AD-A251 237 ·

PL-TR-92-2059 SPECIAL REPORTS, NO. 267



PROCEEDINGS OF THE 14TH ANNUAL REVIEW CONFERENCE ON ATMOSPHERIC TRANSMISSION MODELS, 11-12 JUNE 1991

EDITORS:

L. W. ABREU

F. X. KNEIZYS

26 FEBRUARY 1992



APPROVED FOR PUBLIC RELEASE; DISTRIBUTION UNLIMITED



PHILLIPS LABORATORY
AIR FORCE SYSTEMS COMMAND
HANSCOM AIR FORCE BASE, MASSACHUSETTS 01731-5000

"This technical report has been reviewed and is approved for publication"

WILLIAM A. BLUMBERG, Chief

Simulation Branch

Optical Environment Division

ALAN D. BLACKBURN, Col, USAF, Director

Optical Environment Division

This report has been reviewed by the ESD Public Affairs Office (PA) and is releasable to the National Technical Information Service (NTIS).

Qualified requestors may obtain additional copies from the Defense Technical Information Center. All others should apply to the National Technical Information Service.

If your address has changed, or if you wish to be removed form the mailing list, or if the addressee is no longer employed by your organization, please notify GL/TSI, Hanscom AFB, MA 01731-5000. This will assist us in maintaining a current mailing list.

Do not return copies of this report unless contractual obligations or notices on a specific document requires that it be returned.

UNCLASSIFIED SECURITY CLASSIFICATION OF THIS PAGE

REPORT C	ON PAGE			Form Approved OMB No. 0704-0188	
1a. REPORT SECURITY CLASSIFICATION UNCLASSIFIED	16. RESTRICTIVE MARKINGS				
Za. SECURITY CLASSIFICATION AUTHORITY			/AVAILABILITY O		
2b. DECLASSIFICATION / DOWNGRADING SCHEDU	ι£	1	for publition unlii		lease;
4. PERFORMING ORGANIZATION REPORT NUMBER PL-TR-92-2059	R(S)	S. MONITORING	ORGANIZATION R	EPORT NUI	MBER(S)
SR, No. 267					
63. NAME OF PERFORMING ORGANIZATION Phillips Laboratory	6b. OFFICE SYMBOL (If applicable) GPO	7a. NAME OF MO	ONITORING ORGAI	NIZATION	
6c. ADDRESS (City, State, and ZIP Code)	GFU	7h ADDRESS (Cir.	y, State, and ZIP C	odel	
Hanscom AFB, MA 01731-5000		, and the state of	y, state, and all e		
8a. NAME OF FUNDING/SPONSORING ORGANIZATION	8b. OFFICE SYMBOL (If applicable)	9. PROCUREMENT	INSTRUMENT IDE	NTIFICATIO	ON NUMBER
8c. ADDRESS (City, State, and ZIP Code)		10. SOURCE OF F	UNDING NUMBERS	5	
		PROGRAM ELEMENT NO.	PROJECT NO.	TASK NO	WORK UNIT ACCESSION NO.
·		62101F	7670	09	10
11. TITLE (Include Security Classification) Proceedings of the 14th American area of the 14th American models.	nnual Review	Conference	e on Atmo	spher	ic
12. PERSONAL AUTHOR(S) L.W. Abreu and F.X. Kneizys	· · · · · · · · · · · · · · · · · · ·				
13a. TYPE OF REPORT 13b. TIME CO Reprint FROM	VERED TO	14. DATE OF REPOR 1992 Febru		(ay) 15.	PAGE COUNT
16. SUPPLEMENTARY NOTATION					
17. COSATI CODES	18. SUBJECT TERMS (C	Continue on reverse	if necessary and	identify by	y plock number)
FIELD GROUP SUB-GROUP	Atmospheric Propagation Turbulence; Visible: Inf	Transmitt; Clouds; R Molecular Trared: Spe	ance; Aer ladiative Absorptio	rosols Transi n; Ult	;Atmospheric fer;Optical traviolet;
19. ABSTRACT (Continue on reverse if necessary a	ind identify by block nu	ımber)			
Contains the viewgraphs as	nd other mat	erials for	the 42 p	apers	presented
at the Fourteenth Annual 1	Review Confe	rence on A	tmospheri	c Tra	nsmission
Models held at the Geophys Hanscom AFB, MA 11-12 Jun	sics Directo ne 1991	rate, Phil	lips Labo	rator	y (AFSC),
	•				
20. DISTRIBUTION/AVAILABILITY OF ABSTRACT		21. ABSTRACT SEC		TION	
22a. NAME OF RESPONSIBLE INDIVIDUAL	T. DTIC USERS	226. TELEPHONE (I	ASSIFIED nclude Area Code)	22c. OFFI	ICE SYMBOL
LEONARD W. ABREU		617-377-2	337	GPOS	

	Content
Introduction	vii
Keynote	viii
Session on Aerosols and Clouds	-
Summary of Session 1	1
"Boundary Layer Illumination Radiation Balance Model: BLIRB" A. Zardecki	2
"Relations Between Giant Aerosols Near the Surface and Solar Aureole Brightness" F.E. Volz	14
"The Computation of Radiative Transfer Through the Atmosphere Incorporating Various Aerosol Scenarios" L.C. Rosen	17
"BACKSCAT Lidar Backscatter Simulation: Version 2.0" J.R. Hummel, D.R. Longtin, N.L. Paul, J.R. Jones	28
"Cirrus Cloud Transmission Modelling" W.M. Cornette, J.G. Shanks	34
"ICE-CLOUD - A Model for IR Transmittance Through Cirrus Cloud" W.T. Kreiss, R. Vik	47
"The Status of the Navy Oceanic Vertical Aerosol Model" S. Gathman	54
Session on Atmospheric Propagation Models	
Summary of Session 2	61
"MODTRAN/LOWTRAN: Current Status, Future Plans" L.W. Abreu, F.X. Kneizys, G.P. Anderson, J.H. Chetwynd	64
"FASCODE3: An Update" G.P. Anderson, F.X. Kneizys, J.H. Chetwynd, L.W. Abreu, M. Hoke, S.A. Clough, R.D. Worsham, F.P. Shettle	73

"EOSAEL92" A.E. Wetmore	86
"HITRAN'91: The Contemporary Spectroscopic Molecular Database" L.S. Rothman	98
"SHARC, An Atmospheric Radiation and Transmittance Code for Altitudes from 50 to 300 km" D. Robertson, L. Bernstein, J. Duff, J. Gruninger, R. Sundberg, R. Sharma, R. Healey	107
"Recent Developments of the GENLN2 Line-by-Line Model: Studies in Support of the UARS Project" D.P. Edwards	119
"Present Status of Transmittances and Radiances Modelling at L.M.D." N.A. Scott, A. Chédin, F. Chéruy, B. Tournier	129
"AURIC (Atmospheric Ultraviolet Radiance Integrated Code): an Update" R. Huguenin, R. Hickey, K. Minschwaner, G.P. Anderson, L.A. Hall, R.E Huffman	130
"Ontar's PC Compatible LOWTRAN Package" J. Schroeder, P. Noah	143
"Coupling Atmosphere and Background Effects" W.M. Cornette	152
"SENTRAN7: A Sensitivity Analysis Package for LOWTRAN7 and MODTRAN" D.R. Longtin, F.M. Pagliughi, N.L. Paul	165
"Atmospheric Models in the Strategic Scene Generation Model" W.M. Cornette, D.C. Anding	173
"Review of the Chemical Kinetic Rate Constants Used in the SHARC Model" V.I. Lang, A.T. Pritt, Jr	188
Session on Measurements and Models	
Summary of Session 3	200
"Atmospheric Ultraviolet Radiance and its Variations" R. Link, D.J. Strickland D.E. Anderson, Jr.	202
"Photoabsorption Cross Sections in the Transmission Window Regions of the Schumann-Runge Bands of Oxygen" K. Yoshino, J.R. Esmond, D.E. Freeman, W.H. Parkinson, A.S-C. Cheung	203
"Incorporation of LOWTRAN7 into the ACQUIRE Model" S.G. O'Brien	211
"High-resolution Spectral Measurements of Upwelling and Downwelling Atmospheric Infrared Emission with Michelson Interferometers" H. F. Revercomb	215

"Validation of HIS Spectral Measurements with the FASCODE Line-by-Line Model" S.A. Clough, R.D. Worsham, W.L. Smith, H.E. Revercomb, R.O. Knuteson, H.M. Woolf, G.P. Anderson, M.L. Hoke, F.X. Kneizys, M.V. Wagner, R.M. Goody	. 231
"Improved HNO3 Band Model Parameters" N. Jones, A. Goldman, D. Murcray, F. Murcray, W. Williams	. 242
"Line-by-line Calculations of Atmospheric Fluxes and Heating Rates" S.A. Clough, M.J. Iacono, JL. Moncet	. 249
"Comparison of FASCOD2 and LOWTRAN7 Models with FIT Spectral Transmittance Measurements in the 3-12µm Region" J.M. Thériault	. 263
"Spectral Solar Radiation Modeling, Measurement, and Data Base Activities at the Solar Energy Research Institute" C.J. Riordan, R.L. Hulstrom	. 276
"LOWTRAN 7 Comparisons with Field Measurements" R. Smith, N. McNabb, K. Hammerdorfer, T. Corbin	. 282
"Spectral Smoothing in the Fourier Domain: A Software Package for Line-by-Line Calculations" W. Gallery, M. Esplin	. 314
"A Comparison of Computational Approaches for the Voigt Function" F. Schreier	. 320
Topical Session on Spectral Line Shapes	
Summary of Session 4	. 329
"Basis of the Water Vapor Continuum Coefficients in the GL Models" S.A. Clough	. 333
"Water Vapor Continuum Absorption Measurements with Line Shape Interpretations" M. Thomas	. 341
"Line Coupling for Microwave Oxygen Lines" P.W. Rosenkranz	. 361
"Laboratory Measurements of Line Coupling in CO ₂ and N ₂ O" L.L. Strow	. 370
"Line Mixing: A Near Wing and Far Wing Problem" JM. Hartmann	389

Contributed Papers

and Infrared Regions" R.H. Tipping, Q. Ma	409
"Laboratory Measurements of the 60-GHz O2 Spectrum in Air" H.J. Liebe	419
"Line Coupling in Polar and Nonpolar Molecules" A.S. Pine and J.P. Looney	429
"Study of CO ₂ Blue Wing in the 4.1 µm Region" C. Delaye, M. Thomas	441
"Theoretical Approach to the Line Wing Problem" L. Sinitsa	449
Appendix	
Call for Papers	457
Agenda	459
List of Attendees	465
Author Index	478

INTRODUCTION

The Fourteenth DoD Tri-Service Review Conference on Atmospheric Transmission Models was held at the Geophysics Directorate, Hanscom AFB, Massachusetts on 11-12 June 1991. The purpose of the meeting was to review progress in the modeling of radiation propagating through the earth's atmosphere, identify deficiencies in these models, and make recommendations for improvements.

Approximately 140 scientists and engineers, representing DoD, other government agencies, industry, and the academic community were in attendance. The agenda consisted of forty two papers with sessions on aerosols and clouds, atmospheric propagation models, measurements and models and an extended Topical session on spectral line shapes hosted by Michael L. Hoke which included invited papers and contributed papers.

This proceedings volume summarizes the technical presentations at the conference. The main part of the report consists of the abstracts and copies of the viewgraphs or slides and other material as provided by the authors for the presentations. Preceding the viewgraphs for each session is a commentary prepared by the co-chairpersons on each presentation within that session. The Appendix includes the original call for papers and invitation to the meeting, a copy of the Agenda for the meeting, a list of the attendees, and an author index.

A special thanks is extended to Ronald G. Isaacs, Betty Stenhouse and Atmospheric and Environmental Research, Inc.

Francis X. Kneizys Leonard W. Abreu



Acces	sion For	
NTIS	GRA&I	
DTIC	TAB	ā
Unanr	ounced	ā
Justi	fication	
By Diætr	ibution/	
Avai	lability	Codes
	Avail and	/or
Dist	Special	•
1	1 1	
N'	1 1	
11,	l l	7 , 1

KEYNOTE: Col. Grant Aufderhaar

USAF (OUSDA) Pentagon Washington, DC

DEFENSE CRITICAL TECHNOLOGIES PLAN

SUBMITTED ANNUALLY BY THE

DEPARTMENT OF DEFENSE

IN CONSULTATION WITH THE

DEPARTMENT OF ENERGY



TO THE

COMMITTEES ON ARMED SERVICES UNITED STATES CONGRESS



CRITICAL TECHNOLOGIES PLAN

HISTORICAL CONTEXT

- QUALITATIVE SUPERIORITY PROVIDES UNDERPINNING TO NATIONAL SECURITY
- U.S. SUCCESSFUL IN DOING SO FOR FORTY YEARS (B-52, MINUTEMAN, POLARIS, U-2, AIRCRAFT TURBINES, SENSORS, ACCURACY IN TARGETING, SATELLITES, ETC.)

RECENT TRENDS

- DECLINE IN FUNDING FOR TECHNOLOGY BASE SINCE 1965:
 - FEWER \$ FOR BUDGET CATEGORIES 6.1, 6.2, 6.3A

CONSEQUENCES

- U.S. TECHNOLOGY BASE IS RUSTING
 - CONSISTS OF 80's RESEARCH AND EARLY 80's TECHNOLOGY
- RADICALLY NEW CONCEPTS ARE DIFFICULT TO IMPLEMENT
 - REGARDLESS OF MERIT
 - NOT ENOUGH \$ TO DEMONSTRATE NEW TECHNOLOGIES
- EXPECTATIONS ARE UNSUSTAINABLE



DEFENSE PLANNING GUIDANCE REQUIRES CONTINUED QUALITATIVE SUPERIORITY ...

- ... AND CONTINUED QUALITATIVE SUPERIORITY REQUIRES
 ARRESTING EROSION OF THE TECHNOLOGY BASE THROUGH:
- CLEAR REALISTIC LONG-TERM GOALS
- A HEALTHY INFRASTRUCTURE
- ADEQUATE RESOURCES
 - TO DEVELOP NEW TECHNOLOGIES (6.1, 6.2)
 - TO DEMONSTRATE NEW SYSTEMS CAPABILITY USING NEW TECHNOLOGIES (6.3A)
- AN EFFICIENT MECHANISM FOR TURNING CONCEPTS INTO SYSTEMS
 - THAT ARE CAPABLE OF MEETING THE LONG-TERM GOALS

\$231/321904 V



CRITICAL TECHNOLOGIES PLAN

CONGRESSIONAL MANDATE

PL 101-189

"THE SECRETARY OF DEFENSE ... SHALL SUBMIT ... AN ANNUAL PLAN FOR DEVELOPING THE TECHNOLOGIES CONSIDERED ... MOST CRITICAL TO INSURING THE LONG-TERM QUALITATIVE SUPERIORITY OF UNITED STATES WEAPON SYSTEMS."



PRINCIPAL FEATURES OF THE PLAN

- LINKS CRITICAL TECHNOLOGIES TO DOD SCIENCE AND TECHNOLOGY STRATEGY
- SELECTS 20 CRITICAL TECHNOLOGIES
- PRIORITIZES THEM
- PROVIDES FUNDING ESTIMATES
- INDICATES MILESTONES TO 2005
- PROVIDES INTERNATIONAL COMPARISONS
- INCLUDES INDUSTRIAL BASE AND MANUFACTURING ISSUES

8231/32190/LY



CRITICAL TECHNOLOGIES PLAN

ADDITIONAL CONSIDERATIONS FOR THE FY 1990 PLAN

- BROADER CONGRESSIONAL TASKING
- INCREASED DISCUSSION OF MANUFACTURING ISSUES
- NEW SELECTION CRITERIA
 - (INCLUDES: STRENGTHENING THE INDUSTRIAL BASE)
- FUNDING SHOWN OVER A DECADE (NOT JUST ONE YEAR)
- CRITICAL TECHNOLOGIES PRIORITIZED
- INTELLECTUAL CONSOLIDATION OF SOME CRITICAL TECHNOLOGIES
 - EMPHASIZING TECHNOLOGY RATHER THAN NEED
 - COMBINING CLOSELY RELATED TECHNOLOGIES

ADDITIONAL REQUIREMENT FOR THE 1991 PLAN, AS AMENDED IN THE NATIONAL DEFENSE AUTHORIZATION ACT FOR FY 1991 AND 1992, PL 101-510

"SEC.801. ANNUAL DEFENSE CRITICAL TECHNOLOGIES PLAN

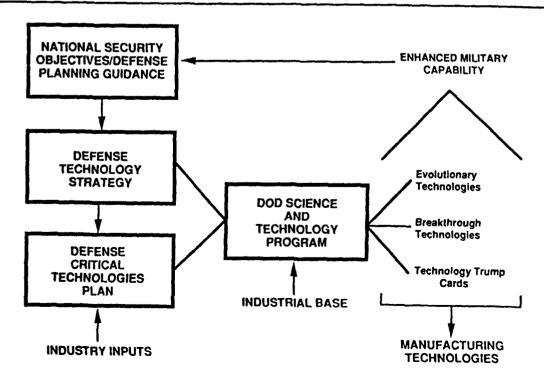
- (A) INCREASED INFORMATION RELATING TO FUNDING ...
 - (3) IDENTIFY EACH PROGRAM ELEMENT ...

FOR WHICH FUNDS ARE BUDGETED FOR THE SUPPORT OF THE DEVELOPMENT OF ANY CRITICAL TECHNOLOGY IDENTIFIED IN THE PLAN: AND

- (4) FOR EACH SUCH ELEMENT --
 - (A) SPECIFY THE AMOUNT [IN FY92] INCLUDED FOR EACH CRITICAL TECHNOLOGY COVERED BY THE PROGRAM ELEMENT ... [AND COMPARE] ... WITH THE AMOUNT ... FOR THE [PRECEDING] FISCAL YEAR [FY91]..."



DEFENSE TECHNOLOGY STRATEGY AND PLANNING





THE PARTICIPANTS

STEERING COMMITTEE: SENIOR S&T MANAGERS FROM DOD,

SERVICES, DOE

WORKING GROUP: OSD (CHAIRMANSHIP)

ARMÝ NAVY AIR FORCE DARPA DIA DNA SDIO JCS

DOE HEADQUARTERS

DOE NATIONAL LABORATORIES: LAWRENCE LIVERMORE LOS ALAMOS SANDIA

B231/32190/LY



CRITICAL TECHNOLOGIES PLAN

SUBJECTS ADDRESSED IN THE REPORT

- DESCRIPTION OF THE TECHNOLOGY
- PAYOFF
- S&T PROGRAMS
- RELATED MANUFACTURING CAPABILITY
- R&D IN THE UNITED STATES
- INTERNATIONAL ASSESSMENT



LIST OF DEFENSE CRITICAL TECHNOLOGIES

- SEMICONDUCTOR MATERIALS AND MICROELECTRONIC CIRCUITS
- SOFTWARE PRODUCIBILITY
- PARALLEL COMPUTER ARCHITECTURES
- · MACHINE INTELLIGENCE/ROBOTICS
- SIMULATION AND MODELING
- PHOTONICS
- SENSITIVE RADARS
- PASSIVE SENSORS
- SIGNAL PROCESSING
- SIGNATURE CONTROL
- WEAPON SYSTEM ENVIRONMENT
- DATA FUSION
- COMPUTATIONAL FLUID DYNAMICS
- AIR-BREATHING PROPULSION
- PULSED POWER
- HYPERVELOCITY PROJECTILES
- HIGH ENERGY DENSITY MATERIALS
- · COMPOSITE MATERIALS
- SUPERCONDUCTIVITY
- BIOTECHNOLOGY MATERIALS AND PROCESSES
- FLEXIBLE MANUFACTURING

Technologies not In priority order



CRITICAL TECHNOLOGIES PLAN

TECHNOLOGY OBJECTIVES

- SEMICONDUCTOR MATERIALS AND MICROELECTRONIC CIRCUITS:
 - HIGH-SPEED COMPUTING AND SIGNAL PROCESSING, AUTOMATIC CONTROL, SENSITIVE RECEIVERS, MILLIMETER WAVE RADAR, PHOTONICS
- SOFTWARE PRODUCIBILITY:
 - AFFORDABLE, TRUSTED SOFTWARE, AUTOMATIC SOFTWARE GENERATION, REUSABLE SOFTWARE
- PARALLEL COMPUTER ARCHITECTURES:
 - ULTRA-HIGH-SPEED COMPUTING
- MACHINE INTELLIGENCE AND ROBOTICS:
 - BUILD HUMAN INTELLIGENCE INTO MECHANICAL DEVICES, MANUFACTURING, MAINTENANCE
- SIMULATION AND MODELING:
 - TESTING CONCEPTS AND DESIGNS WITHOUT EXPENSIVE REPLICAS, TRAINING FOR COMPLEX MILITARY SCENARIOS
- PHOTONICS:
 - ULTRA-HIGH-DENSITY MEMORIES AND HIGH-VOLUME, HIGH-SPEED INFORMATION PROCESING
- SENSITIVE RADARS:
 - NON-COOPERATIVE TARGET IDENTIFICATION, DETECTION OF LOW-OBSERVABLE TARGETS



TECHNOLOGY OBJECTIVES (CONT.)

- PASSIVE SENSORS:
 - SILENT SENSING OF TARGETS OR ENVIRONMENT, MONITORING EQUIPMENT (CONDITION SENSING)
- SIGNAL PROCESSING:
 - PROCESSING SIGNALS FOR INFORMATION EXTRACTION, AUTOMATIC TARGET DETECTION/TRACKING/CLASSIFICATION/RECOGNITION
- SIGNATURE CONTROL:
 - CONTROLLING PLATFORM OR WEAPON SIGNATURES (RADAR, OPTICAL, ACOUSTIC, ETC.) TO ENHANCE THEIR SURVIVABILITY
- WEAPON SYSTEM ENVIRONMENT:
 - UNDERSTANDING OR PREDICTING THE BEHAVIOR OF THE ENVIRONMENT TO ENHANCE WEAPON EFFECTIVENESS
- DATA FUSION:
 - COMBINING AND INTERPRETING DATA FROM SEVERAL SOURCES AND PRESENTING IT IN A CONVENIENT FORM TO THE HUMAN OPERATOR
- COMPUTATIONAL FLUID DYNAMICS:
 - MODELING OF COMPLEX FLUID FLOW TO MAKE DEPENDABLE PREDICTIONS BY COMPUTING, THUS OBVIATING EXPENSIVE FACILITIES AND EXPERIMENTS

0231/32190/LY

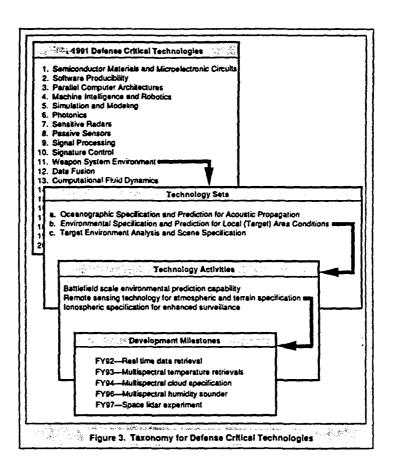


CRITICAL TECHNOLOGIES PLAN

TECHNOLOGY OBJECTIVES (CONT.)

- AIR BREATHING PROPULSION:
 - LIGHT-WEIGHT, FUEL EFFICIENT ENGINES
- PULSED POWER:
 - COMPACT, LIGHT-WEIGHT, LOW-VOLUME DEVICES FOR HIGH-POWER MICROWAVES, HIGH-ENERGY LASERS, ELECTROTHERMAL GUNS, RADARS, ELECTROMAGNETIC LAUNCHERS, PARTICLE BEAMS
- HYPERVELOCITY PROJECTILES:
 - TO PENETRATE HARDENED TARGETS
- HIGH ENERGY DENSITY MATERIALS:
 - SAFE, TRANSPORTABLE, EFFICIENT ENERGETIC MATERIALS FOR EXPLOSIVES AND PROPELLANTS
- COMPOSITE MATERIALS:
 - HIGH-TEMPERATURE, HIGH-STRENGTH, LIGHT-WEIGHT COMPOSITE MATERIALS FOR AEROSPACE APPLICATIONS
- SUPERCONDUCTIVITY:
 - FABRICATION AND EXPLOITATION OF SUPERCONDUCTING MATERIALS
- BIOTECHNOLOGY:
 - SYSTEMATIC APPLICATION OF BIOLOGY IN MILITARY ENGINEERING OR MEDICINE

8231/32190/LY





DEFENSE CRITICAL TECHNOLOGIES PRIORITIZED IN THREE GROUPS

(FY92 FUNDING ESTIMATES FOR S&T PROGRAMS IN \$M)

A		<u>B</u>		Ç
COMPOSITE MATERIALS COMPUTATIONAL FLUID DYNAMICS DATA FUSION PASSIVE SENSORS PHOTONICS SEMICONDUCTOR MATERIALS AND MICROELECTRONIC CIRCUITS SIGNAL PROCESSING SOFTWARE PRODUCIBILITY	\$187 97 112 528 203 512 245 185	AIR-BREATHING PROPULSION MACHINE INTELLIGENCE AND ROBOTICS PARALLEL COMPUTER ARCHITECTURES SENSITIVE RADARS SIGNATURE CONTROL SIMULATION AND MODELING WEAPON SYSTEM ENVIRONMENT	\$389 151 169 194 110 361 393	BIOTECHNOLOGY \$ 40 HIGH ENERGY DENSITY 86 MATERIALS HYPERVELOCITY 188 PROJECTILE PULSED POWER 83 SUPERCONDUCTIVITY 62

• FLEXIBLE MANUFACTURING

<u>MOTE:</u> TECHNOLOGIES ARE LISTED IN ALPHABETICAL ORDER WITHIN EACH GROUP.



CAVEATS

- CRITICAL TECHNOLOGIES ARE NOT THE ONLY IMPORTANT TECHNOLOGIES
 - THEY DO NOT EXIST IN ISOLATION
 - THERE ARE OTHER IMPORTANT TECHNOLOGIES
 - WHICH ARE DESCRIBED IN THE DOD S&T STRATEGY
- THEY ARE NOT TO BE CONFUSED WITH THE
 - "MILITARILY CRITICAL TECHNOLOGIES LIST" USED FOR EXPORT CONTROL PURPOSES
- FUNDING ESTIMATES ARE JUST THAT, NOT BUDGET NUMBERS
- PRIORITY GROUPINGS SHOULD NOT BE OVEREMPHASIZED

8231/32190/LY



CRITICAL TECHNOLOGIES PLAN

FOREIGN TECHNOLOGICAL CAPABILITIES

Critical Technologies	USSR	NATO Allies	Japan
Semiconductor Materials and Microelectric Circuits			
2. Software Producibility			
Parallel Computer Architectures			
4. Machine Intelligence and Robotics			
5. Simulation and Modeling	***		
6. Photonics			
7. Sensitive Radars			
8. Passive Sensors			
9. Signal Processing	146 S.		
10. Signature Control	**		



FOREIGN TECHNOLOGICAL CAPABILITIES (CONT.)

Critical Technologies	USSR	NATO Allies	Japan
11. Weapon System Environment			
12. Data Fusion			
13. Computational Fluid Dynamics			
14. Air-Breathing Propulsion			
15. Pulsed Power			
16. Hypervelocity Projectiles			
17. High Energy Density Materials			
18. Composite Materials			
19. Superconductivity			
20. Biotechnology Materials and Processes			

B231/32190/LY



CRITICAL TECHNOLOGIES PLAN

FOREIGN TECHNOLOGICAL CAPABILITIES (CONT.)

LEGEND:

POSITION OF THE L	JSSR RELATIVE TO THE UNITED STATES	CAPABILITY OF OTH	IERS TO CONTRIBUTE TO THE TECHNOLOGY
	Significant leads in some niches of technology		Significantly ahead in some niches of technology
	Generally on a par with the United States		Capable of making major contributions
En Joseph Seer, and	Generally lagging except in some areas		Capable of making some contributions
	Lagging in all important aspects		Unlikely to make any immediate contribution

DEFENSE CRITICAL TECHNOLOGIES PLAN

TO OBTAIN A COPY OF THE REPORT:

COMPANIES, ASSOCIATIONS, PRIVATE INDIVIDUALS:

CALL

202-697-5737

REPORTERS, PRESS:

CALL

202-695-0192

U.S. GOVERNMENT:

CALL

202-695-0552

TO OBTAIN THE REPORT FROM DTIC, REGISTERED USERS MAY
CALL 202-274-7633 AND REFERENCE "AD" NUMBER AD-A219 300

Session 1

Summary of the Session on Aerosols and Clouds

The session on Aerosols and Clouds included 7 papers. The first paper by Zardecki (Science & Technology Corp.) described the Boundary Layer Illumination Radiation Balance (BLIRB) model, which they are developing for the Army Atmospheric Sciences Laboratory (ASL), in support of the BTI/SWOE program. The model will calculate the direct and scattered sunlight reaching the ground through an atmosphere containing a 3-dimensional distribution of clouds and aerosols. The model, which is based on a modified version of LOWTRAN, includes some interactions between individual clouds, such as partial shadowing of the direct sunlight by an adjacent cloud.

There were two papers on cirrus clouds. The first of these by Cornette & Shanks (Photon Research Associates) reviewed the literature on modeling transmission through cirrus clouds. It provided a reasonable summary of the current research work. Kreiss & Vik (Horizon Technology Inc.) described the ICECLOUD cirrus transmittance model they are developing for AF Wright Labs as part of the IASPM (IR Atmospherics & Signature Prediction Model) project. This model is largely based on the Liou, Heymsfield et al. model in Applied Optics last May and presented at this meeting two years ago.

There were several papers on atmospheric aerosols and their effects on radiation. Volz (PL) showed that his observations of the brightness of the solar aureole are well correlated with the presence of large dust and pollen particles (5 to 50 μ m) in the atmosphere. This aureole brightness has shown a steady decrease over the past twelve years, implying a corresponding decrease in the large aerosol particles in the atmosphere.

Rosen (LLNL) presented preliminary results on modeling the sensitivity of radiation in the atmosphere to different aerosol conditions using LOWTRAN. This work is being done in support of DOE's Atmospheric Radiation Measurements (ARM) program.

Hummel et al. (SPARTA, Inc.) described version 2 of the Lidar backscatter simulation computer code they developed for PL/OPA, named BACKSCAT. This code is written to run stand alone on a PC using the standard LOWTRAN aerosol and cirrus models, which are built in, and external molecular absorption profiles for the lidar wavelength (such as calculated by FASCODE). However, the scientific portion was written in FORTRAN, so it could be easily modified to be directly incorporated into FASCODE, or to run on other computers.

Gathman (NOSC) described the current status of the Navy Ocean Vertical Aerosol Model (NOVAM). This model describes the vertical structure of the optical IR properties of the atmospheric aerosols in the boundary layer above the ocean surface. It uses as input, the surface meteorological conditions and radiosonde profiles. The version of the Navy aerosol model which is currently implemented in LOWTRAN effectively applies the surface values of the NOVAM optical/IR properties to the entire boundary layer.

BOUNDARY LAYER ILLUMINATION RADIATION BALANCE MODEL: BLIRB

A. Zardecki Science and Technology Corporation, 555 Telshor Blvd., Suite 200, Las Cruces, NM 88001

BLIRB provides direct and diffuse solar insolation at the earth's surface in the spectral range 0.4 to 12 μm . The model is an extension of LOWTRAN 7 to 3-D cloud and aerosol distributions in the lower 5 km of the atmosphere. The propagation of radiation through clouds is formulated by a variant of the adding method, supplemented by a stochastic ray tracing algorithm to model the penumbra effect. With a spectral resolution of 20 cm⁻¹, the spatial mesh can reach the size of 40X40X40 grid points in a physical volume whose extent is specified by the user. The full AFGL aerosol data base, including 40 boundary layer aerosol models, can be combined with six model atmospheres and five season-dependent visual range options. LOWTRAN 7 supplies the gaseous transmission to BLIRB, which offers four cloud options including cloud-free, horizontally homogeneous clouds, rectangular clouds, and a Cloud Scene Simulation prototype model developed by TASC.

Boundary Illumination Radiation Balance Model: BLIRB

- A. Zardecki, R. Davis, B. Rappaport
 Science & Technology Corporation
 Las Cruces, New Mexico
- A. Wetmore, J. Martin

 Atmospheric Sciences Laboratory

 White Sands Missile Range, NM

Annual Review Atmos. Transmission Models 1991

Boundary Illumination Radiation Balance Model: BLIRB

- Cloud Options
- Radiative transfer through 3-D clouds
- Atmospheric/aerosol data base
- **■** Example of computation

BLIRB: Cloud Options

- Cloud-free, aerosol loaded atmosphere
- Horizontally homogeneous clouds: cloudiness
- Rectangular clouds: composition
- Clouds Scene Simulation Model TASC

Science & Technology Corp

BLIRB: Radiative Transfer through 3-D Clouds

- Two-stream approximation: Coakley-Chylek 1975
- Doubling method for diffuse radiation
- IR radiation: average flux
- Stochastic ray tracing: penumbra effect

Reflection and transmission functions

$$R(\mu) = \frac{(Q+1)(Q-1)[E-E^{-1}]}{(Q+1)^2 E - (Q-1)^2 E^{-1}}$$

$$\tilde{T}(\mu) = \frac{4Q}{(Q+1)^2 E - (Q-1)^2 E^{-1}}$$

where

$$E = exp(\alpha \tau/\mu)$$

$$Q = \frac{[1 - \omega_0 + 2\omega_0 \beta(\mu)]^{1/2}}{[1 - \omega_0]^{1/2}}$$

$$\alpha = [1 - \omega_0 + 2\omega_0 \beta(\mu)]^{1/2} [1 - \omega_0]^{1/2}$$

Adding Method, Lacis & Hansen 1974

Let

$$S = \frac{R_1 R_2}{1 - R_1 R_2}$$

then transmission & reflection between layers

$$D = T_1 + ST_1 + Se^{-\tau_1/\mu}$$

$$U = R_2 D + R_2 e^{-\tau_1/\mu}$$

Diffuse reflection and transmission

$$R_{12} = R_1 + e^{-\tau_1/\mu}U + T_1U$$

$$T_{12} = e^{-\tau_2/\mu}D + T_2 e^{-\tau_1/\mu} + T_2 D$$

Infrared Radiation

Monochromatic emissivity

$$\epsilon(\nu) = 1 - exp(-\sigma_a z),$$

Flux transmissivity

$$i_F(\nu) = \frac{\int_0^1 exp(-\sigma_a z/\mu) \mu \, d\mu}{\int_0^1 \mu \, d\mu}$$

$$t_F(\nu) = e^{-\tau_a}(1 - \tau_a) + \tau_a^2 E_1(\tau_a)$$

where

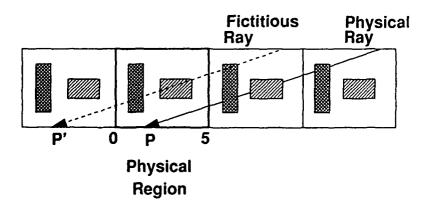
$$E_1(x) = \int_x^\infty s^{-1} exp(-s) ds$$

Average IR flux, w/o scattering

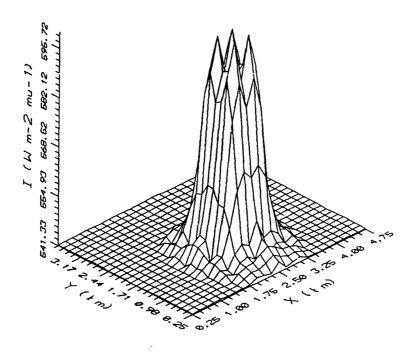
$$F\downarrow (\nu)=\int_{t_F}^1 B(\nu,T)\,dt_F$$

BLIRB: Stochastic Ray Tracing

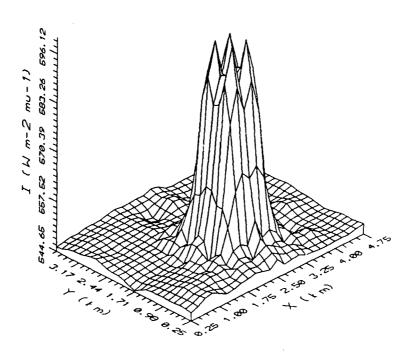
■ Random directions around the normal to earth's surface

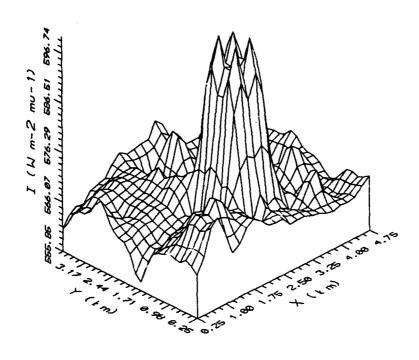


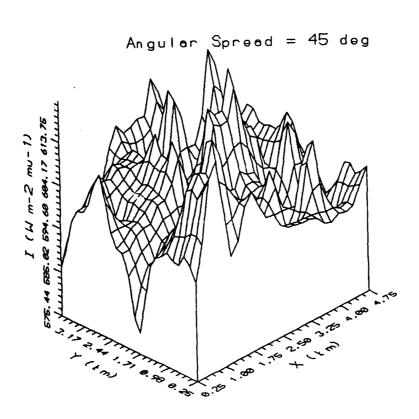
Angular Spread = 5 deg



Angular Spread = 15 deg







BLIRB: AFGL Data Base

- Four layers with different aerosol types
- Rural, urban, maritime, tropospheric aerosols
- RH between 0 and 99%
- Only first two (up to 5km) layers used by BLIRB

Science & Technology Corp

BLIRB: Solar Radiation and Model Atmospheres

- Incident radiation: LOWTRAN 7/numerical fit
- Sky radiance additional source
- **■** Six temperature profiles
- Gaseous absorption from LOWTRAN 7

BLIRB: Rectangular Clouds

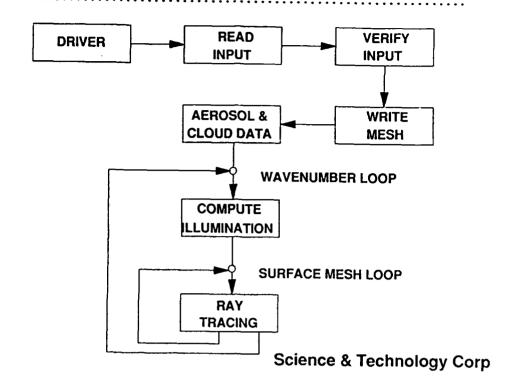
- Regions: ID and bounding coordinates
- Fine mesh structure: MHX(i), XMS(l)
- Material: a mixture of up to 3 aerosols
- Assignment of materials to regions
- PFNDAT phase function data base

Science & Technology Corp

BLIRB: Surface Albedo

- Areas: ID and bounding coordinates
- Albedo: ID and value from input file
- Albedo: tabulated, wavelength-independent
- Spectral albedo arrays pending realistic data

BLIRB: Structure of the Code



BLIRB: Examples of Computation

■ Physical region w. Water Cloud 2x2x1 km

Visible radiation

Stochastic ray tracing: 10 rays

Surface albedo: 0.2, 0.4

Nonuniform mesh

Two rectangular clouds

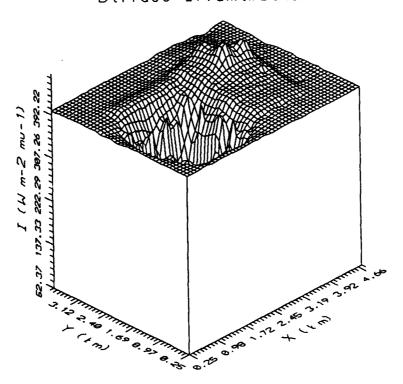
Cloud region: 10 mesh points/km

Background region: 2 mesh points/km

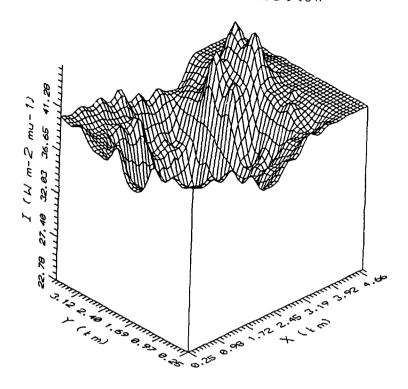
BLIRB: Input File

WAVL	0.55					
VIS	1.0					
BLIRE						
MDL1	22.0000 6.0000	2.0000	0.0000	1.0000		
MDL2	1.0000 292.0000	-1.0000	10.0000	0.0000		
AREA	0.0000 5.0000	0.0000	4.0000	1.0000		
AREA	3.0000 4.0000	2.0000	3.0000	2.0000		
REGN	0.0000 5.0000	0.0000	4.0000	0.0000	5.0000	1.0000
REGN	1.0000 3.0000	1.0000	3.0000	3.0000	4.0000	2.0000
MESX	10.0000 5.0000					
MESY	08.0000 4.0000					
MESZ	10.0000 5.0000					
ALBD	1.0000 0.2000					
ALBD	2.0000 0.4000					
MTRL	1.0000 0.1000	5.0000	0.1000	3.0000	0.0500	
MTRL	-2.0000 3.0000	5.0000	0.1000			
CLDS	2.0000 1.0000	1.0000				
SUN	85.0000 000.0000	1.0000	1.0000			
WAVN	18900.00 18940.00	20.0				
RECL	1.0000					
DONE						
END						
STOP						

Diffuse Illumination



Diffuse Illumination



BLIRB: Conclusions

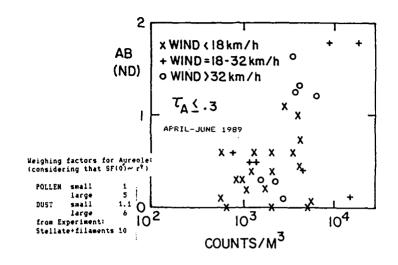
- Integrates clouds, aerosols, and gas absorption
- Direct and diffuse radiation 0.4 12 micro-m
- RT based on adding method and ray tracing
- Mesh 40x40x40 grid points
- AFGL data base for background aerosols
- Four cloud models implemented

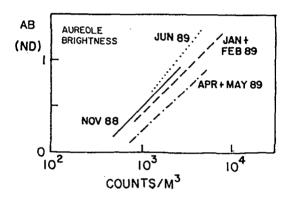
RELATIONS BETWEEN GIANT AEROSOLS NEAR THE SURFACE AND SOLAR AUREOLE BRIGHTNESS

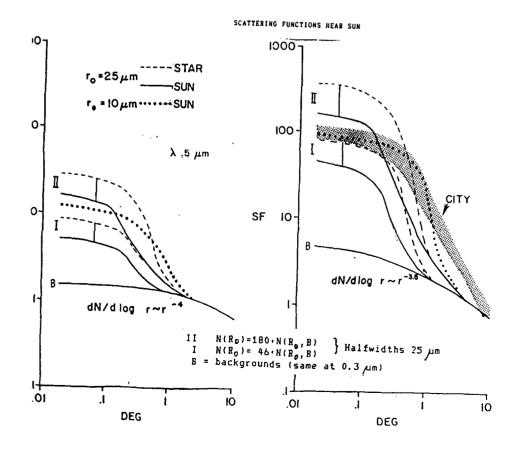
F.E. Volz

Geophysics Directorate, Phillips Laboratory, Hanscom Air Force Base, MA 01731-5000

Observations of the sky brightness at the edge of the sun (aureole) to the west of Boston have shown a gradual decline since about 1979. The number of giant dust particles (with radii from 5 to 50 μ m) suspended in the mixing layer at noontime appears to have decreased by more than a factor of ten. To correlate dust and pollen concentrations near the ground with simultaneous aureole data, those particles were collected by rotating impactor for over one year. Typical scattering functions for size distributions presented in the literature were calculated both for a point source and the sun; small-angle brightness of the latter is considerably lower.







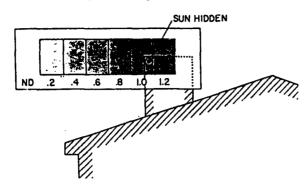
BASIS OF METHOD:

SKY BRIGHTNESS AT SUN'S EDGE (SOLAR AUREOLE), which is governed by particles 3 to 100 microns in size.

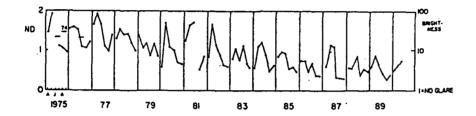
AUREOLE BRIGHTNESS is measured by neutral-density filter needed to suppress glare.

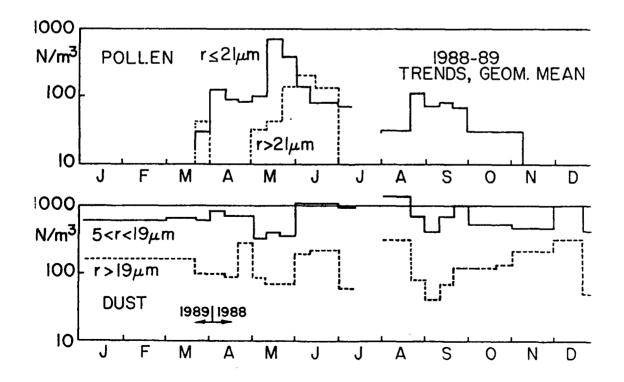
OBSERVATIONS at AFGL and at home (Lexington).

Probably the only continuous date base existing.



AIRBORNE GIANT AEROSOLS - STRONG DECLINE





THE COMPUTATION OF RADIATIVE TRANSFER THROUGH THE ATMOSPHERE INCORPORATING VARIOUS AEROSOL SCENARIOS*

L.C. Rosen

University of California, Lawrence Livermore National Laboratory, Atmospheric & Geophysical Sciences Division, Livermore, CA 94550

The Atmospheric and Geophysical Sciences Division at the Lawrence Livermore National Laboratory is participating in the Atmospheric Research Measurements (ARM) Program. In order to evaluate radiative measurements affected by aerosol environments, calculations are performed utilizing various aerosol scenarios. Mie calculations are done employing appropriate indices of refraction associated with aerosol constituents to yield aerosol extinction coefficients and asymmetry parameters. These results are integrated over aerosol size distributions and are used as data input to the LOWTRAN 7 code. The MIE calculations and integration technique are discussed. The radiative transfer results computed from the LOWTRAN 7 code are compared for the aerosol scenarios. The importance of differing aerosol contributions is discussed.

*Work performed under the auspices of the U.S. Department of Energy by the Lawrence Livermore National Laboratory under Contract No. W-7405-ENG-48.

Physics/G Division



The Computation of Radiative Transfer through the Atmosphere Incorporating Various Aerosol Scenarios

June 11, 1991

L. C. Rosen
Atmospheric & Geophysical Sciences Division
University of California
Lawrence Livermore National Laboratory

Goals



- Develop a capability within the Atmospheric & Geophysical
 Sciences Division, Lawrence Livermore National Laboratory
- Advise Atmospheric Radiation Measurement (ARM) Program
 as to the importance of aerosols to measurement plan

Computational Procedure



For a Given Aerosol Scenario

- Calculate extinction and scattering coefficients, asymmetry parameters from MIE code.
- Integrate extinction and scattering coefficients, asymmetry parameters over size distributions in quadrature code.
- Input averaged extinction, absorption coefficients asymmetry parameters into LOWTRAN7 code to yield radiances and atmospheric transmittances.

MIE Code



- Input indices of refraction
- Output of extinction and scattering coefficients, asymmetry parameters, extinction and scattering efficiency factors.

Quadrature Code

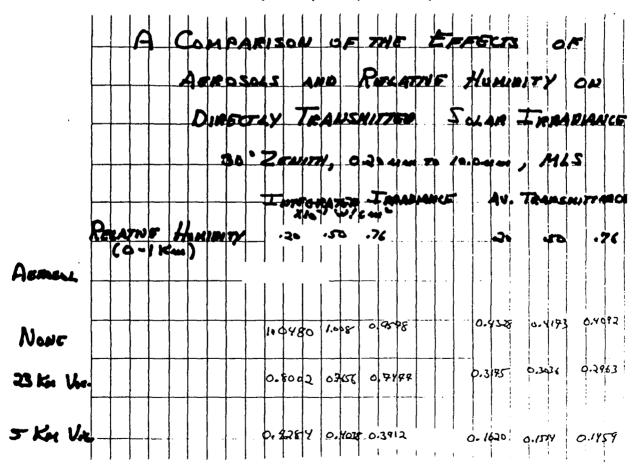


- Input aerosol size distributions, extinction and scattering coefficients, asymmetry parameters, scattering efficiency factors, frequency.
- Output of aerosol extinction and absorption coefficients,
 asymmetry parameters as a function of frequency.



The ICRCCM and other GCM intercomparison programs have highlighted an important area of scientific need associated with the understanding and prediction of global climate change. From the findings of those programs, the following scientific requirements emerge as the most critical:

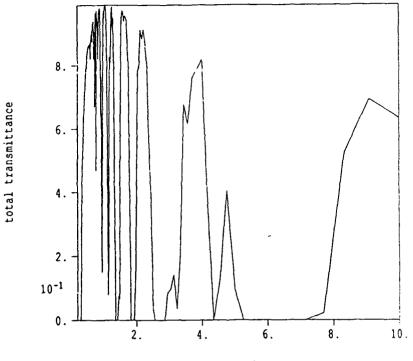
- A quantitative description of the radiative energy balance profile under important physical circumstances must be developed. The descriptions must come from field measurements.
- The processes controlling the radiative balance must be identified and investigated. Validation must come from a direct, comprehensive comparison of field observations with detailed calculations of the radiation field and its cloud and aerosol interactions.
- The knowledge necessary to improve parameterizations of radiative properties of the atmosphere used in GCMs must be developed. This requires intensive measurements at a variety of temporal, spatial and spectral scales.



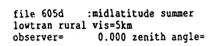
file 605 no aerosol observer=

:midlatitude summer 0.000 zenith angle=

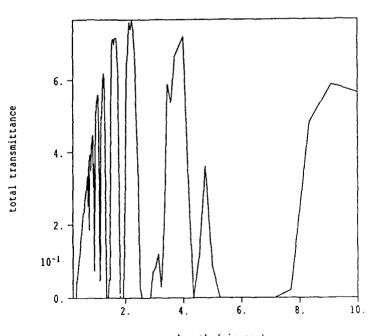
RELATIVE HUMINITY = 76 % MIDLATITUDE SUMMER 30.000



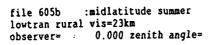
wavelength (microns)



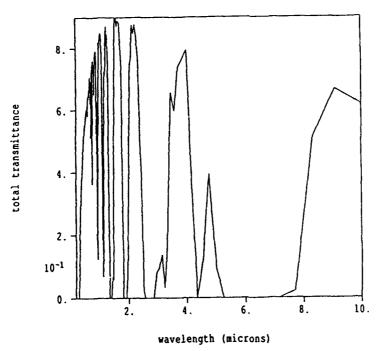
RELATIVE HOLLOWER 30.000

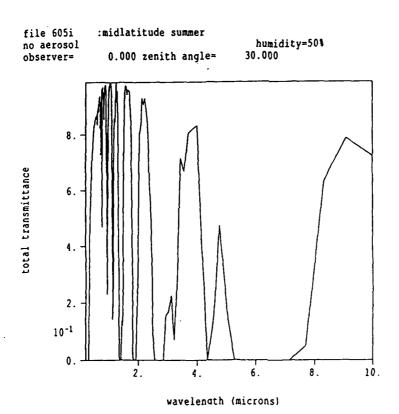


wavelength (microns)



Recarrie Howevery = 76 % MIDLATITUDE SUMMER 30.000





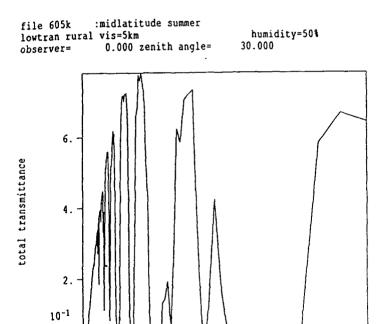
file 605j :midlatitude summer lowtran rural vis=23km humidity=50% observer= 0.000 zenith angle= 30.000

2.

0.

0.

10-1



6.

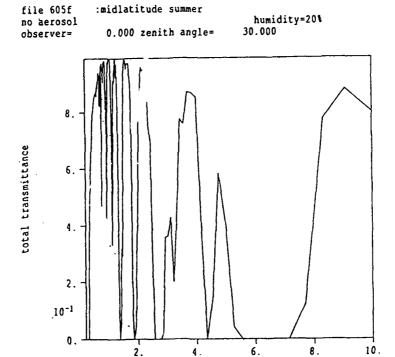
wavelength (microns)

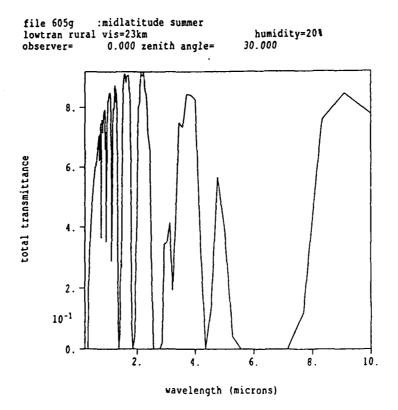
8.

10.

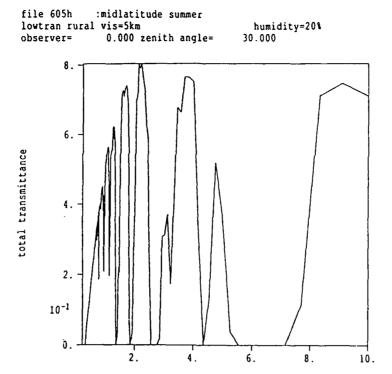
10.

wavelength (microns)

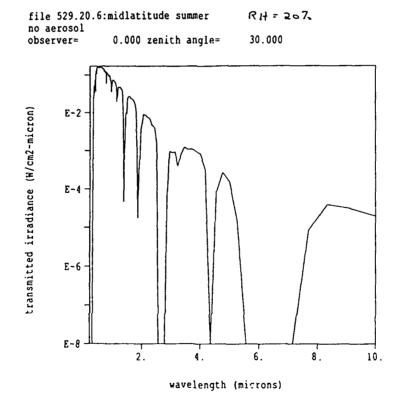


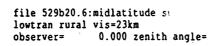


wavelength (microns)

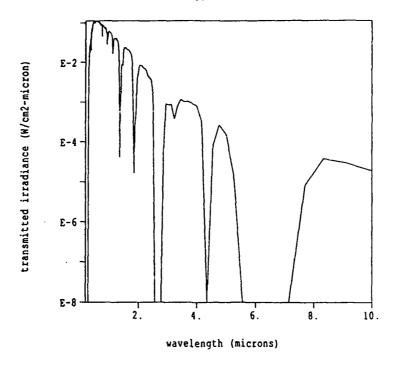


wavelength (microns)



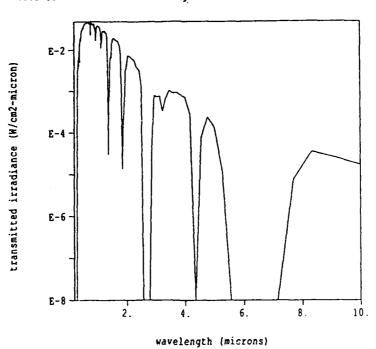


RH-20%

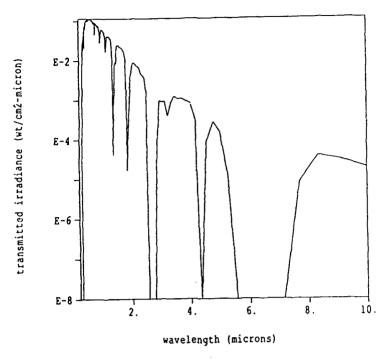


file 529d20.6:midlatitude summer lowtran rural vis=5km observer= 0.000 zenith angle=

RH=20% 30.000



file mie605.6: Recarree Homes, ry = 20 2
Mie integrated, 70% sulfate, 30% dust
altitude= 0.000 zenith angle= 30.000



Future Work

115

- Rural aerosol scenarios
- Marine aerosol scenarios
- Clouds
- Comparison of radiances and atmospheric transmittances

BACKSCAT LIDAR BACKSCATTER SIMULATION: VERSION 2.0

J.R. Hummel, D.R. Longtin, N.L. Paul, J.R. Jones SPARTA, Inc., 24 Hartwell Avenue, Lexington, MA 02173

Backscatter from atmospheric aerosols can produce significant returns in monostatic laser radar (lidar) systems. The Geophysics Directorate of Phillips Laboratory is developing lidar systems that will measure this backscatter. To aid in the design and use of such systems, SPARTA has developed a lidar simulation program, BACKSCAT, that calculates the backscatter return for various lidar systems, viewing aspects, and atmospheric conditions. This paper describes a new version of the simulation system, BACKSCAT Version 2.0. BACKSCAT Version 2.0 has been totally redesigned. Additional aerosol models and cirrus cloud models have been added. In addition, an all new user interface has been developed.

BACKSCAT, LIDAR BACKSCATTER SIMULATION VERSION 2.0

By

John R. Hummel, David R. Longtin, Nanette L. Paul, & James R. Jones

11 June 1991

Annual Review Conference on Atmospheric Transmission Models
Hanscom AFB, Massachusetts

Contract F19628-88-C-0038



BRIEFING OUTLINE

- Background and Objectives of Work
- Overview of BACKSCAT
- New Features in BACKSCAT Version 2.0
- Summary and Recommendations for Future Work



BACKGROUND AND OBJECTIVES

BACKGROUND

- GL has Been Active in Developing and Fielding Atmospheric Backscatter Lidar Systems
- A Need Existed to Simulate the Aerosol Backscatter from Lidar Systems for Repesentative Atmospheric Conditions
- BACKSCAT Version 1.0 Was Developed to Meet That Need Using AFGL Atmospheric Models, circa LOWTRAN 6

OBJECTIVES

- Update BACKSCAT Aerosol Models to LOWTRAN 7 Levels
- Enhance BACKSCAT Based On User Feedback



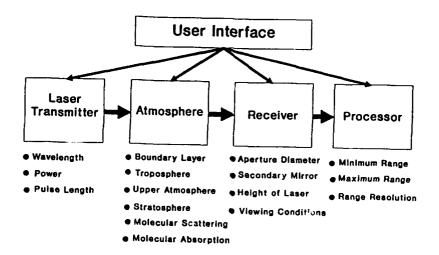
OVERVIEW OF BACKSCAT

- BACKSCAT Simulates the Aerosol Backscatter from a Backscatter Lidar Operating Under User Defined Lidar, Atmospheric, and Viewing Conditions
- A Menu Driven "Front End" Simplifies Operation
- Code Implemented for the IBM PC Environment in "C" (Menu System) and FORTRAN 77 (Science Portion)
- Atmospheric Conditions are User-Defined Employing:
 - Built-in Aerosol and Atmospheric Models
 - User-Supplied Propogation Profile



OVERVIEW OF BACKSCAT (Cont.)

BACKSCAT Version 2.0



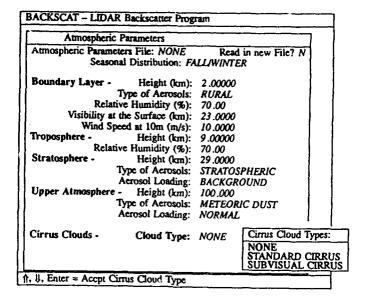


NEW FEATURES IN BACKSCAT VERSION 2.0

- Addition of Cirrus Clouds and Wind-Dependent Desert Aerosol Models
- Molecular Scattering Profiles Based On:
 - Built-in GL Model Atmospheres
 - User-Supplied Radiosonde Data
- Built-in "Quick View" Graphics Package
- All-New Menu Interface System
 - Easier to Use
 - Improved Error Checking

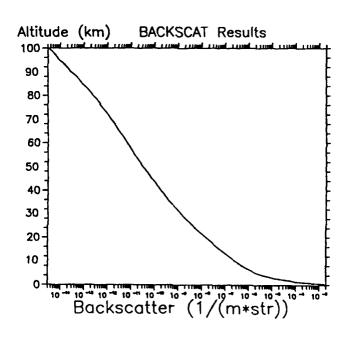


FEATURES OF BACKSCAT VERSION 2.0 (Cont.) - NEW MENU SYSTEM





FEATURES OF BACKSCAT VERSION 2.0 (Cont.) - "QUICKVIEW OPTION"





FEATURES OF BACKSCAT VERSION 2.0 (Cont.) - RADIOSONDE DATA ENTRY

	A	LTTTUDE (m)	PRESSURE (mb)	TEMPERATURE (C)	MOISTURE (RH(%))			
	1 2 3 4 5 6 7	79.00 110.00 555.00 585.00 1017.00 1091.00 1328.00	1003.50 1000.00 950.00 946.84 900.00 892.55 867.92	23.90 23.60 18.60 18.30 15.00 14.50 13.50	74.00 74.00 87.00 88.00 96.00 97.00 96.00			
10)	1498.00 1500.00 1582.00 1717.00	850.68 850.00 842.17 828.93	11.60 11.70 12.60 18.10	74.00 71.00 37.00 11.00			
Ctri-ENTER To ACCEPT DATA ESC from MAIN Menu ALTITUDE REFERENCE MSL UNITS: Alt $\rightarrow m$, P $\rightarrow mb$, T $\rightarrow C$, M $\rightarrow RH(\%)$								



SUMMARY AND RECOMMENDATIONS FOR FUTURE WORK

SUMMARY

- A New Version of BACKSCAT, a Backscatter Lidar Simulation System, is Now Available
- New Features Include:
 - Addition of Cirrus Clouds and Desert Aerosol Models
 - User Defined Molecular Scattering Absorption Profiles
 - New Menu Interface System

RECOMMENDATIONS FOR FUTURE WORK

- Addition of Water Cloud Models
- Compute Aerosol Profiles Based on Fundamental Parameters (ie. Aerosol Size Distributions, Indices of Refraction)
- Extension of Simulation Capability to Other Lidar Systems (ie. Raman, Doppler)

CIRRUS CLOUD TRANSMISSION MODELLING*

W.M. Cornette, J.G. Shanks
Photon Research Associates, Inc., 9393 Towne Centre Drive, Suite 200,
San Diego, CA 92121

The modelling of transmission through a cirrus cloud is of significant concern to a wide variety of users, including IRSTs and satellite systems. A model of cirrus transmission involves a combination of characterizations of cirrus cloud properties and radiative transfer. This presentation will summarize an assessment of current cirrus transmission models, with recommendations for potential upgrades and additions to the existing models. Also, several aspects for modelling transmission through cirrus clouds are applicable to transmission through optically thick atmospheric layers by modelling scattering in the forward direction as being no scattering at all, thereby producing a much more reasonable result.

*This work was funded by the Air Force Geophysics Laboratory under Contract No. F08606-87-C-0035; Dr. Donald Grantham, Technical Monitor.

CIRRUS CLOUD TRANSMISSION MODELING

JUNE 1991

Presented at the 14th Annual Review Conference on Atmospheric Transmission Models 11-12 June 1991, Geophysics Directorate, Phillips Laboratory, Hanscom AFB, MA

Work Funded in Part by the Air Force Geophysics Laboratory Under Contract No. F08606-87-C-0035; Dr. D. Grantham, Technical Monitor

Presented By:

Dr. William M. Cornette Dr. Joseph G. Shanks

PRAM

Photon Research Associates, Inc. 9393 Towne Centre Drive, Suite 200 San Diego, CA 92121



OUTLINE

- Objective
- Cirrus Characterization
 - Mesoscale
 - Microscale
- Radiative Transfer
- Models



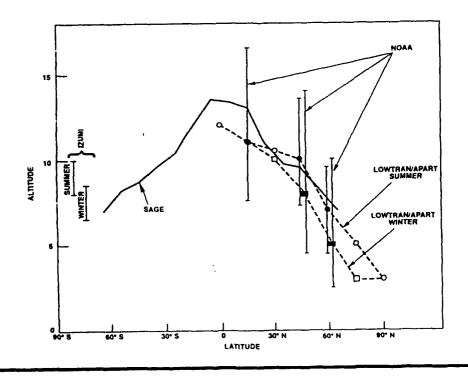
OBJECTIVE

To Assess the Current Capabilities in the Government, Contractor, and University Communities with Respect to the Present State of Technology in Cirrus Analysis and Attenuation Modeling.

- Cirrus (Ci)
- Cirrocumulus (Cc)
- Cirrostratus (Cs)
- Condensation Trails (Contrails)
- Nacreous (Stratospheric)
- Noctilucent (Mesospheric)



CIRRUS CLOUD ALTITUDES

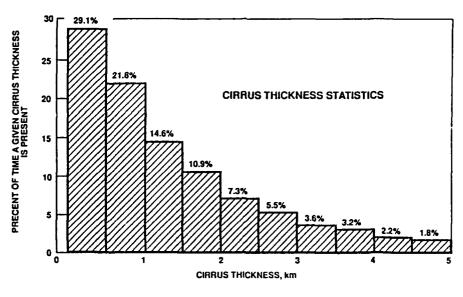


8 467 61 3



CIRRUS THICKNESS

• Median Thickness = 1.0 km

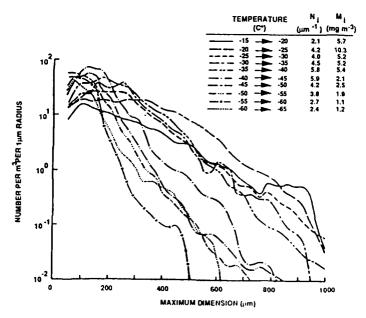


Source: Hall et al. (1984)



OBSERVED SIZE DISTRIBUTIONS

Lidar Measurements



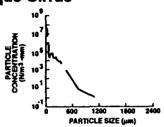
• Sassen, Starr and Uttal, 1989

. 067 81 5

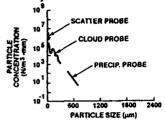


PARTICLE SIZE DISTRIBUTIONS

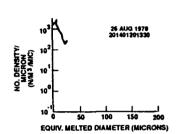
• Opaque Cirrus



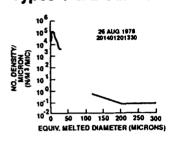
• Thin, Translucent Cirrus



• Type 1 Subvisual Cirrus



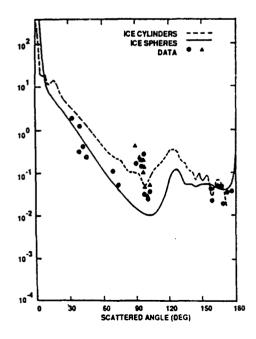
• Types 1 & 2 Subvisual Cirrus



• Barnes (1982)



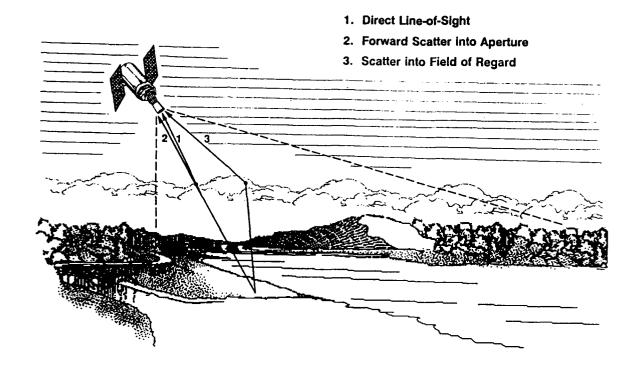
PHASE FUNCTIONS: OBSERVED



- Lyons and Schummers; 1984
- Platt and Dilley; 1984



FIRST-ORDER RADIATIVE TRANSFER





CIRRUS CLOUD MODELS

	RADIATIVE TRANSFER	PARTICLES	VERTICAL PROFILE	SIZE DISTRIBUTION
LOWTRAN	Beer's Law	Spherical	Uniform Layer	-
APART	Beer's Law and First Order Scattering	Spherical	Profile	-
SUBVIS	Beer's Law	Random Hexagonal	Uniform Layer	Temperature Dependent
Liou	Successive Order of Scattering	Random Hexagonal	Uniform Layer	Temperature Dependent
Rockwitz	Successive Order of Scattering	Oriented Hexagonal	-	-

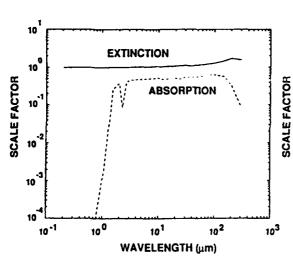


MODELS

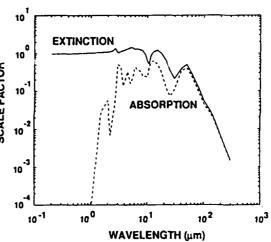
- "Comprehensive" Models
 - LOWTRAN 7
 - APART (Version 7.00)
 - SUBVIS and LOWTRAN
 - Liou
- "Element" Models
 - Pollack and Cuzzi
 - Liou, et al.
 - Rockwitz
 - Barnes
 - Hansen



LOWTRAN/APART CIRRUS MODEL



Standard



. 067 01 11

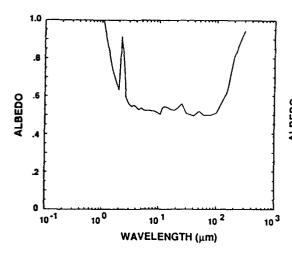
Subvisual

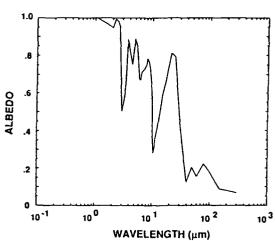


LOWTRAN/APART CIRRUS MODEL



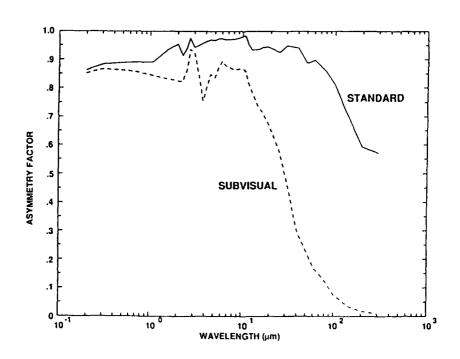
Subvisual





PRAM. Photon Research Associates, Inc.

LOWTRAN/APART CIRRUS MODEL



h 062 #1 17

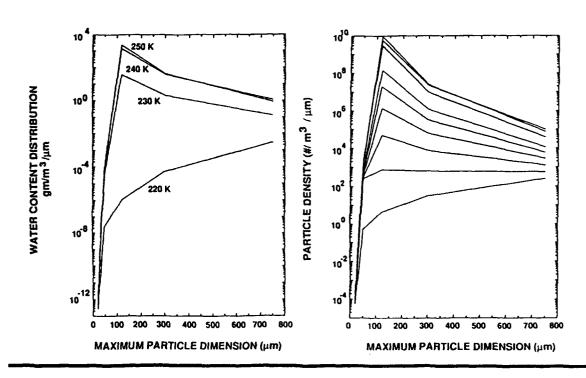


LOWTRAN/APART MODEL DEFICIENCIES

- LOWTRAN
 - Spherical Particles
 - Extinction Only
 - -- Multiple Scatter for Radiation Only, Not Transmittance
 - No Forward Scatter
 - Empirical Scaling Laws Not Based in Phenomenology
- APART
 - Same as LOWTRAN
- EXCEPT -
- Forward Scattering Correction Included for Single Scatter into Field-of-Regard and Aperture



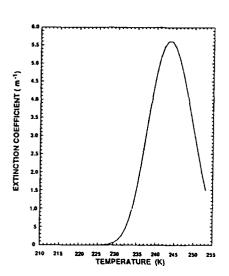
SUBVIS PARTICLE SIZE DISTRIBUTION





SUBVIS CIRRUS CLOUD

- 220, 230, 240, 250 K
- Geometrical Limit





SUBVIS MODEL DEFICIENCIES

- No Phase Functions

 Input to LOWTRAN

 No Multiple Scattering
- Limited Spectral Region (2.2 6.2 μm)
- Geometric Limit on Extinction
 - No Particles Less Than 20 μm Diameter
- Particles Randomly Oriented

8-067 81 17



CORRECTION FOR FORWARD SCATTER

• Replace

$$\sigma_{EXT} = K_{ABS} + \sigma_{SCAT}$$

with

$$\sigma_{EXT} = K_{ABS} + K\sigma_{SCAT}$$

Where g is Asymmetry Factor

• Sample Values of k

- Hansen (1 - g) ≈ 0.49 - Liou ≈ 0.83

- APART ≈ 0.82 - 0.84



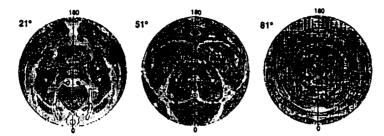
LIOU MODEL DEFICIENCIES

- Apparently Not Available
- Unknown Spectral Region
- Probable Geometric Limit
 - No Particles Less Than 20 μm Diameter
- Particles Randomly Oriented
- Unknown Term in Paper



SINGLE SCATTERING DIAGRAMS

• Upward Scattered Radiation



• Downward Scattered Radiation



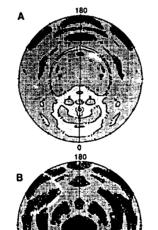


DUAL/TRIPLE SCATTERING DIAGRAMS

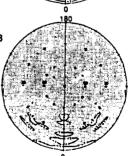
• Dual Scattered

Upward 45°

Downward 45°



В



• Triple Scattered

8 147 90 31

8-067-01-21

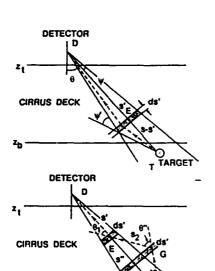


RECOMMENDATIONS

- Incorporate Capabilities into APART/MODTRAN
 - SUBVIS Cirrus Model
 - Forward Scatter Correction (MODTRAN)
 - Different Size Distributions
- Upgrade Capabilities
 - Empirical Phase Function
 - Oriented Particles
 - Small Particle Sizes
- Perform Sensitivity Study

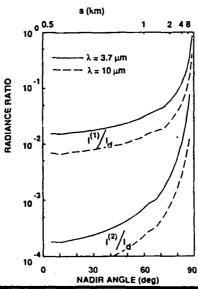


MULTIPLE SCATTERING (LIOU)



Sensor IFOV = 2°
Cloud Top 8.5 km
Cloud Thickness 0.5 km

Midlatitude Winter



ICE-CLOUD A MODEL FOR IR TRANSMITTANCE THROUGH CIRRUS CLOUD

W.T. Kreiss, R. Vik Horizons Technology, Inc., 3990 Ruffin Road, San Diego, CA 92123

ICECLOUD is a model for transmission of IR through cirrus clouds developed for the IASPM project. This task outlines the physical ideas on which the procedure is based. The model sets criteria for the occurrence of ice water and sets parameters defining the number, density and size distribution of the ice particles present. The ice particles are assumed to be hexagonal cylinders. Single particle optical scattering parameters appropriate to these particles (calculated using geometric optics) are used. The model represents transmission through dense cirrus clouds in a narrow region of the IR spectrum. The model can be improved, however, to broaden its applicability.

ICECLOUD

A MODEL FOR TRANSMITTANCE THROUGH CIRRUS CLOUD

BY

ROBERT C. VIK AND WILLIAM T. KREISS HORIZONS TECHNOLOGY, INC. 3990 RUFFIN ROAD SAN DIEGO, CA 92123-1826 (619) 292 8331

PRESENTED AT

THE ANNUAL REVIEW CONFERENCE ON ATMOSPHERIC MODELS
11-12 JUNE, 1991
GEOPHYSICS DIRECTORATE, PHILLIPS LABORATORY
SCIENCE CENTER, BUILDING 1106
HANSCOM AIR FORCE BASE
BEDFORD, MASSACHUSETTS 01731-5000

This work is being supported by the Tri-Services and the Department of Defense under the Defense Nuclear Agency Contract DNA001-90-C-0162.

CIRRUS CLOUDS CAN HAVE SIGNIFICANT EFFECTS ON LONGRANGE IR SENSOR PERFORMANCE

- o IADM/IRSTS FLIGHT TESTS
 - o ANOMALOUS DEGRADATION
 - SUBVISUAL CIRRUS POSSIBLE CAUSE
- o LIDAR/RADIOMETER TEST PROGRAM
 - O CHARACTERIZED CIRRUS AS AN IR ENVIRONMENT
 - o POINTED TO USE OF LOWTRAN7 CIRRUS MODELS
- CONCLUSIONS
 - o BACKGROUND RADIANCE IMPORTANT (AS WELL AS PATH TRANSMITTANCE)
 - o LOWTRAN7 MODELS ARE USEFUL, BUT:
 - o EMPLOY SPHERICAL PARTICLES
 - o PROVIDE OPTICAL DEPTH FROM GEOMETRICAL THICKNESS
- o REQUIREMENT FOR A BETTER CIRRUS MODEL FOR IASPM

REQUIREMENTS FOR A CIRRUS MODEL IN IASPM

- MUST INCLUDE SUBVISUAL CIRRUS
- o MUST TREAT NON-SPHERICAL ICE PARTICLES
- o OPTICAL DEPTHS MUST BE DETERMINED FROM OBSERVATIONAL DATA

EXISTING KNOWLEDGE

- OCCURANCE AND MICROPHYSICS OF CIRRUS CLOUDS (NCAR)
- 0 HEXAGONAL ICE PARTICLE OPTICAL PROPERTIES (UTAH)

"ICECLOUD" MODEL

- GOOD FOR THE TIME
- WE KNOW HOW TO BUILD A BETTER MODEL NOW

PROGRAM ICECLOUD c NCAR MODULES BY JOANNE PARRISH, NCAR, JULY 1986 UTAH MODULES BY LIOU AND TAKANO, LIOU AND ASSOCIATES, AUG 1988 С REAL TREP, ICE TREP and ICE are the average temperature (deg K) and ice-water density (Gm/M**3) in the ice cloud. INTEGER IBOT, ITOP, ML, ICL, MCL С С ER IBOT, ITOP, ML, ICL, NCL ML is the no. of LAYER's, and NCL is the no. in the cloud. ICL is the index of the first ice cloud LAYER. IBOT and ITOP are, respectively, the indices of the bottom and top LEVEL's of the ice cloud. ¢ c CHARACTER*64 INNAME, OUTNAM CHARACTER*72 TITLE PARAMETER (MAXP=1000, MAXL=34) IOS = 0OUTNAM = 'LOCARD' INNAME = 'MOD1.INP' OPEN(UNIT=1,FILE=INNAME,STATUS='OLD',IOSTAT=IOS) Unit 1 ^ is the input file С CALL READSND CLOSE(UNIT=1) CALL PROFILE(ICL, IBASE, CBASE, ITOP, CTOP) HL = 34 IF(ICL.NE.0) THEN PROFILE returns ICL = 1 if there is an ice cloud. CALL CLOUD(IBASE, IBOT, ITOP, TREP, ICE) END IF IF (ICL.NE.O .AND. ICE.GT.1.E-06) THEN CALL LAYERS(NL,IBOT,ITOP,ICL,NCL) CALL BEBA(TREP) ELSE CALL NOICE(HL) END IF CALL NEWCOM CALL ARISPH(ML, ICE, OUTNAM) STOP 1000 FORMAT (A64) END

Pigure 1. ICECLOUD main program

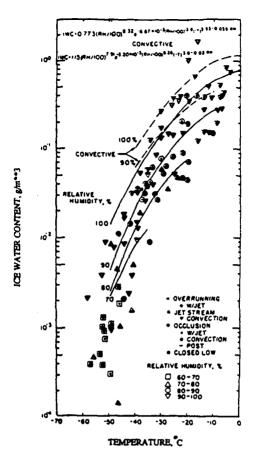


Figure 2. Cirrus cloud ice water content plotted against temperature and parameterized in terms of relative humidity according to convective regions. (Inside symbol: synoptic type; Outside symbol: relative humidity).

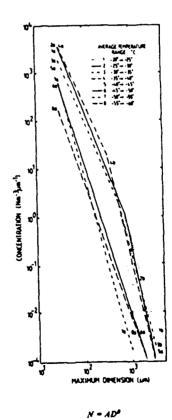
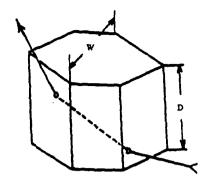


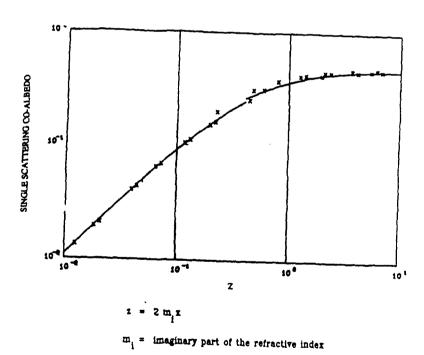
Figure 3. Curves fitted to the average spectra for each temperature range.



The extinction cross-section, averaged over look angles is:

$$C_e = 3/2 (W/2)^2 (43^2 + 4D/W)$$

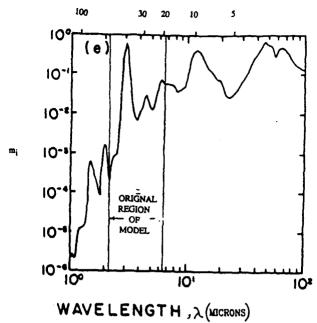
Figure 4. Definition of extinction cross-section.



x = size parameter:

 $z = \frac{2\pi}{\lambda} \frac{W}{2} \left(\frac{3\sqrt{3} D/W}{\sqrt{3} + 4D/W} \right)$

Figure 5. Single scattering co-albedo.



Ce is valid for larger x (smaller) a' forteriori

 $\widetilde{\omega}$ is derived from calculations in the region 0.4 < λ < 2.5 microns

Figure 6. Regions of validity of ICECLOUD.

"ICECLOUD" DEFICIENCIES

- o DOES NOT APPLY TO SUBVISUAL CIRRUS
- o APPLIES ONLY TO NARROW WAVELENGTH REGION
- o SINGLE LAYER TRANSMITTANCE ONLY
- o HIGH ALTITUDE WATER VAPOR MEASUREMENTS ARE DIFFICULT

ELECTO-OPTICAL MODEL FOR AERIAL TARGETING (EMAT) (SUCCESSOR TO IASPM)

EMAT MODEL NEEDS

- o BACKSCATTERING (BACKGROUND SCENES)
- o PATH TRANSMITTANCE
- o PATH RADIANCE
- o MUST APPLY TO THIN AND SUBVISUAL CIRRUS
- O CIRRUS CLIMATOLOGY/MORPHOLOGY
- o A "PRESCRIBED" MODEL (STATISTICAL
- o FULL WAVELENGTH COVERAGE

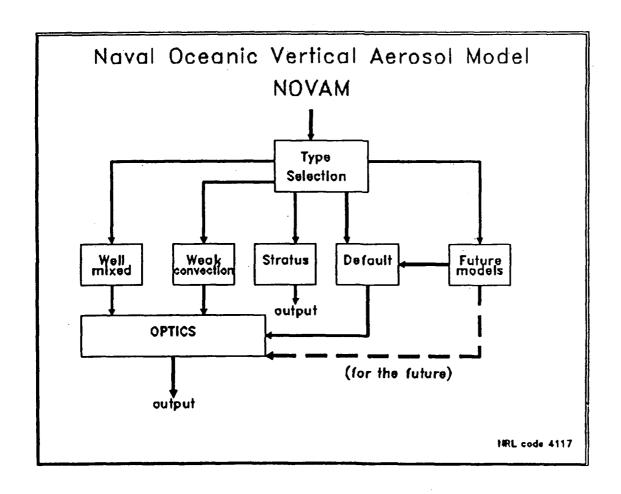
THE STATUS OF THE NAVY OCEANIC VERTICAL AEROSOL MODEL

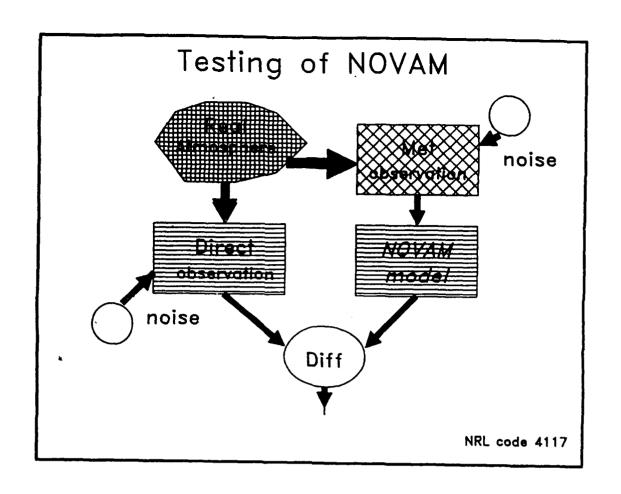
S. Gathman
Ocean and Atmospheric Sciences Division, Naval Ocean Systems Center,
San Diego, CA 92152

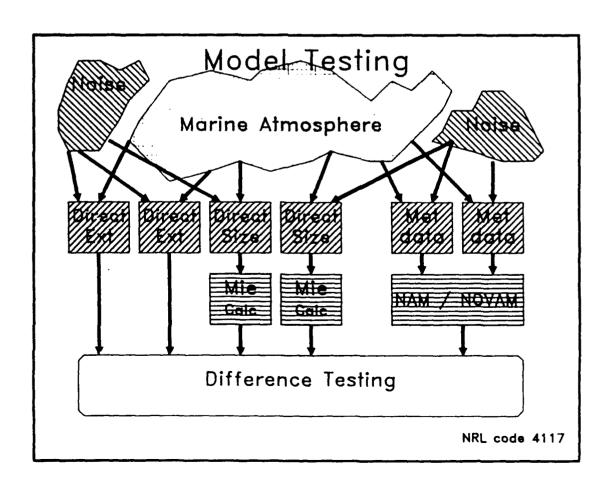
The Navy has been working on the development of a vertical aerosol model called NOVAM for several years. This model uses the navy aerosol model as a kernel for estimation of optical / IR properties of the atmosphere near the ocean surface and provides vertical structure of these properties specifically matched to oceanic conditions. The model utilizes surface meteorological data and radiosonde data as input. The model has been tested off of the California coast during the FIRE experiment and in the tropics during the KEY 90 experiment. This paper shows some of the results of these tests where predicted extinction profiles are plotted along side of measured extinction profiles.

The Status of the Navy Oceanic Vertical Aerosol Model

Stuart G. Gathman NOSC code 543 San Diego, CA







NOVAM Testing



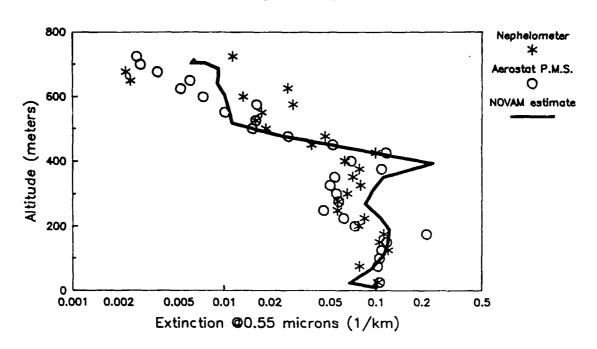
NRL code 4117

Testing Experiments Field tests of NOVAM

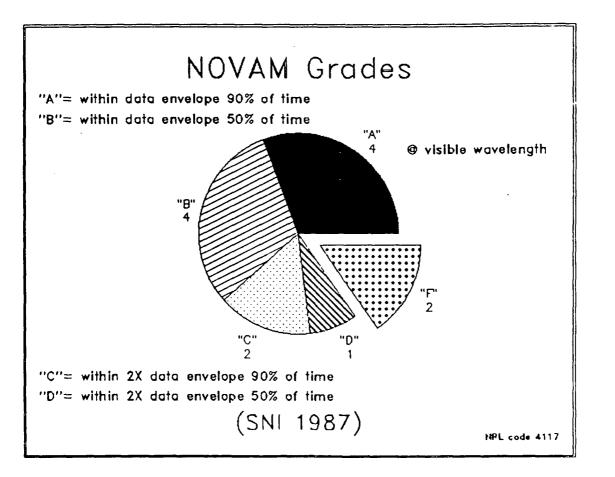
- FIRE experiment at San Nicolas Island, CA. 1987
 Tethered Aerostat Balloon
 NOSC Navajo aircraft
 NPS on the ship, Point Sur
- KEY-90 experiment Marathon Florida, 1990
 Fishing boat for surface data
 NOSC Navajo aircraft
 NRL P-3A aircraft with LIDAR
 Shore base LIDAR
- East Coast Experiment plans for 91/92
 Cooperation with IRAMMP, Summer 91
 Cooperation with ONR/NRL ATI, FALL 91/92

NOSC code 543

Aerostat Measurements SNI-87 (flight 1814)



NRI code 4117

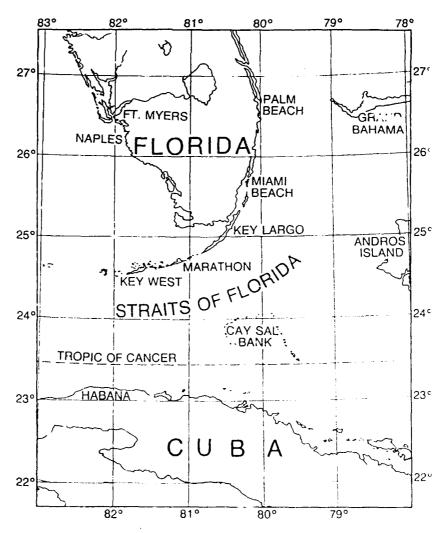


KEY-90 - Verification of NOVAM in a "tropic like" environment

MEASURED EXTINCTION PROFILE

- Measured profile of Aerosol size distribution (Extinction calculated from Mie theory)
 NOSC aircraft with PMS probes
- Surface Aerosol size distribution
 Boat: UMIST PMS probe + TNO rotorod.
 (Extinction calculated from Mie theory)
- Surface extinction @ 3-5 and 8-12 bands Boat: PVM instrument.
- Downward looking lidar using aureole measurement.
 NRL P3 aircraft.
- TNO's lidar using the Kunz calibration. Shore based measurement.

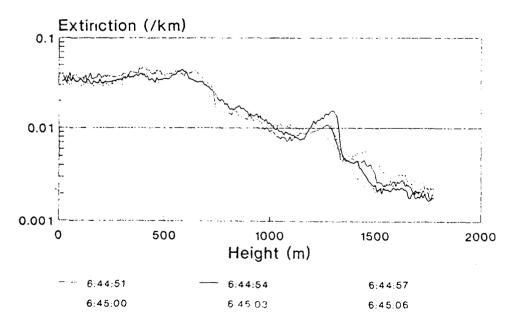
NRL code 4117



KEY - 90

		E	κрε	eri	m	en	ł C	a _V	's,		Jul	У	19	90)		
veriable	Instrument	23		5 6						12	13	14	ŀ	16	17	18	19
tatr	Teather pak	•••	ſ	•	•	1	•			٠	•	•		•	•	•	•
utair	UMST Ophir device			•	•1•	1	•	•	•	•	•	•	Ì		•	•	ldot
tmendry	Sling Psycrometer	10		•]	•	۰	•	•	•	•		lacksquare	•	•	⊡
bucket	Precision therm.	•		•	• [•	Ì	lacksquare	٠		•	٠	•	ŀ	led	٠	•	Ð
est	Boet's thorm.			•	1)		•	٩	•	•	•		•	۰	•	•
rh.	Weather pak	• •		•	1		•			٠	•	•		lee	•	•	•
	UMST Ophir device			•	• •	1	•	٠	٠	۰	٠	•		•	٠	٠	$oldsymbol{\cdot}$
chum	Capacitor device			\perp	L			٠	•	•	•	•		٠	•	•	ᆜ
	Sling Paycrometer	199	L	<u>•</u>		l	•	•	•	•	٠	•		Ŀ	•	٠	•
	NELTO bireans	1		•	_	l	•	•	•	•	•	•		٠	•	٠	\mathbf{L}
	Weather pak	100		•		!	•			•	•	•		\cdot	٠	•	ᆜ
	UMIST Sonic	Ш	L	1	-	1	╚	•	•	\cdot	•	\cdot		브	•	•	dot
	Hand held device	199	-	4	_		•	•	٠	•	٠	•		•	•	•	-
	NEED bivene	100		• •	_		•	٠	٠	•	•	٠		•	•	•	-
	Weather pak	199	L	•			٠	Щ		۰	۰	٠		•	•	٠	
	NEL's compass		L	-			•	•	٠	•	•	•		•	•	•	
	Weather pak		L	_			•	Н	Ш	•	-	•		÷	•	÷	\vdots
	Weather pak		L	#	+	1	H			÷	÷	H			$\dot{\cdot}$	÷	\exists
	Precision barometer Environment 1		ı ı	+	-	ł	H	÷	-	÷	÷	÷	١.,	H	÷	÷	\exists
_		1.:			;	l	H	÷	÷	÷	$\ddot{\cdot}$	H		\vdash	$\dot{-}$	÷	H
hesi		111		+	-		H	\div	-	$\ddot{\cdot}$	÷	÷		Н	_	_	Н
	HSS visibility meter Gerber Scientific	1	L	#			÷	÷	÷	$\ddot{\cdot}$	÷	÷		\vdash		-	\vdash
	NRL's redon counter	1	ŀ	#		1	÷	÷	÷	H	÷	H		-	•	•	
I wood	TNO rotorods		ŀ	-	-	1	-	÷	÷	÷	÷	-		H	•	÷	
	UMIST FSSP	1		:	1	l	÷	÷	÷	÷	÷	÷		H	·	÷	1
estolor	MOSC Aircraft.	1.1.	L	: 1	_	ı	H	÷	•		÷	·		H	•	-	
	NPS radiosonde	HH	ŀ	+	+	l	•	•	•	÷	•	•		÷	٠	•	-
	NRL Aircraft	HH	· }	+	╁╴		•	\vdash	÷	٠	•	-		Н	Н		H
ł	INO's Lider	1.1	· •	1	٠.	1	•		•	•	•	•			•	•	\dashv
	Sun Photometer	1.	ŀ	٦,		ı	-		Н		-			•		•	\vdash
	Yave Spectra	H	ŀ	╅	+	1			Н	\vdash	\vdash	-		H			Н
	Key West Met. Data	HH	·	+	✝	1	H	Н	Н		\vdash	-		H			Н
	and area one name	ليليا	· t			•		لب		لــا		نـــا			-	_	

Extinction Profiles (for NRL lidar)



7/14/90;shots:726-730;24⁰38¹N,80⁶58¹W

Session 2

Summary of the Session on Atmospheric Propagation Models

The status of atmospheric propagation models is steadily improving. Problems that once appeared intractable are now being implemented on PCs. LOWTRAN has become a triservice/industrial standard that is now commercially available. Other codes are also following suit. The increased resolution of new codes has allowed for examination of different problem areas. In particular, Non-LTE and other upper atmospheric problems are now being considered. This has brought attention to the altitude mismatch in results between various codes that work in the lower atmosphere and those which have been designed to operate in the upper atmosphere. This problem is being worked and should be resolved in the near future.

Comments on specific presentations:

MODTRAN/LOWTRAN: CURRENT STATUS, FUTURE PLANS Presented by L. Abreu

MODTRAN compares well with SHARC. Favorable comparisons have also been done with LOWTRAN7 and FASCOD3. Improvements in MODTRAN will be in the area of radiative transfer (multiple scattering algorithms). World wide model atmospheres will be added, and the code will be made more modular. MODTRAN and APART will be integrated for work on spectral backgrounds.

FASCODE3: An Update Presented by G. Anderson

The history of FASCODE development was presented. Currently FASCODE is trying to produce "exact" results in an optimized fashion (e.g. mathematical line shape, layer selection, etc.). Improvements underway currently consist of improving the portability, radiance algorithm, cross-sections, HITRAN capability, and dealing with non-local thermodynamic equilibrium (NLTE) and transitions from LTE to NLTE. Finally FASCODE3 has not been released because too many corrections/additions were needed.

EOSAEL 92 Presented by A. Wetmore

The 1992 version of the Electro-Optical Systems Atmospheric Effects Library (EOSAEL) will leave unchanged the following modules: NMMW, CLTRAN, COPTER, GRNADE, MPLUME, OVRCST, FCLOUD, ILUMA, FASCAT, LASS, GSCAT, NOVAE, and RADAR. The following modules will be upgraded: LOWTRN, LZTRAN, KWIK, XSCALE, TARGAC, COMBIC. The SABRE and MSCAT modules will be dropped. Four new modules will be added: BITS - to be used for broad-band integrated transmittance; FASCODE - GD's model; NBMSCATT - a radiative transfer approximation; and UVTRANS - a UV transmission, fluorescence, and lidar program. The various modules are also being made interactive.

HITRAN '91: The Contemporary Spectroscopic Molecular Database Presented by L. Rothman

Major molecular parameter updates have been done for H₂0, CO₂, O₃, methane, CO, NO, NO₂, HNO₃, and the hydrogen halides (HCl, HF, HI, HB). There have been minor changes in the trace gases (H₂O₂, C₂H₂, HCH₆, SF₆) and COF₂ is being added. Provisions are also being made to convert HITRAN to run on a PC.

SHARC, An Atmospheric Radiation and Transmittance Code for Altitudes from 50 to 300 km Presented by D. Robertson

SHARC was initially developed for SDIO for modeling radiance in the upper atmosphere. SHARC will handle Non-LTE conditions found in the upper atmosphere (50 - 300 km) in either ambient or auroral conditions. Current resolution is .5 inverse centimeters at wavelengths from 2 to 40 microns. A manual is currently being printed and will be available shortly.

Recent Development of the GENLN2 line-by-line model: studies in support of the UARS project Presented by D. Edwards

GENLN2 is a line-by-line Non-LTE atmospheric transmittance and radiance code. It contains six GD model atmospheres, is modular, and will produce plots using NCAR graphics. Comparisons with ATMOS have been favorable, with reasonably good transmission over a variable spectral grid.

Present status of Transmittances and Radiances Modeling at L.M.D. Presented by N. A. Scott

L.M.D. is investigating the impact of high resolution measurements for/on signatures. The fast-running, versatile codes compute transmittance and/or radiance for a variety of conditions.

AURIC (Atmospheric Ultraviolet Radiance Integrated Code): An Update Presented by R. Huguenin

AURIC is being developed as an atmospheric UV spectral transmission and solar irradiance code. MODTRAN is the starting point; AURIC's structure will try to stay with MODTRAN's. The initial release will not include airglow, will have a resolution of 1 wavenumber with interpolation to .5 wavenumber. Optimum methods are being employed, particularly in the temperature dependent model, in order to have the code run faster.

ONTAR's PC Compatible LOWTRAN7 Package Presented by J. Schroeder

ONTAR entered into a cooperative R & D agreement with GP in 1988. Since then, ONTAR has released various versions of GP's LOWTRAN code. The most recent version, release 3.8, has the full LOWTRAN7 implemented. Online help is available with this interactive version of LOWTRAN as are plotting routines which include overlays for different runs.

ONTAR's LOWTRAN7 has been certified by GP and runs in 640K on a PC with no memory extender required: however, a coprocessor is recommended.

Coupling Atmospheric and Background Effect Presented by W. Cornette

The development of a computer model to determine thermal clutter in a scene with changing atmospheric conditions was described. The model is sensitive to solar radiation and includes numerous terrain materials for background effects. Terrain scenes and several cloud models at varying altitudes are included.

SENTRAN7: A Sensitivity Analysis Package for LOWTRAN7/MODTRAN Presented by D. Longtin

SENTRAN7 was described as a user active analysis code designed to perturb various input parameters of LOWTRAN7 or MODTRAN. Graphical outputs are created in 2D and 3D formats. The code is currently designed to operate on VAX/VMS and SUN Unix systems. A complete description of the user input commands and the graphical requirements required was presented.

Atmospheric Models in the Strategic Scene Generation Model Presented by W. Cornette

The Strategic Scene Generation Model was described in detail with special emphasis on the atmospheric propagation models currently implemented in the code. The background scene modules APART, GENESIS and CLDSIM were described with 2D simulations of terrain and cloud scenes. Simulations on varying resolution of transmittance, calculations were shown and some subtle differences between MODTRAN and APART were explained.

Review of the Chemical Kinetic Rate Constants Used in the SHARC Model Presented by A. Pritt

As the title indicates, this was a comprehensive review of the chemical kinetic rate constants being used in the SHARC model. A basic explanation of SHARC and NLTE conditions was given, along with an explanation of the derivation of H₂0 and CO rate constants. The presenter showed numerous comparisons between SHARC and a large and impressive series of measurements.

MODTRAN/LOWTRAN: CURRENT STATUS, FUTURE PLANS

L.W. Abreu, F.X. Kneizys, G.P. Anderson, J.H. Chetwynd Geophysics Directorate, Simulation Branch (OPS), Hanscom Air Force Base, MA 01731-5000

MODTRAN (public release: November 1990) is a 2 parameter (P&T) band model code with moderate spectral resolution (2 cm⁻¹ full width-half maximum). The MODTRAN band model parameters were calculated by utilizing the HITRAN-86 data base. The code is fully compatible with LOWTRAN 7 and the results can be degraded to between 2 and 50 wavenumber spectral resolution.

Future plans include an improved more accurate multiple scattering algorithm as well as a realistic modelling of the atmosphere-to-background-to-atmosphere coupling technique. A definitive set of worldwide model atmospheres is presently under development.

MODIRAN/LOWIRAN: CURRENT STATUS, FUTURE PLANS

L.W. ABREU, F.X. KNEIZYS, G.P. ANDERSON and J.H. CHETWYND

ANNUAL REVIEW CONFERENCE ON ATMOSPHERIC TRANSMISSION MODELS

11-12 JUNE 1991

GEOPHYSICS DIRECTORATE PHILLIPS LABORATORY

SOFTWARE DESCRIPTION FOR ATMOSPHERIC PROPAGATION MODELS AND DATA BASE: FASCODE, MODTRAN, LOWTRAN, HITRAN

o Common Elements:

Transmittance and Radiance Geometry, thermal multiple scattering Default amospheric profiles (molecular, aerosol, particulates) Spectral range: 0 to 50,000 cm⁻¹ (0.2µm to 2) Interpolation, Scanning, and Filter Functions

o FASCODE (FASCOD2-1986; FASCOD3-1990)

Resolution: Line-by-line (high)
Physics:
Altitude Range:
Applications: High resolution simulations
(LTE, NUTE, Laser, Lidar)
Slow (or large spectral ranges:
Requires external database (HITRAN)
Requires NUTE specifications
Recognized litternational Standard

o MODTRAN (1990)

Resolution: Physics: Altitude Range: Applications: Comments:

2 cm⁻¹ (moderate)
2-parameter band model (P and T)
60 km
Moderate resolution simulations,
solar (direct and scattered)
Moderate time consumption
No NLTE
Spectral database stored in 1 cm⁻¹ bins

o LOWTRAN (1989)

Resolution: Physics: Altitude Range: Applications: Comments:

20 cm⁻¹ (low)
1-parameter band model (P)
0 to 50 km (limited by band model)
Broad band spectral simulations
Solar (direct and scattered)
Efficient (no time penalty)
Loss of small scale spectral character
Recognized International Standard

o HITRAN (HITRAN86-1987, HITRAN90-1990)

Resolution: Physics:

Applications

Infinite
Complete spectroscopic parameters for
over 350,000 transitions for
28 separate molecular species
Molecular cross sections for 9
additional species.
Source data for high resolution line byline synthesis of molecular
adsorption properties
Used directly by FASCOBE
Source of derivative bond molecular.
MCOTRAN and LOWTEAN
Recognized International Standard

THE LUWIRAN MUDEL

ATMOSPHERIC TRANSMITTANCE/BACKGROUND RADIANCE
- 20 CM-1 RESOLUTION

33 LAYER ATMOSPHERIC MODEL

- CHOICE OF MODEL ATMOSPHERES, AEROSOL MODELS
- USER DEFINED

GEOMETRY FOR ANY SLANT PATH

- LOOKING UP/DOWN
- TANGENT HEIGHTS
- HORIZONTAL PATHS

PRODUCT TRANSMITTANCE DUE TO

- MOLECULAR ABSORPTION (BAND MODEL)
- MOLECULAR SCATTERING
- AEROSOL EXTINCTION
- CONTINUUM ABSORPTION

THERMAL EQUILIBRIUM IN EACH ATMOSPHERIC LAYER

LOWTRAN?

AB SOR3 ER	SPECTRAL RANGE (CH ⁻¹)				
Water Vapor (H ₂ O)	0-17860				
Ozone (0 ₃)	0- 200, 515-1275, 1630-2295, 2679-3260, 13000-24200, 27500-50000				
Uniformly Mixed Gases.					
Methane (CH ₄)	1065- 1775, 2345- 3230, 4110- 4690, 5865- 6135				
Nitrous Oxide (N ₂ O)	0- 120, 490- 775, 865- 995, 1065- 1385, 1545- 2040, 2090- 2655, 2705- 2865, 3245- 3925, 4260- 4470, 4540- 4785, 4910- 5165				
0xygen (0 ₂)	0- 265, 7650-8080, 9235-9490, 12850-13220, 14300-14600, 15695-15955				
Carbon Monoxide (CO)	0- 175, 1940- 2285, 4040- 4370				
Carbon Dioxide (CO ₂)	425-1440, 1805-2855, 3070-4065, 4530-5380, 5905-7025, 7395-7785, 8030-8335, 9340-9670				

LOWTRAN?

AR	Sn	22	ER	

SPECTRAL RANGE (CH-1)

Trace Gases:			
Nitric Oxide (NO)	1700- 2005		
Nitrogen Dioxide (NO ₂)	580- 925,	1515- 1695,	2800- 2970
Ammonia (NH ₃)	0- 2150		
Sulphur Dioxide (SO ₂)	0- 185, 2415- 2580	400- 650,	950-1460,

LONTRAN 7 BAND MODEL

TRANSMITTANCE FUNCTIONS

$$T = EXP C - (CW)^{a} \exists$$

$$W = (P/P_{o})^{n} \times (T_{o}/T)^{m} \times U$$

where:

a, n, m are BAND MODEL PARAMETERS

U = ABSORBER AMOUNT

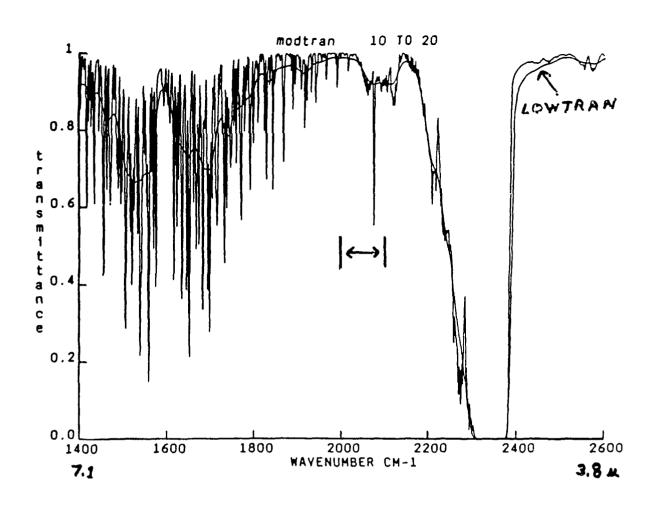
C = BAND MODEL ABSORPTION COEFFICIENT

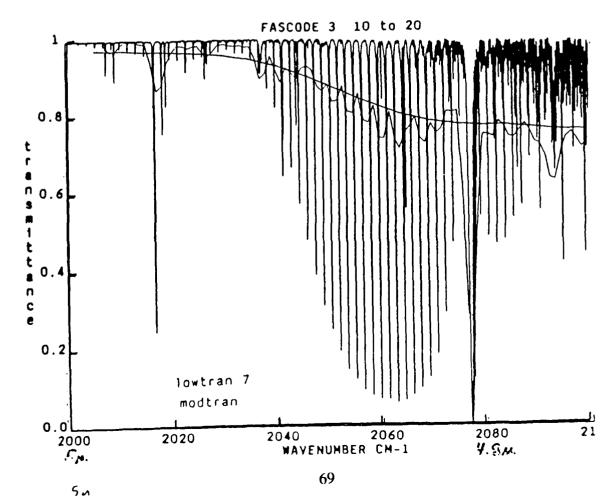
MODTRAN: Specific Attributes

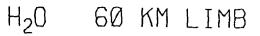
- * Moderate Spectral Resolution 2 cm⁻¹ (FWHM)
- * 2 Parameter Band Model (P,T) $1~{\rm cm}^{-1} \quad {\rm Bins~Stored~On~Tape}$ Calculated From 1986 HI/RAN Data Base (0 17900 ${\rm cm}^{-1}$)
- * Internal Triangular Slit Function
 Begradable To Desired Spectral Resolution
- * Atmospheric Molecules :

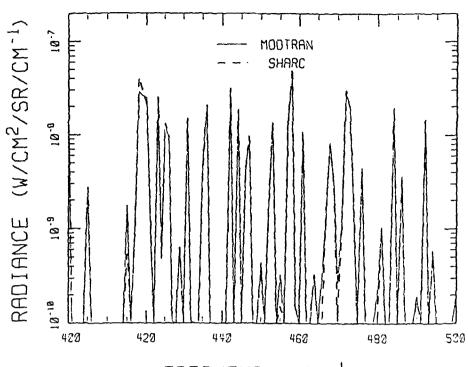
EXPANDED APPLICABILITY

- * MODTRAN IS BETTER SUITED THAN LOWTRAN FOR ATMOSPHERIC PATHS ABOVE 30 KM
 - Band Model Parameters Are Both Temperature and Pressure Dependent
 - Transmittance Is Modeled With A Voigt Lineshape
- * HOWEVER, MODTRAN STILL ASSUMES LOCAL THERMODYNAMIC EQUILIBRIUM

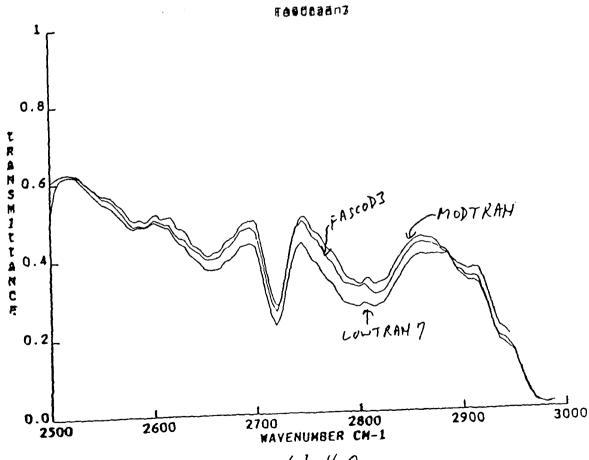








FREQUENCY (CM-1)



Ruge 1km at SFC 20 2 m/m3 H2O

GL ATMOSPHERIC PROPAGATION MODELS

GENERAL	PROPERTIES	FASCODE	MODTRAN	LOWTRAN
SPECT	TRAL RESOLUTION			
	HIGH MODERATE LOW	x x x	x x	x
CAPAE	BILITIES			
	TRANSMITTANCE	x	x	x
	BACKGROUND RADIANCE			
	THERMAL SOLAR/LUNAR	х	X X	X X
	NON-LTE	X	Λ	^

SPECIFIC AFPLICATIONS	FASCODE	MODIRAN	LOWTRAN
LASER PROPAGATION	X		
PLUME SIGNATURES	X	X	
TARGET CONTRAST	x	x	X
REMOTE SENSING	x	X	x

FUTURE PLANS

- * IMPROVED MULTIPLE SCATTERING ALGORITHM BASED OF THE DISCRETE-ORDINATE-METHOD
- * WORLD-WIDE DATA BASE OF MODEL ATMOSPHERES
- MODULARIZATION OF CODES
- * INTEGRATION OF MODIFAN AND APART
- * SPECTRALLY DEPENDENT BACKGROUNDS
- * IMPROVED GEOMETRY ROUTINES FOR 32 BIT MACHINES

DOD POINT OF CONTACT FOR LOWTRAN 7 AND MODTRAN IS:

LEONARD W. ABREU GL/OPS(AFSC) HANSCOM AFB, MA 01731 (617) 377-2337 Autovon 478

DOD POINT OF CONTACT FOR FASCOD3 IS:

GAIL P. ANDERSON GL/OPS(AFSC) HANSCOM AFB, MA 01731 (617) 377-2335 Autovon 478

NOTE: DOD Contractors, please have your contract monitor make the request.

The codes are publicly available through:

National Climatic Data Center, NOAA Environmental Data Services Federal Building Acheville, NC 28801

FASCOD3: AN UPDATE

G.P. Anderson, F.X. Kneizys, J.H. Chetwynd, L.W. Abreu, M.L. Hoke Geophysics Directorate, Hanscom Air Force Base, MA 01731-5000

S.A. Clough, R.D. Worsham Atmospheric and Environmental Research, Inc., 840 Memorial Drive, Cambridge, MA 02139

> E.P. Shettle Naval Research Laboratory, Code 6522, Washington, DC 20375

FASCOD3, a line-by-line atmospheric radiance-transmittance code, is currently available in a beta-test version. As with FASCOD2, the program is applicable to spectral regions from the microwave to the middle ultraviolet, employing standard spectroscopic parameters supplied from external line atlases. New FASCOD3 capabilities include: multiple scattering of thermal radiation, CO₂ and O₂ temperature-dependent line coupling for selected bands, UV diffuse absorption (0₂ and 0₃), improved weighting functions, enhanced non-local thermodynamic equilibrium (NLTE) calculations, and, perhaps most importantly, compatibility with the HITRAN91 database, including temperature-dependent cross sections. NLTE input requirements include LTE temperature and density profiles plus adequate descriptions of the NLTE population profiles for the specified excited vibrational states. Auxiliary NLTE line positions, halfwidths, strengths and vibrational-rotational assignments must also be provided.

FASCOD3: An Update

G.P. Anderson, F.X. Kneizys, J.H. Chetwynd, L.W. Abreu, M.L. Hoke (Geophysics Lab (AFSC))

S.A. Clough, R.D. Worsham (Atmospheric and Environmental Research, Inc.)

E.P. Shettle (Naval Research Laboratory)

Presented at the:

Annual Review Conference on Atmospheric Transmission Models 11-12 June 1991

FASCODE: Fast Atmospheric Signature Code

Version $3 - \beta$

AFGL: F.X. Kneizys | - Primary | S.A. Clough¹ |

G.P.Anderson - UV, Constituent Profiles

J.H. Chetwynd - Programming, Validation

L.W. Abreu - LOWTRAN7 Compatibility

W.O. Gallery¹ - Geometry

LS. Rothman - Line Atlas

M.L. Hoke - Line Coupling

E.P. Shettle² - Aerosols/Hydrometcors

R.D. Worsham³ - X-sections, etc.

¹ currently at Atmospheric and Environmental Research, Inc.

² currently at Naval Research Laboratory

³ at Atmospheric and Environmental Research, Inc.

Some thoughts on FASCOD3 presentation:

1 June 1991

- 1. Authorship 2. History/Contractor Support
- 3. FASCOD2/FASCOD3 in 1990 "The Way We Were"
- 4. Delays in FSC3 release why?

FASCODE: Fast Atmospheric Signature Code

Version 2 and Version 3-β

Visidyne:	H.J.P. Smith	- contributions to FASCOD1C (1978)
Visitylic.	11.J.L. SHILLI	· continuations to 1 ASCODIC (1970)

D.J. Dube M.E. Gardner

T.C. Degges - NLTE theory (1977, 1985)

Sonicraft: W.L. Ridgway - contributions to FASCOD2 (1985)

R.A. Moose A.C. Cogley

AER, Inc.: R.G. Isaacs - multiple scattering (1987)

R.D. Worsham - programming contributions to FASCOD3 & MS (1988-91)

S.A. Clough - radiance algorithm, etc. (1990-1991)

FASCODE2/3: Fast Atmospheric Signature Code

Introduction: (or "Just what is so difficult anyway?" and "Why bother?")

o Line-by-Line Radiance/Transmittance Model which attempts:

to provide "exact" solution to radiative transfer problem -

Beer's Law $[T = \exp(-a(i) \cdot N(i))]$

Planck Function [B=fn(T)]

Radiance Eqn [R=BdT]

to optimize mathematics for rapid solution

to account for realistic atmospheric lines-of-sight (not including non-linear "seeing")

to maintain "state-of-the-art" spectroscopy

to unify physical description for all frequencies

to accommodate intrument design characteristics

o Limiting Considerations

Spectral sampling - governed by "true" line shape

Atmospheric layering - governed by Curtis-Godson approximation

Computer allocations - historic

o Solutions (?)

Optimize:

line shape per layer layer selection merging of adjacent layers

Provide "all" default options (realistic)

Maintain LOWTRAN compatibility for all non-molecular parameters

Support user-friendly I/O:

documentation, distribution, maintenance user services

FASCODE2/3: Fast Atmospheric Signature Code

Basic Input/Output:

o INPUT

Mode

- optical depth
- transmittance
- radiance

Spectroscopic variables for line-by-line calculations

- external data bases (HITRAN86, NLTE, coupling coef.)
 [driven by LNFL routines for FASCOD3;
 BCDMRG routines for FASCOD2]
- internal block data (mm with coupling coef.)
- line shape including far wings and continua

Spectral range and sampling

- 500 cm⁻¹ limit
- "buffering" at boundaries
- monochromatic option (laser)
- "natural" frequency spacing dv = 4 pts/halfwidth
- "instrumental" frequency spacing scanning and filter options

Line-of-sight/geometry

- horizotal
- H1 to H2 $(-/+90^{\circ})$
- tangent
- layering (boundaries and/or selection criteria)

Path characterization

- pressure, temperature
- constituent (trace) profiles
- hydrometeor profiles (clouds, rain, fog)
- particulate profiles (aerosols, dust, etc.)

FASCODE2/3: Fast Atmospheric Signature Code

Basic Input/Output:

o OUTPUT

Echo all input parameters

Path description

- layer selection
 pressure, temperature
 atmospheric constituent profiles*
 aerosol/hydrometeor profiles
 line shape, halfwidth
- geometry

 path type
 bending
 integrated amounts (layer, total)
 particulate absorption (layer, total)

Spectroscopic

- number of lines/species
- layer specific

v₁, v₂, dv(natural)

optical depth, transmittance, radiance

- total path

(same)

- scanned

dv(scan), type (triangular, rectangular, etc.)

- filtered

v₁, v₂, shape

- plotted (all of above)

- layer boundary info: T/p(l), T/p(l-1), etc.

FASCOD3: Fast Atmospheric Signature Code

Version 3

Generic Capabilities:

- o Line-by-line molecular spectroscopy including line coupling
- o Uniform physical definitions (0-50000cm-1)
- o Full geometric path flexibility, 0-120 + km, all lines of sight with spherical refraction
- o Access to arbitrary databases (HITRAN91/86, NLTE, etc.)
- o Voigt line shape at all altitudes and/or pressures
- o Mathematical optimization for layering and spectral sampling algorithms
- o Default or user-supplied atmospheric profiles, p, T, and mixing ratios for 28 constituents
- o Absorption x-section implementation from HITRAN86/90
- o Additional default & user specifications for 10 green-house gases
- Default or user-supplied aerosol and hydrometeor profiles; full LOWTRAN7 compatibility
- o Laser (monochromatic) options
- Non-local thermodynamic equilibrium; NLTE populations must be provided from outside source (i.e. Degges, SHARC, AARC, etc.)
- o Weighting functions, merge options, ground reflection
- o Thermal multiple scattering, layer fluxes
- o Standard "user" options (plot, scan, filter, etc)

4. Delays in FSC3 release - why?

90/91 SCIENCE:

	i.	improved radiance algorithms:
		Tbar(1) replaced by weighted $(T(b)+T(b+1))$
		[non-compatible with m.s. algorithm??]
		Default "fine" layer at observer
	ü.	x-sections including:
		p-broadening, T-dependence,
		default profiles from M. Allen, 1990
	iii.	"linear" Planck function interpolation
	iv.	HITRAN91 compatibility:
		Line coupling and cross sections
	v.	TIPS: Total Internal Partition Sum
		from Gamache & Rothman, with FSC3 extrap.
	vi.	isotopic implementation
	vii.	revised NLTE coding,
		including efficient 4th function
	viii.	dayside NLTE populations from SHARC (Sharma
		and Robertson), ARC (Wintersteinner &
		Picard), and HAIRM (Degges) (composite)
	iix.	nightside NLTE populations being explored
•	ix.	H2O continuum extrapolation altered in near IR
		(based on measurements at 1.06 microns)
	x.	new defaults:
		simple CO2 mixing ratio modification:
		330ppmv can be replaced with single option
		default alpha(0) adjust, for line coupling:
		0.04cm-1 instead of 0.08 at 1 atm STP
		default line rejection values:
		fraction of Optical Depth & Continuum
	xi.	possible inclusion of GL/NRL Constituent
		Climatologies (CIRA-based)
		,
	00 /01 (20	NINE ENTER A NICEN PENERS.
	90/91 CC	DDE ENHANCEMENTS:
	<u>i</u> .	scanning/interpolation upgrades:
	ь	SINC, SINC**2, fixed sampling
		FTS simulations/functions (Gallery)
	ii.	much improved "weighting function" options:
	и,	renamed "sequential" transmittance/radiance
		reduced storage requirements, E/O systems
		compatibility
	iii.	improved efficient 4th function sampling
	iv.	corrected FASLOW compatibility (layering)
	14.	LO improvements. ASCII/bings. options

90/91 OTHER:

portability!!

v.

vi.

i. future directions -? (let's get there first!)

I/O improvements: ASCII/binary options

NCAR/IDL Graphics

UNIX, IBM, CRAY(?), Workstation, Apollo, etc.

SPECIAL OPTIONS:

o Thermal multiple scattering - (Radiance ONLY)

encouraged for long slant paths at moderate to high
pressure (i.e. below 15km) in the presence of
scatterers (aerosols and/or clouds)
10-20% effect in IR
activated by IMS=1
directionally dependent
increases total radiance when looking down
decreases " " " up
strong function of viewing angle
function of scattering opacity vs total opacity
** increases FASCOD3 runtime by at least a factor of 2-3
modularized coding (if IMS=0, normal FASCOD3
execution occurs)
new input parameters - surface T and emissivity
- min and max altitudes for calc.

o Non-local thermodynamic equilibrium (NLTE) - Radiance

appropriate for spectral ranges and altitudes where "hot" bands occur

potentially large effects, particularly for paths
above 50km
activated by HIRAC=4
new input parameters - vibrational ID's
- vibrational Ts or populations
- standard line parmeters (S, v)
modularized coding
improved line shape for far wings
increases runtime in proportion to no. of lines

FASCOD3: Fast Atmospheric Signature Code

SPECIAL OPTIONS (con't #1):

o Line coupling - Optical depth, transmittance, and radiance

important in vicinity of strong Q-branches and other

"dense" band systems for which coupling coefficients
are available (CO2 and O2 for now)

moderate effects (contamination of remote sensing channels
leading to T-determinations with errors > 5-10K)

default option; activated whenever coef. are supplied
new input parameters - coupling coef. as a fn(T)

(recognized by LNFL routines)

embedded coding
modifies line shape and continua
small effect on runtime

o Weighting Functions (Sequential Calculations)

instrument design tool for ascertaining signature source regions as a fn(distance from observer) calculates cumulative transmittance from observer to points (layer boundaries) along the line-of-sight activated by IMRG = 3-8, 13-18, 23-28saves "layer-defined" monochromatic transmittances at dv(natural) for IMRG = 3-8; can consume large amnts of storage for moderate spectral range for IMRG = 13-18, will save only spectrally scanned cumulative transmittances while preserving proper line-by-line calculation for IMRG = 23-28, will save only filtered (spectrally integrated) cumulative transmittances, while preserving proper line-by-line calculation coding dependent on viewing geometry: line-by-line calc original pre-stored ground to space (IMRG = 4, 14, 24 6, 16, 26) space to ground (IMRG = 3, 13, 23, 5, 15, 25) tangent (IMRG = 7, 17, 27, 8, 18, 28)timing increases minimal to moderate

does NOT work with IAERSL = 1,7 or IMS = 1

FASCOD3: Fast Atmospheric Signature Code

SPECIAL OPTIONS:

o Cross Section Capability - Radiance and Transmittance

(activated by: IXSECT = 1)

Currently reads HITRAN86 cross sections
Will read HITRAN90 T-dependent cross sections
Incorporates cross section into layer optical depths
at the coarsest resolution possible:

i.e. Function 1 $(\pm 4\alpha)$

Function 2 ($\pm 16\alpha$)

Function 3 ($\pm 64\alpha$)

Function 4 (± 25 cm⁻¹)

** Pressure broadened with Lorentzian convolution**
Layer-dependent

10 New default profiles for important greenhouse gases (based on M. Allen, 1990 photochemistry)

FASCODE2/3: Fast Atmospheric Signature Code

Recent Comparisons/Validation:

o Theoretical

WMO Intercomparison of Transmittance and Radiance Algorithms (ITRA) - 1985-1988 and 1990-1991

- compared with 6 line-by-line codes for limb, nadir, and microwave test cases
- IR and mm wavelengths
- line shape (including continua)
- layering algorithm
- transmittance, radiance, and weighting functions

SHARC - Strategic High Altitude Radiance Code for NLTE comparisons (Sharma & Robertson)
ARC/NLTE - Atm. Radiance Code (Picard & Wintersteiner)

o Laboratory (partial list; historic validation)

Line coupling (Lafferty & Hoke, 1986-87) etc.

o Atmospheric Instruments

- SCRIBE (Stratospheric Cryogenic Interferometric Balloon Experiment, AFGL) 1984-1988; multiple balloon flights with very high spectral resolution (0.06cm⁻¹); limb and nadir radiance
- HIS (High-Resolution Interferometer Sounder, Univ. of Wisconsin) 1985-1988; multiple airborne (balloon, aircraft, and shuttle) flights with high spectral resolution (0.5cm⁻¹); limb and nadir radiance
- ATMOS (Atmospheric Trace Molecule Spectroscopy instrument, JPL/NASA) 1985; spacelab (shuttle) flight with very high spectral resolution (0.01cm⁻¹); solar occultation (transmittance)
- IMORL (Infrared Mobile Optical Radiation Laboratory, NRL) 1976-1979; ground-based Fourier-transform spectrometer with very high resolution (0.06cm⁻¹); transmittance

FASCOD3: Fast Atmospheric Signature Code

Version 3

Applications:

- o Laser Propagation/ Ground Based Laser
- o Plume Signature/ Infrared Search and Track
- o Target Contrast/
 Tactical Decision Aids
- o Remote Sensing/ Inproved Point Analysis Models
- o Data Simulation/ UV, Visible, IR, microwave NLTE, line coupling
- o Instrument design & development/
 Information content, etc.
- o Heating-Cooling Rate Calculations/ Greenhouse gas absorption described by x-sections

DOCUMENTATION:

o "Instant" User Instructions (upon release)

Read tape

Unpack

Machine conversions

I/O "Parameter" definitions

Test cases

Sample output

Database access

(File management)

o User's Manual (release plus 5 months)

Expansion of "Instructions"

Scientific definitions

References

Description/justification of "default" choices

Subroutine descriptions and flow charts

Segment load file

File management

o Scientific Report (release plus 10 months)

All of the above AND:

Philosphy/history of FASCODE

Algorithm descriptions

Line-by-line functions *

Line shape

Line coupling

Continua

Diffuse functions

Geometry

Layering selection

Layer merging

Weighting functions

Standard profiles (p, T, constituent) *

Aerosol/hydrometeor profiles (LOWTRANT)

NLTE

Multiple scattering

X-sections (greenhouse gases)

Test cases/templates

Validation

Comparisons

References

Hints/cautions

etc.

COMMON ELEMENTS: Model Atmospheres

Topics:

- o Available "default" profiles for pressure, temperature, density, and molecular constituents: FASCODE, LOWTRAN, and MODTRAN all employ the same set; see AFGL Atmospheric Constituent Profiles (0-120km).
- o User input options for these parameters:

Again, the same type of options are employed by all three codes. However, the details of the input procedures differ, based primarily on the number of constituent variables (28 for FASCODE, 12+ for LOWTRAN and MODTRAN) and historic usage.

- o New FASCOD3 "greenhouse" gas option: access to the molecular absorption cross sections available on the HITRAN86/90 databases has necessitated the addition of 10 new profiles.
- o Natural climatological variability:

 Near-term availability of climatologically varying profiles and their statistical evaluation.

GREENHOUSE GAS PROFILES: New FASCOD3 Default Options

- o HITRAN86/90 provides molecular absorption cross sections for: ClONO2, HNO4, CHCl2F, CCl4, CCl3F, CCl2F2, C2Cl2F4, C2Cl3F3, N2O5, HNO3, and CF4
- o FASCOD3 now includes "default" profiles for these gases, plus the capability to implement layer-by-layer optical depth/transmittance calculations.
- o These profiles are based on a "one/two-dimensional photochemical model" with upgraded 1990 chemistry and/or measurements. (M. Allen, JPL)

EOSAEL92

A.E. Wetmore U.S. Army Atmospheric Sciences Laboratory, White Sands Missile Range, NM 88002-5501

The U.S. Army Atmospheric Science Laboratory (ASL) is planning to release the next version of the Electro-Optical Systems Atmospheric Effects Library (EOSAEL) during the first quarter of fiscal year 1992. This paper reports what the EOSAEL users have to look forward to. The climatology (CLIMAT) database has been expanded to include the continental United States and most of Canada. The aerosol phase function database (PFNDAT) database used by the EOSAEL has been expanded to include models of desert aerosols and lidar backscatter coefficients. A new Narrow Beam Multiple Scattering code will replace many of the previous scattering codes. An ultraviolet transmission and lidar code is being included. We are replacing LOWTRAN-6 with LOWTRAN-7 and including the capability of calculating contrast transmission. The target acquisition (TARGAC) and natural aerosol extinction (XSCALE) model have been improved and laser transmission (LZTRAN) should have several new wavelengths added. Several of the modules will sport an interactive interface.

EOSAEL92

Alan E. Wetmore U.S. Army Atmospheric Sciences Laboratory White Sands Missile Range, New Mexico 88002-5501, USA

FALL 1991 DISTRIBUTION

The U.S. Army Atmospheric Sciences Laboratory (ASL) is planning to release the next version of the Electro-Optical Systems Atmospheric Effects Library (EOSAEL) during the first quarter of fiscal year 1992. There will be new models, upgrades to existing models, and obsolete models. Distribution will continue to be on magnetic tape and free to qualified recipients.

UNCHANGED MODELS

Many of the modules are unchanged in their physics. These are the near millimeter wave (NMMW), cloud transmission (CLTRAN), obscuration due to helicopter lofted snow and dust (COPTER), self-screening applications (GRNADE), missile smoke plume obscuration (MPLUME), contrast transmission (OVRCST) and contrast transmission (FCLOUD), natural illumination under realistic weather conditions (ILUMA), fast atmospheric scattering (FASCAT), large area screening systems applications (LASS), nonlinear aerosol vaporization and breakdown effects (NOVAE), and millimeter wave system performance (RADAR) modules.

UPGRADES TO EXISTING MODELS

- atmospheric transmittance and radiance (LOWTRN)
- laser transmission (LZTRAN)
- climatology (CLIMAT)
- munition expenditure module (KWIK)
- natural aerosol extinction (XSCALE)
- target acquisition (TARGAC)
- combined obscuration model for battlefield-induced contaminants (COMBIC)

LOWTRAN 7

- ASL researchers are incorporating the Geophysics Laboratory's (GL's) latest upgrades to LOWTRAN 7, modifying the input routines to use the EOSAEL record order independent routines, and making some changes to improve portability.
- The largest upgrades are the vertical structure algorithms. Bob Fiegel described this work last year.
- We are writing The Complete LOWTRAN Manual.
- Much of our time has been spent increasing the portability and putting reasonable limits and checks on many mathematical operations.

LZTRAN

- Several new laser wavelengths will be added.
- It is not too late to request that your favorites be added.
- Remember that LZTRAN is a near earth transmission code.

CLIMAT

- Data for Canada and the continental United States has been added.
- An option to print out the summary data for all climate classes was added.





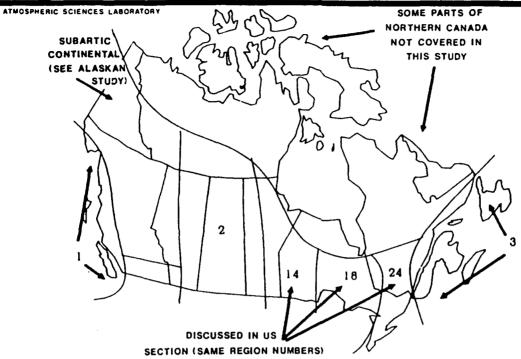
ATMOSPHERIC SCIENCES LABORATORY





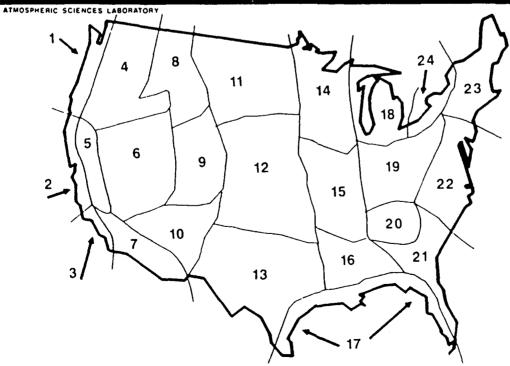
CANADA











KWIK

- No new smoke munitions.
- Refinements to the calculation of extinction coefficients.
- The values of transmission reported by XSCALE are modified to better agree with experimental data.

XSCALE

- Increased speed in the calculations using the vertical structure models.
- The inversion-haze case has been compared with field data; good agreement was obtained.
- XSCALE now calculates transmission through thin cloud and haze layers. These paths may extend from above the layer, through the layer, to the ground below the layer.

TARGAC

- TARGAC has been upgraded to use the EOSAEL routine ILUMA.

 This replaces an independent routine that calculated illumination levels.
- A new thermal model (TCM2) for surfaces has been added.

 Turbulence and clutter calculations have been included in this model.
- An improved method of calculating the sky-to-ground ratio uses a delta Eddington model to account for path radiance and surface reflectance.

COMBIC

- COMBIC has had several modifications to fix minor bugs.
- A paper on using non-inventory smokes has been prepared.
- Instructions illustrating methodologies for adding "experimental" obscurants.

MODELS TO BE DROPPED

- The simulation of aerosol behavior in realistic environments (SABRE) and aerosol multiple scattering (MSCAT) modules will be dropped from the EOSAEL distribution.
- The SABRE model required too much customization to be used for different geographic sites.
- The MSCAT Monte Carlo code leaves far too many chances for misapplication. Most users who need a Monte Carlo code probably have their own. For those who were satisfied with MSCAT, the ASL will continue to supply it as a research code.

NBMSCAT

- NBMSCAT is a radiative scattering code developed by Luc Bissonnette of the Defence Research Establishment Valcartier, Canada.
- This code is an approximation to the radiative transfer equations suitable for narrow beams of light and observation points near the propagation axis.
- It handles arbitrary inhomogeneous obscurant clouds.

UVTRANS

- UVTRANS is an ultraviolet transmission, fluorescence, and lidar program developed for near earth applications.
- UVTRANS differs from LOWTRAN
 - flat earth and atmosphere approximations,
 - pressure parameterization valid for near earth only,
 - single aerosol model valid for visibilities less than 50 kilometers,
 - includes some different trace gasses.

USER INTERFACE IMPROVEMENTS

- We are developing an interactive user interface.
- There will be a demonstration available during the breaks.

 We would appreciate any comments on the work that is shown.
- We hope to have both a generic interface that can be used on any computer system and a more customized version for MS-DOS PC's.
- The interactive interface will also create a normal EOSAEL input file for later reuse or modification.

GRADE OF SOFTWARE

The ASL will be evaluating all of the modules to assign a grade. These grades are not the same as "validating" the codes.

Research	Describes phenomena based on a physical or meteorological theory.
	Limited evaluations in the field or laboratory.
Developmental	Tailored version of a research model. Limits of applicability have been defined.
Fieldable	At least "several" evaluations have been made. Applicability has been defined.
	Confidence has been established throughout the community. "Many" evaluations have been "passed". The model has been verified for its stated usage.

AVAILABILITY

- EOSAEL92 is available to U.S. Department of Defense (DoD), specified allied organizations, and DoD authorized contractors at no cost. DoD agencies needing EOSAEL92 should send a letter of request, signed by a branch chief or division director, to the ASL. Contractors should have their DoD contract monitor send the letter of request. Allied organizations must request EOSAEL92 through their national representative.
- Please include, within security restrictions, your intended use(s). Also, indicate what type of nine-track tape your computer can read. We can make "ASCII" tapes, VAX VMS BACKUP tapes, and UNIX "tar" format tapes in either 1600 or 6250 bpi.

(505) 678-5563 Commander/Director

FAX (505) 678-2432 U.S. Army Atmospheric Sciences Laboratory

DSN 258-5563 ATTN: SLCAS-AA-A (Dr. Wetmore)

awetmore@wsmr-emh73.army.mil White Sands Missile Range, New Mexico 88002-5501

BATTLEFIELD ATMOSPHERICS CONFERENCE

Formerly the EOSAEL/TWI Conference 2-6 December 1991 Fort Bliss, Texas

Mailing Address:

Commander/Director
U.S. Army Atmospheric Sciences Laboratory
ATTN: Battlefield Atmospherics Conference
White Sands Missile Range, New Mexico 88002-5501

HITRAN'91: THE CONTEMPORARY SPECTROSCOPIC MOLECULAR DATABASE

L.S. Rothman
Geophysics Directorate, Optical Environment Division, Simulation Branch (OPS),
Hanscom Air Force Base, MA 01731-5000

The spectroscopic molecular database, HITRAN, is the DOD and international standard compilation of absorption parameters that enable the calculation of atmospheric spectral simulations from the microwave through the visible. A new edition of HITRAN has been made available in the first quarter of 1991. The current edition contains over 65 megabytes of high resolution data of transitions for 30 species and their atmospherically significant isotopic variants. In addition, there is a file of new cross-sections for heavy molecular species, with bands at several representative temperatures that should facilitate some quantitative retrievals. This task will summarize some of the major updates, improvements, and modifications.

HITRAN'91: The Contemporary Spectroscopic Molecular Database

Laurence S. Rothman

Geophysics Directorate
Optical Environment Division
Simulation Branch (OPS)
Hanscom AFB, MA 01731-5000 USA

Abstract

The spectroscopic molecular database, HITRAN, is the DOD and international standard compilation of absorption parameters that enable the calculation of atmospheric spectral simulations from the microwave through the visible. A new edition of HITRAN has been made available in the first quarter of 1991. This current edition contains over 65 Megabytes of high resolution data of transitions for 30 species and their atmospherically significant isotopic variants. In addition, there is a file of new cross-sections for heavy molecular species, with bands at several representative temperatures that should facilitate some quantitative retrievals. This talk will summarize some of the major updates, improvements, and modifications.

Major Molecular Parameter Updates

- O H₂O
- O CO₂
- **O** O₃
- O CH₄
- O CO, HNO₃, HCI, HF, HI, HBr...
- ✿ Cross-sections (CIONO₂, CFC's, N₂O₅...)

Water Vapor (H₂O)

	V _{min}	V_{max}	# bands	# lines
0	5904	7965	9	3112*
0	8036	9482	9	1874
•	9603	11 481	9	2484
•	11 661	12 741	5	714*
6	13 238	22 657	41 (39,2)	4608
6	782	2745	2	*

Water Vapor (H₂O)

All new regions have been taken at the Kitt Peak Solar Observatory using the FTS and long-path cell. These data replace older parameters that were observed using grating spectrometers and a path through the atmosphere. Most notable improvement in intensities of weak lines. In the case of data from Toth, a hybridization with '86 lines was used to supplement his data

- Toth, JPL
- Flaud & Camy-Peyret (FCP), Paris
- FCP
- Toth
- **6** FCP | extends spectral range of compilation
- Toth

Carbon Dioxide (CO₂)

- New Line Positions: New fit of observed high resolution data by Hawkins & Rothman (including some DND points to supplement data). New data includes very high vibrational 4.3-μm observations of Bailly et al. (Orsay) and the 15-μm observations of Esplin et al. (GL)
- **New Intensities**: New intensity observations of Dana *et al.* (Paris) and Johns (NRC). Calculations by Wattson & Rothman for unobserved bands, include Herman-Wallis coefficients.
- **Revised Halfwidths:** Self- and Foreign-broadened halfwidths and temperature dependence now pased on work at Ecole Centrale.

Ozone (O₃)

	V_{min}	$V_{\sf max}$	# bands	# lines	
0	557	900	2	12 085	
2	919	1271	18	42 500	
•	934	1178	4	13 590	
•	1319	2322	19	44 926	

Ozone (O₃)

- New data for v_2 and $2v_2 v_2$ from Pickett (JPL) et al.
- **②** Revamping of 10-μm region. This time includes many new bands and hot bands.
- $\mbox{\bf 8}$ Isotopic bands of 10- μm region from FCP & Rinsland (NASA Langley)
- Many new combination bands from Goldman (Denver)

Methane (CH₄)

	V_{min}	V_{max}	# bands	# lines
0	0	6185	31 (21,6,4)	37 207
9	2902	3147	3	309

- Major improvement by Brown (JPL).
- Updated mono-deuterated methane bands by Brown.

Other Molecular Species

- CO (carbon monoxide): Update, primarily for HITEMP (*Tipping*)
- O NO (nitric oxide): Update of fundamental (*Ballard*)
- O NO₂ (nitrogen dioxide): Update of v_3 region (*Perrin*, *FCP*)
- O HNO₃ (nitric acid): Addition of new bands (fundamentals and combinations, 410 to 1400 cm⁻¹) (Goldman, Maki, Perrin, et al.)
- HCI, HF, HI, HBr (hydrogen halides):
 Update, primarily for HITEMP (*Tipping, et al.*)

Other Molecular Species (continued)

- H₂O₂ (hydrogen peroxide): Update of ν₆ band, 138-1500 cm⁻¹ (Hillman)
- C₂H₂ (acetylene): Addition of v₅ band, 1192-1470 cm⁻¹ (Rinsland et al.)
- C₂H₆ (ethane): Addition of ν₇ band, 2973-3000 cm⁻¹ (Goldman, Dang-Nhu, Bouanich)
- © COF₂, SF₆: New species on compilation (*Goldman, Rinsland, et al.*)
- OCS, N₂ ...

Updates generally include all parameters of HITRAN format.

Cross-sections (Supplemental files)

CFC's now at six temperatures: 203, 213, 233, 253, 273, and 293K. N_2O_5 at 233, 253, 273, and 293K. $CIONO_2$ at 213 and 296K.

Species	V_{min}	V_{max}	# lines
CFC-11 (CCl₃F)	830	860	
n	1060	1107	31 146
CFC-12 (CCl ₂ F ₂)	867	937	
"	1080	1177	67 542
CFC-13 (CCIF ₃)	765	805	
V	1065	1140	
IJ	1170	1235	72 804
CFC-113 (C ₂ Cl ₃ F ₃)	780	995	
u	1005	1232	5304

Cross-sections (continued)

Species	V _{min}	V _{max}	# lines
CFC-114 (C ₂ Cl ₂ F ₄)	815	860	
"	870	960	
"	1030	1067	
"	1095	1285	146 418
CFC-115 (C₂CIF₅)	955	1015	
"	1110	1145	
"	1167	1260	76 038
N_2O_5	<i>555</i>	600	
"	720	765	
n	1210	1275	
n	1680	1765	1988
CIONO ₂	740	840	
n	1240	1340	
"	1680	1790	26 622

SELECT OPTIONS

Input:

- 2 Molecule
- 3 Isotope
- v', v" (upper and lower "global" quanta)
- S S_{crit} (Intensity cutoff)

Output:

- Batch file for input
- Files for input to subsequent programs (direct image; '82 format; user defined)
- Temperature Correction
- Hard copy listing
 (codes converted to spectroscopic and chemical notations;
 80 or 132 columns printers)

MAJOR CONTRIBUTORS

D. C. Benner	J. W. C. Johns
L. R. Brown	A. G. Maki
V. Dana	S. T. Massie (NCAR)
V. Malathy Devi	C. P. Rinsland
JM. Flaud	L. Rosenmann
R. R. Gamache	M. A. H. Smith
A. Goldman	R. Tipping
J. M. Hartmann	R. A. Toth
R. L. Hawkins	R. B. Wattson

SUMMARY

- ★ New Edition of HITRAN published March 1991.
- ★ Improvements notable for remote sensing, laser transmission, climate modeling, use of heavy species...
- * References and Error criteria now implemented.
- ★ SELECT faster and more flexible.
- A New media and structure for the database to materialize.
- * HITEMP to be available in '91.

SHARC, AN ATMOSPHERIC RADIATION AND TRANSMITTANCE CODE FOR ALTITUDES FROM 50 TO 300 KM

D. Robertson, L. Bernstein, J. Duff, J. Gruninger, R. Sundberg Spectral Sciences, Inc., 111 S. Bedford Street, Burlington, MA 01803

R. Sharma
Geophysics Directorate, Phillips Laboratory, Hanscom Air Force Base, MA 01731-5000

R. Healey
Yap Analytics, Inc., 594 Marrett Road, Lexington, MA 02173

The latest version of the Strategic High-Altitude Radiance Code (SHARC), SHARC-2, is now available. The new version contains significant upgrades, the most important being a fully integrated auroral model with time-dependent chemistry, extension down to 50 km altitude, and incorporation of the minor isotopes of CO₂. SHARC calculates atmospheric radiance and transmittance over the 2-40 µm spectral region and includes arbitrary paths within 50 and 300 km altitude. It models radiation due to NLTE (Non-Local Thermodynamic Equilibrium) molecular emission which are the dominant sources at these altitudes. It calculates molecular radiation on a line-by-line basis and has a spectral resolution of 0.1 cm⁻¹. SHARC uses an equivalent-width formalism to obtain the total transmittance for each line, thus alleviating the need for the usual numerical integration over the line shape.

SHARC THE STRATEGIC HIGH-ALTITUDE RADIANCE CODE

BY

DAVID ROBERTSON, LARRY BERNSTEIN,
JAMES DUFF, JOHN GRUNINGER, ROBERT SUNDBERG,
SPECTRAL SCIENCES, INC.,

RAMESH SHARMA, PHILLIPS LABORATORY/OPS

REBECCA HEALEY, YAP ANALYTICS, INC.

11 JUNE 1991

OUTLINE

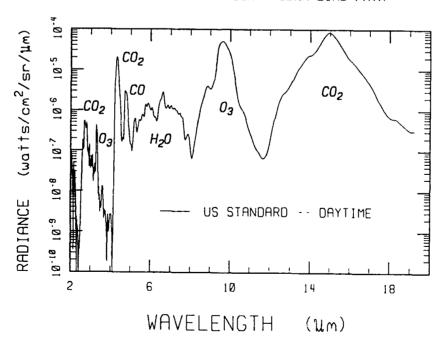
- SHARC-2 OVERVIEW
- MAJOR MODULES
 - RADIATIVE EXCITATION (NEMESIS)
 - AURORAL MODULE
- VALIDATION EXAMPLES
- ILLUSTRATIVE RUN TIMES
- CONCLUDING REMARKS

SHARC-2 OVERVIEW

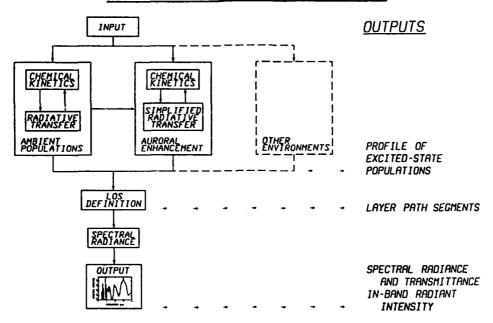
- SHARC CALCULATES NLTE RADIATION FROM AMBIENT AND AURORAL ATMOSPHERES
- BASIC FEATURES:
 - 50-300 km ALTITUDE REGIME
 - 2-40 µm WITH RESOLUTION OF 0.5 cm⁻¹
 - ARBITRARY VIEWING GEOMETRIES
 - INTERACTIVE INPUT MODULE WITH ERROR CHECKING
 - ADJUSTABLE CHEMICAL KINETICS MECHANISMS/RATES
 - AUTOMATICALLY INCLUDES LTE & NLTE CONTRIBUTIONS
 - AMBIENT MOLECULES INCLUDE: H_2O , O_3 , CO, NO, OH, CO_2 , ITS IMPORTANT ISOTOPES
 - AURORAL MODULE WITH: NO+, NO, CO2
 - MULTIPLE OUTPUT OPTIONS
 - FORTRAN SOURCE CODE PROVIDED

ILLUSTRATIVE SHARC CALCULATION

SPACE VIEWING THROUGH A 50km LIMB PATH



SHARC-2 FLOW CHART



AMBIENT POPULATIONS MODULE

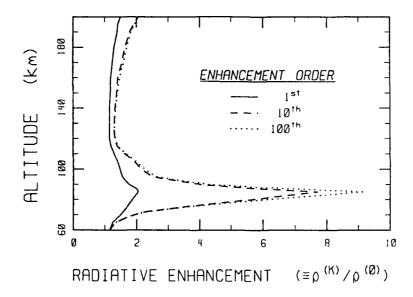
- SYMBOLIC DESCRIPTION OF CHEMICAL KINETICS MECHANISM
 - BASED ON WIDELY USED SANDIA CHEMKIN CODE
 - EXAMPLE: $M + O + O_2$ -> $M + O_3(000)$ $M + O_3(001)$ -> $M + O_3(000)$ $O_3(001)$ -> $O_3(000) + h\nu$
- RATE EQUATIONS SOLVED IN STEADY STATE
 - ASSUMES RATE EQUATIONS DEPEND LINEARLY ON VIBRATIONAL POPULATION
- MONTE CARLO CALCULATION FOR FIRST-ORDER RADIATIVE ENHANCEMENT
 - MULTIPLE APPLICATION YIELDS HIGHER ORDER ENHANCEMENTS

RADIATIVE EXCITATION MODULE (NEMESIS)

- RADIATIVE EXCITATION SIGNIFICANTLY ENHANCES
 THE EXCITED-STATE POPULATIONS OF STRONG BANDS
 AND HENCE THE STRENGTH OF THEIR EMISSIONS
- BASIC MODEL ASSUMPTIONS
 - SEMI-INFINITE PLANE-PARALLEL HOMOGENEOUS LAYERS
 - VOIGT LINESHAPE
 - TRANSLATIONAL-ROTATIONAL EQUILIBRIUM
 - COMPLETE LINE FREQUENCY REDISTRIBUTION
 - COMPLETE ROTATIONAL LEVEL REDISTRIBUTION
 - NO LINE OVERLAP

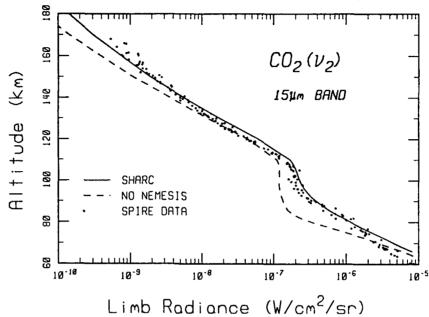
ENHANCEMENT OF $CO_2(\nu_2)$

POPULATION ENHANCEMENT FACTOR DUE TO RADIATIVE EXCITATION



RADIATIVE ENHANCEMENT FOR CO2

NO-NEMESIS CALCULATION SKIPS RADIATIVE EXCITATION



SPECTRAL RADIANCE MODULE

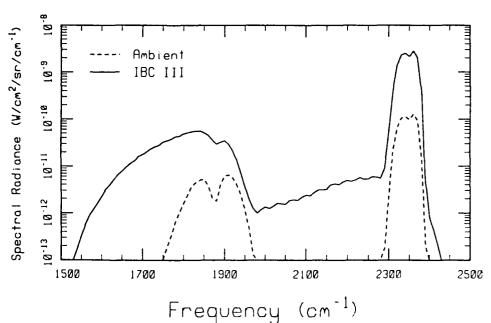
- RADIATION TRANSPORT CALCULATION PERFORMED FOR EACH MOLECULAR LINE
 - USES GL ATMOSPHERIC ABSORPTION LINE DATABASE (HITRAN)
- ullet RODGERS-WILLIAMS APPROXIMATION FOR THE EQUIVALENT WIDTH (W) OF A SINGLE LINE WITH A VOIGT LINESHAPE NASA HANDBOOK APPROXIMATION FOR W_D AND W_L
- LAYER-DEPENDENT LINE STRENGTHS
 VIBRATIONAL AND ROTATIONAL TEMPERATURES
- CURTIS-GODSON APPROXIMATION
 AVERAGING PROCEDURE FOR INHOMOGENEOUS PATHS
- LINE OVERLAP CORRECTION FOR DENSE REGIONS
- 50-70 TIMES FASTER THAN TRADITIONAL LBL APPROACH

SHARC AURORAL MODULE

- AURORAL PHENOMENOLOGY
 - STARTING POINT IS GL AARC CODE
 - ELECTRON DEPOSITION MODELS FOR DIFFERENT STRENGTH AURORAS: CLASS II, III, III+
 - SOLVES TIME/ENERGY DEPENDENT RATE EQUATIONS TO CALCULATE BOTH SECONDARY ELECTRON DISTRIBUTIONS AND THE KINETICS FOR IR RADIATORS
 - PRESENT IR MOLECULES ARE: NO, NO⁺, CO₂
- SHARC AURORAL UPGRADE
 - GEAR'S STIFF ODE ALGORITHM USED AS REQUIRED
 - CAN ADD NEW RADIATORS VIA USER-DEFINED INPUT FILES
 - LOS CALCULATION COUPLED WITH AMBIENT REGION
- UPGRADED GEOMETRY MODEL INSURES THAT LOS TRAJECTORIES INTERSECT AURORA AS DESIRED

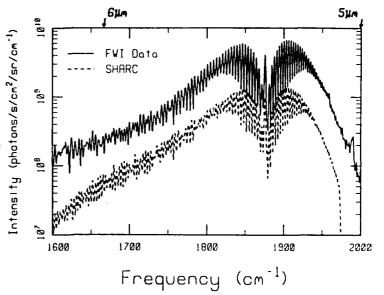
<u>ILLUSTRATIVE AURORAL ENHANCEMENT</u>

RELATIVE STRENGTHS FOR PATH 90 km - SPACE



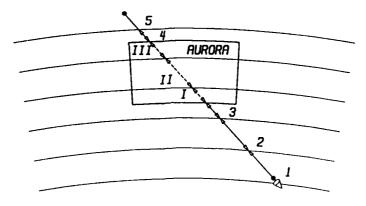
<u>COMPARISON TO AURORAL FIELD DATA</u>

- FWI DATA (FIELD WIDENED INTERFEROMETER)
- VERTICAL PATH TO SPACE FROM 90 KM
- CLASS II AURORA (~12 K RAYLEIGHS)
- SHARC CALCULATION FOR CLASS II (10 KR)
- MODEL CALCULATION USES A CONSTANT ELECTRON DOSE RATE
 BUT
- AURORA IS LIKELY STRONGLY PREDOSED



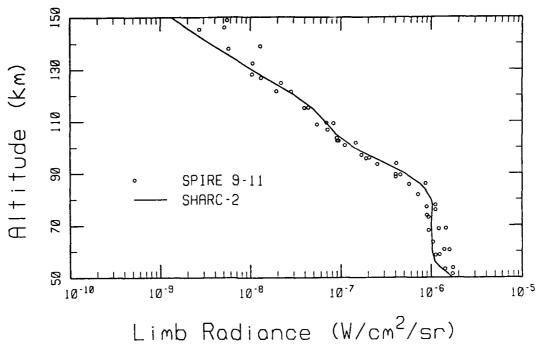
LOCALIZED ATMOSPHERIC REGIONS

- EXTENDED ATMOSPHERE PLUS LOCAL (AURORAL) REGIONS
 POPULATIONS DEFINED IN EACH REGION
- LOS IS COMPOSED OF MULTIPLE HOMOGENEOUS SEGMENTS WITHIN EACH REGION



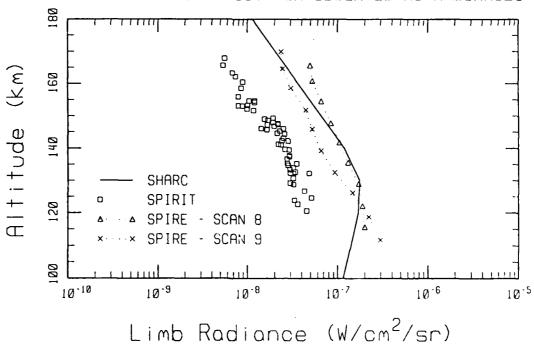
SPIRE: DAYTIME CO2 (4.3 µm)

STRONG SOLAR PUMPING VIA EXCITATION OF 2.7µm BAND



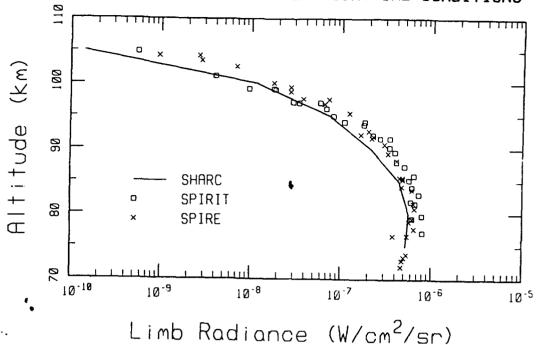
COMPARISON TO NO (5.3 µm) DATA

SIGNIFICANT VARIABILIITY IN OBSERVED NO RADIANCES



COMPARISON TO 03 (9.6 14m) DATA

SPIRIT 1 AND SPIRE DATA FOR NIGHTTIME CONDITIONS



RUN TIMES - CHEMISTRY

- CHEMISTRY ONLY REPEATED FOR MODIFIED ATMOSPHERE
- AMBIENT POPULATIONS
 - 89 BANDS OF $\rm H_2O$, $\rm CO_2$, $\rm O_3$, $\rm CO$, $\rm NO$, $\rm OH$ 26 OF WHICH REQUIRE RADIATION TRAPPING TREATMENT
 - 66 ATMOSPHERIC LAYERS FROM 50 TO 300 KM

DATA GENERAL AVIION AV5100 (20 MIPS) : 15.2 MIN DEC VAX 8800 : 10.8 .*
DEC VAX 780 : 80.1 .*

- AURORAL POPULATIONS (ADDITIONAL TO AMBIENT)
 - 31 VIBRATIONAL STATES: NO(13), NO † (14), CO $_{2}$ (4)
 - 37 RADIATING BANDS: NO (23), NO (13), CO (1)
 - 36 LAYERS FROM 80 TO 150 KM

DATA GENERAL AVIION AV5100 (20 MIPS) : 7-12 MIN DEC VAX 8800 : 5-8.5 DEC VAX 780 : 37-64

RUN TIMES - LOS RADIANCE

- SPECTRAL RADIANCE SINGLE BAND
 - 14-16 µm BAND OF CO2 WITH 890 LINES
 - 131 LAYERS (50 KM LIMB)

DATA GENERAL AV: 10N AV5100 (20 MIPS) : 5.2 SEC DEC VAX 8800 : 3.7

DEC VAX 8800 : 3.7 • DEC VAX 780 : 27.6 •

- SPECTRAL RADIANCE MULTIPLE BANDS
 - 1-40 μ m BANDPASS: H_2O , CO_2 , O_3 , CO, NO, OH 84,000 LINES
 - 131 LAYERS (50 KM LIMB)

DATA GENERAL AVIION AV5100 (20 MIPS) : 6.3 MIN

DEC VAX 8800 : 4.5 •

DEC VAX 780 : 33.4 •

SUMMARY

- SHARC WAS DEVELOPED TO MEET SDIO REQUIREMENTS FOR A HIGH-ALTITUDE RADIANCE MODEL
 - AURORAL AND QUIESCENT ATMOSPHERES
 - MODULARIZED STRUCTURE
 - ARBITRARY PATHS ABOVE 50 km
 - FULLY INTEGRATED & LOCALIZED AURORAL REGION
- COMPATIBLE WITH SSGM STRUCTURE
- VALIDATED WITH GL FIELD DATA

SHARC STATUS

- SHARC-2 WILL BE DISTRIBUTED IN JULY, 1991
 - CODE IS READY
 - MANUAL IS BEING PRINTED
- REQUEST (ON LETTERHEAD) FROM:

 DR. RAMESH SHARMA

 PHILLIPS LABORATORY (OL-AA) / GP/OPS

 HANSCOM AFB, MA Ø1731-5000
- ENCLOSE A 9-TRACK 1600-BPI TAPE

RECENT DEVELOPMENTS OF THE GENLN2 LINE-BY-LINE MODEL: STUDIES IN SUPPORT OF THE UARS PROJECT

D.P. Edwards National Center for Atmospheric Research, Box 3000, Boulder, CO 80307

Recent developments of the general purpose line-by-line atmospheric transmittance and radiance model GENLN2 are described. Results will be presented of radiative transfer studies in support of algorithm development for the temperature sounding channels of infrared instruments aboard the Upper Atmosphere Research Satellite (UARS). The implications of spectral line shape modelling and line mixing have been considered for low altitude limb views and comparisons are made with spectra taken during the ATMOS experiment. The effect of high altitude non-LTE radiance in these channels has also been investigated.

BENLN2

Recent Developments and Studies in Support of the *UARS* Project

DAVID P. EDWARDS

Atmospheric Chemistry Division National Center for Atmospheric Research Boulder, CO

GENLN2 PROGRAMS

HITLIN

Purpose: Create fast access line data base.

- Binary, direct access line data base, allowing :-
- Fast search for first useful line
- Pointer on each line to next line of same gas
- Every 200 lines a record containing line number of next line of each gas
- Ability to merge new lines into data base
- Status number for each line indicating origin
- Line strength scaling to avoid underflow of weak lines.

GENLN2 PROGRAMS

LAYERS

Purpose: Perform atmospheric layering.

- Model or user supplied atmospheric profile
- User specified viewing geometry
- Layer structure calculated according to max ΔT and $\Delta \alpha_{Voigt}$ across a layer or user supplied
- Ray tracing accounting for atmospheric refraction and variation of g.
- Curtis-Godson mean values for T, p and gas amount.

GENLN2 PROGRAMS

GENLN2

Purpose: Line-by-line calculations.

- Spectral line shapes: Voigt (Humlicek, 1982), Doppler, Lorentz, Gross, Van-Vleck & Huber or user supplied
- CO₂ sub-Lorentzian line wings (Cousin et al., 1985)
- Line mixing (Edwards & Strow, 1991)
- Water vapour continuum (Clough et al., 1981)
- Heavy molecule absorption cross-sections (McDaniel et al., 1991)
- N₂ and O₂ pressure induced continua (Orlando et al., 1991)
- Temperature variation of line partition functions (Gamach et al., 1990)
- Non-LTE model based on vibrational temperature profile input (*López-Puertas et al.*, 1986).

GENLN2 PROGRAMS

GENLN2

- Two stage line-by-line calculation: fine absorption grid close to line center, wider in the line wings
- Line cutoff at specified minimum intensity and at maximum value of $|\nu \nu_0|$
- Vertical calculation: at any time the optical depth is known separately for each gas in every layer over a narrow wavenumber interval
- Parallel transmittance and radiance calculations
- Surface boundary options for radiance calculations
- Single gas emission studies for sensitivity calculations
- Gas-correlation, PMR and LMR calculation options.

GENLN2 PROGRAMS

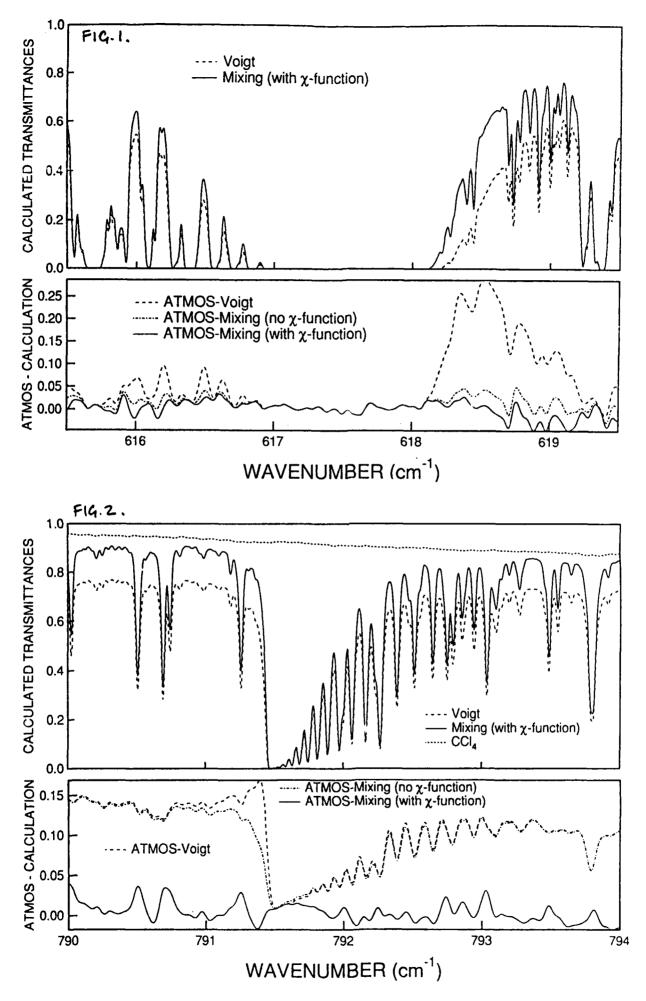
GENGRP

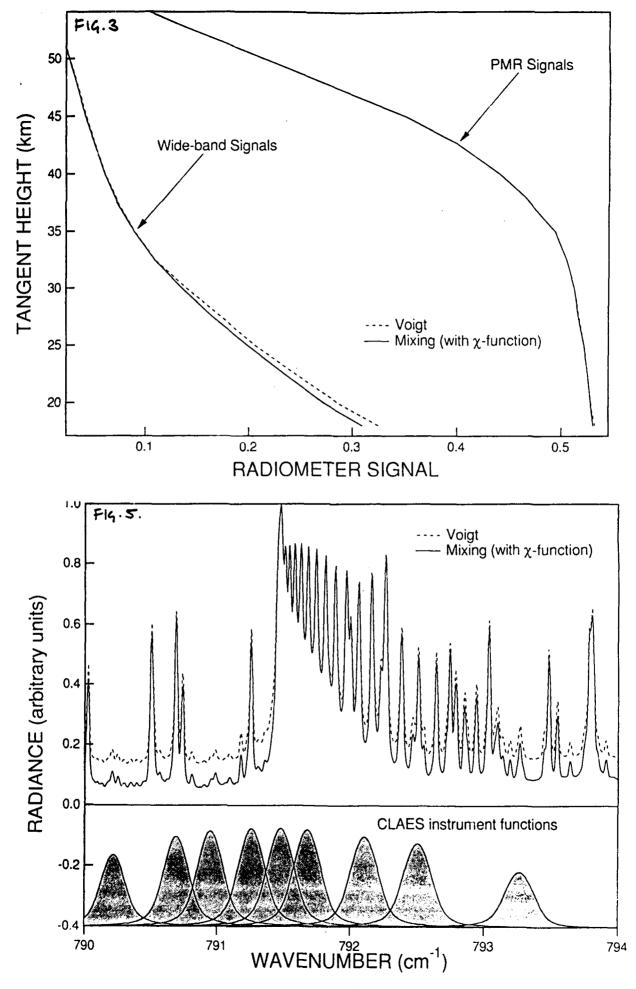
Purpose: Graphics and spectra manipulation.

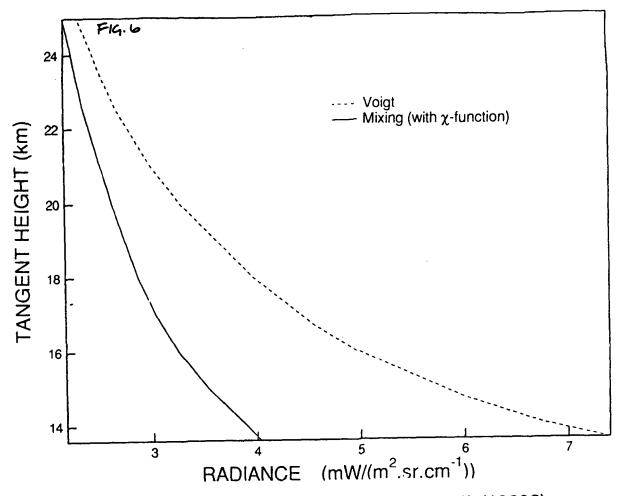
- Spectrum plotting based on NCAR graphics
- Spectra can be convolved with instrument function in the Fourier domain
- Boxcar, triangle, spectrometer (with apodizing functions) or user supplied instrument functions
- Spectrum convolution with broadband radiometer response
- Calculation of equivalent brightness temperatures.

Figure Captions

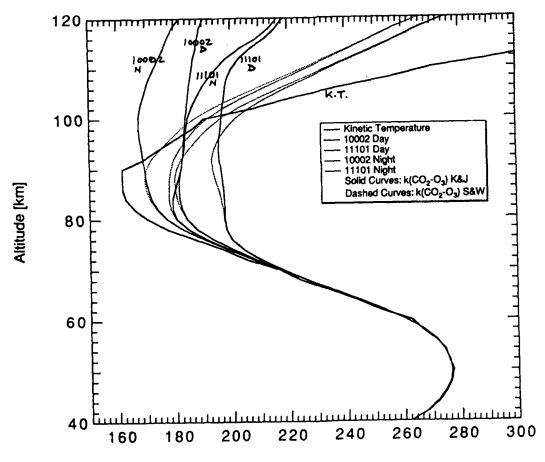
- Fig. 1. A comparison of calculated transmittances and ATMOS spectra for a 22.4 km tangent height at the 617 cm⁻¹ CO₂ Q-branch. The upper panel shows calculated transmittance spectra (dashed line for simple Voigt model, solid line for line mixing model with sub-Lorentzian line wings). The lower panel shows the differences between the calculated transmittances and the ATMOS spectra (dashed line for the Voigt model, chain line for line mixing model with Lorentzian line wings and solid line for the line mixing model and sub-Lorentzian line wings).
- Fig. 2. A comparison of calculated transmittances and ATMOS spectra for a 13.6 km tangent height at the 791 cm⁻¹ CO₂ Q-branch. The upper panel shows calculated transmittance spectra (dashed line for simple Voigt model, solid line for line mixing model with sub-Lorentzian line wings). The contribution of the CCl₄ band is also shown (dotted line). The lower panel shows the differences between the calculated transmittances and the ATMOS spectra (dashed line for the Voigt model, chain line for line mixing model with Lorentzian line wings and solid line for the line mixing model and sub-Lorentzian line wings).
- Fig. 3. ISAMS channel 7.1 radiometer signal at different tangent heights for the Voigt model (dashed line) and the line mixing model with sub-Lorentzian line wings (solid line). The wide-band signals are shown left and the PMR signals right.
- Fig. 5. Calculated radiance spectra for a 13.6 km tangent height at the 791 cm⁻¹ CO₂ Q-branch. The upper panel shows calculated radiance spectra (dashed line for simple Voigt model, solid line for line mixing model with sub-Lorentzian line wings). The lower panel shows the CLAES blocker filter 8 etalon channel positions.
- Fig. 6. CLAES blocker filter 8 etalon 3 channel radiance at different tangent heights for the Voigt model (dashed line) and the line mixing model with sub-Lorentzian line wings (solid line).





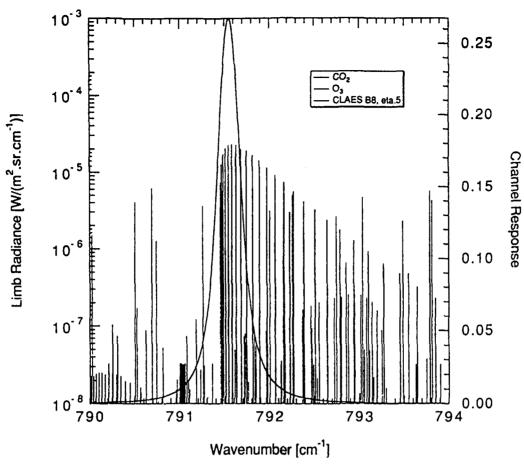


Vibrational Tempertures for CO₂ (11101)-(10002)

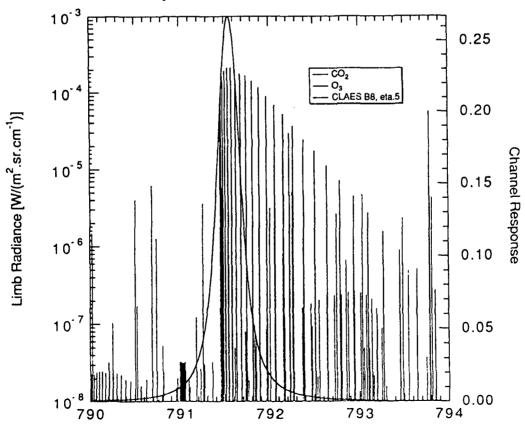


Temperature IKI 126



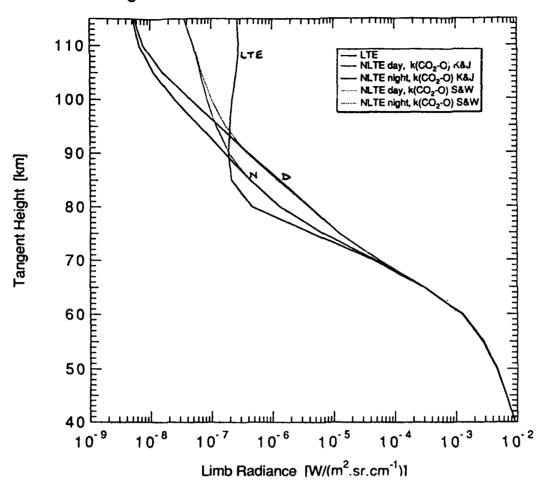


NLTE 80km Day Limb Radiance: Subarc.Sum.#4, S&W.



Wavenumber [cm⁻¹]

CLAES High Altitude Radiance: B8, eta 5. Subarc.Sum.#4.



PRESENT STATUS OF TRANSMITTANCES AND RADIANCES MODELLING AT L.M.D.

N.A. Scott, A. Chédin, F. Chéruy, B. Tournier (ARA/LMD) Ecole Polytechnique, 91128 Palaiseau Cedex, France

The ARA/LMD group has years of experience in the modelling of transmittances and radiances: STRANSAC (1974), 4A (Automated Atmospheric Absorption Atlas, 1981) and 3R (Rapid Radiance Recognition, 1986) represent three generations of forward radiative transfer models characterized by their increasing efficiency regarding the computation time. They have already been and are involved in several international campaigns of intercomparisons (ITRA: Intercomparison of Transmittance and Radiance Algorithms, IRC/IAMAP). STRANSAC and 4A are presently used within the context of the modelling of high spectral resolution radiance measurements (AIRS experiment of the NASA EOS - Earth Observing System - Programme, and IASI experiment of the CNES-GLOBSAT Program. ne).

A description of these models as well as a report on the work in progress will be given at the time of the Conference.

"AURIC (ATMOSPHERIC ULTRAVIOLET RADIANCE INTEGRATED CODE): AN UPDATE"

R. Hugeunin, R. Hickey Aerodyne Research, Inc., 45 Manning Road, Billerica, MA 01821

> M. Minschwaner Harvard University, Cambridge, MA 02138

G.P. Anderson, L.A. Hall, R.E. Huffman Phillips Laboratory, Hanscom Air Force Base, MA 01731-5000

AURIC is an atmospheric ultraviolet spectral transmission and solar irradiance code that is being developed as a modification of MODTRAN. The modification provides an extension of atmospheric structure to allow more than 34 layers, including layers above 100 km. The modification also provides an extension of wavelength to 100 nm. Atmospheric specification will allow compatibility with layer specifications in SHARC. A new O₂ Schumann Runge model is being developed for AURIC, but the initial release will not include airglow emissions.

AERODYNE RESEARCH, Inc. SYSTEMS



ARI FILE NO. 1579-011 V6S/183

AURIC

(ATMOSPHERIC ULTRAVIOLET RADIANCE INTEGRATED CODE)

AN UPDATE

ROBERT HUGUENIN AND ROBERT HICKEY (AERODYNE RESEARCH, INC.)

KEN MINSCHWANER (HARVARD UNIVERSITY)

GAIL ANDERSON, AL HALL AND ROBERT HUFFMAN
(PHILLIPS LABORATORY/GEOPHYSICS DIRECTORATE/AF SYSTEMS COMMAND)

PRESENTED AT
ANNUAL REVIEW CONFERENCE ON ATMOSPHERIC MODELS
PHILLIPS LABORATORY/GEOPHYSICS DIRECTORATE
AFSC, HANSCOM AFB, MA

11-12 JUNE 1991

45 Manning Road Billerica, Ma. 01821-3976 (508) 663-9500 Fax: (508) 663-4918 SYSTEMS



AURIC DEVELOPMENT PROGRAM

GOAL: DEVELOP AN ATMOSPHERIC ULTRAVIOLET SPECTRAL TRANSMISSION AND SOLAR IRRADIANCE CODE FOR DELIVERY TO SDIO BY 30 SEPTEMBER 1991



AURIC DEVELOPMENT PROGRAM

TECHNICAL APPROACH: MODIFY MODTRAN TO INCLUDE AN EXTENSION OF

ATMOSPHERIC STRUCTURE AT ALTITUDES ABOVE 100 KM AND AN EXTENSION OF WAYELENGTH TO 100 NM.

AIRGLOW EMISSIONS WILL NOT BE INCLUDED

SYSTEMS



HIGH ALTITUDE VERTICAL STRUCTURE EXTENSION

- . MODTRAN/LOWTRAN7 CODE MODIFICATION TO REMOVE 33 LAYER LIMITATION
 - MODIFICATION OF EXISTING DIMENSION STATEMENTS
 - DEVELOPMENT OF NTW ORDER INTERPOLATION ROUTINE FOR CONSTITUENT PROFILES
- . USER-DEFINED N-LAYER SPECIFICATION
 - LAYERS CAN BE ADDED ABOVE 100 KM
 - NUMBER OF LAYERS CAN BE INCREASED BELOW 100 KM
 - ALLOWS COMPATIBILITY WITH SHARC LAYER SPECIFICATIONS
- . CONSTITUENT PROFILES WILL BE EXTENDED TO 1000 KM
 - BLOCK DATA STATEMENT EXTENSIONS
 - PROFILE SPECIFICATION IN PROGRESS



SYSTEMS IN THE



HIGH ALTITUDE VERTICAL STRUCTURE EXTENSION (CONT'D)

- STORAGE REQUIREMENTS (VIRTUAL MEMORY USED)
 - TESTS PERFORMED ON MICROVAX WITH MODTRAN CONSTITUENT PROFILES

MODTRAN - APPROXIMATELY 533 KBYTES
AURIC (50 LAYERS) - APPROXIMATELY 558 KBYTES
AURIC (100 LAYERS) - APPROXIMATELY 670 KBYTES
AURIC (200 LAYERS) - ESTIMATED, APPROX. 1 MBYTE

ALL CURRENT FUNCTIONALITY OF MODTRAN/LOWTRAN7 HAS BEEN RETAINED

SYSTEMS



EXOATMOSPHERIC SOLAR IRRADIANCE EXTENSION

- INITIAL WAVELENGTH EXTENSION TO 1205A
 - USE OF SUSIM (4000 1205A) TABLES PLANNED
 - NOMINAL 14 RESOLUTION DATA WITH INTERPOLATION
- · SELECTION OF SOLAR ACTIVITY MODEL IN PROGRESS



02 SCHUMANN-RUNGE MODEL UPGRADE

- BASED ON FIRST PRINCIPLES MODEL BY K. MINSCHWANER AND M. MCELROY (HARVARD UNIVERSITY)
- DEVELOPMENT OF FACTORABLE TEMPERATURE DEPENDENCE MODEL FOR COMPATIBILITY WITH MODTRAN/LOWTRAN TRANSMISSION FORMULATION

SYSTEMS



HARVARD SCHUMANN-RUNGE MODEL FEATURES

- . $\chi^3\Sigma_G^-$ and $B^3\Sigma_U^-$ energy levels from spectroscopic constants (yeseth and Lofthus, 1974; cheung et al. 1986)
- ROTATIONAL DEPENDENCE OF PREDISSOCIATION WIDTHS (CHEUNG ET AL, 1990; LEWIS ET AL, 1989)

SYSTEMS -



HARVARD SCHUMANN-RUNGE MODEL FEATURES (CONT'D)

- BAND OSCILLATOR STRENGTHS (YOSHINO ET AL, 1983; LEWIS ET AL, 1986); HÖNL-LONDON FACTORS (TATUM AND WATSON, 1971); FULL BOLTZMAN CALCULATION TO DETERMINE INDIVIDUAL LINE STRENGTHS
- VIBRATION: V' = 0, 1 AND 2 V" = 0 TO 19
- ROTATION: N" = 1 TO 51 N' = 0 TO 50



SYSTEMS



HARVARD SCHUMANN-RUNGE MODEL FEATURES (CONT'D)

- . 2 PRINCIPAL BRANCHES (AN = AJ = ± 1)
- 6 SATELLITE BRANCHES ($\Delta N = \pm 1$; $\Delta J = 0$, ± 1 ; $\Delta N + \Delta J$)
- 2 FORBIDDEN LINES ($\Delta N = \pm 3$, $\Delta J = \pm 1$)
- . ISOTOPIC OXYGEN LINES 160 180
- . UNDERLYING HERZBURG, SCHUMANN-RUNGE CONTINUA INCLUDED



HARVARD SCHUMANN-RUNGE MODEL FEATURES (CONT'D)

- INPUT
 - 02 SPECTROSCOPIC CONSTANTS
 - BAND OSCILLATOR STRENGTHS
 - LINE WIDTHS (FUNCTIONS OF UPPER STATE VIBRATIONAL /ROTATIONAL LEVELS)
 - TEMPERATURE
- CALCULATION
 - ENERGY LEVELS
 - POPULATION DISTRIBUTION
 - LINE POSITIONS
 - LINE STRENGTHS
- SPECTRAL CALCULATION

 $\sigma(v) = \Sigma$ ALL LINES WITHIN 500 CM-1; VOIGT LINE PROFILES

 VALIDATION AT 79°K AND 300°K FROM MEASUREMENTS BY HARVARD-SMITHSONIAN GROUP



SYSTEMS



SCHUMANN-RUNGE TEMPERATURE DEPENDENCE MODEL

. MODTRAN/LOWTRAN TRANSMISSION FORMULATION

$$\tau_{v} = \exp \left\{ -\sum_{t} (a_{v} + b_{v} T_{t} + C_{v} T_{t}^{2}) n_{t} \right\}$$

$$= \exp \left\{-a_{v} \sum_{\underline{\ell}} N_{\underline{\ell}} - b_{v} \sum_{\underline{\ell}} T_{\underline{\ell}} n_{\underline{\ell}} - c_{v} \sum_{\underline{\ell}} T_{\underline{\ell}}^{2} n_{\underline{\ell}}\right\}$$

STORED COLUMN AMOUNTS

• TEMPERATURE DEPENDENCE MUST BE FACTORABLE, YIELDING (A., B., C.) vs. v

$$eg \ \sigma_{_{\boldsymbol{V}}} \ (T) = a_{_{\boldsymbol{V}}} + b_{_{\boldsymbol{V}}} \ T + c_{_{\boldsymbol{V}}} \ T^2$$

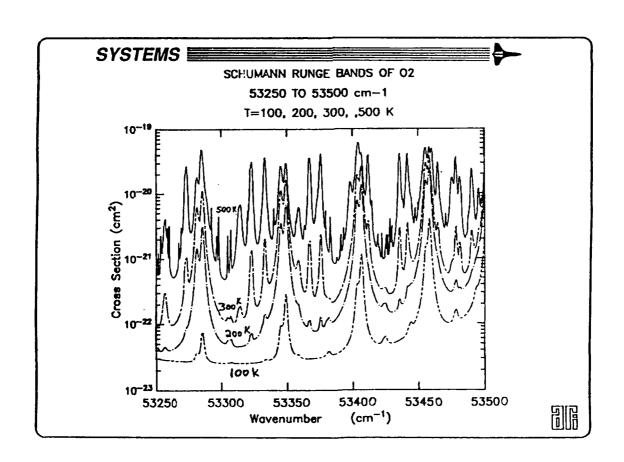
or
$$\sigma_{v}(T) = a_{v} + b_{v}T^{2} + c_{v}T^{4}$$

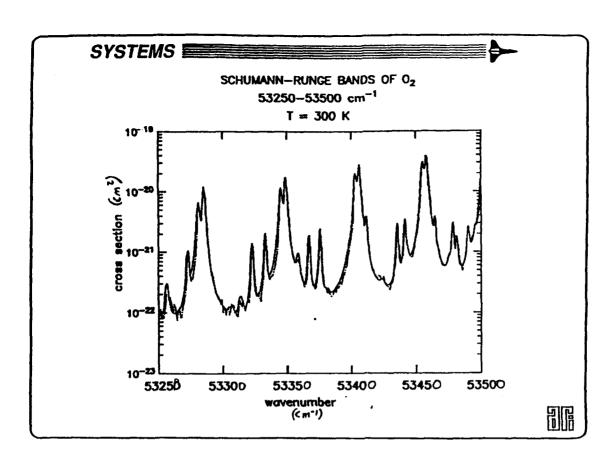


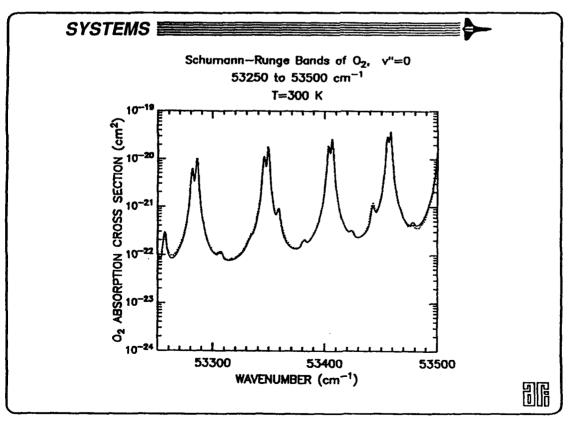


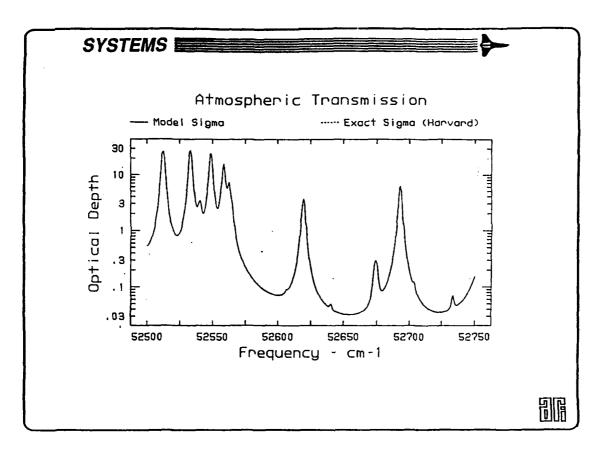
SCHUMANN-RUNGE TEMPERATURE DEPENDENCE MODEL (CONT'D)

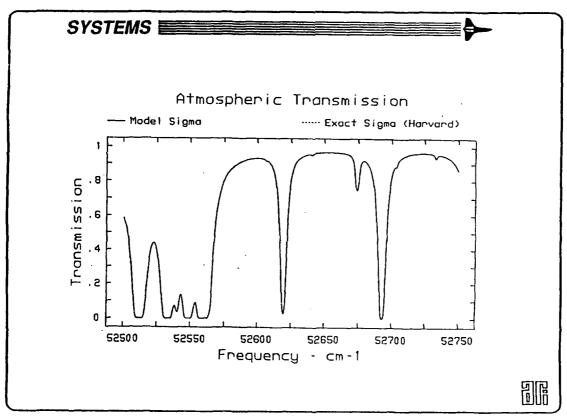
- WORK IS PROCEEDING TO DETERMINE THE BEST SET OF BASIS FUNCTIONS AND OPTIMAL FITTING PROCEDURES TO COVER TEMPERATURE RANGE OF 100 - 500°K
 - HOT AND COLD BANDS HAVE DIFFERENT TEMPERATURE DEPENDENCES
 - ATTEMPTING TO FIT CROSS-SECTIONS WITH POLYNOMIALS IN TEMPERATURES
 - DIFFERENT FITTING PROCEDURES REQUIRED ABOVE AND BELOW 275-300°K
 - DOUBLE QUADRATIC FIT, PINNED TO 275°K DATA POINT YIELDS PROMISING RESULTS

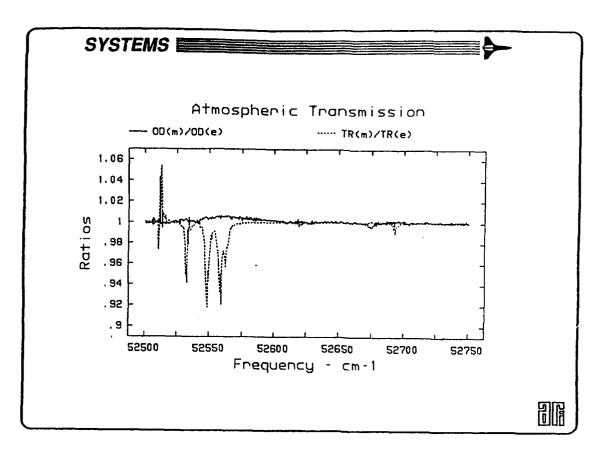


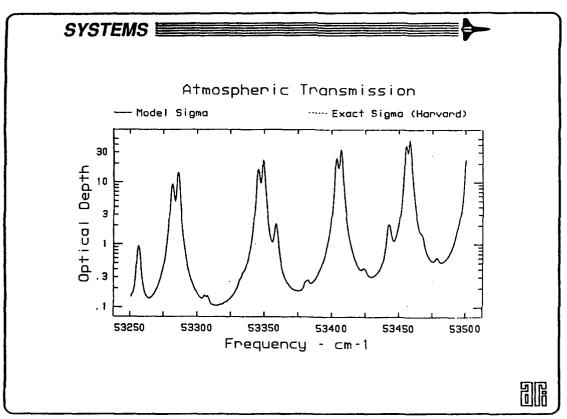


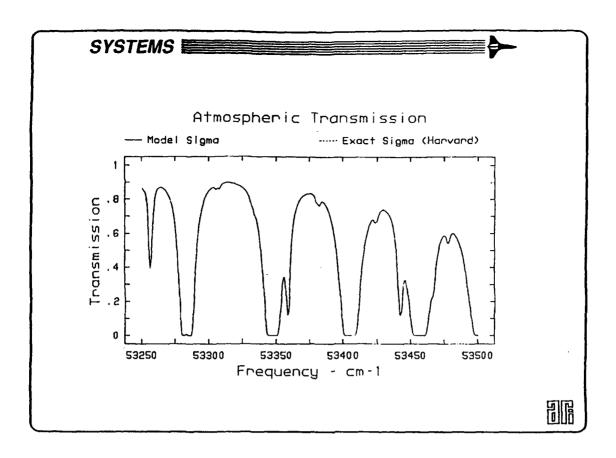


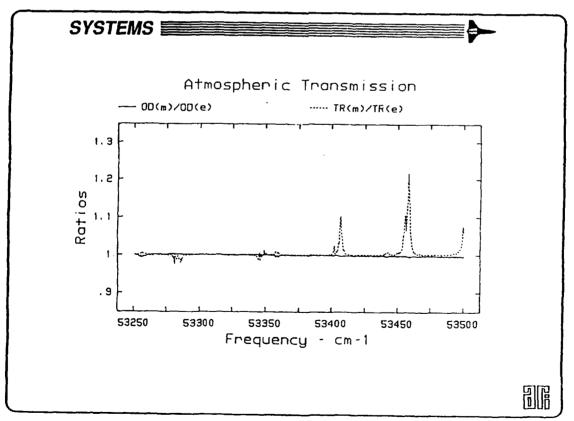














SUMMARY

- . AURIC IS AN EXTENSION OF MODTRAN
 - EXTENDED ATMOSPHERIC STRUCTURE
 - = 33 LAYER LIMITATION REMOVED
 - = LAYERS CAN BE ADDED ABOVE 100 KM
 - CONSTITUENT PROFILES EXTENDED TO 1000 KM
 - WAVELENGTH RANGE EXTENDED TO 1205 &
 - = EXTENSION OF EXOATMOSPHERIC SOLAR IRRADIANCE
 - ADDITION OF IMPROVED 02 SCHUMANN-RUNGE MODEL
 - FULL MODTRAN FUNCTIONALITY RETAINED
- AURIC PROVIDES ATMOSPHERIC SPECTRAL TRANSMISSION AND SOLAR IRRADIANCE
- . AURIC 1.0 WILL NOT INCLUDE AIRGLOW EMISSIONS
- . DELIVERY TO SDIO BY 30 SEPTEMBER 1991

ONTAR'S PC COMPATIBLE LOWTRAN7 PACKAGE

P.V. Noah, J. Schroeder Ontar Corporation, 129 University Road, Brookline, MA 02146

PCTRAN7 is an implementation of the Phillips Laboratory/Geophysics Directorate's LOWTRAN7 model and associated software for the IBM and compatible family of personal computers. The package contains software for input generation, help for LOWTRAN7 parameters, an ASCII text file viewer for output files, screen graphics capability, and hard copy graphics. The software has been validated by the PL/GP under a cooperative IR&D agreement with Ontar.

This paper will describe PCTRAN7, Version 2a, and demonstrate the capabilities of the package.

PCTRAN 7 [c]: An Implementation of the GP's LOWTRAN 7 Model for the Personal Computer

USERS MODELING WORKSHOP (LOWTRAN/MODTRAN/FASCODE-HITRAN)

PL/GP Hanscom AFB, MA

11 June 1991

Paul V. Noah and John Schroeder

Ontar Corporation
129 University Road
Brookline, MA 02146 - 4532

Tel: 617-739-6607 FAX: 617-277-2374



Cooperative R & D Agreement

With Geophysics Laboratory - Hanscom AFB, MA

September 1988

PC Implementation of a Software Package - LOWTRAN 7 - PCTRAN 7 [c]



LITERATURE AVAILABLE

SOFTWARE DEMONSTRATION

Ontar Corporation
129 University Road
Brookline, MA 02146 - 4532

Tel: 617-739-6607 FAX: 617-277-2374 Bulletin Board: 617-277-6299



PL/GP LOWTRAN 7 CODE

Computes Atmospheric Transmission and Radiance.

0 to 50,000 Cm⁻¹ Spectral Coverage @ 5 to 20 Cm⁻¹ Resolution.

All Viewing Geometries.

Default Atmospheric Profiles from Sea Level to 100 Km.

Capability for User Supplied Profiles.

Cloud, Rain and Aerosol Models.

Band Models for H_2O , O_3 , N_2O , CH_4 , CO, O_2 , CO_2 , NO, NO_2 , NH_3 and SO_2 . New UV parameters for O_2 (Schumann-Runge bands and Herzberg continuum) and updated O_3 Hartley and Huggins bands.



PCTRAN 7 [c] * Version 2a

PC Version of the PL/GP LOWTRAN 7 Atmospheric Radiance & Transmission Code

Complete Implementation of the LOWTRAN 7 Code - Release 3.8.

Installation Program.

Interactive User Input Software.

Help Screens for All Input Variables.

Screen and Hard Copy Graphics Output.

Tabular Output in ASCII Format.

Batch Processing Input Software.

Plotting from Different LOWTRAN Calculations.

Expert Help.

CERTIFIED for ACCURACY by the GEOPHYSICS DIRECTORATE.



Hardware and Software Requirements

Personal Computer - XT, AT, 80386, 80486 (Compatible, Clone)

1.2 Mbyte Diskette Drive, Hard Disk

640 Kbytes of Memory

CGA, EGA, or VGA Graphics Board and Monitor - for Screen Plots

Printer - for Hard Copy

Numeric Co-processor Highly Recommended



Setup Program

Semi-automatic Installation Procedure.

Copies all files to target drive.

Sets up Printer Support.

Defines Graphics Adapter Type.

Capable of Printer ONly Installation.

Checks Available Disk Space.

ONTAR Corporation, 129 University Road, Brookline, MA 02146, 617-739-6607

4MMA

ONTAR's LOWTRAN Modules Program Suite -- Version 7.2a LOWTRAN7/MODTRAN/SENTRAN

a.	Input Shell
b.	Execute Program
c.	Data Plotting
d.	Printer Plotting
e.	View Data Output
f.	View FILE7
g. h.	View FILE8
	Filter Input
i.	Execute Filter Program
j. k.	View Filter Output
k.	Execute Scanning Program
l.	Scanning Plotting
m.	View FILE9
n.	Multiple FILE7 Plots
0.	Expert Help
x.	Return to DOS

Input Function:

4217A21

Initial Altitude (km)	1.500
Final Altitude/Tangent Height (km)	10.000
Initial Zenith Angle (degrees)	.000
Path Length (km)	.000
Earth Center Angle (degrees)	.000
Radius of Earth (km) [.000 - default]	.000
Type of Path	Short

Initial Frequency 2000.000 cm-1 Wavelength 4.000 m

Final Frequency 2500.000 cm-1 Wavelength 5.000 m

Frequency Increment (wavenumber) 5.000

Run # 2 of 4 LOWTRAN7 Cards 3 & 4

OHTAR

PC-TRAN7 Batch Mode Manager.

ESC -	Quit LOWIN (write LOWIN and LOWPLT.DAT)
F0	

F2 - Edit current run.

F3 - Edit next run.

F4 - Edit previous run.

F5 - Add new run (to end) and go to that run

F6 - Delete current run.

F7 - Go to run.

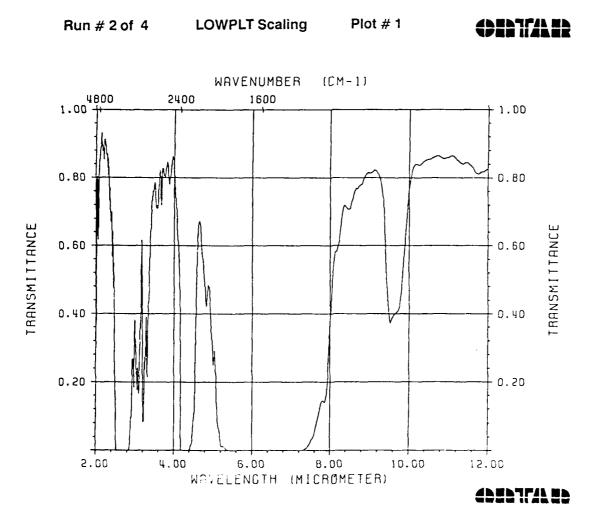
Database name MCASE3

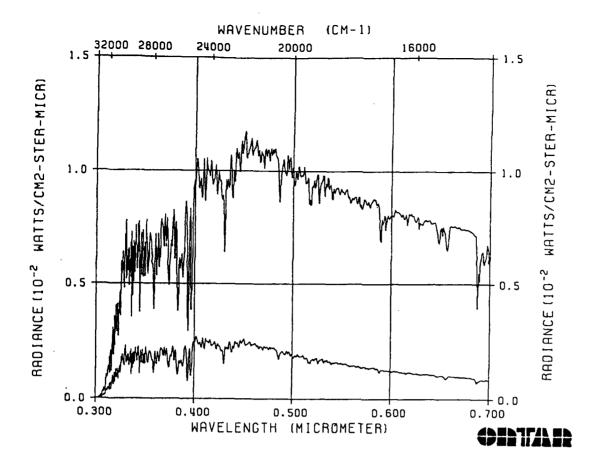
Number of runs in this database 4 Current run 3

LOWTRAN7 Card 5

GENTALE

Plot Type	Transmittance in m
Type of X Axis	Linear
Type of Y Axis	Linear
Number of Decimal Digits for Y Axis	2
Length of X Axis (in inches)	7.0000
Beginning Wavenumber/Wavelength	4.0000 m
Ending Wavenumber/Wavelength	5.0000 m
X Axis Annotation Interval	.2000 m
X - Number of Minor Ticks / Division	5
Length of Y Axis (in inches)	6.0000
Autoscale Y Axis	No
Minimum Transmittance/Radiance	.00E+00
Maximum Transmittance/Radiance	1.00E+00
Y Axis Annotation Interval	2.00E-01
Y - Number of Minor Ticks / Division	5
Plot Grids (Graph Paper)	Coarse Grid



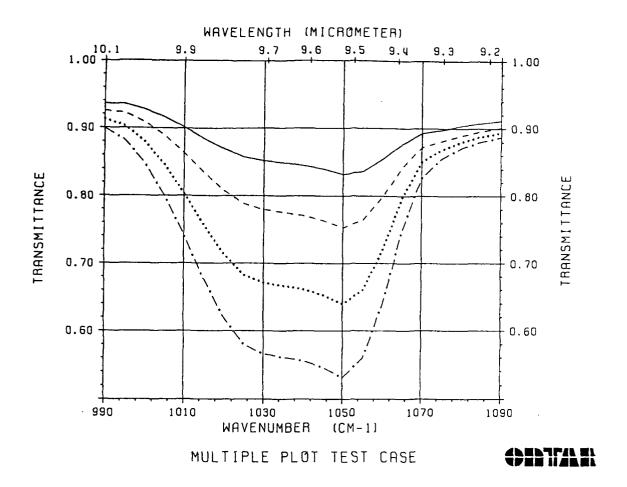


Multiple Run Plotting Inputs

Filename	Run	Plot Mode	Title
CASE-A CASE-A CASE-A CASE-B CASE-B CASE-B CASE-B CASE-C CASE-C	1 2 3 4 1 2 3 4 1 2 3	Transmittance Transmittance Radiance /w Scattering Radiance Transmittance Radiance Radiance /w Scattering Transmittance Transmittance Radiance Radiance Radiance Radiance Radiance	1976 U S STANDARD SUBARCTIC WINTER SUBARCTIC SUMMER MIDLATITUDE SUMMER 1976 U S STANDARD TROPICAL MODEL MIDLATITUDE SUMMER SUBARCTIC SUMMER 1976 U S STANDARD TROPICAL MODEL New Model Atmosphere Met Data (Hor Path)
CASE-C	4	ransmillance	Met Data (1101 Fath)

LOWMPIN Select Runs





PCTRAN7 Expert Help

Online Expert Help.

Guides you through common user problems.

Draws on over 5 years of PCTRAN user support.

Aides in selecting Appropriate Model:



Helps in model parameter selection/setup.



COUPLING ATMOSPHERE AND BACKGROUND EFFECTS*

W.M. Cornette
Photon Research Associates, Inc., 9393 Towne Centre Drive, Suite 200,
San Diego, CA 92121

The available atmospheric transmission models typically represent the atmosphere in significant detail, but have traditionally modelled the background very simplistically, if at all. The impact that the atmosphere has on the background (e.g., convection, evaporation, condensation, evapotranspiration, radiative loading, cloud shadowing) has recently been modelled in some detail in a computer code developed for the U.S. Army Atmospheric Sciences Laboratory (ASL). This presentation will outline the model and will discuss some of the additional atmosphere-to-background and background-to-atmosphere coupling required (e.g., surface air heating by the background).

*This work was funded by the U.S. Army Atmospheric Sciences Laboratory under

Contract No. DAAD07-90-C-0149; Dr. Patti Gillespie, Technical Monitor

COUPLING ATMOSPHERE AND BACKGROUND EFFECTS

JUNE 1991

Presented at the 14th Annual Review Conference on Atmospheric Transmission Models 11-12 June 1991, Geophysics Directorate, Phillips Laboratory, Hanscom AFB, MA

Work Funded in Part by the U.S. Army Atmospheric Sciences Laboratory Under Contract No. DAAD07-90-C-0149; Dr. P. Gillespie, Technical Monitor

Presented By:

Dr. William M. Cornette

Photon Research Associates, Inc. 9393 Towne Centre Drive, Sulle 200 San Diego, CA 92121

8-068 81



OBJECTIVE

Development of a Computer Model Which May be Used to Characterize the Amount of Thermal Clutter in a Scene Viewed by a Thermal Imager and How the Clutter Level Changes with Changing Atmospheric Conditions



ATMOSPHERIC EFFECTS ON BACKGROUND

- Temperature
 - Convection
 - Evaporation/Condensation/Evapotranspiration
- Radiative Loading
 - Direct Solar Loading
 - Scattered Solar Loading
 - Thermal Loading
 - Scattered Thermal Loading
- Background Type
 - Polar Regions
 - Mid-Latitudes
 - Deserts
 - Tropics

PRAM

ENERGY FLUX

- Radiation
 - Emitted
 - Absorbed Solar
 - Absorbed Thermal
- Sensible (Direct)
 - Free Convection
 - Forced Convection
- Latent (indirect)
 - Evaporation
 - Condensation
 - Evapotranspiration
- Ground/Submedium
 - Conduction
 - Convection (Water)

9 048 91 3

8-068 B1 Z



TERRAIN MATERIALS

- Water
- Snow
- Ice
- Broadleaf Trees
- Pine Trees
- Irrigated Low Vegetation
- Meadow Grass
- Tundra
- Scrub
- Sand
- Rock
- Packed Dirt
- Tilled Soil
- Urban Commercial
- Urban Residential
- Asphalt
- Concrete
- Metal Building Roof
- Summer and Winter Variations

PRA-

PARAMETERS

- Atmosphere
 - Pressure Profile
 - Temperature Profile
 - H₂O, CO₂, O₃ Profiles
 - Wind Speed
 - Cloud Cover and Altitude
- Background
 - Solar Absorptivity
- From Reflectivity
- Thermal EmissivityThermal Conductivity
- Submedium Temperature
- Roughness
- Density
- Specific Heat
- General
 - Latitude
 - Time
 - Date

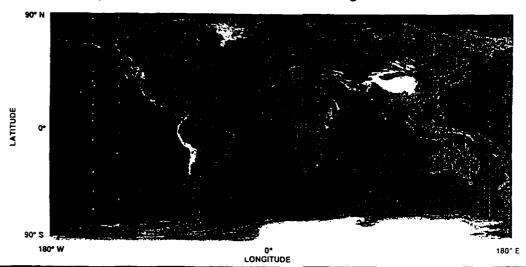
8 040 01 5

.



TERRAIN ALTITUDE MAP

- National Geophysical Data Center (NGDC) Global 10-Minute Terrain Data Base
- Resample with 1º Latitude and Variable Longitude Resolution





GLOBAL TERRAIN SCENES (DETERMINISTIC)

- City/Harbor Land/Sea Interface
- Arctic Tundra Land/Sea Interface
- Forested Low Relief Terrain
- Subarctic Rocky Land/Sea Interface
- Forested Terrain/Agricultural Terrain
- Flat Agricultural
- Desert Pavement with Dunes
- Desert Land/Sea Interface
- Forested Mountains/Cultural
- Multi-Year Sea Ice
- Arctic Mountains with Scrub
- Arctic Tundra with Melt Lakes
- Open Ocean
- Mixed Farmlands/Orchards
- Southern California Land/Sea Interface

San Diego, CA
Point Barrow, AK
Wa Wa, Ontario, Canada
Trondheim, Norway
Fulda, Germany
Alberta, Canada
Imperial Valley, CA
Salton Sea, CA
Santa Cruz, CA
Beaufort Sea
Brooks Range, AK

Camarillo, CA Southern California

.....

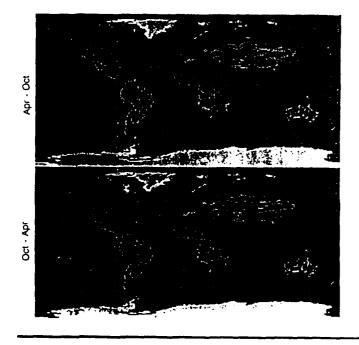


GLOBAL TERRAIN SCENES (MODIFIED)

- Tundra
- Pine Forest
- Mixed Forest/Farmland
- Grass Land Savannah
- Scrub Chaparral
- Scrub Desert
- Urban
- Rural Land/Sea Interface
- Tropical Forest
- Tropical Savannah
- Tropical Desert
- Tropical Land/Sea Interface



SCENE TYPE MAP



Blue - Ocean

Light Blue - Sea Ice

White - Continental Ice

Green - Tropical Forest

Tan - Grassland

Brown - Scrub Desert

Grey - Mixed Forest/Farmland

Red - Forested Mountains

Pink - Arctic Mountains

Purple - Tropical Savannan

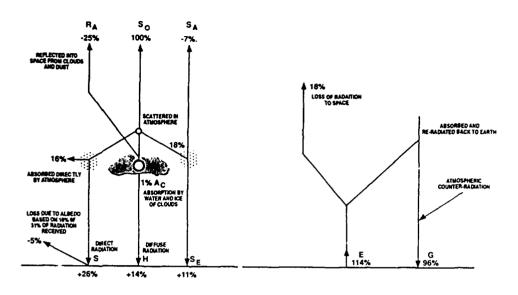
Black - Other



HEAT BALANCE OF THE EARTH

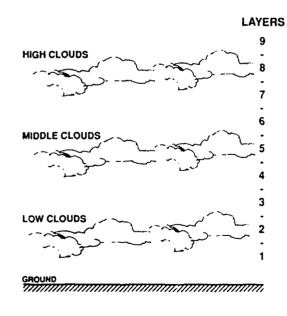
Solar Radiation

• Terrestrial Radiation



PRAM

HEAT TRANSFER



- Short Wave (α_s) (0.25 - 4.0 μm)
 - Direct Beam
 - Upward Diffuse
 - Downward Diffuse

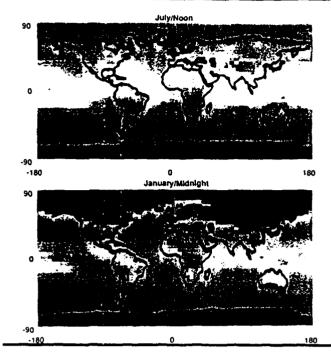
8-046 61 10

. ...

- Long Wave (ϵ_{th}) (4.0 μ m 25 μ m)
 - Upward Diffuse
 - Downward Diffuse
- Multiple Scattered



SURFACE TEMPERATURE MAPS



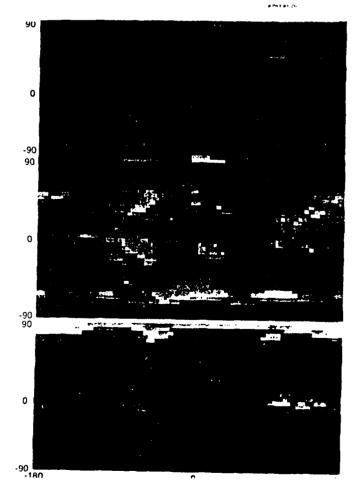
- NOAA Nimbus-7 C-Matrix Data Base
- Air Force Surface Temperature Analysis Base



CLOUD COVER MAPS

(NOAA NIMBUS-7 C-MATRIX DATA BASE)

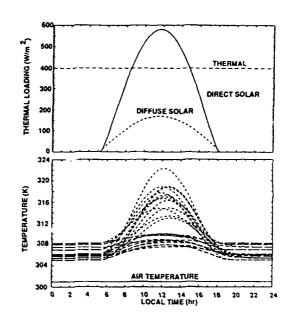
JANUARY/MIDNIGHT





TROPICAL ATMOSPHERE

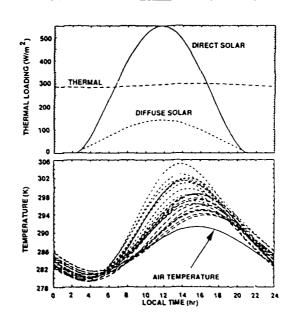
- Thermal Loading by Atmosphere Dominates at Night
- Heavy Cloud Cover Prevents Cooling at Night
- No Day-Night Air Temperature Variations





SUBARCTIC SUMMER ATMOSPHERE

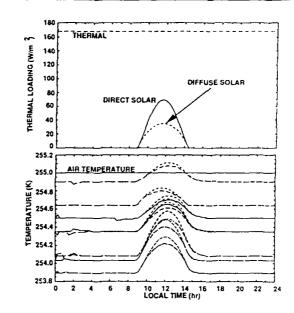
- Driven by Local Air Temperature
- Cooling Observed at Night Below Local Air Temperature
- Large Day-Night Air Temperature Variations





SUBARCTIC WINTER ATMOSPHERE

- Small Thermal and Solar Effects
- No Day-Night Air Temperature Variations
- Numerical "Noise" of Algorithm Seen in Temperature Curves



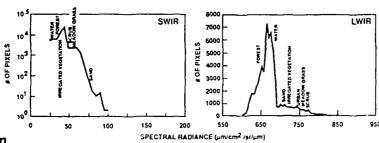
8-068-91-14

....

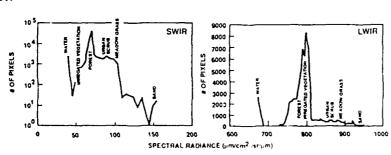


SANTA CRUZ, CALIFORNIA, SCENE

• Dawn Plus One Hour



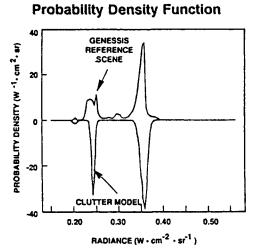
• Noon



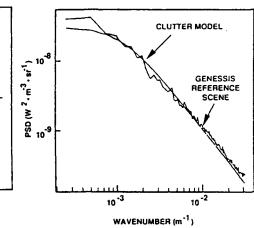


FULDA, GERMANY, SCENE

- Noon
- 3.7 4.1 µm



Power Spectral Density

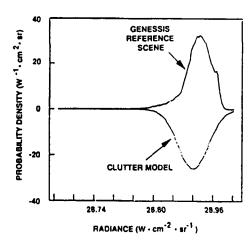




OPEN OCEAN SCENE

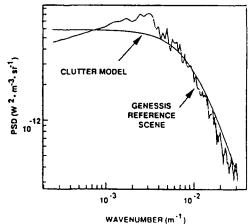
• 8 - 12 µm

Probability Distribution Function



Power Spectral Density

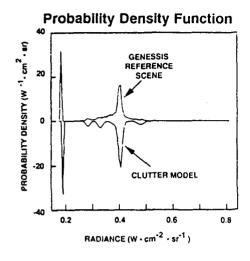
.....

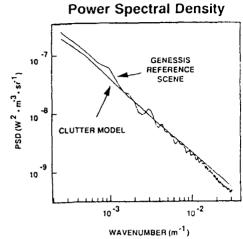




SAN DIEGO, CALIFORNIA, SCENE

- Noon
- 3.7 4.1 µm





SKY NOISE

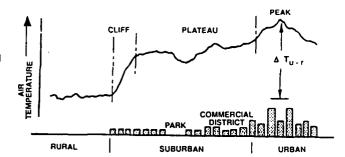
- Thermal Sky Noise

 - Due to Temperature Fluctuations
 Derived from C_n² Profiles
 Based on Work of Kent and Korf at AMOS
- Scatter Sky Noise (Pending)
 - Variations in Aerosol Number Density
 - Variations in Aerosol Particles
 - Variations in Molecular Density
 - Variations in Index of Refraction



BACKGROUND EFFECTS ON ATMOSPHERE

- Altitude/Profile
- Atmospheric Heating
- Free Convection
- Wind Speed and Direction
- Relative Humidity
- Pollutants
- Aerosols
- Turbulence
- Cloud Cover/Type/Altitude



PR/4---

CURRENT STATUS

- CLUTTR Code Developed
 - Calculates PDF's and PSD's
 - Includes Atmospheric Thermal Sky Noise
 - Includes Sensor Effects, Including Human Factors
- Future Development
 - Add Atmospheric Scatter Sky Noise
 - Improve Interfaces
 - Validate Algorithms and Data Bases
 - Extend Data Bases

8-068 81 20

SENTRAN7: A SENSITIVITY ANALYSIS PACKAGE FOR LOWTRAN 7 AND MODTRAN

D.R. Longtin, F.M. Pagliughi, N.L. Paul SPARTA, Inc., 24 Hartwell Avenue, Lexington, MA 02173

The computer code SENTRAN, originally developed by researchers at The Pennsylvania State University, permits users to rapidly evaluate transmittances and radiances from LOWTRAN in response to perturbations of input atmospheric conditions. The code provides a friendly and efficient interface to create multiple LOWTRAN input decks as well as graphical representation of the output in both 2D and 3D formats.

In the current effort, SENTRAN has been upgraded for use with LOWTRAN 7 and MODTRAN. The new computer code is called SENTRAN7. As part of the upgrade, SENTRAN7 contains improved error checking on user inputs, an enhanced online help capability and smarter editing restrictions that reflect inputs from other LOWTRAN 7 or MODTRAN input cards. Additionally, users are able to graphically display results from the standard TAPE7 and TAPE8 files. New features of SENTRAN7 include the capability to run LOWTRAN 7 or MODTRAN internally, and screen display of available input files. Finally, the framework for a sensitivity package for FASCODE will be discussed.

SENTRAN7: A SENSITIVITY ANALYSIS PACKAGE FOR LOWTRAN7/MODTRAN

Presented at

The Annual Review Conference on Atmospheric Transmission Models

June 12, 1991

David R. Longtin, Nanette L. Paul and Frank M. Pagliughi

SPARTA, Inc. 24 Hartwell Avenue Lexington, MA 02173

Contract F19628-88-C-0038



Acknowledgements

- We Wish to Thank the Following Individuals
 - Gail Anderson and Jim Chetwynd of The Geophysics Directorate
 - Charles Randall of The Aerospace Corporation
 - Charles Lo Presti of The Battelle Pacific Northwest Laboratory
 - Ken Tomiyama and Michael Hogan of The Pennsylvania State University



Outline of Talk

- Introduction to SENTRAN7
 - Software and Hardware Requirements
- Capabilities of SENTRAN7
 - Examples of Menus
 - New Features
- Ongoing Efforts
 - Sensitivity Package for FASCODE, SENCODE



What Is SENTRAN7?

- User Interface System Designed to Evaluate the Sensitivity of LOWTRAN7/MODTRAN* Transmittances and Radiances to Input Variations
 - Interactive Input Module to Perturb LOWTRAN7/MODTRAN Input Parameters
 - Automatic Generation of LOWTRAN7/MODTRAN Input Decks
 - Autonomous Post-Processing of TAPE7 and TAPE8 Outputs
 - Graphical Representation of Output in 2D and 3D Formats
- Based on Original SENTRAN for LOWTRAN6 By K. Tomiyama and M. Hogan
- * MODTRAN: Moderate Resolution Model for LOWTRAN7 Developed By Spectral Sciences, Burlington, MA



Software and Hardware Details For SENTRAN7

- Structural Design
 - SENTRAN7 Coded in Fortran-77
 - Graphics Consistent with Tektronix 4014 Standards
 - Terminal Control Follows ANSI Standards
- Hardware Requirements
 - Software Developed for VAX/VMS and SUN Unix Computer Systems
 - Interactive Viewing of SENTRAN7 Graphics Use VT240 Terminal or Emulator
 - Hard Copy Output Requires Tektronix 4014 Compatible Printer/Plotter or Device Able to Interpret Tektronix 4014 Files via Special Translating Programs
- SENTRAN7 Utilizes Standard Input and Output Formats from LOWTRAN7/MODTRAN Codes



Main Menu of SENTRAN7

SENTRAN7 SUN4/Unim Version	SPARTA, Inc
WELCOME TO SESTRANT	
THE SENSITIVITY ANALYSIS PROGRAM FOR LOWTRANT,	HODTRAH
1 - LOAD/SAVE	
2 - ZDIT	
3 - COMPILE	
4 - SELECT LOWIRAM7/MODTRAM	
5 - ROW LOWTRAN7	
6 - CRAPH & AMALYZE	
7 - HELP	
8 - QUIT	
n	
7 []	

MARTA NG.

Description of Main Modules

- LOAD/SAVE: Load or Save SENTRAN7 Methodology Files
 - Methodology Files Contain Images of LOWTRAN7 Input Cards and Directives for Their Perturbation
- EDIT: Interactive Editing Module for Specifying LOWTRAN7 Cards and Directives for Their Perturbation
 - Editor Emulates Logical Flow Through LOWTRAN7 Input Decks
 - Each LOWTRAN7 Input Described by a Nominal Value and an Optional Perturbation Directive
- COMPILE: Creates LOWTRAN7 Input Decks Based on Information in the EDIT Module
 - Provides List of Active Molecular Absorbers in the Spectral Interval of Interest



Description of Main Modules (cont.)

- SELECT LOWTRAN7/MODTRAN: Determines Code To Be Run.
- RUN LOWTRAN7/MODTRAN: Executes Selected Code
- GRAPH AND ANALYZE: Generates Graphical Plots of Data
 - Screen or Files For Hard Copy Available
 - Additional Features Include Data Manipulation and Analysis
- HELP: Provides Information About and Examples For Most SENTRAN7 Commands
- QUIT: Exit SENTRAN7 Code



Edit Module: Editing Card 3

SENTRAN	7 : SUN4/Unix	Version		SPARTA, Inc.			
SENTRAN7 EDITING UTILITY							
EDITING CARD 3							
t				1			
LOTTOMING	PARAMS. USE A	PERTURBATION	VALUE				
н1	0.000 TO	20 STEP 2					
н2	0.000						
	0.000						
RANGE	1.000 TO	10					
	0.000						
	0.000						
LOTTOMING	PARAM. USES A	PERTURBATION	LIST (* IMPLIES	PERTURBATION RESTRICTIONS)			
LEN A	0						
	U						
1							
1							
ALL PARAMI	TERS FOR CARD	3 O.K. (Y/N)	r⊠ı				
			·D·				
1							



Graph and Analyze Module

Main Capabilities

- Handles TAPE7 and TAPE8 Files from LOWTRAN7 Plus Raw X-Y-Z Data Files
- Includes Tools for Data Analysis and Archiving
- Generates Screen Plots of Data and Graphics Files for Hard-Copy Output

• 3-D Plotting Details

- Permits User-Defined Rotation Angles
- X and Y Axes Can Represent Wavenumber, or the First or Second LOWTRAN7 Variables Perturbed
- Conversion to Micrometers Are Available
- Plots For Layer-By-Layer Calculations from TAPE8 Always Make X-Axis the Wavenumber and and Y-Axis the Layer Number



Available Plots in SENTRAN7

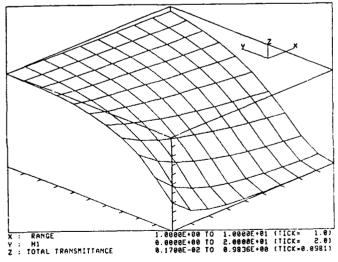
PLOT CATEGORY1	SPECIFIC PLOTS				
Raw-XYZ					
Transmittance	Transmittance: total, log of total, uniform mixed gases, trace gases, molecular scattering, H ₂ O, H ₂ O continuum, O ₃ , N ₂ continuum, aerosol and hydrometeor, CO ₂ , CO, CH ₄ , N ₂ O, O ₂ , NH ₃ , NO, NO ₂ , SO ₂ , HNO ₃ Aerosol and Hydrometeor Absorption				
Thermal Radiance	Transmittance: total, log of total Atmospheric Radiance				
Differential Transmittance and Black Body Function	Differential Transmittance (DTAU), DTAU/layer thickness DTAU*BB function, DTAU*BB function/layer thickness				
Fluxes/Irradiance	Fluxes: upward total, upward solar, downward total, downward solar Direct Solar Irradiance				
Solar/Lunar Radiance	Transmittance: total, log of total Radiance: total, atmospheric, path scattered, single scattered, total ground reflected, direct reflected				
Direct Solar Radiance	Transmittance: total, log of total, solar irradiance Incident Solar Irradiance				

¹ Plot Category Determined By Values of IEMSCT, IMULT, NOPRT



Example 3-D Plot From SENTRAN7

SPARTA INC.



Total Transmittance at 1300 cm⁻¹ Versus H1 and RANGE for a Horizontal Path

Other Features of SENTRAN7

- Original SENTRAN Code Upgraded for Use with LOWTRAN7
 - Smarter Editing Restrictions That Reflect Previous User Inputs
 - Improved Error Checking on User Inputs
 - Refined Identification of Major Molecular Absorbers
- New Features in SENTRAN7
 - Compatibility with the Moderate Resolution Code, MODTRAN
 - Ability to Access LOWTRAN7/MODTRAN Codes Internally
 - Screen Display of Available Methodology and Other Input Files
 - Safeguards to Prevent Existing Files From Being Overwitten
 - Increased Portability Across Hardware Platforms
 - Online Help Available Within Editing Module
 - Tick Marks on Plots
 - Graphical Display of User-Defined Trace Gas Profiles, Card 2C Series



Ongoing Work: Sensitivity Package For FASCODE, SENCODE

SPARTA INC.

- General Approach
 - Develop Parallel Package For FASCODE, But Retain SENTRAN7 Framework
 - Use Many of SENTRAN7's Supporting Routines
 - Limit Those FASCODE Input Cards That Can Be Perturbed
- Future Obstacles
 - Method of Effectively Dealing With FASCODE Output Files
 - Output May Exceed SENTRAN7's Plotting Capabilities
 - Some Sensitivity Studies May Grossly Interfere with FASCODE's Atmospheric Layering Package

ATMOSPHERIC MODELS IN THE STRATEGIC SCENE GENERATION MODEL*

W.M. Cornette, D.C. Anding Photon Research Associates, Inc., 9393 Towne Centre Drive, Suite 200, San Diego, CA 92121

The Strategic Scene Generation Model (SSGM) produces scenes of interest to a strategic space-based sensor, including terrain, clouds, earth limb, aurora, zodiacal light, and stars as background; and missile plumes and fuselages, post-boost and reentry vehicles as targets. In support of the various components of the SSGM are several atmospheric codes, which provide basic information regarding transmission and emitted and scattered path radiance, plus additional information required by the various background and target models. An overview of the SSGM will be presented, with emphasis on how the various atmospheric models are utilized. Comparisons between the codes will be presented, together with recommendations for upgrades to insure consistency.

*This work is being funded by the Naval Research Laboratory under Contract No.

N00014-89-C-2283; H. Heckathorn, Technical Monitor.

ATMOSPHERIC MODELS IN THE STRATEGIC SCENE GENERATION MODEL

JUNE 1991

Presented at the 14th Annual Review Conference on Atmospheric Transmission Models 11-12 June 1991, Geophysics Directorate, Phillips Laboratory, Hanscom AFB, MA

Work Funded in Part by Naval Research Laboratory Under Contract No. N00014-89-C-2283 H. Heckathorn, Technical Monitor

Presented By:

Dr. William M. Cornette David C. Anding

PRAM

Photon Research Associates, Inc. 9393 Towne Centre Drive, Suite 200 San Diego, CA 92121

PRA-MPhoton Research Associates, Inc.

STRATEGIC SCENE GENERATION MODEL (SSGM)



TASC

- Definition
 - Computerized Methodology Founded on State-of-Science Knowledge, Empirical Data Bases, Phenomenological Models to Generate LOS Radiometrics, 2-D Radiance Maps, Time-Sequenced Scenes, and Observables Data Bases for SDI Applications



- Objectives:
 - Provide Focus for SDIO Scene Generation Requirements



- Serve as a Standard for Testing SDI Concepts and Designs Which is Traceable to a Consistent Set of Physical Assumptions, Conditions
- Requirements:

GO TELEDYNE

- Phenomenology = Targets, Target Related Events, Natural and Nuclear Backgrounds

- Scenarios
- All Vehicle Types (Launch, Midcourse, Re-Entry)Spatial, Temporal, Spectral Sampling Regimes
- DimensionsGeometry
- = All Sensor/Scene/Target Locations and Time-History



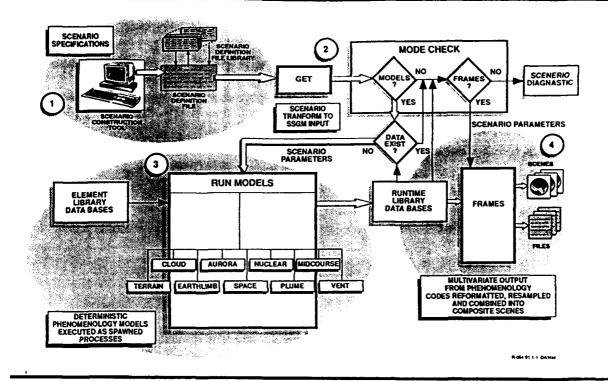
- Connectivity
- Event-Driven, Both Passive and Active (Illuminated)
 Signatures

9-068 91

Sequences



SSGM FUNCTIONAL FLOW DIAGRAM DESIGN



8 066 91 2



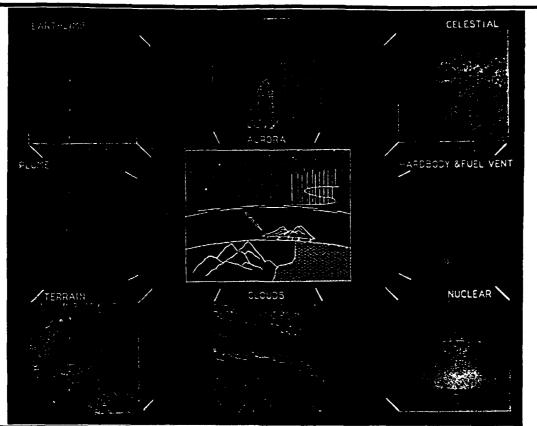
SSGM ATMOSPHERIC MODELS

- Earthlimb
 - MODTRAN (<60 km)
 - SHARC (>60 km)
- Backgrounds
 - APART (Terrain)
 - APART (Clouds)
- Targets
 - APART (TARSIS)
 - SIRRM (Plumes)
 - Simple Extinctions (Plumes)

175

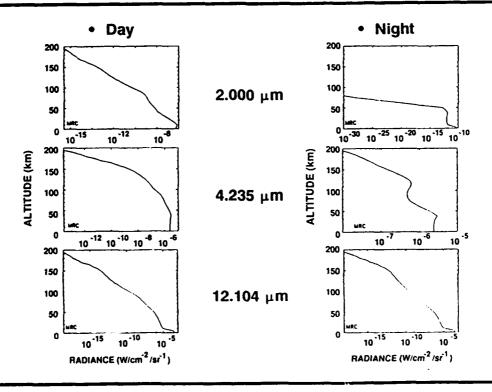


SSGM PHENOMENOLOGY



PRA---

SSGM EARTH LIMB PROFILES

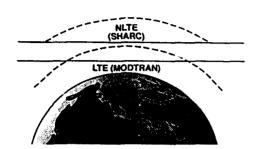


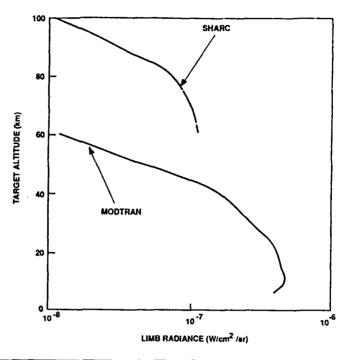
5 046 S t



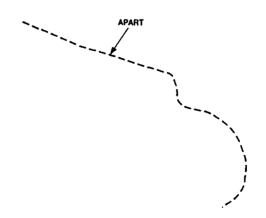
EARTH LIMB MODELING

- U.S. Standard Day
- 2.5 2.9 μm





B-000-81







BACKGROUND SCENE MODELS

- GENESSIS (Generic Scene Simulation Software) and CLDSIM (Cloud Simulation) are Collections of Computer Codes Which Generate 2-D Images of Terrestrial and Cloud Scenes
- GENESSIS Uses First-Principles Algorithms Which Include Those for:
 - Surface Temperature Heat Transfer
 - Solar-Viewer Shadowing and Scene Projection
 - Thermal Emission, Solar-Skyshine Reflection
 - Atmospheric Absorption, Scattering, Emission

Using an Input Scene Data Base Consisting of:

- Digital Elevation Map
- Earth Surface Material Assignment
- CLDSIM Uses the Following Assumptions and Treatments:
 - Cloud Tops are Treated as Surfaces, Emitting and Reflecting According to a Bidirectional Reflectance Function (BRDF). BRDF Varies with Cloud Optical Properties, Altitude, and Wavelength.
 - Clouds Can be Optically Thin and Transmit Radiation from Below
 - Cloud Top Temperatures Set Equal to Ambient
 - Skyshine Reflection Neglects Radiation from Neighboring Clouds

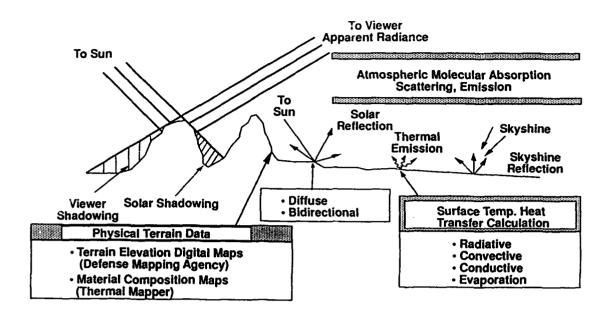
Using an Input Scene Data Base Consisting of:

- Digital Cloud Top Altitude Map
- Cloud Types

8-000-01 7



GENESSIS TERRAIN SCENE MODEL



R-006-90,8 DA/Mac

8-066-91



GENESSIS SIMULATION OF SOUTHERN CALIFORNIA COASTLINE (NADIR VIEW)

1024 x 1024 Pixels, 400 Meter Resolution, 10 - 12 μm





GENESSIS SIMULATION OF CAMARILLO, CALIFORNIA (NADIR VIEW)

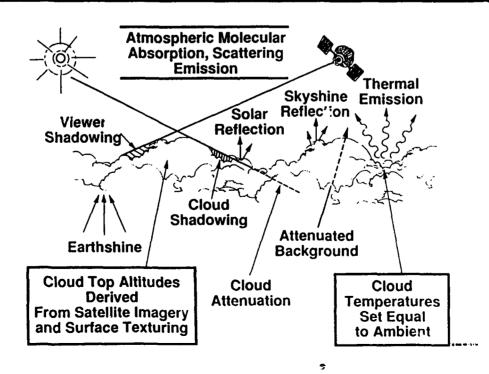
512 x 512 Pixels, 30 Meter Resolution, 3.6 - 4.0 μm



Photon Research Associates, Inc.

CLDSIM CLOUD SCENE MODEL

8 086 81 10





CLDSIM SIMULATION OF MULTIPLE CLOUD TYPE HORIZON SCENE

4000 x 4000 Pixels, Nominal 400 Meter Resolution, 2.6 - 2.8 μm



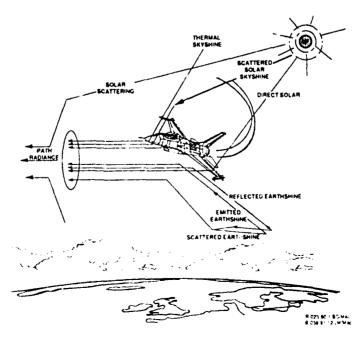
B-064 81 12



APART RADIATIVE ENVIRONMENT CODE

- Full LOWTRAN 7 Compatibility
- Observables-Driven Architecture
- Molecular Absorption
 5 cm⁻¹ Resolution

 - 0.2-50 μm
 - Five Parameter Volght Model
- Five-Flux Multiple Scattering
- Turbulence/Sky Noise
- Forward In-Scatter
- **Backgrounds**
 - Contrast
 - Structured
 - Global Data Base
 - **Bidirectional Materials**
- Giobal Atmosphere Data Base
- Hydrometeors
 - Clouds (Water/ice)
 - Fog
 - Rain
 - Snow





ATMOSPHERE MODELS

- Latitude Dependent
 - Equatorial (Summer/Winter)
 - Tropical (Summer/Winter/Annual)
 - Subtropical (Summer/Winter)
 - Midlatitude (Summer/Winter/Spring-Fall)
 - Subarctic (Summer/Winter/Special)
 - Arctic (Summer/Winter)
 - Polar (Summer/Winter)
- Special
 - U.S. Standard (1976)
 - Israeli Standard (Day/Night)
 - User-Defined



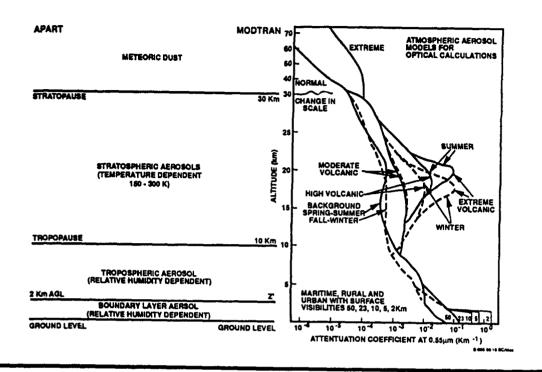
NORTHERN HEMISPHERE MODEL ATMOSPHERES

Туре	Latitude	Seasons
Equatorial	0°	Summer Winter
Tropical	15°	Annual Summer Winter
Subtropical	30°	Summer Winter
Midiatitude	45°	Summer Winter Spring/Fall
Subarctic	60°	Summer Winter Winter (Cold) Winter (Warm)
Arctic	75°	Summer Winter Winter (Cold) Winter (Warm)
Polar	90°	Summer Winter
U.S. Standard	-	
Israeli Standard		Day/Night

9-066-91.14



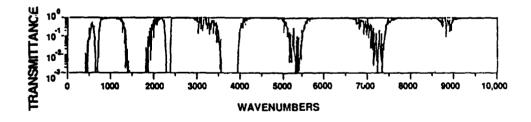
AEROSOL TYPES AND HAZE PROFILES



8-066-81.16



RADIATIVE TRANSFER



- Three Parameter Band Model
- Voight Line Shape
- Foreign-Broadened Line Wings
- Self-Broadened Line Wings

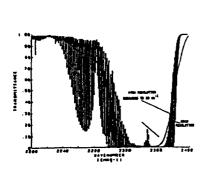
- Spectral Region 0.20 0.50 μm
- Band Parameters from 1986 AFGL Line Atlas
- User-Defined Resolution (5 200 cm⁻¹)
- Molecular Oxygen Model Added in UV

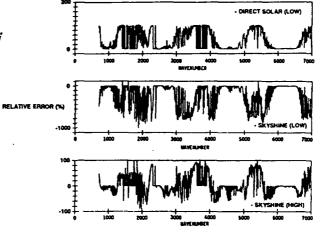
5-060-01 17



BAND CORRELATION

- A Passive Observable Consists of
 - Thermal Emission
 - Solar Reflections
 - Skyshine Reflections
 - Earthshine Reflections
- Each Components Transmits Differently Due to Band Averaging



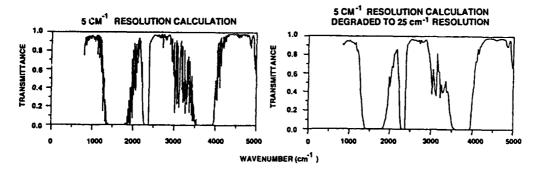


-156-00 11 JJMac

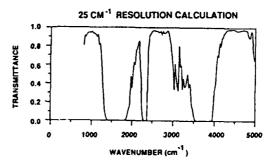
8-048-61.18

174/4~

VARIABLE RESOLUTION



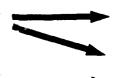
- Options
 - 5 cm⁻¹ Resolution
 - Multiples of 5 cm⁻¹ Resolution
 - "Constant" Wavelength Resolution





ATMOSPHERIC TURBULENCE EFFECTS

- Turbulence Induced Irregularities Cause Spatial and Temporal Variations of Atmospheric Index of Refraction
 - Spatial and Temporal Variations of Wavefront Amplitude



Scintillation

 Spatial and Temporal Variations of Wavefront Phase

Image Blur

- Turbulence Induced Irregularities Also Cause Atmospheric Radiance Variations
 - Sky Noise
 - Increased Path Radiance
- These Effects Can be Estimated Using Weighted Integrals of C_n², the Index of Refraction Structure Parameter, Over the Propagation Path

6-066-81 20



APART/MODTRAN DIFFERENCES

- BAND PARAMETERS
 - Spectral Resolution
 - Spectral Range
 - Variable Resolution
 - Wavelength Resolution
- REFRACTIVITY
- RAY TRACING
- FULL SOLAR GEOMETRY
- SOLAR AND LUNAR EPHEMERIS
- MOLECULAR SCATTERING
- RELATIVE HUMIDITY (GOFF-GRATCH)
- MODIFIED PHASE FUNCTION

- ADDITIONAL MODEL ATMOSPHERES
- MULTIPLE SCATTER
 - Four-Stream
 - Exponential Sum Fit
 - Coupling
- EQUATION OF TRANSFER
- TEMPERATURE DEPENDENT BACKGROUND STRATOSPHERIC AEROSOL (150 - 300 K)
- HAZE PROFILE AND AEROSOL TYPE
 - Boundary Layer
 - Tropopause
 - Stratosphere
- HYDROMETEORS



ADDITIONAL APART CAPABILITIES

- TURBULENCE
 - Thermal Sky Noise
 - Scatter Sky Noise
 - Scintillation
- ATMOSPHERE
 - Diumal Variations
 - Geographic Variations
- HEAT TRANSFER
 - Cloud Cover
 - Surface Temperature
 - Background Temperatures
- CORRECTION FOR LAYERING PROBLEM
- LINE CORRELATION
- INTEGRATION WITH OTHER CODES
 - Target
- Multiple Scatter
- Plume
- Heat Transfer
- Terrain
- Cloud

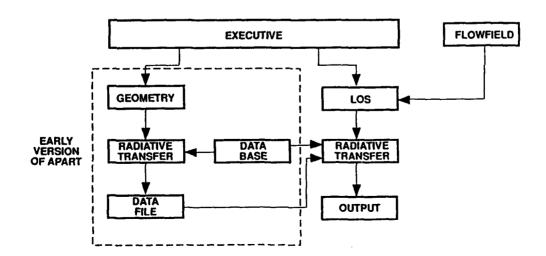
- FORWARD SCATTER
- BACKGROUNDS
 - Space (Zodiacal, Stars, Galactic)
 - Global Scene Types
 - Materials
 - Diffuse
 - -- Directional
 - Bidirectional
 - Terrain Blockage
- . USER-DEFINED
 - Atmosphere
 - Aerosol (Layered Species)
 - Hydrometeors
 - Background Scenes and Materials
- ULTRAVIOLET
 - O₂ N₂O
 - 03 NO2
 - H₂O N₂O₂
 - SO₂ D₂O₂

6-046-61,2



SIRRM ATMOSPHERIC MODEL

• SIRRM Uses Early (1981) Version of APART



Can Easily Upgrade SIRRM for Latest Version of APART



CONCLUSIONS

PROBLEM	CURRENT SOLUTION	DESIRED SOLUTION
LTE/NLTE "Discontinuity"	Interpolate	Single Code
Earthlimb vs. Backgrounds	None	Compatible or Single Code
Plume vs. Background	None	Compatible or Single Code

8-066-81.2

REVIEW OF THE CHEMICAL KINETIC RATE CONSTANTS USED IN THE SHARC MODEL

V.I. Lang, A.T. Pritt, Jr.
The Aerospace Corporation, PO Box 92957, Los Angeles, CA 90009

The SHARC (Strategic High Altitude Radiance Code) predicts the infrared (1-40 µm) radiance background of the Earth's atmosphere from 50 - 300 km for a variety of viewing geometries. At these altitudes the molecular species are no longer in thermodynamic equilibrium, requiring that the state populations of each emitter be calculated based on a steady state solution to a set of first-order differential equations describing the kinetic development of each emitter. Presented here is a review of the rate constants used to calculate specific vibrational level populations for H₂O, CO₂, and O₃ which are important molecular species emitting in the infrared.

REVIEW OF THE CHEMICAL KINETIC RATE CONSTANTS USED IN THE SHARC MODEL

V. I. Lang and A. T. Pritt, Jr. The Aerospace Corporation

prepared for the Annual Review of Atmospheric Models June 11 - June 12, 1991

work supported by the Geophysics Directorate, Phillips Laboratory Dr. R. Sharma, Program Manager

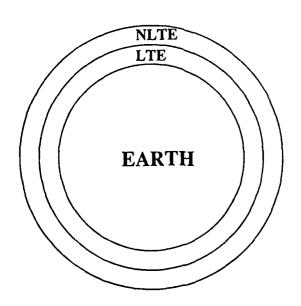


STRATEGIC HIGH ALTITUDE RADIATION CODE (SHARC)

Features:

NLTE Code 1 - 40 μm 50 - 300 km

Quiescent and Auroral Vaious Viewing Geometries





OUTLINE

WHAT IS SHARC?

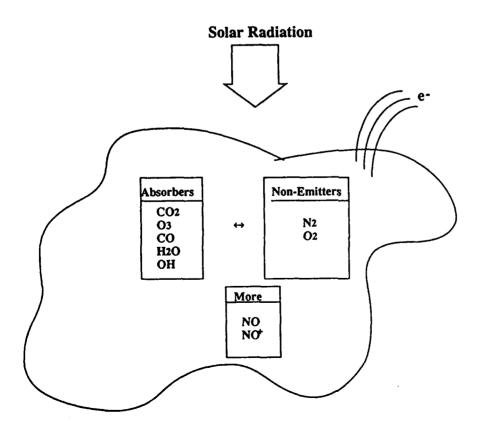
WHY AN NLTE MODEL?

CO RATE CONSTANTS

H2O RATE CONSTANTS

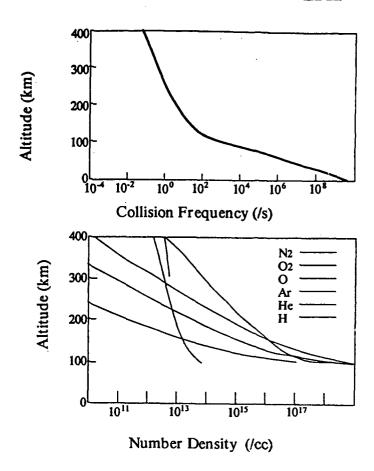
NEW WORK



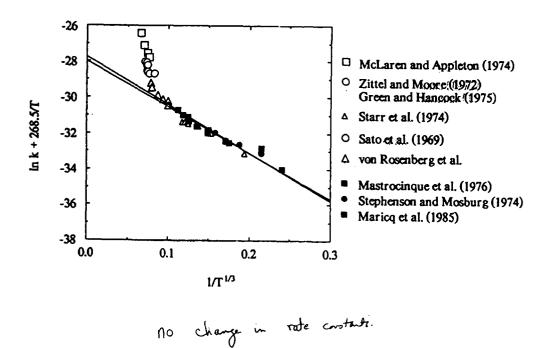




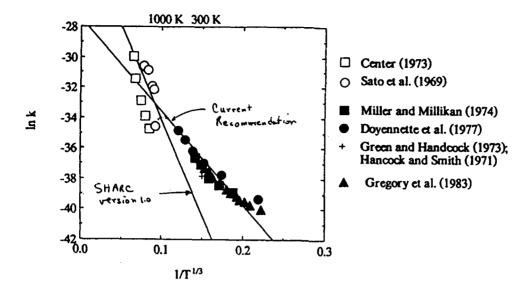
EARTH'S ATMOSPHERE



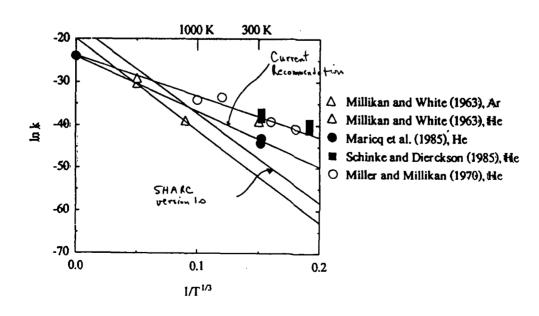
$$CO(1) + N_2(0) \rightarrow CO(0) + N_2(1)$$



$CO(1) + O_2(0) \rightarrow CO(0) + O_2(1)$



$$CO(1) + M \rightarrow CO(0) + M$$



$CO(1) + O \rightarrow CO(0) + O$

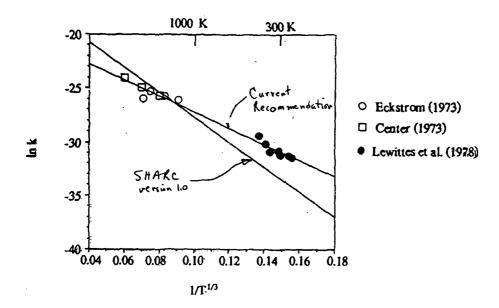


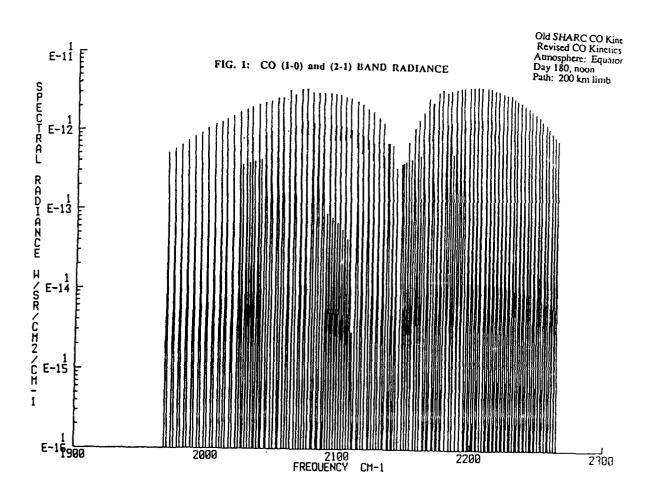
TABLE 1: Revisions to CO Kinetics

	Current Si A _i	HARC Coeffi Ci	cients ⁽²⁾ D _i ^(b)	Revised A _i	Coefficients $^{(a)}$	D _i (b)
V-T Reactions(c).(d)						
M + CO(1) - M + CO(0) N ₂ /1.0/ O ₂ /1.0/	6.67e-08	208.3	0.0	3.78e-11	129.2	0.0
M + CO(0) - M + CO(1) N ₂ /1.0/ O ₂ /1.0/	6.67e-08	208.3	3083.7	3.78c-11	129.2	3083.7
M + CO(2) - M + CO(1) N ₂ /1.0/ O ₂ /1.0/	1.33e-07	208.3	0.0	7.56e-11	129.2	0.0
M + CO(1) - M + CO(2) N ₂ /1.0/ O ₂ /1.0/	1.33e-07	208.3	3045.6	7.56e-11	129.2	3045.6
M + CO(2) - M + CO(0) N ₂ /1.0/ O ₂ /1.0/	1.33e-07	208.3	0.0	7.56e-11	129.2	0.0
M + CO(0) - M + CO(2) N ₂ /1.0/ O ₂ /1.0/	1.33e-07	208.3	6129.3	7.56e-11	129.2	6129.3
O + CO(1) - O + CO(0)	9.90e-08	118.1	0.0	5,39e-11	48.8	0.0
O + CO(0) - O + CO(1)	9.90e-08	118.1	3083.7	5,39e-11	48.8	3083.7
O + CO(2) - O + CO(1)	1.98e-07	118.1	0.0	1.08e-10	48.8	0.0
O+CO(1)-O+CO(2)	1.98c-07	118.1	3045.6	1.08e-10	8.8	3045.6
O + CO(2) - O + CO(0)	1.98e-07	118.1	0.0	1,08c-10	48.8	0.0
O + CO(1) - O + CO(2)	1.98c-07	118.1	6129.3	1.08e-10	48.8	6129.3

TABLE 1 (cont.): Revisions to CO Kinetics

	Current S Ai	HARC Coo	fficients D _i	Revised C A _i	oefficients C _i	D _i
V-V Reactions(d)					·	
$CO(0) + N_2(1) - CO(1) + N_2(0)$	6.98c-13	25.6	0.0	2.20e-13	18.7	0.0
$CO(1) + N_2(0) - CO(0) + N_2(1)$	6.98e-13	25.6	268.5	2.20e-13	18.7	268.5
$CO(0) + O_2(1) - CO(1) + O_2(0)$	3.50e-10	124.0	844.4	1.68e-13	50.2	844.4
$CO(1) + O_2(0) - CO(0) + O_2(1)$	3.50e-10	124.0	0.0	1.68e-13	50.2	0.0
hv Emission(e)		•				
CO(1) - CO(0) + hv	30.96	0.0	0.0	30.96	0.0	0.0
CO (2) - CO(1) + hv	60.45	0.0	0.0	60.45	0.0	0.0
CO (2) - CO(0) + hv	1.03	0.0	0.0	1.03	0.0	0.0

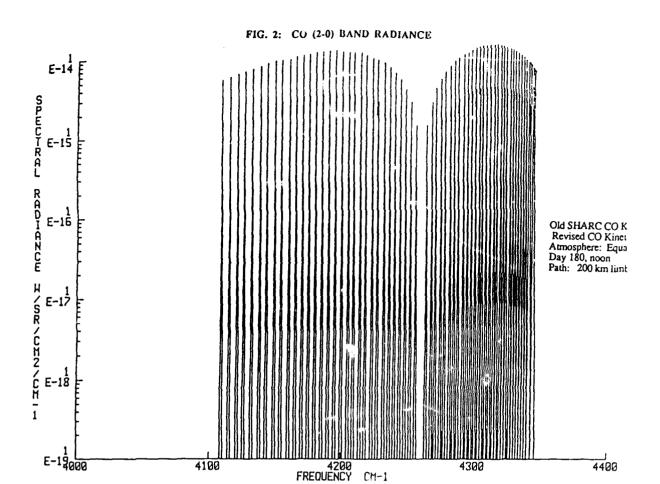
a) Landau - Teller function $k = A_i T^{-B_i} \exp(-C_i T^{-333} - D_i T^{-1})$; $B_i = 0$ for all reactions included here.

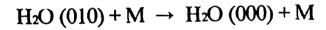


b) $D_i = \Delta E (cm^{-1})/1.44$ c) efficiences of collsion partner are listed below each reaction

d) rate units are cm3 molecules-1 s-1

e) rate units are s-1; rates for reverse processes are zero





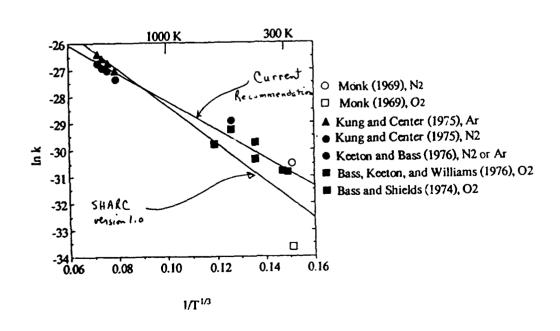


TABLE 1: Rate Coefficients for Relaxation of 11_2O $\{k_i = A_i T^{\beta i} \exp(-C_i T^{-.333} - E_i/T)\}$

REACTIONS				REVISED RATE COEFFICIENTS				
<u> </u>				_	Ai	β_i	Ci	**E _i
M + H2O(010) = M + H2O(000) N2/1.0/ O2/1.0/	5.37E-10	0.0	70.0	0.0	1.13E-10	0	52.5	0
M + H2O(100) = M + H2O(020) N2/1.0/ O2/0.7/	4.60E-13	0.0	0.0	0.0	4.60E-13	0	0	0
M + H2O(001) = M + H2O(020) N2/1.0/ O2/0.7/	4.60E-13	0.0	0.0	0.0	4.60E-13	0	0	0
M + H2O(020) = M + H2O(010) N2/1.0/ O2/1.0/	5.37E-10	0.0	70.0	0.0	2.26E-10	0	52.5	0
M + H2O(030) = M + H2O(020) N2/1.0/ O2/1.0/	5.37E-10	0.0	70.0	0.0	3.39E-10	0	52 .5	0
M + H2O(110) = M + H2O(100) N2/1.0/ O2/1.0/	5.37E-10	0.0	70.0	0.0	1.13E-10	0	52.5	0
M + H2O(011) = M + H2O(001) N2/1.0/ O2/1.0/	5.37E-10	0.0	70.0	0.0	1.13E-10	0	52.5	0
M + H2O(110) = M + H2O(030) N2/1.0/ O2/0.7/	4.60E-13	0.0	0.0	0.0	4.60E-13	0	0	0
M + H2O(011) = M + H2O(030) N2/1.0/ O2/0.7/	4.60E-13	0.0	0.0	0.0	4.60E-13	0	0	0
O2(0) + H2O(010) - O2(1) + H2O(000) O2(1) + H2O(000) - O2(0) + H2O(010) O2(0) + H2O(020) - O2(1) + H2O(010) O2(1) + H2O(010) - O2(0) + H2O(020) O2(1) + H2O(030) - O2(1) + H2O(020) O2(1) + H2O(010) - O2(0) + H2O(030) O2(0) + H2O(110) - O2(1) + H2O(100) O2(1) + H2O(100) - O2(0) + H2O(110) O2(1) + H2O(011) - O2(1) + H2O(011) O2(1) + H2O(001) - O2(0) + H2O(011) H2O(010) - H2O(000) + HV H2O(020) - H2O(000) + HV	1.00E-12 1.00E-12 1.00E-12 1.00E-12 1.00E-12 1.00E-12 1.00E-12 1.00E-12 1.00E-12 1.00E-12	0.0 0.0 0.0 0.0 0.0 0.0 0.0 0.0 0.0	0.0 0.0 0.0 0.0 0.0 0.0 0.0 0.0 0.0	0.0 55.2 0.0 0.7 0.0 -59.3 0.0 31.0 0.0 27.3 0.0	2.9E-12 2.9E-12 5.8E-12 5.8E-12 8.7E-12 8.7E-12 2.9E-12 2.9E-12 2.9E-12 2.9E-12 2.9E-12	000000000000000000000000000000000000000	000000000000000000000000000000000000000	0 55.2 0 0.7 0 59.3 0 31.0 0 27.3
H2O(100) - H2O(000) + HV H2O(001) - H2O(000) + HV	3.37 78.40	0.0 0.0	0.0 0.0	0.0 0.0	5.00 76.58	0 0	0 0	0 0

		•		R	EVISED R	ATE CO	EFFICIE	NTS
REACTIONS (cont.)				Ā		Bi	Ci	D_{i}
H2O(030) - H2O(000) + HV H2O(110) - H2O(000) + HV H2O(011) - H2O(000) + HV H2O(011) - H2O(000) + HV H2O(020) - H2O(010) + HV H2O(020) - H2O(010) + HV H2O(030) - H2O(010) + HV H2O(030) - H2O(010) + HV H2O(110) - H2O(010) + HV H2O(110) - H2O(010) + HV H2O(030) - H2O(020) + HV H2O(030) - H2O(020) + HV H2O(000) + HV - H2O(010) H2O(000) + HV - H2O(011) H2O(000) + HV - H2O(011) H2O(000) + HV - H2O(011) H2O(010) + HV - H2O(010) H2O(010) + HV - H2O(030)	0.349 17:22 0 33:74 0.612 3.70 1.11 0 4.17 65.98 36.87 0.0 0 0.0 0.0 0 0.0 0.0 0 0.0 0.0 0 0.0 0.0	0.0 0.0 0.0 0.0	0.0	.C .7 1' 4 1. 2 1 4	i 0065 680 7.23 1.29 3.36 1.15 .21 .53 1.49 0.06	B _i 0 0 0 0 0 0 0 0 0	000000000000000000000000000000000000000	0 0 0 0 0 0 0 0 0 0 0 0 0 0
H2O(010) + HV - H2O(011) H2O(020) + HV - H2O(030)		0.0 0.0						

^{*}Numbers in italics indicate that no change has been made from the original SHARC value

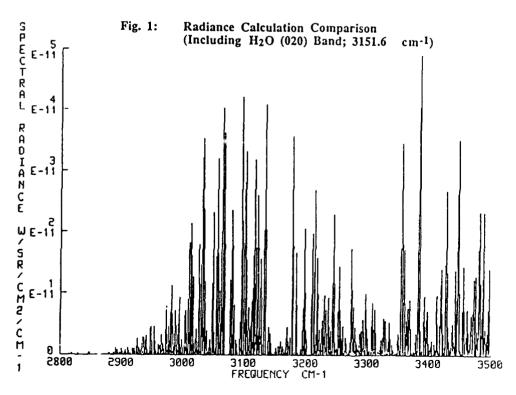
** The E; terms (ie. the energy differences between levels) are not listed here for the V-T processes because these are obtained from the H2OSTAT.DAT file in SHARC 2.0.

H Z O
TABLE 2: BAND RADIANCE COMPARISON

Transition	Frequency	Band Radiance (W Old Kinetics	V/SR/cm ²) New Kinetics	Radiance Ratio Old:New
(010)-(000)	1594.750	0.37277c-6	0.35466e-6	1.05
(020)-(000)	3151.630	0.11184c-8	0.21412e-9	5.22
(100)-(000)	3657.053	0.87024e-9	0.47780e-9	1.82
(001)-(000)	3755.930	0.35921e-7	0.36124e-7	.994
(030)-(000)	4666.793	0.11070e-11	0.87792e-13	12.6
(110)-(000)	5234.977	0.63862e-11	0.24911e-11	2.56
(011)-(000)	5331.269	0.20763e-8	0.12812e-8	1.62
(020)-(010)	1556.880	0.39202e-7	0.75069e-8	5.22
(100)-(010)	2062.303	0.13254e-9	0.73330e-10	1.81
(001)-(010)	2161.180	0.16949e-8	0.16950e-8	1.00
(030)-(010)	3072.043	0.17710e-9	0.14089e-10	12.6
(110)-(010)	3640.227	0.39018e-10	0.15291c-10	2.55
(011)-(010)	3736.519	0.82490e-8	0.50967e-8	1.62
(030)-(020)	1515.163	0.32288e-8	0.25724e-9	12.6
Pure Rotational Line	×s ·	0.99151e-10	0.99151e-10	1.0
Total Overlap Corrected Band Pass Radiance		0.46488e-6	0.40686e-6	1.14

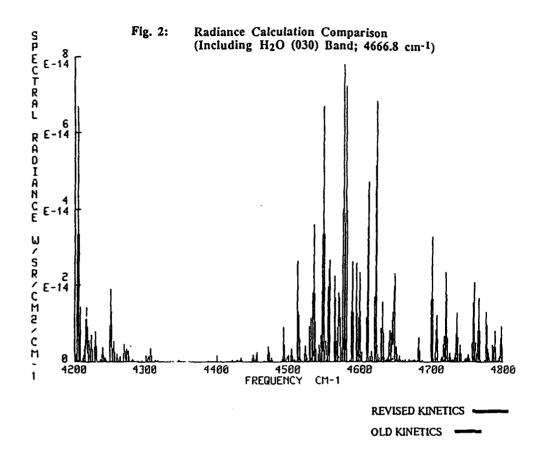
Model Atmosphere: DAYSUBAR.DAT Lat. 00, Long. O0 Solar Zenith Angle O0

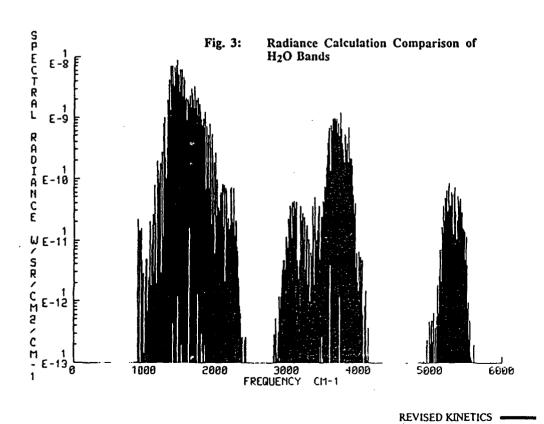
Limb View, 64 km Tangent



REVISED KINETICS •

OLD KINETICS -





OLD KINETICS

NEW WORK

OZONE RATE CONTANTS

NO RATE CONSTANTS

OH RATE CONSTANTS

LIMITATIONS OF KUYMER-JAMES MODEL

REVIEW ARTICLE

Session 3

Summary of the Session on Measurements and Models

This session addressed model applications, enhancements, validations, and potential new directions; the singular laboratory measurement paper described work on the UV Schumann-Runge bands. Because of the large number of separate issues covered, this synopsis is arbitrarily divided into two categories: "New Directions" and "Measurements and Validations".

NEW DIRECTIONS:

"Atmospheric Ultraviolet Radiance and its Variation": In the realm of new directions for PL/GP models, Computational Physics (CPI) outlined its approach to modeling UV/Visible airglow features and their variability. This modeling effort will eventually be merged with the lower atmosphere AURIC, MODTRAN, and SHARC (see previous papers, Huguenin et al.; Abreu et al.; Robertson et al.). Such syntheses will eventually produce a seamless code covering solar, thermal, and airglow features throughout the ultraviolet to far IR spectral ranges.

"Improved HNO₃ Band Model Parameters": Currently a full spectroscopic description for HNO₃ at 11.3 microns requires thousands of transitions. Implementing this system into a line-by-line algorithm consumes large amounts of time and storage; therefore, the authors propose an efficient temperature dependent band model, suitable for incorporation into LOWTRAN and MODTRAN.

"Line-by-Line Calculations of Atmospheric Fluxes and Heating Rates": Interest in Global Climate Change within the scientific community has driven the evolution of FASCOD3 into the arena of energy deposition within the atmosphere. AER has extended the code to produce heating and cooling rates for a variety of atmospheres, comparing those results to prior calculations (ICRCCM). The contour plots of line-by-line heating and cooling rates, as a function of both pressure and frequency, readily demonstrates the importance of correct detailed spectroscopy, particularly regarding "feature overlap" and the H₂O continuum, on potential global change predictions.

"A Comparison of Computational Approaches for the Voigt Function": F. Schreier of the Optoelectronics Institute, Germany, presents a comprehensive (and elegant) investigation of computational procedures for calculating the Voigt function. Coding implementation and subsequent timing runs were described.

"Spectral Smoothing in the Fourier Domain: A Software Package for Line-by-Line Calculations": With the growth of Fourier transform spectrometric techniques, used in both laboratory and field measurements (surface, airborne, balloon, shuttle, and satellite), the need for rapid FTS simulation capability became apparent. This new routine (developed at Optimetrics and Stewart Radiance Lab) provides a set of FTS scanning functions, including apodization, that can be used in conjunction with FASCOD3 output. The functions include sinc, sinc², Beer, Hamming, and Hanning.

MEASUREMENTS AND VALIDATIONS:

"Photoabsorption Cross Sections in the Transmission Window Regions of the Schumann-Runge Bands of Oxygen": This paper describes laboratory work done at Harvard-

Smithsonian to improve the measurements of the Schumann-Runge Band absorption in the window regions between stronger rotational lines, including the pressure dependence. These data are particularly important when calculating penetration of solar UV into the mesosphere and stratosphere. Eventually, full cross sections based upon the Harvard measurements will be incorporated into AURIC (see previous papers: Hugeunin et al., Link et al.).

"High-Resolution Spectral Measurements of Upwelling and Downwelling Atmospheric Infrared Emission with Michelson Interferometers": FASCOD3 validation is critically dependent upon good high-resolution radiance and transmittance measurements; the atmospheric data presented by the University of Wisconsin-Madison provide well calibrated IR radiances at both surface and aircraft altitudes (downwelling and upwelling). The data are of sufficient quality to infer necessary changes to CO₂ and H₂O spectral line parameters; independently those same parameters were updated for HITRAN91 based on laboratory data (see Rothman). The role of FTS data in interpreting the atmosphere (temperature, constituent, and particular profiles) is strongly reinforced by this excellent program.

"Validation of HIS Spectral Measurements with the FASCODE Line-by-Line Model": This is a companion paper to the Wisconsin (Revercomb et al., above) instrument presentation, further describing inferences drawn from comparisons between HIS atmospheric measurements and FASCOD3 calculations. Cloud (sub-visual cirrus) and fluorocarbon signatures, in addition to ozone, water, and carbon dioxide, are readily apparent, supporting the development of high resolution measurements in more operational modes.

"Comparison of FASCOD2 and LOWTRAN7 Models with FIT Spectral Transmittance Measurements in the 3-12 micron Region": The Canadian research group has compared high resolution interferometric transmittance measurements (winter and summer, high and low humidity) with both FASCOD2 and LOWTRAN7 (after degrading the data to LOWTRAN resolution; agreement is, in general, very good (<|8%|). However, their analyses point out some of the same problem areas in H₂O lines (updated in HITRAN91), along with concerns about the self and foreign continua. This latter problem is being addressed; see Special Session discussion.

"LOWTRAN7 Comparisons with Field Measurements": As the title indicates, the Army Night Vision Laboratory conducted an extensive set of comparisons of LOWTRAN7 with transmissometer measurements at 1.54, 3-5, and 8-12 micron frequencies. Measurements were made in Virginia, Panama, Alaska, and Utah. The quality of agreement was, in most cases, as good as the supporting meteorological data (humidity, etc.). An initial comparison of MODTRAN and high resolution Fourier transform transmissometer measurements also showed excellent agreement, furthering the arguments for the E/O community to convert from LOWTRAN to MODTRAN.

"Spectral Solar Radiation Modeling, Measurement, and Data Base Activities at the Solar Energy Resolution Institute (SERI)": SERI outlined their interest, motivation, and measurement program in the near UV through near IR spectral ranges. This program is driven by the need to assess performance of solar energy conversion devices. Both MODTRAN and LOWTRAN provide similar modeling capability, so the SERI development offers parallel validation of the DoD codes.

"Incorporation of LOWTRAN7 into the ACQUIRE Model": LOWTRAN7 has been modified for the Army to be compatible with EOSAEL 92; this has required changing the input to EOSAEL flexible formatting and adding target contrast calculations along with new aerosol and multiple scattering algorithms.

ATMOSPHERIC ULTRAVIOLET RADIANCE AND ITS VARIATIONS

R. Link, D.J. Strickland, D.E. Anderson, Jr. Computational Physics, Inc., P.O. Box 788, Annandale, VA 22003

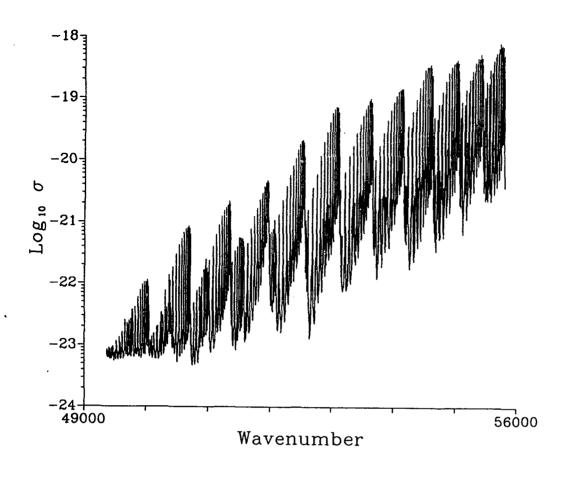
CPI is developing numerical codes for the Atmospheric Ultraviolet Radiance Integrated Code (AURIC) development effort of the Phillips Laboratory Geophysics Directorate in the area of Ionospheric Impact on Air Force Systems - Ultraviolet Remote Sensing. The modules will calculate thermospheric emission spectra and radiances in the 1000 - 6500 Å wavelength region for dayglow, nightglow, twilight and electron aurora, and will account for solar, photoelectron, auroral electron, and chemical excitation processes, pure and self absorption, and multiple scattering effects. The modules will provide the capability to calculate emission spectra as a function of wavelength and look angle, or provide radiances integrated over specified wavelength intervals for user-selected viewing geometries. An orbit code will be provided for satellite viewing geometries. An interface to MODTRAN will be provided for calculating Rayleigh scattering contributions. The integrand codes will provide the analyst with a powerful tool for predicting UV optical backgrounds, analyzing optical data, and designing sensors.

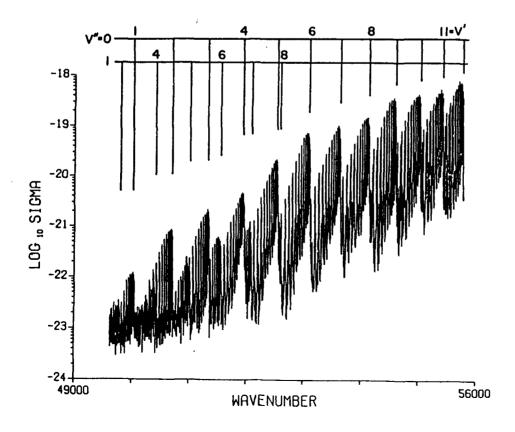
PHOTOABSORPTION CROSS SECTIONS IN THE TRANSMISSION WINDOW REGIONS OF THE SCHUMANN-RUNGE BANDS OF OXYGEN

K. Yoshino, J.R. Esmond, D.E. Freeman, W.H. Parkinson Harvard-Smithsonian Center for Astrophysics, 60 Garden Street, Cambridge, MA 02138

> A.S-C. Cheung Chemistry Department, University of Hong Kong, Hong Kong

We have completed measurements of the absorption cross sections of the Schumann-Runge bands in the window regions between the rotational lines in the wavelength region 180-199 nm. The measurements have been done with many different pressures of oxygen, 50-76 torr, so that the pressure dependent absorption can be separated from the main cross sections. The measured cross section $\sigma_p(\lambda)$ at the window region is linearly dependent on the pressure P of O2, $\sigma_p(\lambda) + \alpha(\lambda)P$. σ_2 is the cross section of O2 extrapolated to zero pressure and $\sigma_p(\lambda)P$ is the cross section involving two molecules of O2. They are used to eliminate the pressure dependent part of the cross sections from the measured cross sections in the transmission window regions. The absorption cross sections at the window region have been obtained for $\sigma_p(\lambda) - \sigma_p(\lambda) + \sigma_p($





$$\sigma_{P}(\lambda) = \sigma_{0}(\lambda) + \alpha(\lambda)P$$

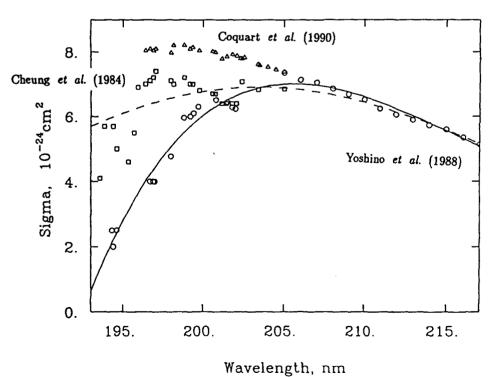
$$\sigma_0(\lambda) = \sigma_{SR}(\lambda) + \sigma_H(\lambda) + \sigma_R(\lambda)$$

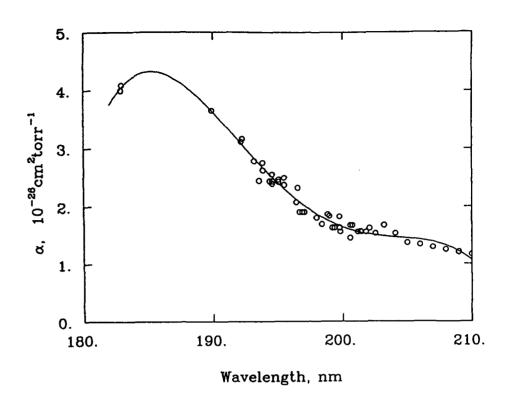
 $\sigma_{SR}(\lambda)\!\!:$ Wing effects of the Schumann-Runge bands Temperature dependent

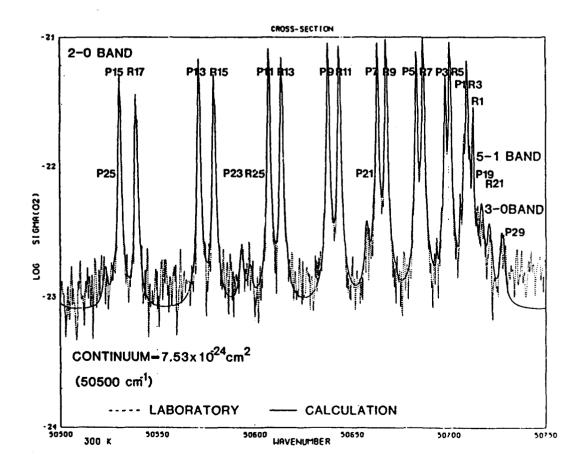
 $\sigma_{\rm H}(\lambda)$: Herzberg continuum

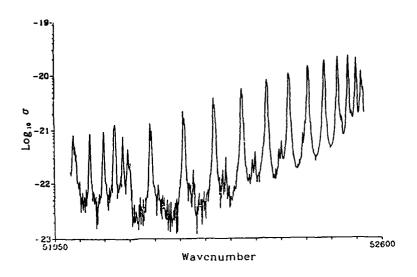
Rayleigh scattering $\sigma_{\mathbb{R}}(\lambda)$:

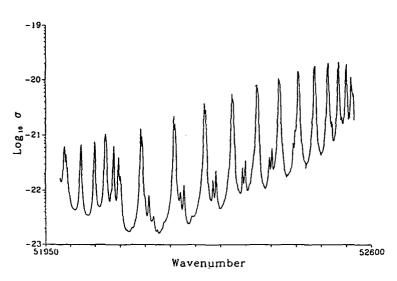
Herzberg Continuum Cross Sections, $\sigma_{\rm H}$

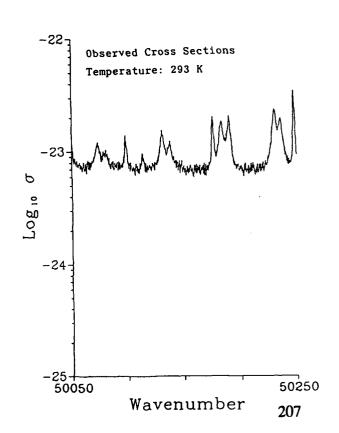


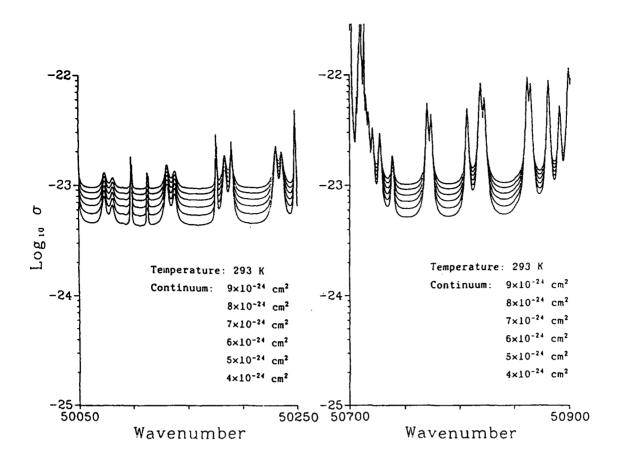


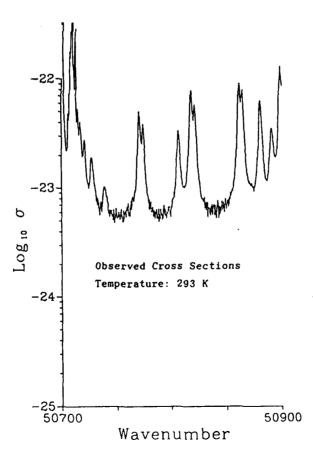


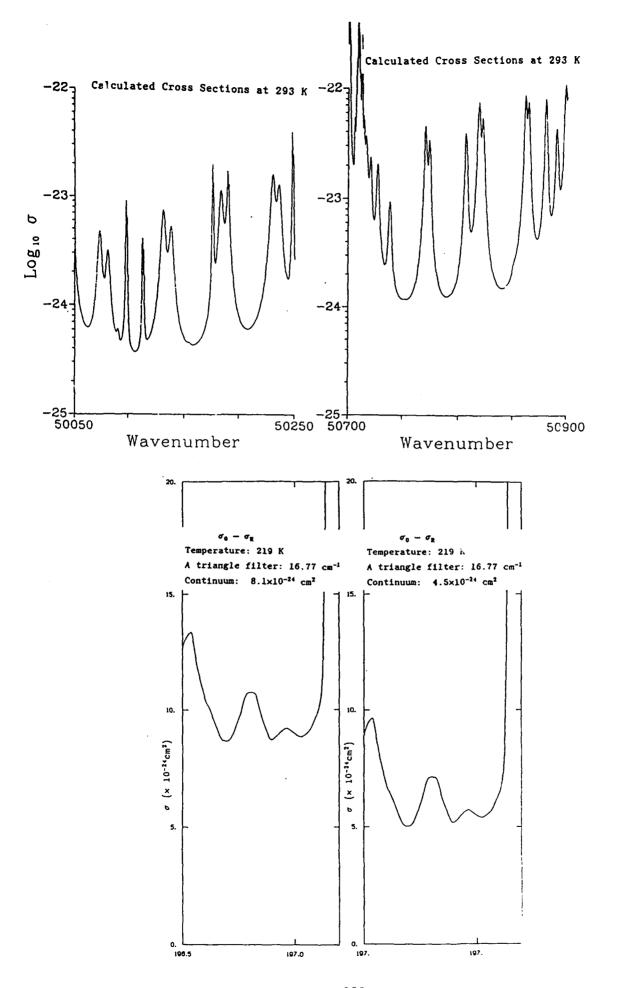


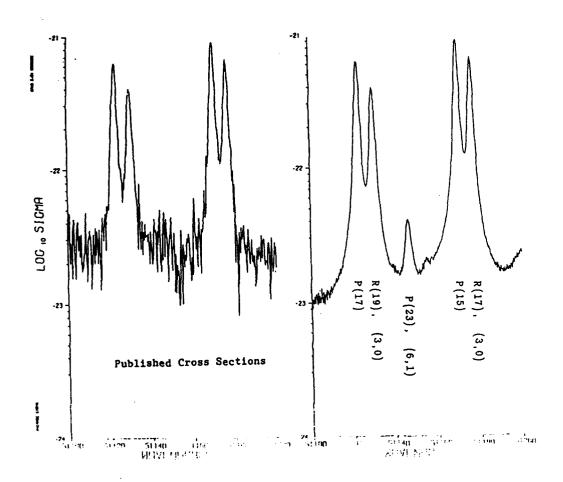












INCORPORATION OF LOWTRAN 7 INTO THE ACQUIRE MODEL

S.G. O'Brien
Las Cruces Scientific Consulting, 3373 Solarridge Street, Las Cruces, NM 88001

The Night Vision Laboratory ACQUIRE computer program is designed to calculate range performance predictions that are based upon results from the FLIR90 sensor performance model. ACQUIRE combines MRT data, target characteristics, and atmospheric conditions to predict the probability of accomplishing various acquisition tasks as a function of range. The addition of a modified version of LOWTRAN 7 to perform the atmospheric characterization task is described.

Incorporation of LOWTRAN 7 into the ACQUIRE Model

Sean G. O'Brien Las Cruces Scientific Consulting

Incorporation of LOWTRAN 7 into ACQUIRE

Implementation

- o Use ACQUIRE as the driver
- o Input of negative transmission triggers LOWTRAN 7 execution
- o Modified LOWTRAN 7 (EOSAEL LOWTRAN) already performs target contrast computation
- o Modify ACQUIRE range performance algorithms to include contrast results

Incorporation of LOWTRAN 7 into ACQUIRE

Goals

- Use modified LOWTRAN 7 to calculate observer-target and observer-background transmissions and radiances in ACQUIRE, and calculate target contrast
- o Modify ACQUIRE to adjust target acquisition results using LOWTRAN 7 target contrast results
- o Test and document the resulting code

NVL ACQUIRE Model Input/Output

- o Input
 - target: height, length, delta T

 - device: * of MRT data points, number of resolvable cycles on target corresponding to 50% probability of performing tasks #1 and #2 (#2 is used for search detection task), WFOV/NFOV ratio, search time
- o Output
 - echo of input
 - NFOV P(#1), P(#2), and P(#2,t) as functions of range
 - NFOV R(#1), R(#2) as functions of probability
 - Corresponding WFOV results (if any)

NVL ACQUIRE Model

- o Uses FLIR90 model output as input
- o FLIR90 predicts device-dependent performance parameters measurable in the laboratory
 - NETD (noise equivalent temperature difference)
 MTF (modulation transfer function)

 - MRTD (minimum resolvable temperature difference)
- o ACQUIRE accepts MRTD data and predicts field performance
 - probability of detection and recognition of military targets as a function of range

 - 2-D range performance optional 1-D range performance
- o NVL search model is embedded in ACQUIRE
 - allows time-dependent probability of detection analysis, given search period criterion

Modifications to LOWTRAN 7

- o Adapted to be driven by EOSAEL 92 control program
- Change of input format to EOSAEL card order-independent
- o Addition of target contrast calculation
- o Comparison to UV transmission models and data
- o Documentation of LOWTRAN 7
 - upgrade to include new features:

target contrast new aerosol models (e.g., desert model) multiple scattering of atmospheric radiance

HIGH-RESOLUTION SPECTRAL MEASUREMENTS OF UPWELLING AND DOWNWELLING ATMOSPHERIC INFRARED EMISSION WITH MICHELSON INTERFEROMETERS

H.E. Revercomb University of Wisconsin - SSEC, 1225 W. Dayton Street, Madison, WI 53706

The University of Wisconsin Space Science and Engineering Center has developed instruments for the measurement of accurately calibrated atmospheric emission both from the ground and from an aircraft platform (NASA ER-2). These instruments have been used in recent field experiments to obtain extensive data sets of combined radiances and in-situ atmospheric measurements. Some of the interesting results from these experiments that will be presented include: clear air spectroscopic differences with line-by-line code, ice and liquid water cloud radiative signatures, and atmospheric state parameter retrievals from the infrared measurements. Results of comparisons of observations with FASCOD2 and Beta-FASCOD3 will be presented as well as the impact of improvements in the CO2 line parameters over those found in HITRAN86.

COMPARISONS OF FASCODE SPECTRA WITH HIS OBSERVATIONS (II)

H.E. Revercomb, R.O. Knuteson, W.L. Smith, H.M. Woolf*, and H.B. Howell*

University of Wisconsin
Space Science and Engineering Center
1225 West Dayton Street
Madison, WI 53706
USA

* NOAA/NESDIS Systems Design and Applications Branch, 1225 West Dayton Street, Madison, WI 53706

> for Annual Review Conference on Atmospheric Transmission Models Geophysics Laboratory Hanscom AFB, MA

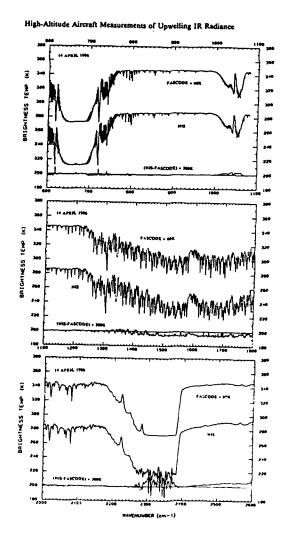
> > 11-12 June 1991

TOPICS

- HIS (High-resolution Interferometer Sounder)
 OBSERVATION HISTORY
- SUMMARY OF 1989 FASCOD2 / HIS COMPARISONS
- CO₂ RESULTS FROM FASCOD3
- NEW 1991 OBSERVATIONS

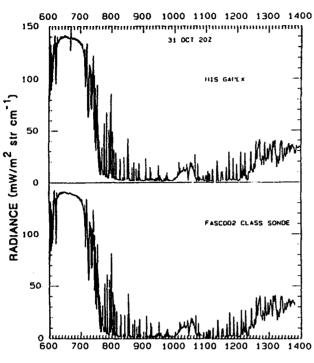
6-YEAR HISTORY OF ATMOSPHERIC OBSERVATIONS

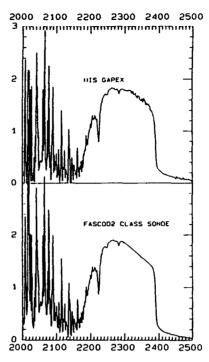
- NASA U2/ER2 AIRCRAFT (NADIR VIEWING)
 - KITT PEAK, APRIL 1986
 - COHMEX, JUNE / JULY 1986
 - FIRE, WISCONSIN, OCT / NOV 1986
 - NASA AMES, PACIFIC OCEAN, MAY 1991
 - CAPE, SERON, FIRE; 2ND HALF 1991
- NOAA P3 AIRCRAFT (NADIR VIEWING)
 - MIAMI, 1 TEST FLIGHT, NOV 1988
- GROUND BASED (ZENITH VIEWING)
 - MADISON, NOV 1986
 - GAPEX, DENVER, OCT / NOV 1988
 - MADISON / LIDAR, NOV / DEC 1989
 - WISP: COLORADO, FEB / MAR 1991
 - NSF SHIP, POINT SUR, MAY 1991



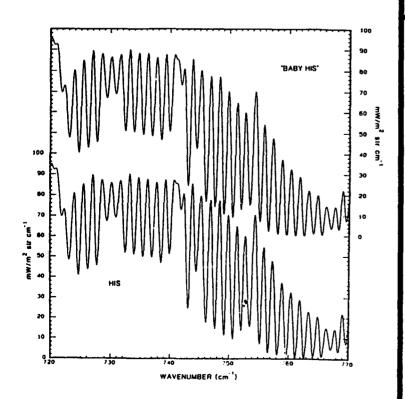
HIS GROUND-BASED OBSERVATIONS (Downwelling Compared to FASCODE)







WAVENUMBER (cm⁻¹)



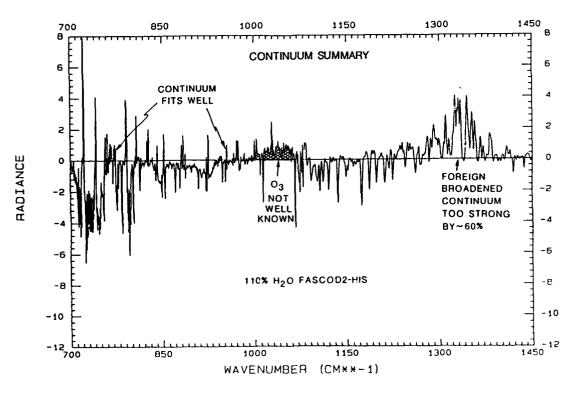
University of Wisconsin
Space Science and Engineering Center

DEMONSTRATION OF
ABSOLUTE
RADIOMETRY
(Intercomparison of 2
different interferometric
systems)

H2O CONTINUUM: 1989 Summary

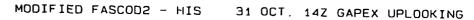
- HIS AGREES REASONABLY WELL WITH FASCOD2
 FROM 750 TO 1000 cm⁻¹ (10 TO 13 μm)
 (A 10% increase of the continuum strength would improve agreement)
- REDUCTION OF THE FOREIGN-BROADENING CONTINUUM BY 60% BETWEEN 1300 AND 1400 cm⁻¹ (8 TO 9 μm) WOULD ACCOUNT FOR THE DISCREPANCY BETWEEN HIS AND FASCOD2 FOR DRY ATMOSPHERES.

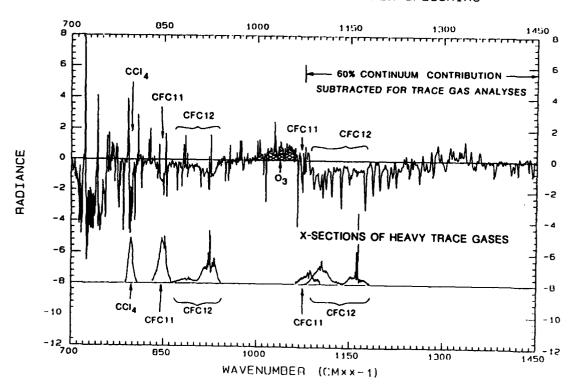
FASCOD2 - HIS 31 OCT. 14Z GAPEX UPLOOKING



TRACE GASES: 1989 Summary

- CFC 11 AND CFC 12 ARE IDENTIFIABLE IN THE REGION FROM 1050 TO 1200 cm⁻¹, IN ADDITION TO THE REGION PREVIOUSLY IDENTIFIED FROM 840 TO 940 cm⁻¹
- CCl4 IS IDENTIFIABLE CENTERED AT ABOUT 800 cm⁻¹

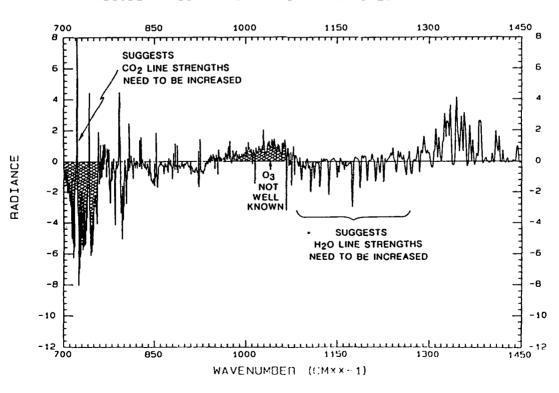




LINE STRENGTH ADJUSTMENTS: 1989 Summary

- H2O LINE STRENGTHS FROM 1090 TO 1200 cm⁻¹ NEED ABOUT 30% INCREASE
- CO2 LINE STRENGTHS FROM ABOUT 700 TO 760 cm-1 NEED TO BE INCREASED

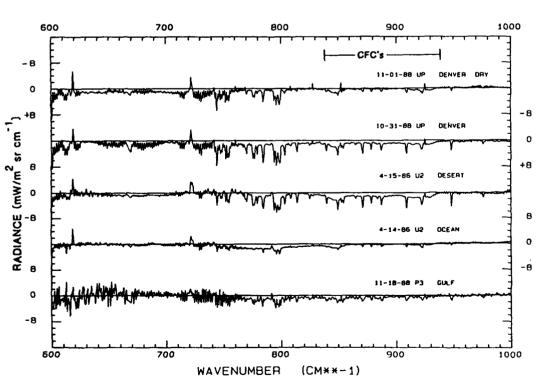
FASCOD2 - HIS 1 NOV. 11Z GAPEX UPLOOKING



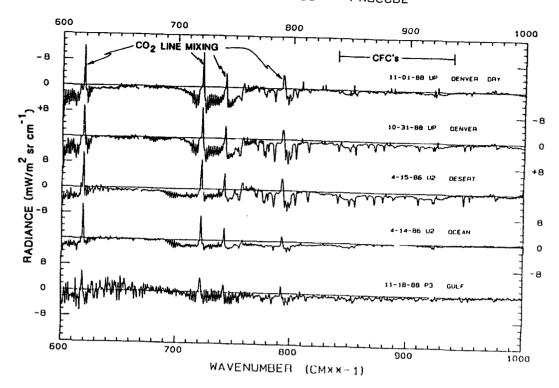
CO2 RESULTS FOR FASCOD3

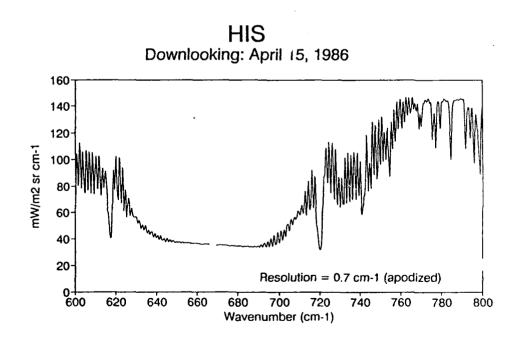
- AUGUST 1990 BETA TEST VERSION OF FASCOD3
- 1990 WATTSON / ROTHMAN CO2 LINES
- RINSLAND H2O LINES AUGMENTING HITRAN '86

RADIANCE DIFFERENCES HIS - FASCOD3

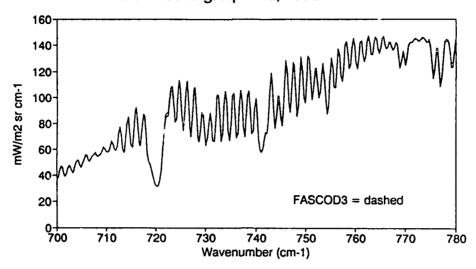


RADIANCE DIFFERENCES HIS - FASCOD2

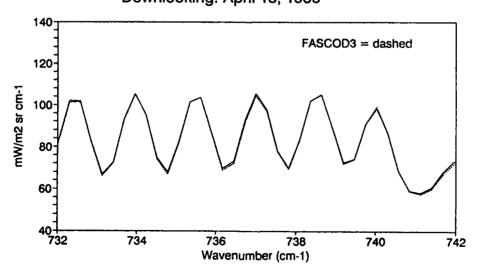




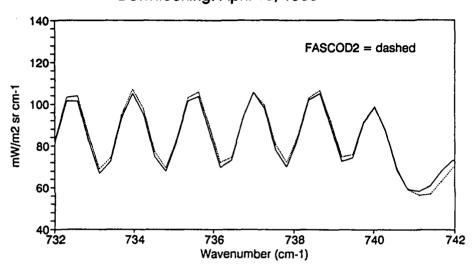
HIS & FASCOD3 Downlooking: April 15, 1986



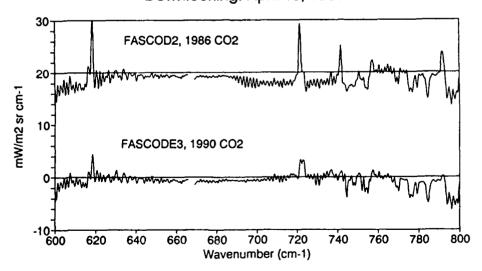
HIS & FASCOD3 Downlooking: April 15, 1986



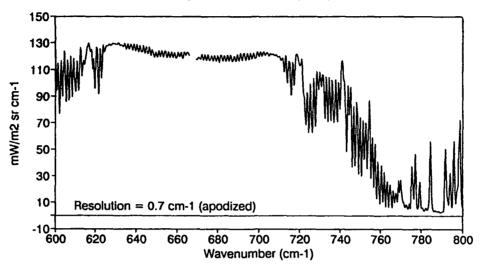
HIS & FASCOD2 Downlooking: April 15, 1986



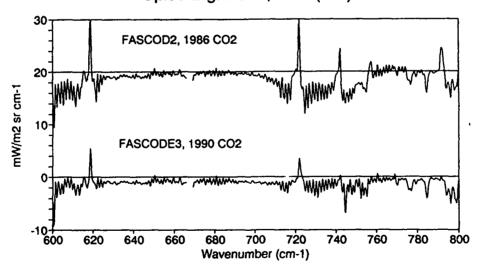
-FASCODE+ HIS Downlooking: April 15, 1986



HIS Uplooking: Nov 1, 1988 (11Z)

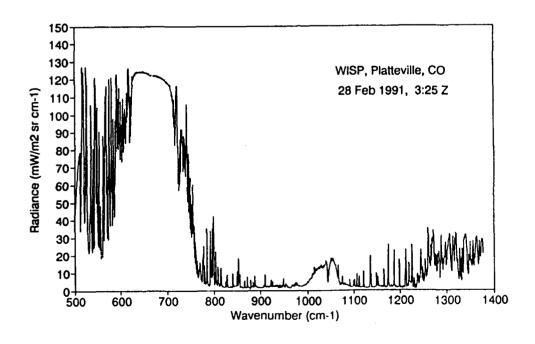


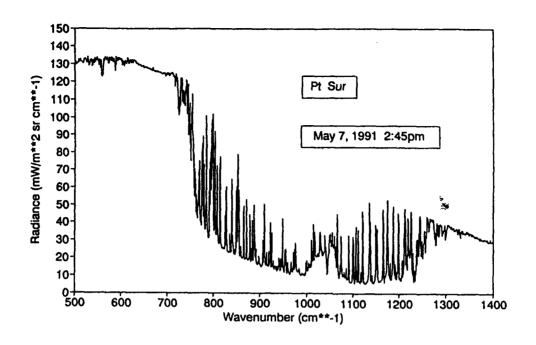
FASCODE - HIS Uplooking: Nov 1, 1988 (11Z)

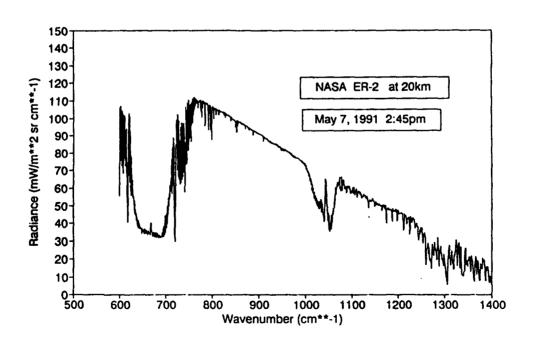


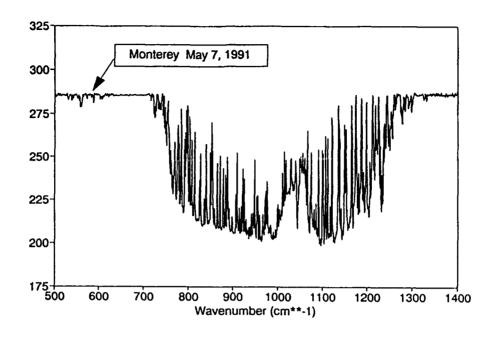
NEW 1991 OBSERVATIONS

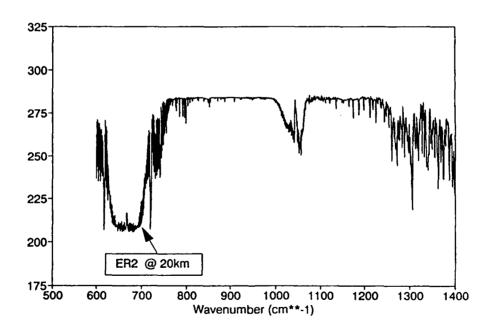
- PLATTEVILLE, COLORADO (WISP): UPLOOKING,
 VERY DRY, 26 FEB 15 MAR 1991
- PACIFIC OCEAN, OFF MONTEREY: UPLOOKING FROM SHIP "PT SUR" & DOWNLOOKING FROM NASA ER2, VERY MOIST, 7-9 MAY 1991
- CAPE CANAVERAL (CAPE) & SOUTHEAST US (SERON):
 DOWNLOOKING FROM NASA ER2, JULY-AUGUST 1991
- COFFEYVILLE, KANSAS (FIRE & SPECTRE):
 DOWNLOOKING FROM NASA ER2 & UPLOOKING,
 NOV-DEC 1991











SUMMARY

- FASCOD3 WITH LINE MIXING AND THE NEW WATTSON / ROTHMAN CO2 LINES SUBSTANTIALLY IMPROVES AGREEMENT WITH HIS OBSERVATIONS IN THE 15 μm REGION.
- NEW HIS OBSERVATIONS FOR DIFFERENT ATMOSPHERIC CONDITIONS HAVE BEEN ACQUIRED DURING 1991 AND MORE ARE EXPECTED.

VALIDATION OF HIS SPECTRAL MEASUREMENTS WITH THE FASCODE LINE-BY-LINE MODEL

S.A. Clough, R.D Worsham Atmospheric and Environmental Research, Inc., 840 Memorial Drive, Cambridge, MA 02139

> G.P. Anderson, M.L. Hoke, F.X. Kneizys Geophysics Laboratory (OP), Hanscom AFB, MA 01731

M. Wagner, R.M. Goody Harvard University, Department of Applied Sciences, Pierce Hall, Cambridge, MA 02138

An extended version of FASCODE (Clough et al., 1986) has been utilized in conjunction with the GL HITRAN database (Rothman et al., 1987) and carbon dioxide line coupling coefficients (Hoke et al., 1988), to perform spectral radiance comparisons with data from the High-Resolution Interferometer Sounder (HIS; Revercomb et al., 1987). Validations have been performed with down viewing spectra from 19.6 km and up viewing spectra from the surface for the 600-1100 cm⁻¹ spectral region. Effects that are observed include improvements relating to the 1991 HITRAN line parameters for water vapor and carbon dioxide, line coupling effects in carbon dioxide and absorption by anthropogenic molecules including CCl₄, CFC11, and CFC12. Of particular interest is the apparent effect of attenuation by sub-visual cirrus clouds and the correlation of the spectral residuals with carbon dioxide quantum number.



Validation of HIS Spectral Measurements with the FASCODE Line-by-Line Model

S.A. Clough

Atmospheric and Environmental Research, Inc.

R.D. Worsham

W.L. Smith

University of Wisconsin

H.E. Revercomb

R.O. Knuteson

H.M. Woolf

G.P. Anderson

Geophysics Directorate

M.L. Hoke

F.X. Kneizys

M.V. Wagner

Harvard University

R.M. Goody



Platform

Altitude

View

Surface

Instrument Temp.

Resolution (unappodized)

Photometric Calibration

absolute

relative

U2

19.6 km

nadir

ocean

ambient

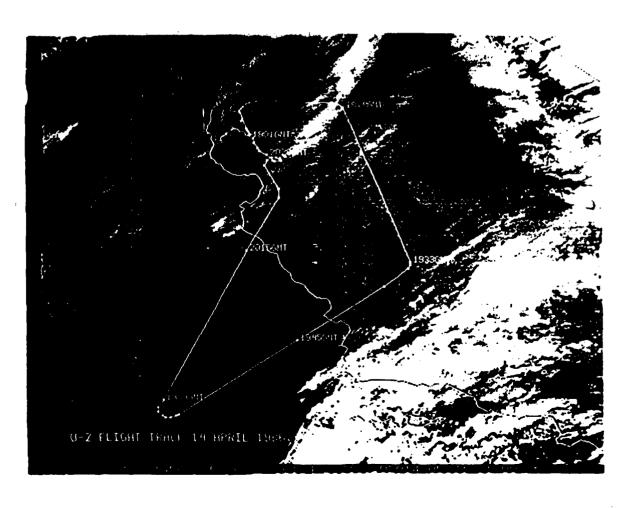
Bimpicit

0.365 cm-1

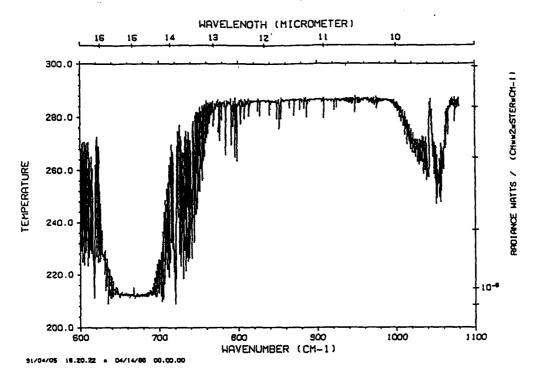
~1K

~0.5K





Radiance spectrum in equivalent brightness temperature for the long wave spectral region from 600 to 1100 cm⁻¹. The data were taken with the U. of Wisconsin High-Resolution Interferometer Sounder (HIS), Smith et al. (1983).





HIS/FASCODE Comparison

Data: unappodized

field of view correction in time domain

FFT to spectral domain

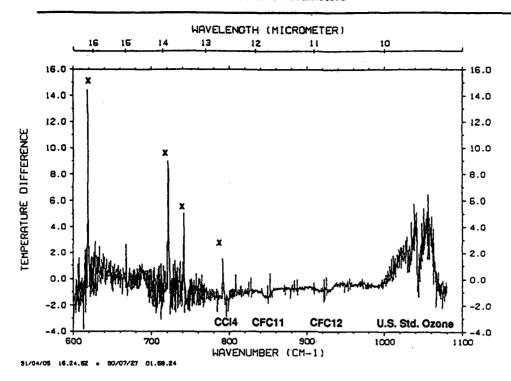
Calculation: line by line (FASCODE)

sinc scanning function

radiances at same spectral values as data



HIS - Calculated
HITRAN 86 Line Parameters



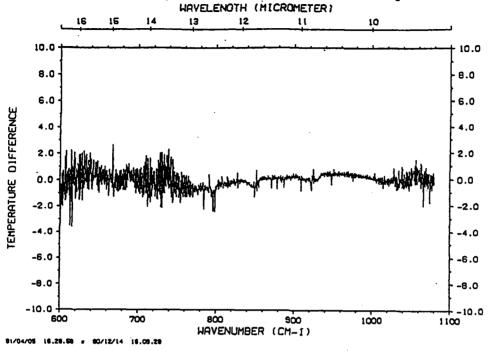
x - line mixing: CO2 Q branches



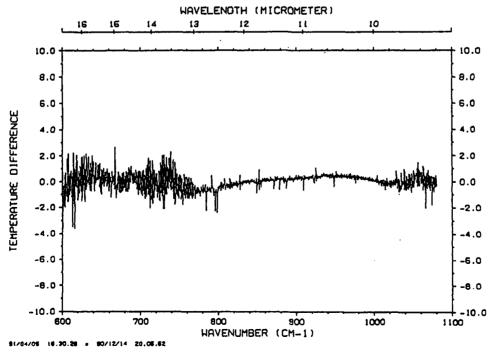
Parameters for FASCODE Calculation

Spectral parameters	1986 HITRAN database
Temperature profile	radiosonde
Water vapor profile	radiosonde
Ozone profile	U.S. Standard profile
Surface temperature	obtained from window radiance

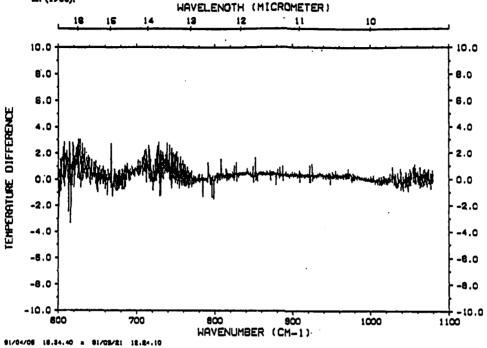
The effects of line coupling including its temperature dependence have been accounted for using the line coupling coefficients of Hoke et al. (1988) multiplied by a factor of 1.3 based on this and related spectra. Essential to these results are improved interim carbon dioxide line parameters provided by L.S. Rothman (1990). The improvements in the carbon dioxide line intensities are qualitatively consistent with those developed for ATMOS, Brown et al. (1987). The residuals for ezone have been reduced through the application of a retrieval algorithm to obtain an improved ozone profile. The remaining residual associated with the main Q-branch of carbon dioxide at 667 cm⁻¹ is due to warmer gas close to the instrument.



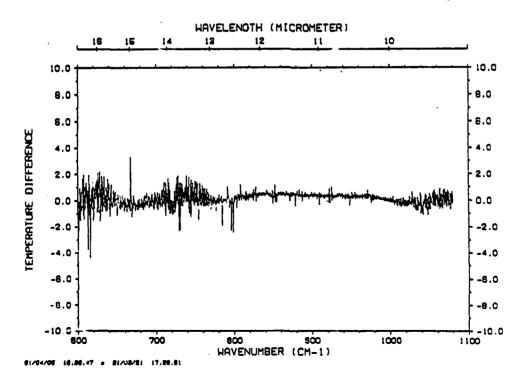
The same as the previous figure except that the effects of the absorption by the heavy molecules have now been included. This has been accomplished by using the cross sections of Massie et al. (1985) and the mixing ratios from the AER/NASA community model. The broad spectral features associated with CCl4, CFC11 and CFC12 are well accounted for.



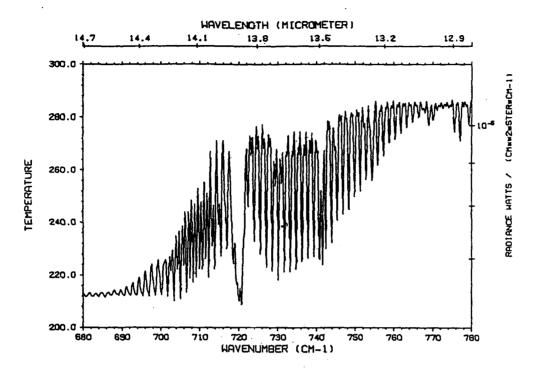
The same as the previous figures except that the effects of extinction due to a thin cirrus cloud at 13km have been included. The cloud has an optical thickness of 0.05 at 0.55 microns. For computational expediency conservative scattering has been invoked. The cloud model used for this example is one developed for LOWTRAN7 by Bric Shettle; spherical particles are assumed with a mode radius of four microns. The spectral characteristic of this cloud type provides a marked improvement in the spectral residuals. The idea of looking at this issue had its origins with the paper by Prabhakara et al. (1988).



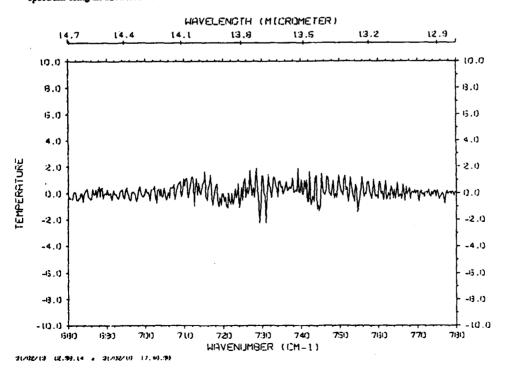
The effect on the spectral residuals of performing a temperature retrieval based on the spectral interval from 680-780 cm⁻¹. It may be noted that the mean error is improved from Fig. 5, but that the rms error about the mean is not greatly improved. Most of the irregular spaced residuals are due to incorrect intensities of pure rotational water lines.

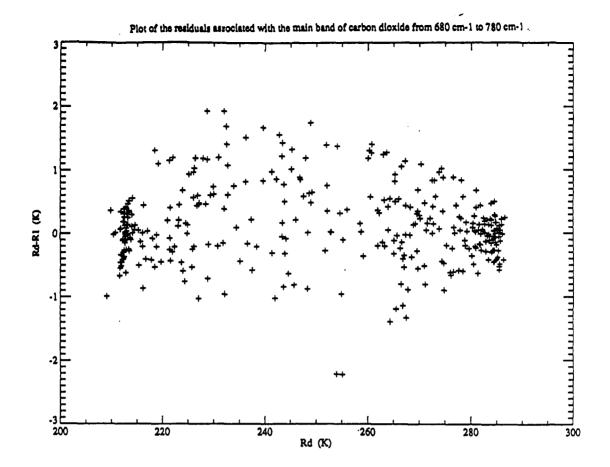


Radiance spectrum in equivalent brightness temperature for the long wave spectral region from 680 to 780 cm⁻¹. The data were taken with the U. of Wisconsin High-Resolution Interferometer Sounder (HIS), Smith et al. (1983).



The difference spectrum in equivalent brightness temperature between the HIS spectrum and a calculated spectrum using an advanced version of FASCODE.



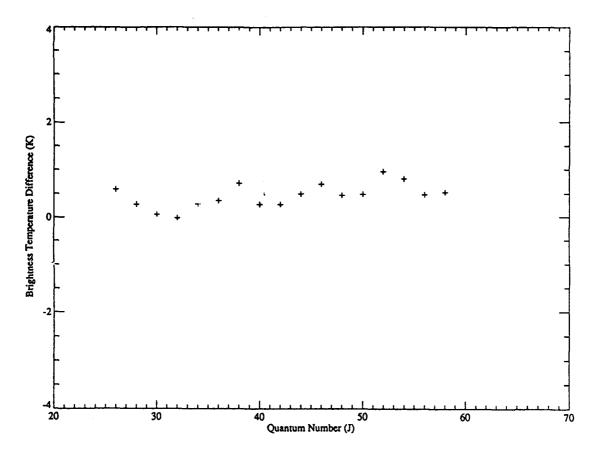




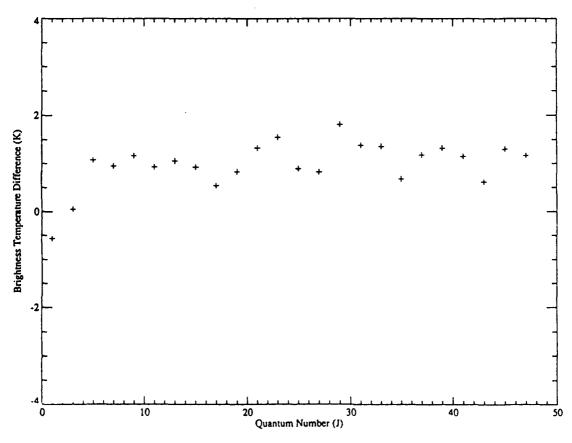
Residual Correlations

- 1) residuals vs. brightness temp. 680-780
- a) all points
- b) peaks
- c) valleys
- 2) residuals vs. brightness temp. for reduced spectral regions
- 3) residuals vs. quantum number by band
- a) 667 2-1
- b) 720 5-2

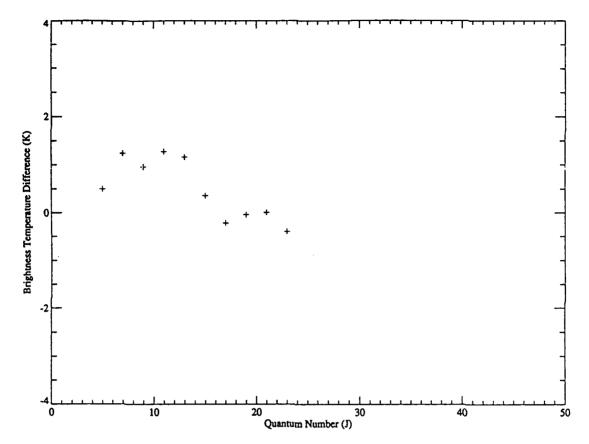
- residuals at the peak
 - doubly sampled data from U. of Wisconsin
- 4 point interpolation
- doubled the sampling frequency for calibration -
- 4 point interpolation



Band 2-1, R lines.



Band 5-2, R lines.



Band 5-2, P lines.



Summary

Conclusions:

- data are extremely good
- '91 line parameters significantly better than '86
- line coupling (some remaining issues)
- cross sections
- effects of thin cloud (Prabhakara et al.)

Remaining Issues:

- residuals ~1-2 K in CO2 region
 - not calibration
 - not temperature profile
 - CO2 line parameters: widths, strengths?
 - additional intervening cloud?
- residuals associated with water vapor lines
 - pure rotation: strengths and widths

IMPROVED HNO₃ BAND MODEL PARAMETERS

N. Jones, A. Goldman, D. Murcray, F. Murcray, W. Williams Department of Physics, University of Denver, Denver, CO 80206

Band model temperature dependent parameters for HNO₃ have been recalculated for the 11.3 µm bands using the best available molecular parameters and integrated band strengths. Parameters are calculated with a 1 cm⁻¹ resolution and for several temperatures appropriate to the lower stratosphere. The new parameters should be suitable for both MODTRAN and LOWTRAN. A brief presentation of the calculations as well as sample results will be included.

IMPROVED HNO $_3$ BAND MODEL PARAMETERS FOR THE 11.3 μ REGION

Nicholas Jones Aaron Goldman David Murcray Frank Murcray and Walter Williams

University of Denver Department of Physics Denver, CO 80208

Annual Review Conference on Atmospheric Transmission Models Hanscom AFB

11-12 June, 1991

ABSTRACT

- HISTORY
- METHODS
- PRELIMINARY RESULTS
- COMPARISONS
- FUTURE WORK

HISTORY OF HNO3 MODELS

Date	Group	Data Base	Model
1971	U of D	Lab Meas. Amb Temp	5 cm ⁻¹ B-M
1975	U of D	Lab Meas. Multi-Temp	5 cm ⁻¹ B-M
1978	G.L.	5 cm ⁻¹ B-M	LOWTRAN 4
1981	U of D NASA/Ames	Lab Meas. Multi-Temp	5 cm ⁻¹ B-M
1984	NASA/Ames U of D	Lab Meas. Multi-Temp	1 cm ⁻¹ B-M
1984/6	Maki et al	Lab Meas. High Res	Line-by-Line
1987	G.L.	Line-by-Line	HITRAN 1986
1991	U of D	Line-by-Line	1 cm ⁻¹ B-M w/Temp

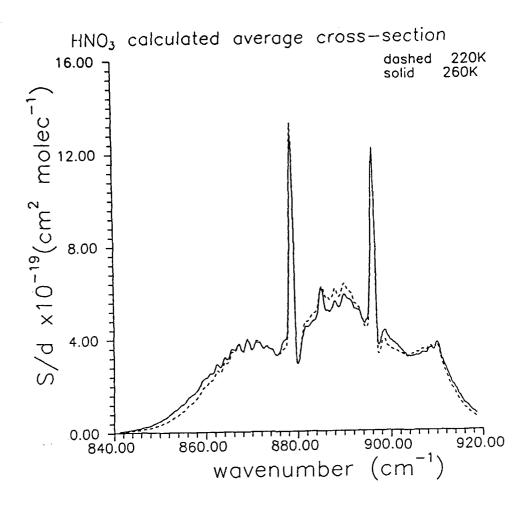
HNO₃ BAND MODEL PARAMETERS Method of calculation

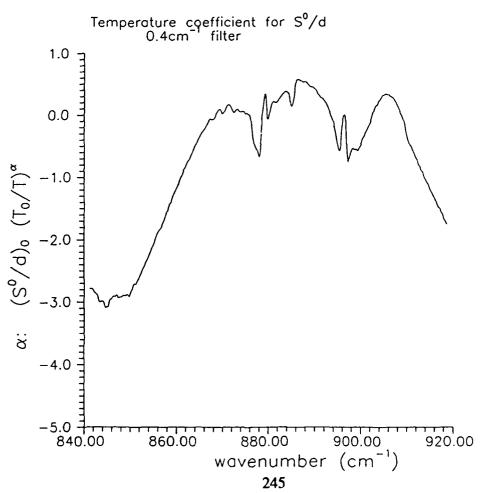
. Calculate Band Model Coefficients for several temperatures using \mbox{HNO}_3 line parameters and Goodys' Statistical method

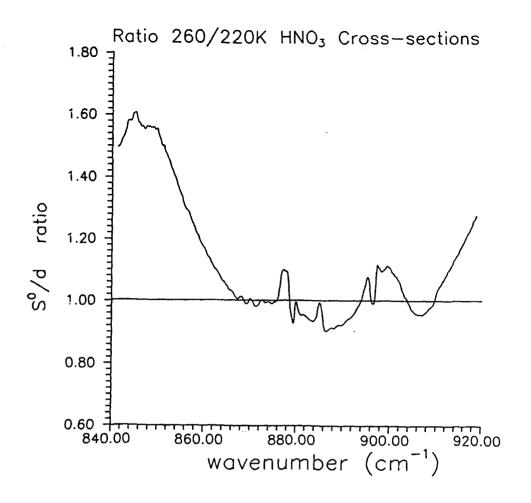
$$x/L - \frac{S^{0}}{2\pi\gamma^{0}} - \frac{1}{8} \frac{\left(\sum_{i=1}^{N} S_{i}^{0}\right)^{2}}{\left[\sum_{i=1}^{N} \left(S_{i}^{0} \gamma_{i}^{0}\right)^{1/2}\right]^{2}}, \quad \beta - \frac{2\pi\gamma^{0}}{d} - \frac{8}{\Delta\nu} \frac{\left[\sum_{i=1}^{N} \left(S_{i}^{0} \gamma_{i}^{0}\right)^{1/2}\right]^{2}}{\sum_{i=1}^{N} S_{i}}.$$

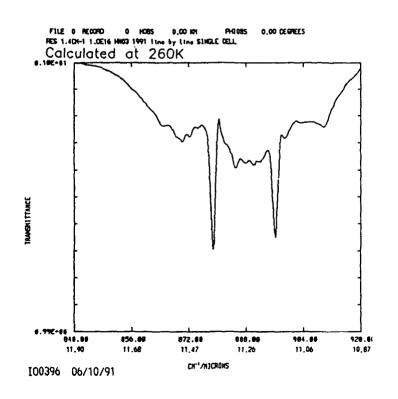
$$S^{0}/d - \left(\frac{2\pi\gamma^{0}}{d}\right) \left(x/L\right) - \frac{1}{\Delta\nu} \sum_{i=1}^{N} S_{i}^{0}$$

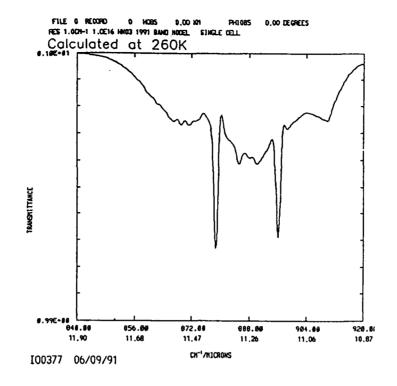
- Approximate Band Model Coefficients with Linear Coefficient $K {=} \, S^0 / d$
- Derive Temperature Dependent Linear Coefficients $K(T) \approx K_O(T_O) (T_O/T)^{V}$

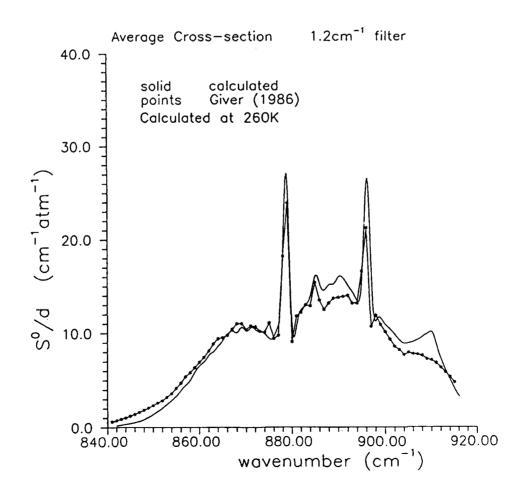












SIGNIFICANCE OF TEMPERATURE DEPENDENCE

T-Dep Results

- Many Spectral Regions have ≤ 5% T-Dep
- Some Spectral Regions have ≥ 20% T-Dep
- Strongest T-Dep in Wings
- Incomplete "Hot Bands" Analysis

Applications

Select Optimum Spectral Regions for HNO₃
 Measurements:

Regions w/wo Interference (F11, F12, H₂O)

Regions w/wo T-Dep

• Verify T-Profile used for Analysis of Emission Data

REMAINING TASKS

- Extend Coefficients into the Wings
- Further Compare Line Parameters and Band Model Parameters with High Resolution and Low Resolution Lab Data
- Publish Results
- Make Data Base Available

LINE-BY-LINE CALCULATIONS OF ATMOSPHERIC FLUXES AND HEATING RATES

S.A. Clough, M.J. Iacono, J.-L. Moncet Atmospheric and Environmental Research, Inc., 840 Memorial Drive, Cambridge, MA 02139

A rapid and accurate radiance algorithm has been developed to provide enhanced capability for the line-by-line calculation of fluxes and heating rates using FASCODE for thermally inhomogeneous non-scattering atmospheres. First moment quadrature is utilized to obtain fluxes from the radiances, providing accuracies of 1% for two angles and 0.2% for three angles. Optical depths are calculated for a single zenith angle, generally the nadir. Extensive calculations have been performed for water vapor using the mid-latitude summer atmosphere in the context of the ICRCCM campaign. Comparisons with other line-by-line models have been conducted. Effects of line cutoff procedures have been studied in detail and will be discussed. The role of the water vapor continuum (Clough et al., 1989) will be described in detail. The heating rate and flux calculations are presented spectrally to provide insight into the correlation of the radiative effects between spectral domain and altitude. The importance of the 300-600 cm⁻¹ region for the upper tropopause will be discussed. Calculations have also been performed for the tropical and subarctic winter atmospheres with important implications related to the water vapor continuum.



Line-by-line Calculations of Atmospheric Fluxes and Heating Rates: Application to Water Vapor

S. A. Clough

M. J. lacono

J.-L. Moncet

Atmospheric and Environmental Research, Inc.

12 June 1991

ICRCCM: InterComparisons of Radiation Codes for Climate Models

LBL: W.L. Ridgway - Goddard Laboratory for Atmospheres (GLA)

Model Atmospheres:

Mid-Latitude Summer

Tropical

66 layers

Sub Arctic Winter

Line-by-Line Calculation
Advanced version of FASCODE.

G.P. Anderson & F.X. Kneizys

Radiance Algorithm

Topics

Calculation:

heating rate:

flux divergence

flux:

first moment quadrature

radiance:

inhomogeneous atmosphere

spectral integration:

box car

Application:

spectral sampling error at high altitudes (GLA)
of quadrature points
spectral extent of line contributions
water vapor continuum
model atmospheres
spectral mapping of cooling rate vs. altitude

Heating Rate:

$$\left(\frac{\partial T}{\partial t}\right)_{IR} = -\frac{1}{c_P P} \frac{\Delta F}{\Delta Z}$$

F: net flux
$$F_{i} = F_{i}^{\uparrow} - F_{i}^{\downarrow}$$

$$\Delta F = F_{i} - F_{i-1}$$

Flux:

$$F_{v}^{\uparrow\downarrow} = \int_{0}^{2\pi} \int_{0}^{\frac{\pi}{2}} I_{v}(\theta, \phi) \cos \theta \sin \theta d\theta d\phi$$

 I_v : monochromatic radiance

$$=2\pi\int_0^1 I_v(\mu)\mu d\mu$$

 μ : direction cosine

$$=2\pi\sum_{j=1}^N w_{j,N}I_v(\mu_j)$$

 $w_{l,N}$: first moment quadrature

Radiance Algorithm:

↑	I	t U	B_v^U
			D_{v}

$$\hat{B}_{v}$$

- Isothermal (old FASCODE)

$$I_{v}^{\uparrow} = \hat{B}_{v}(1 - T_{v})$$

 T_{v} : layer transmittance

$$T_{v}$$
: $\exp(-\tau_{v})$

- linear in τ

$$I_{v}^{\uparrow} = B_{v}^{U} (I - T_{v}) - (B_{v}^{L} - B_{v}^{U}) T_{v} + \frac{B_{v}^{L} - B_{v}^{U}}{\tau_{v}} (1 - T_{v})$$

 τ_{v} : layer optical depth

- new algorithm (new FASCODE)

$$I_{v}^{\uparrow} = \left\{ \left(\hat{B}_{v} + a\tau_{v} \ B_{v}^{U} \right) / \left(1 + a\tau_{v} \right) \right\} \ \left(1 - T_{v} \right)$$

 $a \sim 0.2$

- limits:

isothermal

linear in au

new

thin
$$(\tau \rightarrow 0)$$

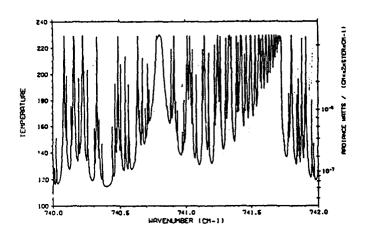
thin $(\tau \to 0)$ $\hat{B}_v \tau_v$ $\frac{B_v^U + B_v^L}{2} \cdot \tau_v$

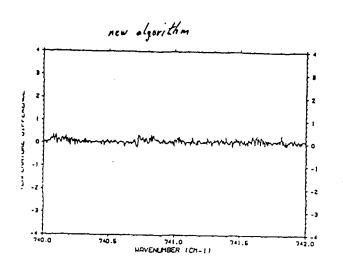
 $\hat{B}_{\upsilon}\tau_{\upsilon}$

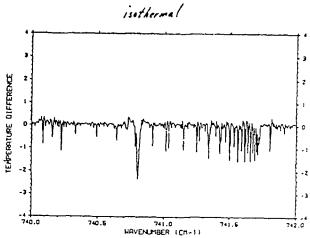
thick
$$(\tau \to \infty)$$

 \hat{B}_{v}

Spectral Radiance







Approx: 1 loyer

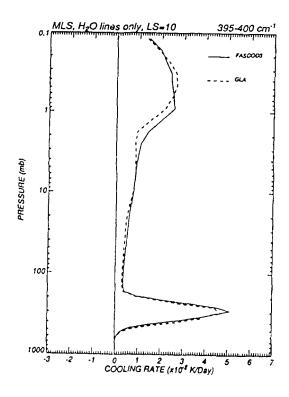
2.5 km thick

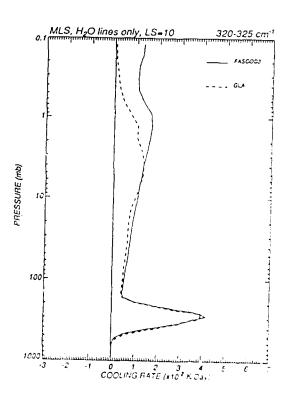
5.2 K J. Staroutia 1

"Correct": 5 layers

ceck layer 0.5 ha thick

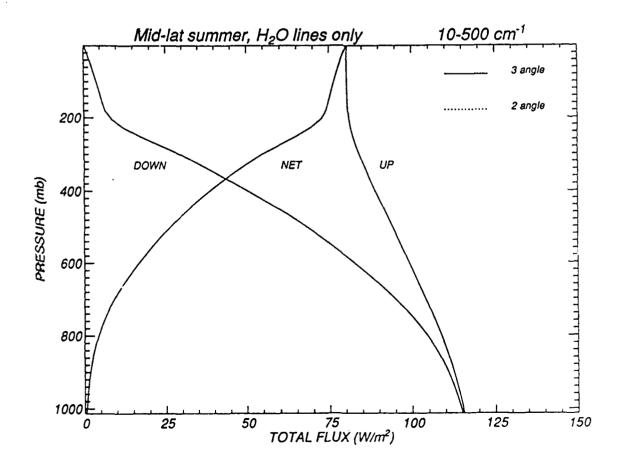
uses new elgorithm for redinace

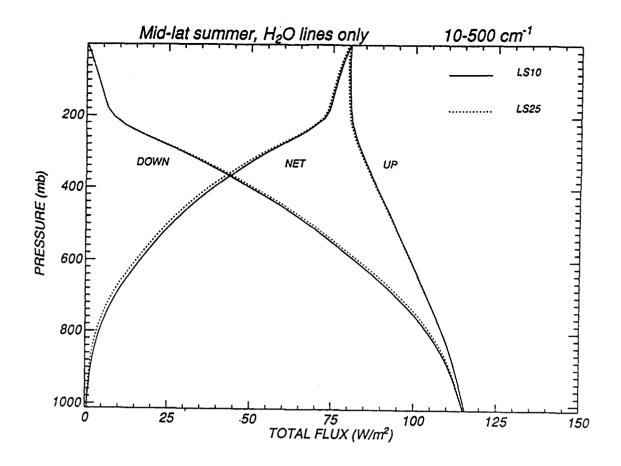


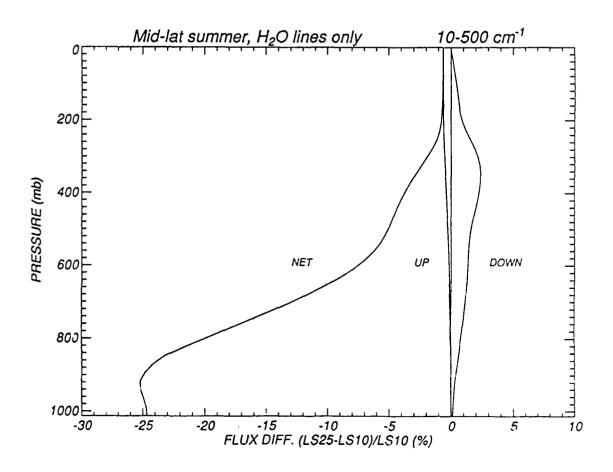


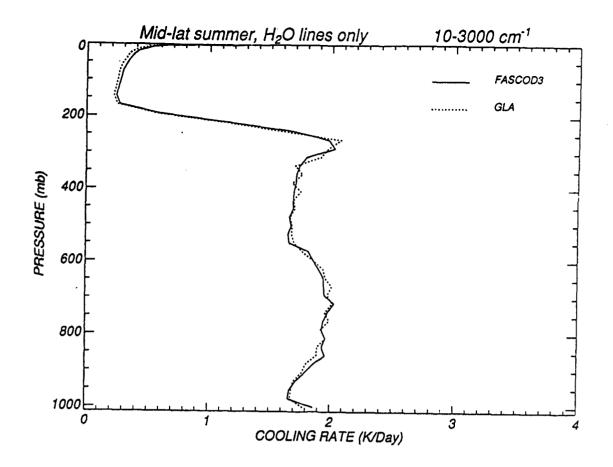
Flux Errors (%): Quadrature vs. 25 pt. trapezoidal

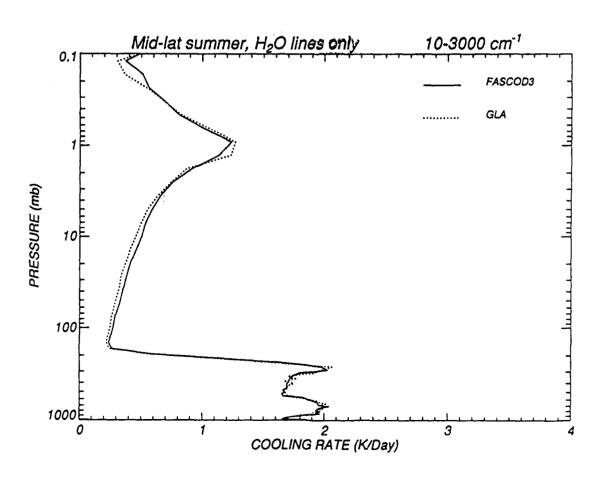
# angles	quad	rature	first moment quadrature	
	up	down	up	down
1	-2.3	8.5	0.7	-4.5
2	-0.13	0.99	0.05	-0.58
3	0.006	0.16	0.007	-0.063
4	-0.009	0.04	0.003	0.020

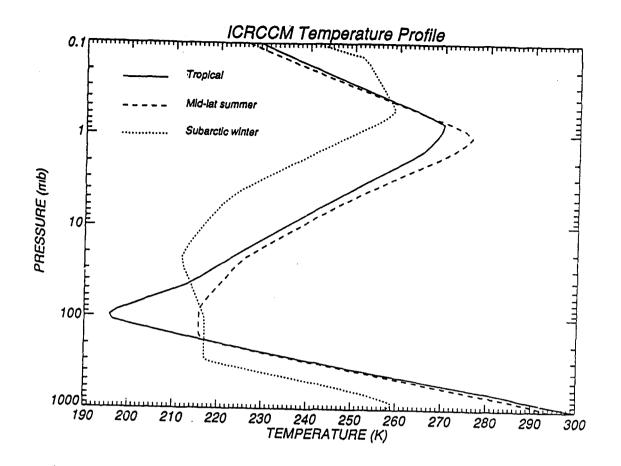


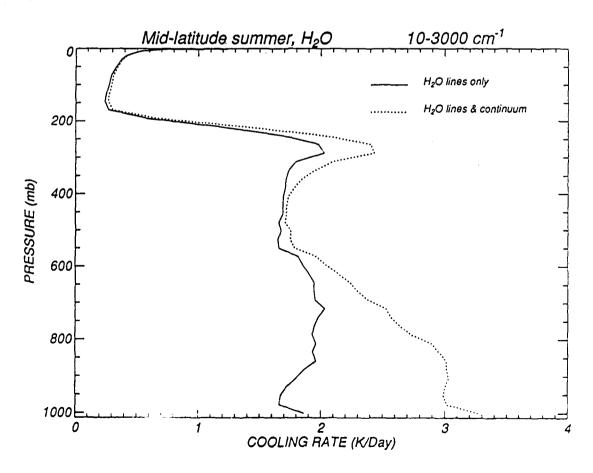


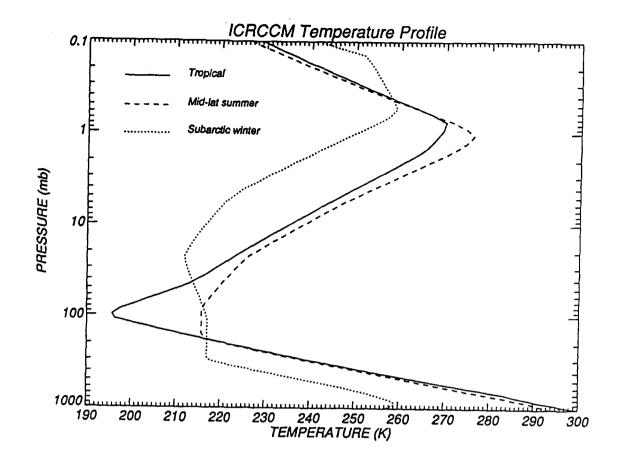


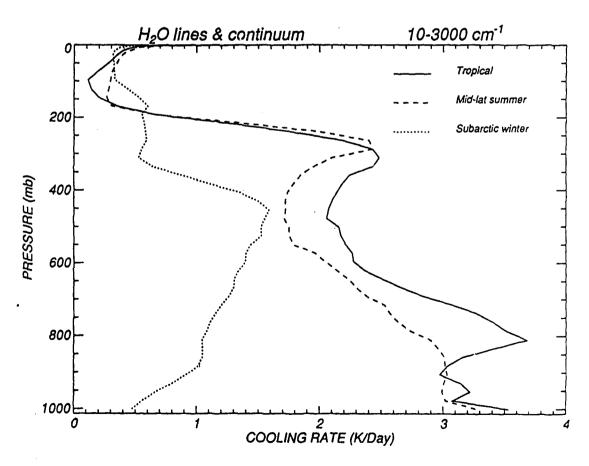


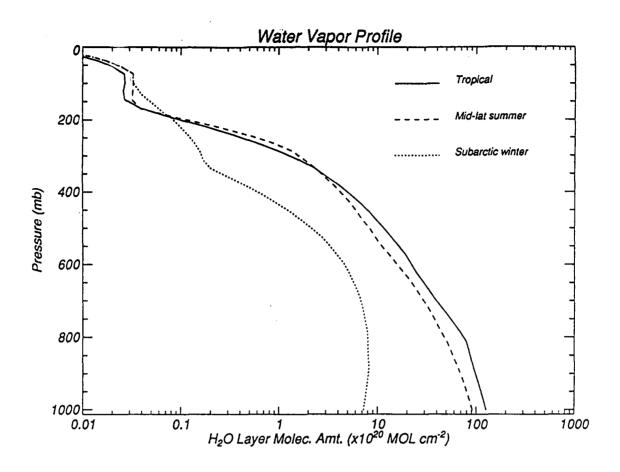


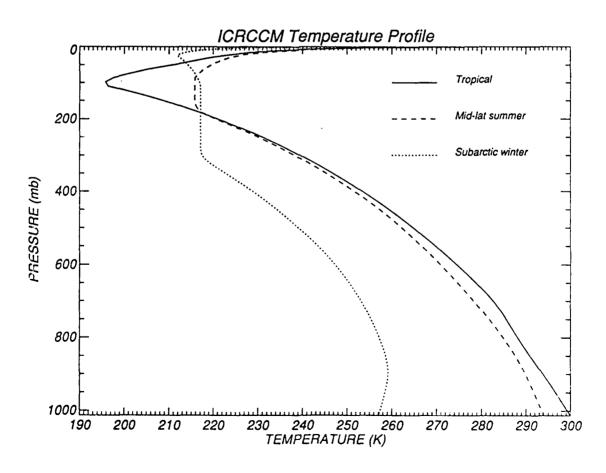


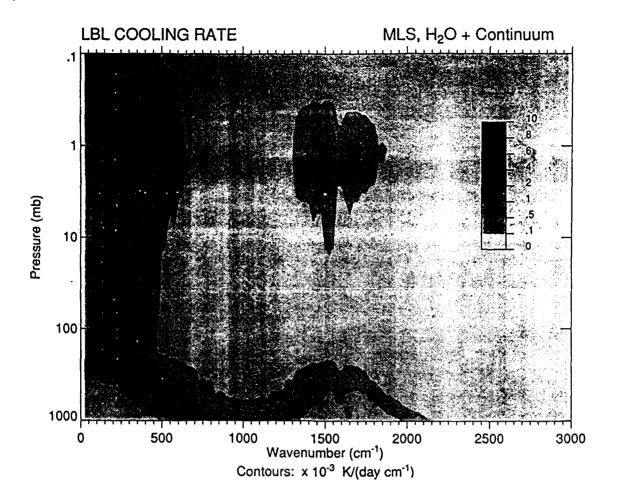


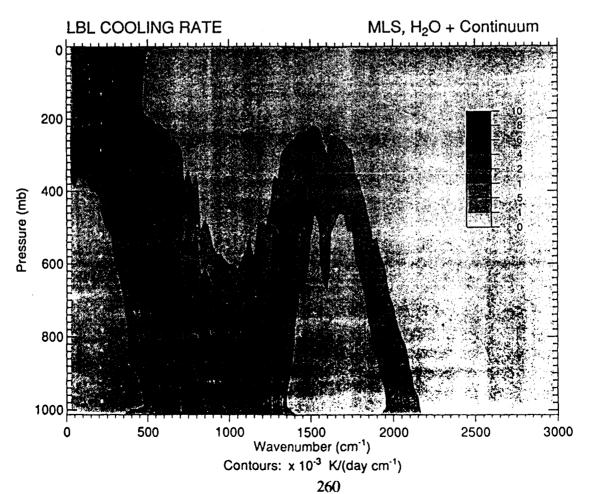


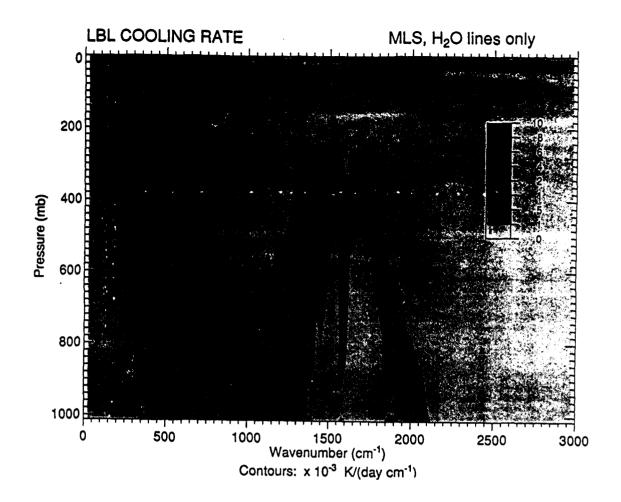


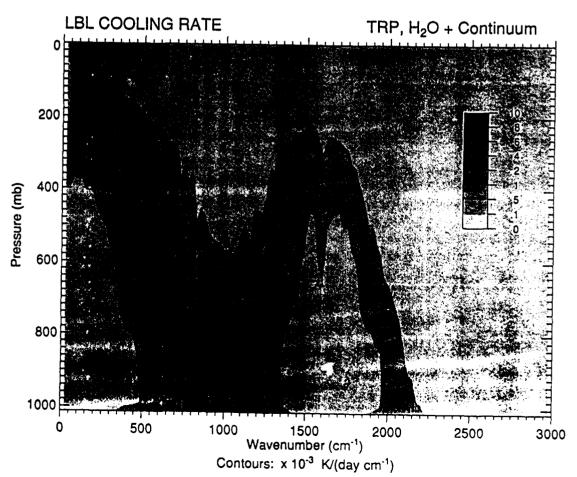


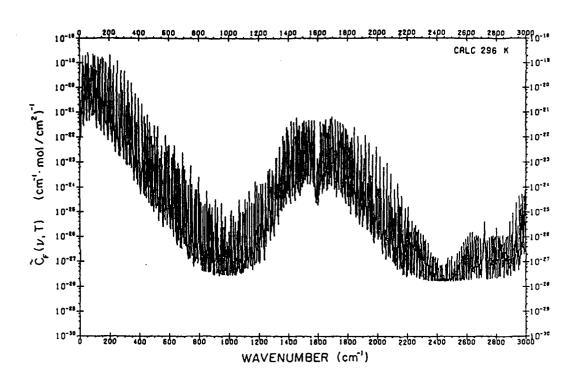












COMPARISON OF FASCOD2 AND LOWTRAN7 MODELS WITH FIT SPECTRAL TRANSMITTANCE MEASUREMENTS IN THE 3-12 μm REGION

J.M. Thériault
DREV-Defense Research Establishment Valcartier,
P.O. Box 8800, Courcelette, Québec, Canada, GOA-1RO

A comparison is made between FASCOD2 and LOWTRAN7 predictions with experimental measurements carried out at DREV over a 5.7 km transmission path under a wide range of ambient temperature (-9° to 30° C) and humidity conditions (1.1 to 14.2 g/m³). Following a brief review of the FIT instrumentation¹, low and high resolution measurements (20 and 1 cm⁻¹) of atmospheric transmittance in the 3-12 μ m region are reported. The most significant differences have been recorded in winter and spring conditions. The analysis of the results suggests that the water vapor continuum modeling in the 7-12 μ m region has some limitations at low ambient temperature in both models. Furthermore, the comparison of LOWTRAN7 with measurements has revealed an unexpected difference of 12%, independent of temperature and humidity conditions in the important transmission window near 3.6 μ m. This difference is attributed to the modeling of the 3020 cm⁻¹ absorption hand of methane.

¹Theriault, J.M., Roney, P.L. and Reid, F., "Atmospheric Transmission in the 2.8-5.5 µm Region; Description of the Fourier Interferometric Transmissometer and

Typical Result at Low Temperatures", Appl. Opt. 29, 3654-3666 (1990).

COMPARISON OF FASCOD2 AND LOWTRAN7 MODELS WITH FIT SPECTRAL TRANSMITTANCE MEASUREMENTS IN THE 3-12 µm REGION

J.-M. Thériault

DREV-Defence Research Establishment Valcartier P.O. Box 8800, Courcelette, Quebec, Canada, GOA-1RO

also with (Mar. 91- Feb. 92)

CIMSS-Cooperative Institute for Meteorological Satellites Studies University of Wisconsin Space Science and Engineering Center 1225 West Dayton Street Madison, WI 53706

Presented at the 1991 Annual Review Conference on Atmospheric Transmission Models, AFGL 11-12 June 1991

Propagation Group

High Resolution Atmospheric Transmission Measurement

- 5.7-km transmission range
- FIT-Fourier Interferometric Transmissometer
- Quebec city area: Wide range of ambiant temperature and humidity conditions

Current work:

- Transmissometer calibration techniques
- Water vapor and temperature effects
- Comparison with FASCOD2 and LOWTRAN7 predictions

FIT-Receiver:

- 1 Parabolic Newtonian 17-in diameter F/4.6 telescope
- 2 BOMEM DA2.02 field Interferometer:
 - Resolution from 0.04 cm⁻¹ to 64 cm⁻¹
 - Clear optical beam cross section ~ 14 cm²
 - Bandpass: 2.8-12 µm MCT det. and BaF2 beamsplitter
- 3 System field of view: 0.5 mrad

FIT-Calibration:

$$T_{atm}(v) = \frac{1}{K(v)} \frac{P_{d}(v)}{P_{loc}(v)}$$

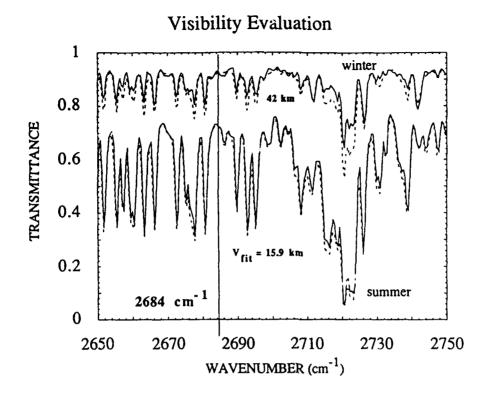
- Calibration factor:

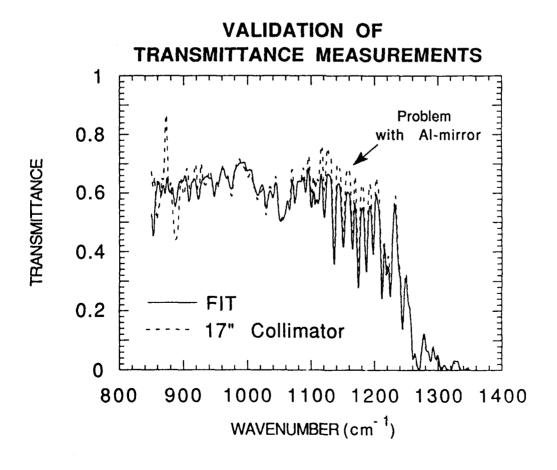
$$K(v) = \frac{(R)}{d^2} \frac{A_m}{A_{ap}} \frac{f_1^2 f_3^2}{f_2^2} (RQ)$$

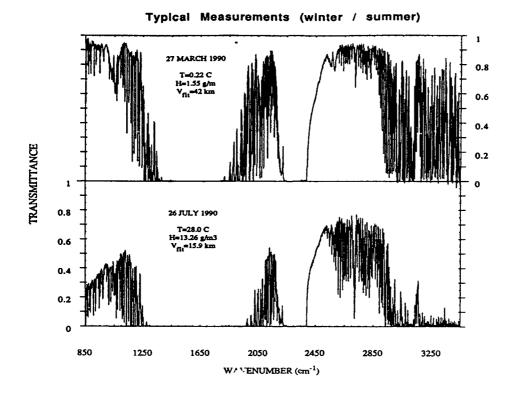
- In the Mid-IR: Verification of results with a wideband transmissometer (3.4-4.1 μm).
- In the Far-IR : Correction Factor $F_c(\mu) = R^2(\mu) \cdot Q$

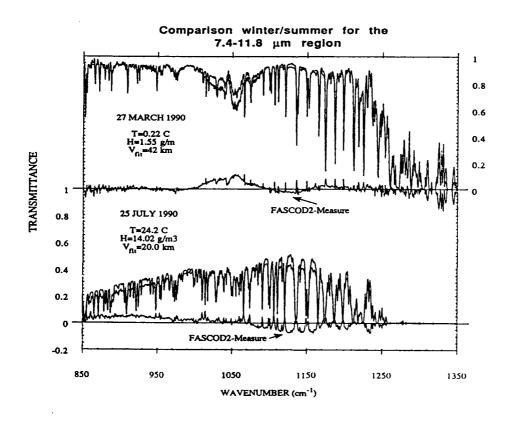
Comparison of Measurements with FASCOD2:

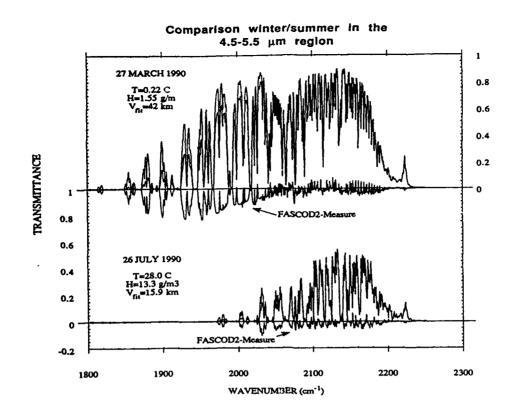
- 1 Resolution of 1 cm⁻¹
- 2 Spectral region: 850-3500 cm⁻¹
- 3 Temperature Range: -8.55 to 29.4 C
- 4 Humidity Range: 1.16 to 14.2 g/m³
- 5 HITRAN Database: 1986 Edition
- 6 Contributions of other active molecules namely O₃,
 N₂O, CH₄, CO, O₂, and N₂: AFGL Mid-summer or Mid-winter conditions except for the CO₂ (350 ppm)
- 7 Aerosol model: Rural Type
- 8 Visibility evaluation: Matching FASCOD2 spectra with measurements at 2684 cm⁻¹

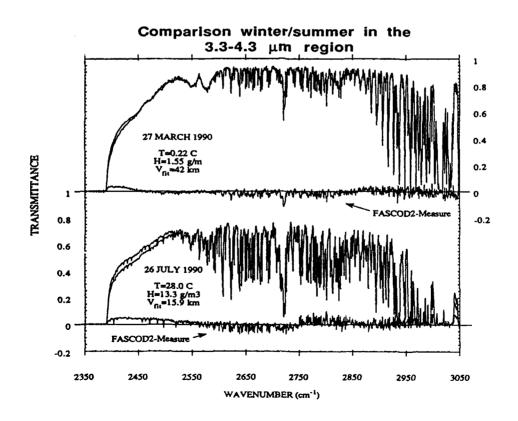


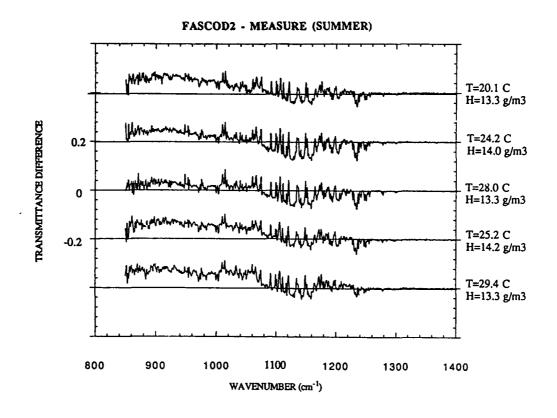


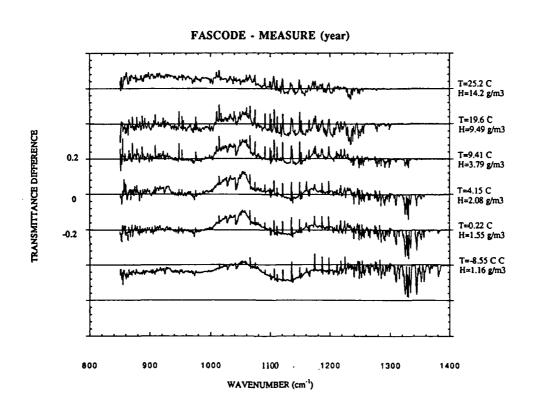


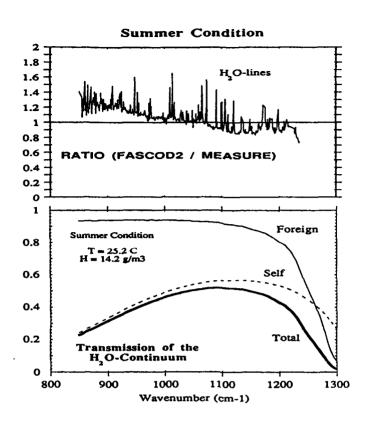


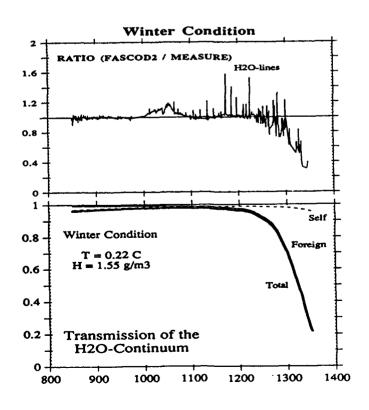




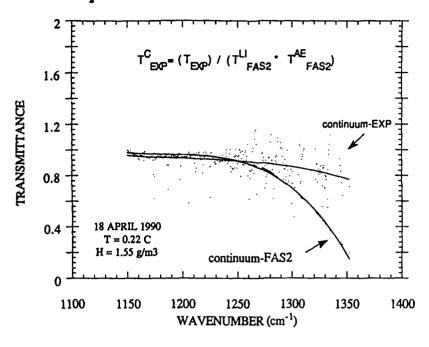


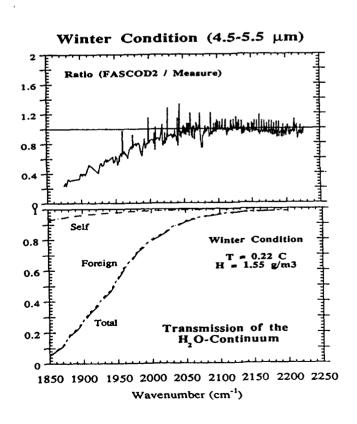




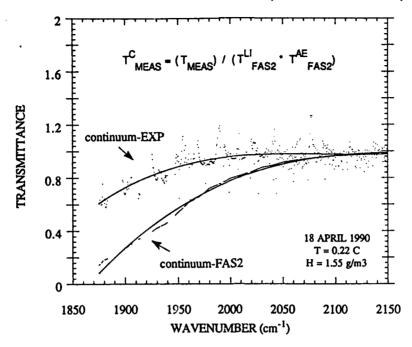


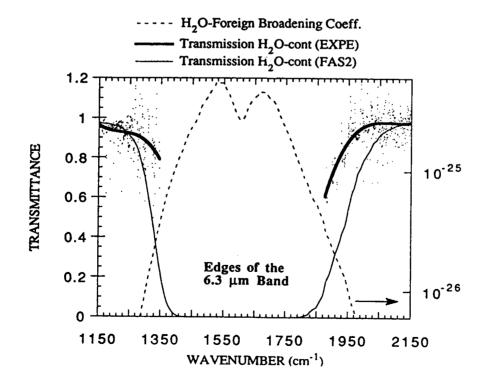
H₂O-continuum evaluation (cold conditions)





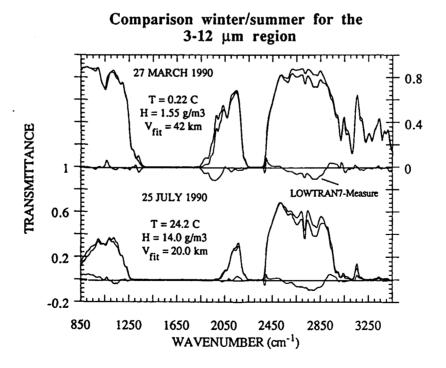
H2O-continuum evaluation (cold conditions)

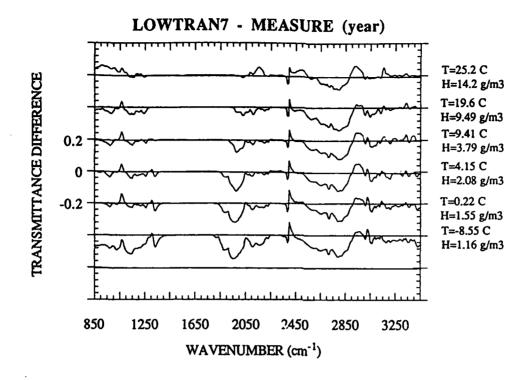


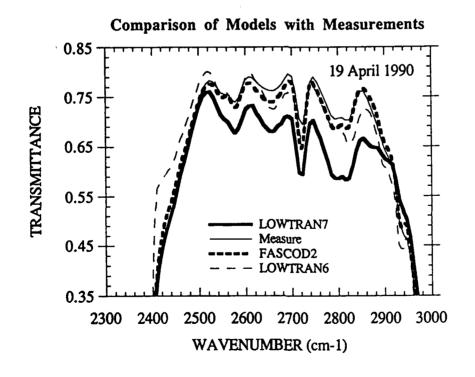


Comparison of Measurements with LOWTRAN7:

- 1 Resolution degraded to 20 cm⁻¹
- 2 Spectral region: 850-3500 cm⁻¹
- 3 Temperature Range: -8.55 to 29.4 C
- 4 Humidity Range: 1.16 to 14.2 g/m³
- 6 Contributions of other active molecules namely O₃, N₂O, CH₄, CO, O₂, and N₂: AFGL Mid-summer or Mid-winter conditions except for the CO₂ (350 ppm)
- 7 Aerosol model: Rural Type
- 8 Visibility evaluation: Matching FASCOD2 spectra with measurements at 2684 cm⁻¹







SUMMARY(FASCOD2)

- 1 Overall agreement with measurements is very good. The average difference over the 3-12 μm region is generally smaller than I5I% (ΔT/T). The remaining differences have been attributed to the water vapor and to the ozone.
- 2 The analysis of results suggest that for
 - H₂O The self broadening continuum absorption should be increased by approximately 10-15% in the 850-1000 cm⁻¹·
 - The Foreign broadening continuum absorption should be reduced by approximately 50 % at the edges of the 6.3 μm absorption band (5.3 μm and 7.5 μm): Assuming that the lines parameters are perfect.
 - The absorption of several lines in the 1100-1250 cm⁻¹ region should be increased by approximately 20-50%.
 - O₃ Generally for temperatures smaller than 10 C, the FASCOD2 transmittance of the ozone band at 9.6 μm is higher than the experimental one by approximately 10% on the average. Both the concentration and the absorption parameters may be the cause of this.

SUMMARY(LOWTRAN7)

- 1 The average difference is generally smaller than 181%.
- 2 The analysis of results suggest that for
 - H₂O Continuum: (same remarks as for FASCOD2)
 - CH₄ In the transmission window near 3.6 μm, LOWTRAN7 is always smaller than the measured one by approximately 12%, independently of the temperature and humidity conditions. It is attributed to the modeling of the 3020 cm-1 absorption band of methane.

SPECTRAL SOLAR RADIATION MODELING, MEASUREMENT, AND DATA BASE ACTIVITIES AT THE SOLAR ENERGY RESEARCH INSTITUTE

C.J. Riordan, R.L. Hulstrom Solar Energy Research Institute, 1617 Cole Boulevard, Golden, CO 80401

The Solar Energy Research Institute uses atmospheric transmission codes and data to characterize spectral solar radiation (0.3-3.0 μ m) at the earth's surface for designing and predicting the performance of spectrally selective solar energy conversion devices, such as solar electric cells (photovoltaics). We use a simple model called SPCTRAL2 that was developed at SERI using comparisons with more complex codes, such as LOWTRAN, and comparisons with limited measured data. We also maintain a data base with 3000 measured spectra, 0.3-1.1 μ m at a 2-nm resolution. Our current activities include participation in a new International Energy Agency, Solar Heating and Cooling Program, Task 17 on Measuring and Modeling Spectral Radiation Affecting Solar Systems and Buildings. We will present an overview of all of our spectral solar radiation modeling, measurement, and data base activities at SERI.

Spectral Solar Radiation Modeling, Measurement, and Data Base Activities at the Solar Energy Research Institute

Carol Riordan and Roland Hulstrom

Solar Energy Research Institute Golden, Colorado 303-231-1344 303-231-1220

June 1991



Objective

Briefly describe SERI's interests and activities in spectral solar radiation, and identify conference participants with similar interests

Tektronix

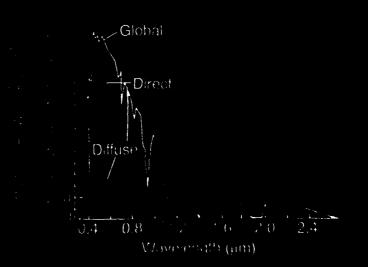
Interests

Spectral solar radiation at the earth's surface from 280 to 3000 nm at about 1-nm resolution for designing and predicting the performance of spectrally selective solar energy conversion devices (e.g.,photovoltaics)

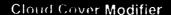
23 4 16 13

Modeling

logad Salar Zerath Asig e Turk eldy Proceedable Shater Ancie Sale New Year



Modeling





Reference there were than communities of the experience of the exp

Modeling - Measurements

International Energy Agency
Solar Heating and Cooling Programme Annex 17
Measuring and modeling spectral
radiation affecting solar systems and buildings

- A: Narrow-band spectral and broad-band infrared radiometry
- **B**: Broad-band visible radiometry
- C: Narrow-band spectral radiation data acquisition and analysis
- D: Narrow-band spectral radiation modeling-SERI
- E. Broad-band visible radiation data aquisition and analysis
- F. Broad-band infrared radiation data aquisition and analysis

Measurements

Spectroradiometers

Geophysical Environmental Research 300-3000 nm

LI-COR LI-1800

300-1100 nm

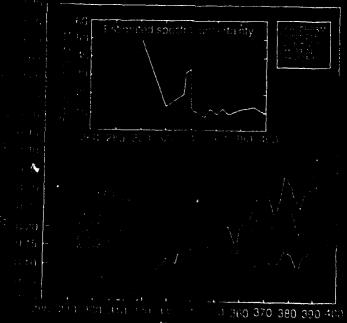
Optronic Laboratories - 752D

200-800 nm

Instruments S.A. DH10

200-800 nm

Direct Normal UV Spectral Irradiance SERI/Solar Radiation Research & Metrology Branch (SRR&M) ISA/DH10 Spectroradiometer Jan 05 1990





Measurements

Department of Energy Atmospheric Radiation Measurement (ARM) Program

Characterizing, evaluating, and calibrating instruments for measuring atmospheric properties and radiation at the Clouds and Radiation Testbed (CART) Sites

Taktmniv

LOWTRAN 7 COMPARISONS WITH FIELD MEASUREMENTS

R. Smith, N. McNabb, K. Hammerdorfer, T. Corbin TECOM Fort Belvoir Met Team, AMSTE-TC-AM (BE) CCNVEO, Ft. Belvoir, VA 22060

This paper presents comparisons between LOWTRAN 7 and field measurements taken during a number of field tests conducted by the US ARMY Center for Night Vision and Electro-Optics. The data was taken by the TECOM Ft. Belvoir Meteorological Team. Transmission data in the .4 to .7 micron, 3 to 5 micron, and 8-12 micron bands were taken at Ft. A.P. Hill, VA in March and April 1991. Data at 1.54 micron was taken at Ft. Greely, AK in February and at Ft. Clayton, Panama during March and April 1991. A description of the equipment is provided along with the input values used for the LOWTRAN calculations.

LOWIRAN 7 COMPARISONS WITH FIELD MEASURMENTS

R.W. SHITH, T. CORBIN, N. HCHABB, K. HAKKERDORPER TECOM FT BELVOIR METEOROLOGICAL TEAM

This paper presents comparisons between LOWTRAN 7 and field measurments taken during a number of field tests conducted by the US ARMY Center for Might Vision and Electro-Optics at several different locations. The data was collected by the TECON Ft Belvoir Meteorological Team. Data includes transmission at 1.54 microns, 3-5 microns, and 8-12 microns. A brief description of the equipment and meteorological parameters are presented along with the measured transmission and calculations using LOWIRAM 7 and in

INTRODUCTION

not possible or practical to use our measurement equipment due to size of the test or other considerations. For example, it is generaly not practical to provide support which takes four days to set up to support a one day test. At times, we must support one test up to support a one day test. At times, we must support test. We also use LOWTRAN to monitor the behavior of our neasurement equipment by making real time calculations which our technicians compare to the measured data. In this manner, we can detect problems quickly and take corrective action. This is built One of the most important measurements made by this team in support of test operations is that of atmospheric transmission. It is essential to evaluate the performance of the many different articles our customers test ranging from R&D to operational evaluation. Transmission models are also of great importance to us. We use them in studies and we use them in studies and ye use them in studies. In field support, In field support, we often use LOWTRAN calculations whenever it is into our automated run stream and serves as a great quality control mechanism. It is obvious then that we must have confidence in the transmission model in use and have a feel for how it performs under various conditions.

A few comments may be appropriate before we launch into the data. First is that this data was collected as part of testing programs with specific objectives and unfortunatly collecting have to live with real world problems of power, equipment changes, unwanted vehicle traffic, etc. These will be pointed out whenever possible. The second comment concerns the meteorological data. In some tests, we have to use locally collected data which is not designed to support E-0 testing. Some problems with this will be pointed out. During large tests where we are collecting all data ourselves, we feel much more comfortable in its quality and nice clean data for these comparisons were not amoung them. So we

our equipment at the beginning, then we will look at data collected at Pt AP Hill, Va in the 3 to 5 micron band and the 8-12 micron band. Visible data could not be obtained during this test because of a broken beam combiner at the transmissometer

oredit to Major(Dr) Bob Hughes of the Wright-Patterson Arm Staffmet office for supplying the pc version of LOWINAME.I should point out that lowtran was run using 1.54 microns +/- 10 wave source.Mext we will look at data taken for the Miniature Eyesafe Laser Infrared Observation System at 1.54 microns. This data was in Alaska, Panama, and Utah. Finally, and example involving MODTRAN will be presented. In all the comparisons, I must give numbers.

1. INSTRUMENTATION:

calibrated by abutting the source and receiver to eliminate atmospheric and system effects. Then appropriate corrections for range and optics were applied. The result is a measurement of absolute transmission. Discussion of the equipment used for the higher resolution data is described in that section. section on modtran was a Barnes 4.5 inch research radiometer system with a 1000 c blackbody source for the 3-5 and 8-12 bands, an InSb detector for 3-5 microns and MCf for the 8-12 band. Both detectors are LM2 cooled. For the 1.54 transmission, a Germanium detector was used with a high intensity quarts halogen light source. Presision optics are used for even distribution of the energy and the beam is highly collimated. The system was The transmissometer system used for all the data except the

2. Ft A.P. Hill, Va Data

first kilometer of the path. Temperature and humidity measurements were done with Vaisala humicaps, visibility using a HSB visibility meter, rate of rain with a BTI optical rainrate instrument, pressure by an AIR digital barometer and ceiling with a Vaisala Laser Ceilometer. Hany other parameters were measured, The following data was taken as part of the MultiBensor Automated Targeting field test. This data was taken over a two kilometer path with extensive meteorological measurements taken at both ends and optical turbulence measurements taken over the first kilometer of the path. Temperature and humidity such as soil temperature, solar radiation, and wind and are available on floppy disk. Meteorological data are collected on an automated system and represent 15 minute averages. Two days of data are presented. The data is presented in charts at the end of the text, hopefully in the correct order. a. 20 Mar 91: This was a partly cloudy day with no clouds below 12000ft. Optical turbulence was in the light range so that data is not presented. Looking first at the met data, it is quite unexciting except for three spikes. These are periods were equipment was being changed or repaired causing a period of bad data (eliminated in the official test data base).Only site one data is included because site two data is identical.

The discussion will be organized with a brief description of Power stability problems due to cool weather with its use equipment at the beginning, then we will look at data of heaters and due to the number of test participants.During the have a select amplifier in use on the 3-5 system so holding a good signal was difficult. We did achieve stable power by 1400 and The first comparison shows 3-5 microns. We had significant the comparison to lowtran now becomes quite good. One minute data

shows the problems clearly especially the two periods when the lock-in amplifiers were turned off to reset the system.

The 8-12 system had a select amplifer so we actually obtained good data sconer. The one minute data indicates that while the data stabilizes easier, twiking the system takes longer. I should point out that the spike at about 0900 coincident with the met equipment problem is just that- coincidence.

and a period of rain, Site one data only for temperature and pressure are shown because they are identical. Both sites are shown for RH and visibility because differences are indicated. Note that differences in visibility increase with increasing visibility. That is common with the HSB instrument. But below 10 km the differences are real. Cloud height is shown as is a comparison of the rain rates (sites 354 are further down range). The difference between site one and two were verified by our observations. In this case we show our data compared to lowtran using data from both met sites. You are invited to make your own comparisons. I will say that these comparisons are consistent 22 Mar 91: This day brings change with higher humidity with what we usually observe.

micron region. Again we had a two kilometer path length but this time looking down some 300 meters and crossing the panama canal as shown on the map. Met data comes from the receiver site so its Next we will travel south to Panama and look at the representiveness is in question. Two days are presented.

is that the visibility was estimated by a human and is not representative of the path. Many fires from burning crops were in the area and especially dense during one afternoon period. The break in the measured data was caused by lunch. Note the very a.30 Mar 91: The only comment to be made about the met data good agreement during the last hour. b. 1 Apr 91: This day had no fires to contend with and the comparison is straight foward. Some of the difference is probably due to our detector band width.

This was done with the cold weather testing of the MELIOS at the Cold Regions Test Center, Ft Greely, Alaska. Part of this test involved smokes. Again, met data was taken at the receiver site. The comparison chart shows mainly why were still in business. Between generator smoke and the obscurant smoke, comparisons are not really possible. For this paper, we will not discuss the type of obscurant used

Proving Ground in Utah. Met data is again at the receiver site by a human, the path is two kilometers and very flat, but now the altitude is near 4000ft. In this case three days are shown. The final stop on our support of MELIOS was the Dugway

was a clear warm day and had very strong optical turbulence. I would estimate in the 10E-12 range. The first comparison shows one hour averaged data with measured being somewhat lower that lowtran. Near the end of the day, dust from vehicles came over our path dropping the transmission but the observer could still see the top of the mountain 90 miles away. The fact that we could not see the base 10 miles away was not recorded. The effect of The met data is included for reference. the turbulence can be seen on the one minute data. a.21 May 91:

turbulence was slight. Now we have excellant agreement between measured and calculated. The one minute data captures a vehicle which kept crossing our line of sight, a problem we were able to b.22 May 91: This day was cloudy and cooler and the observed resolve with our powers of persuasion. c.23 May 91: This day was partly cloudy with moderate turbulence. Lack of turbulence measurments is a bother. But again in this case, with a uniform path and moderate turbulence, we found very good agreement with lowtran 7.

6. Summary

The above data gives us considerable confidence in using LOWTRAN7 as a tool of great usefullness. When one has good met measurements which describe the path, good comparisons can be obtained. As for scintillation, it most certainly is a factor in obtaining field measurements, but that is another topic which we intend to address in another paper.

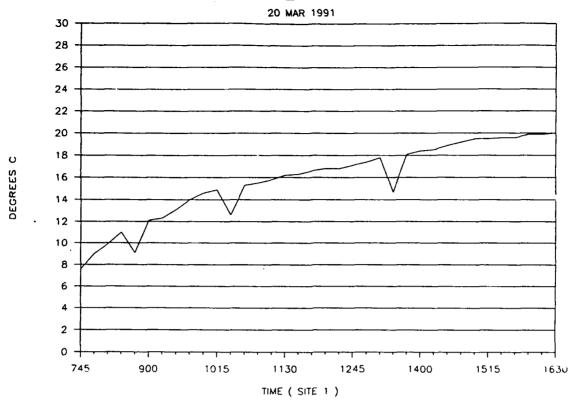
7. Bonus

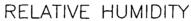
We would like to present some data we took in Germany in 1988 using our Nicolet FTIR transmissometer. This instrument has a MCTA detector with a ZnSe beamsplitter and can produce a two wave number resolution. The data were taken over a path of about 700 meters. The first chart shows the data obtained. The DF refers to distance and optics corrections. The second chart is a lowtran run using met data at both ends of the path including measured visibility. Incidently, that was also our data. The third chart shows a MODTRAN run of the same time. The agreement is very good, in fact remarkable considering our field conditions with the very sensitive FTIR. We are eagerly awaiting a pc version of MODTRAN and feel that it will eventually replace LOWTRAN in some of our support activities. Our manning and workload has interfered with our workwith the FIIR but we think that that will soon change.

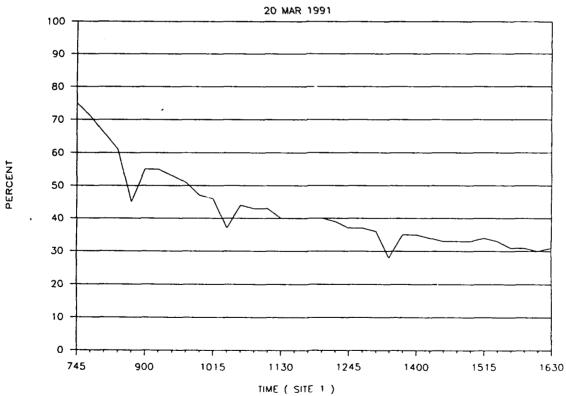
FINAL BUMMARY

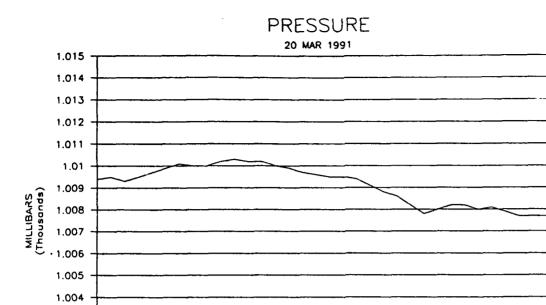
To provide support to our customers in the E-O world, we must have the capability for both measuring and calculating atmospheric transmission. We in fact use LOWTRAN7 as a quality an accurate product. We feel that it is, at least to the accuracies we need and in our near the ground application, our data shows that if the input data is accurate, so is the result. control tool. Accordingly our confidence must be high that it is



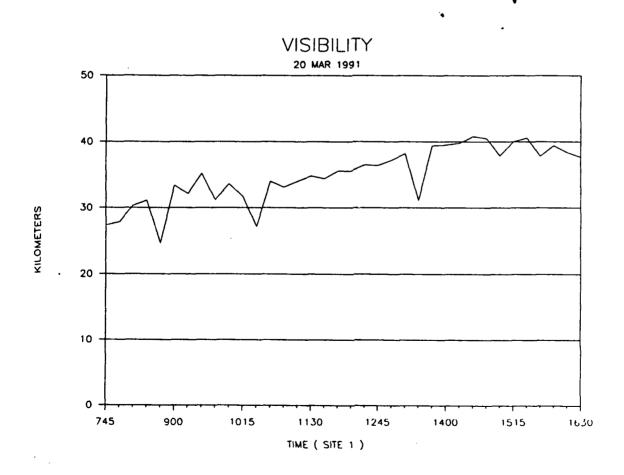






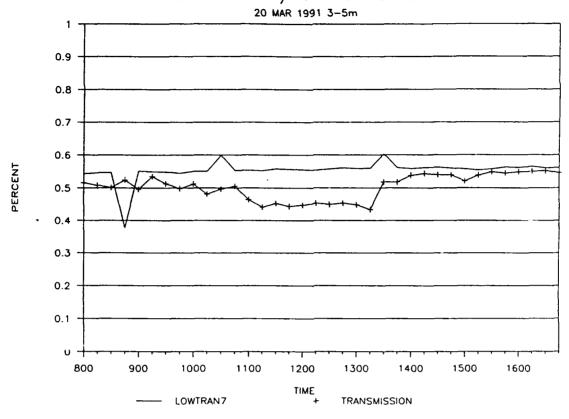


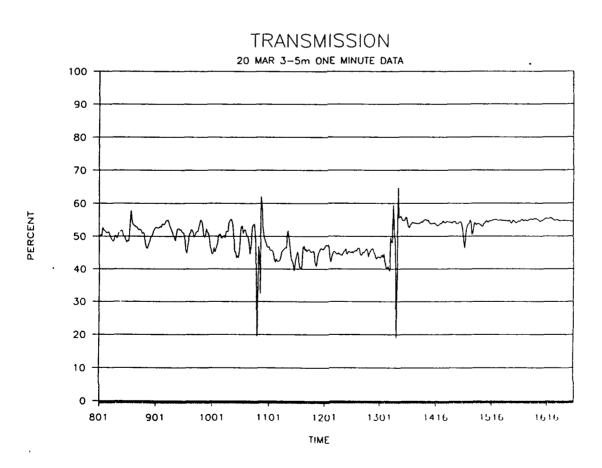
1.003 1.002 1.001



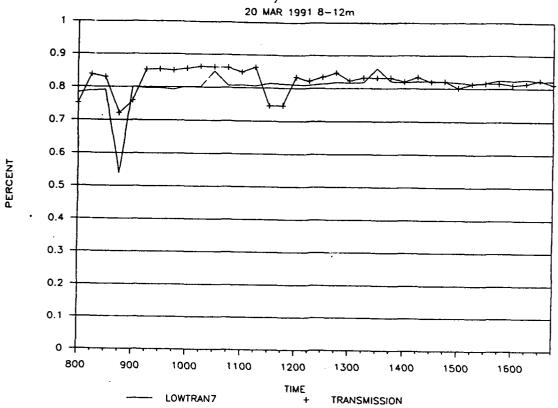
TIME (SITE 1)

LOWTRAN7/TRANSMISSION

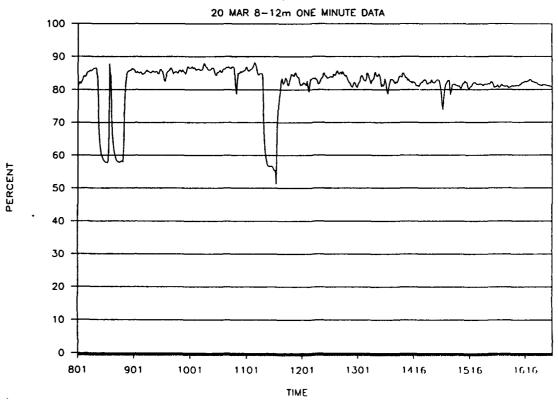




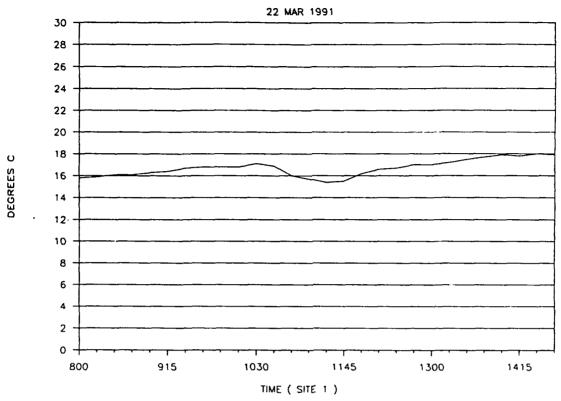
LOWTRAN7/TRANSMISSION

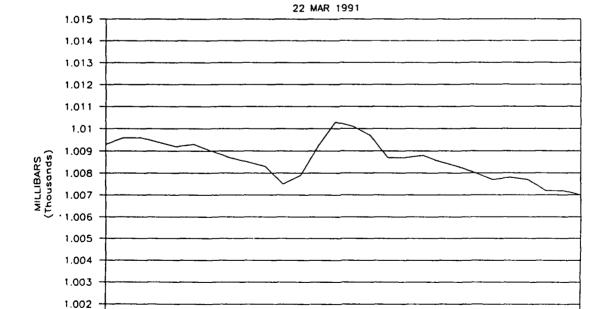


TRANSMISSION





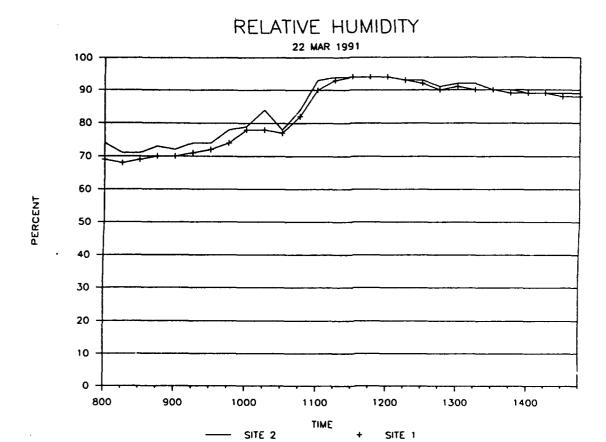


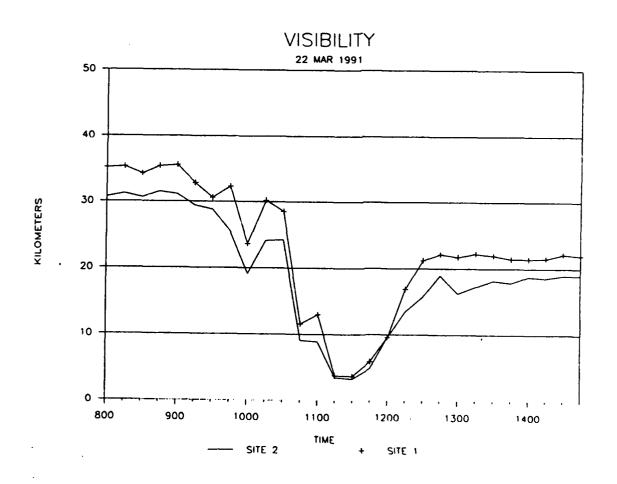


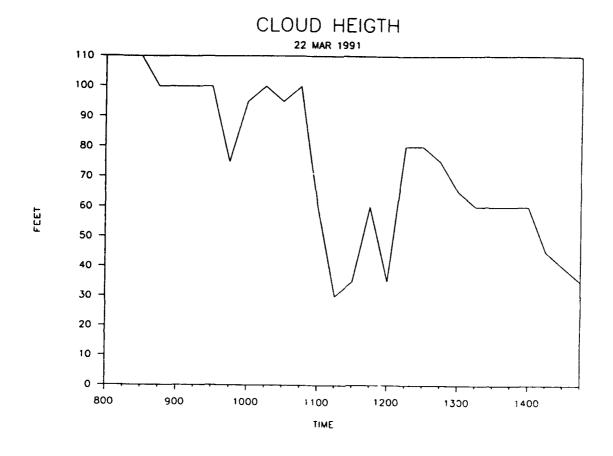
TIME (SITE 1)

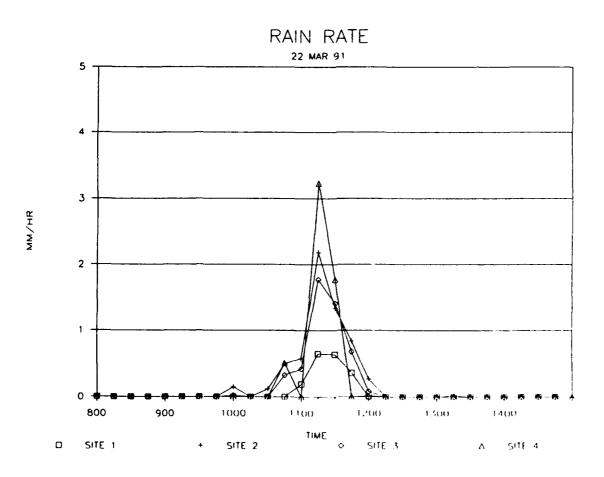
1.001

PRESSURE

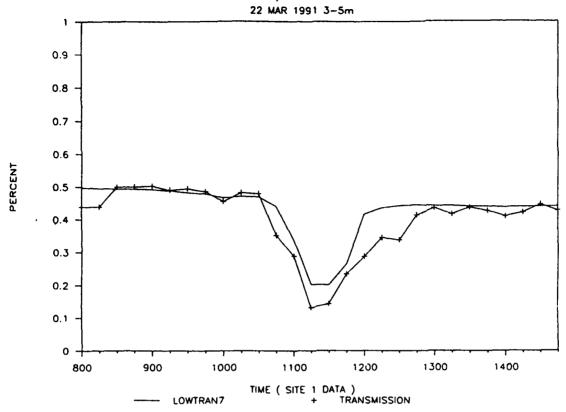




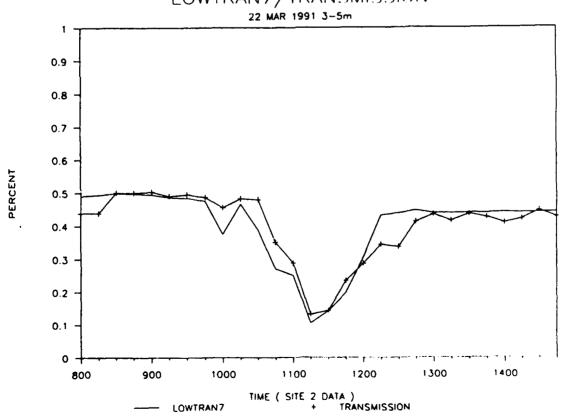




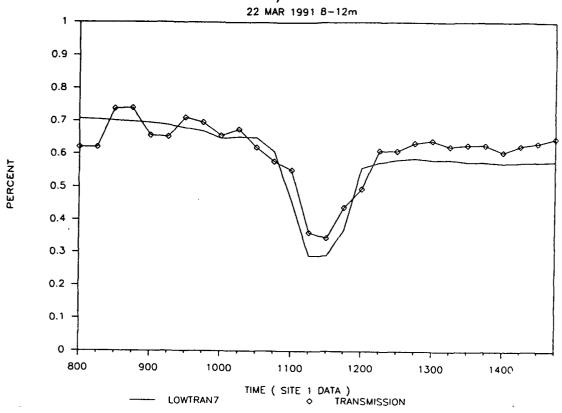
LOWTRAN7/TRANSMISSION

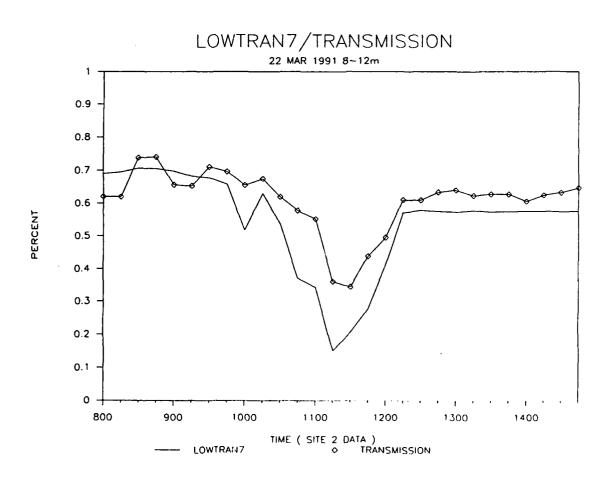


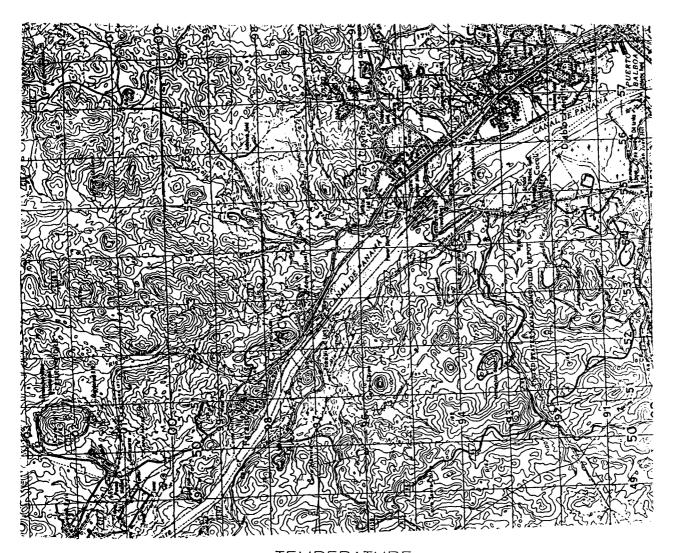
LOWTRAN7/TRANSMISSION



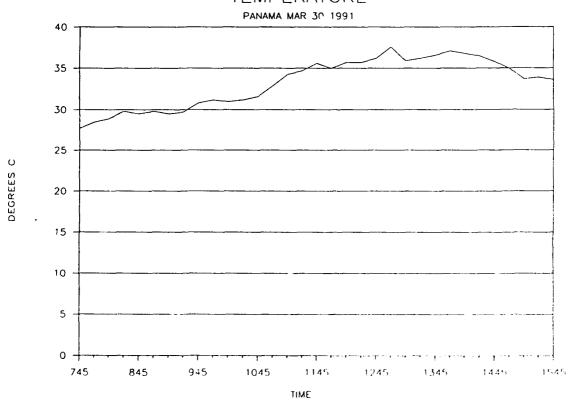
LOWTRAN7/TRANSMISSION



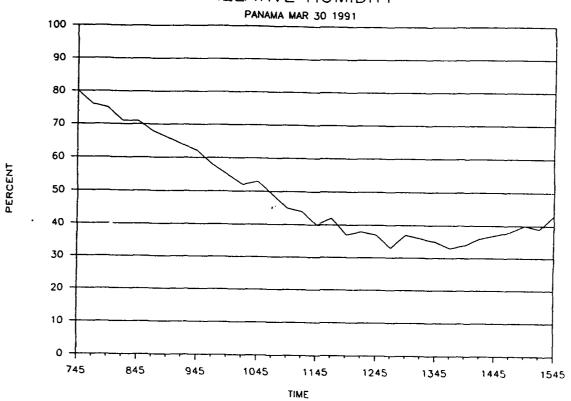




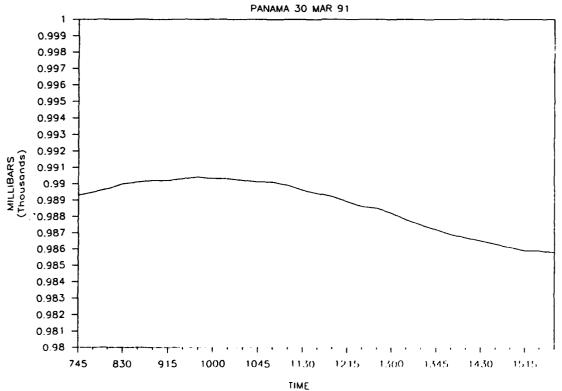


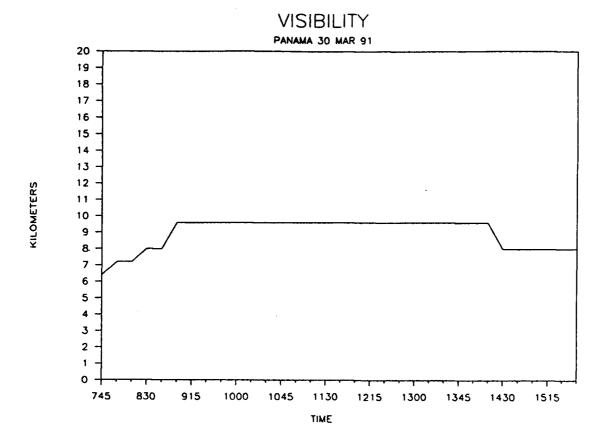


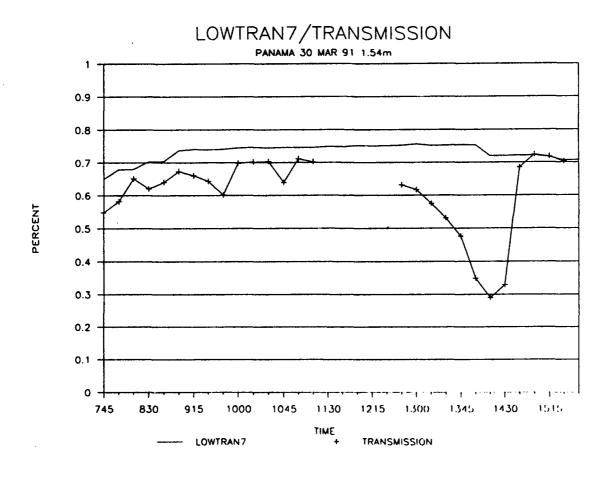
RELATIVE HUMIDITY



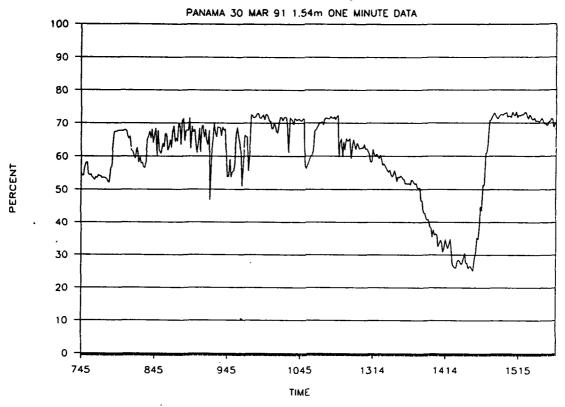


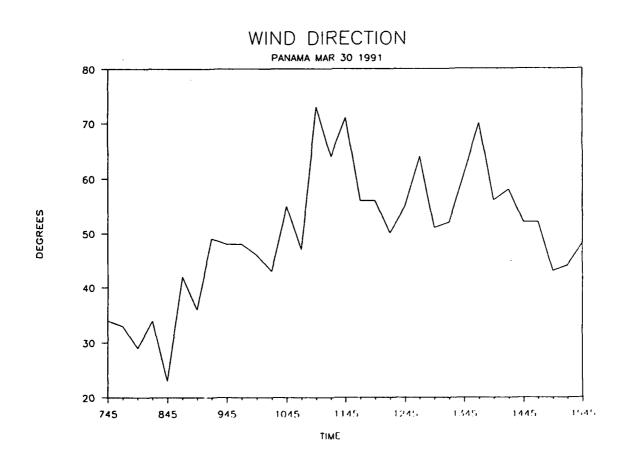


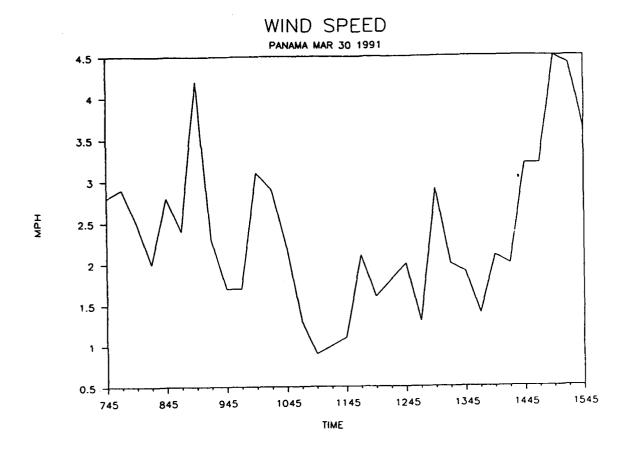


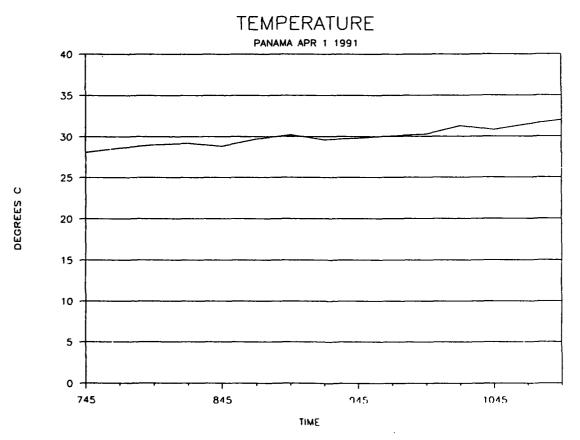


TRANSMISSION

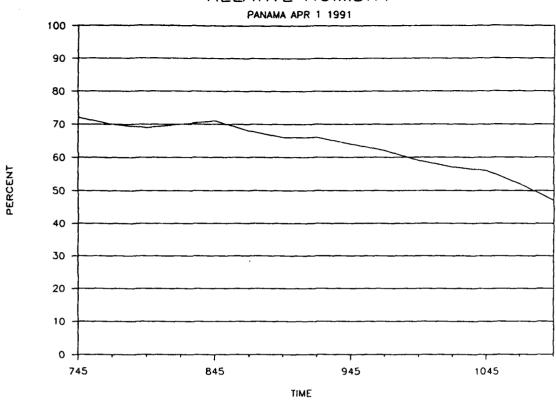


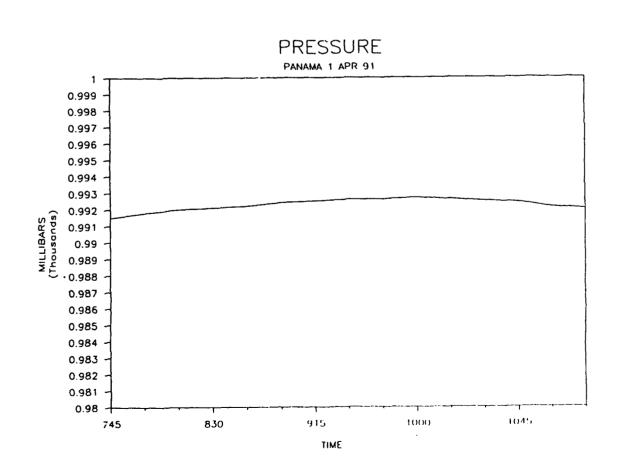


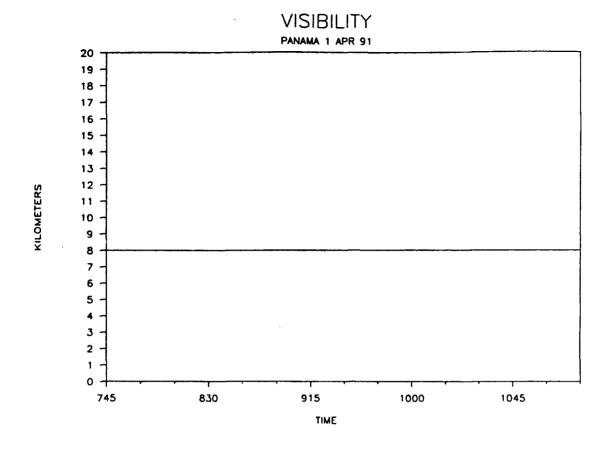


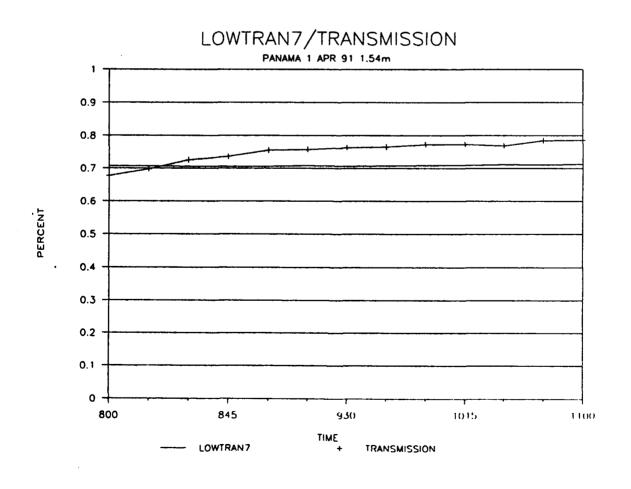


RELATIVE HUMIDITY

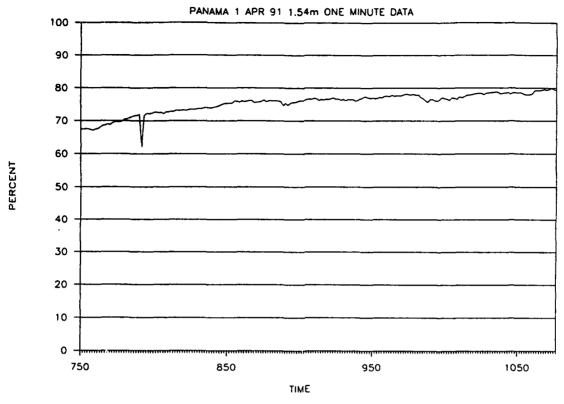


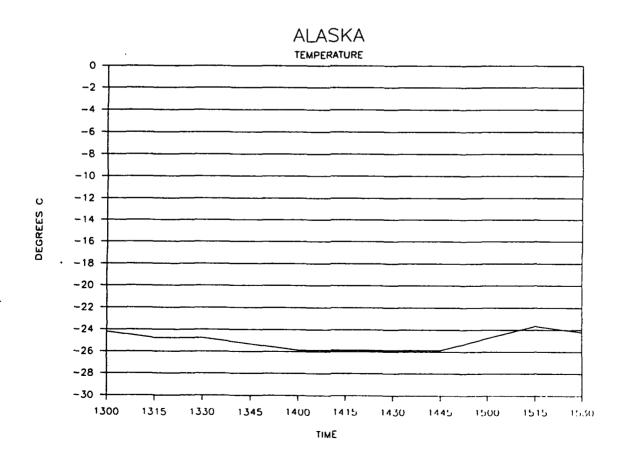


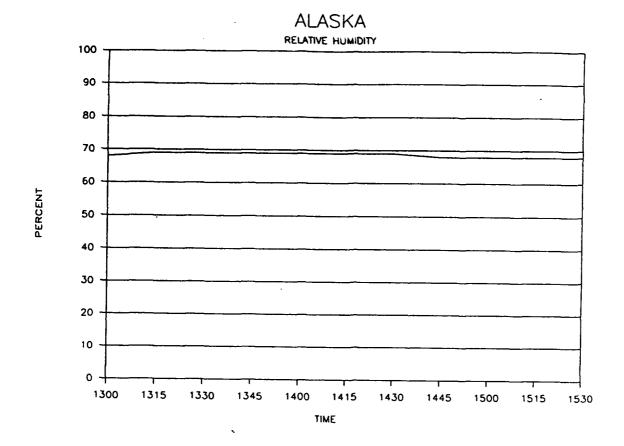


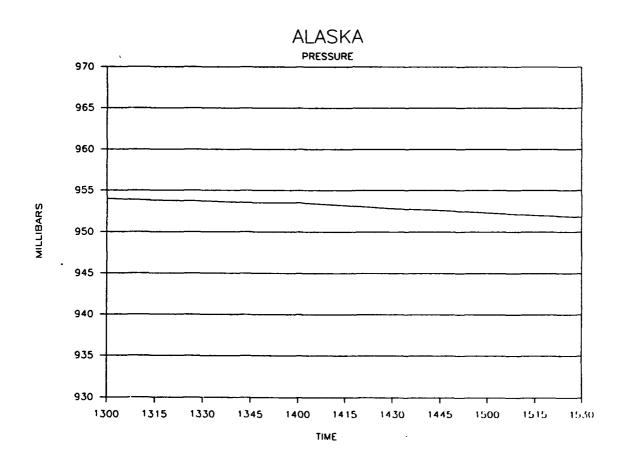


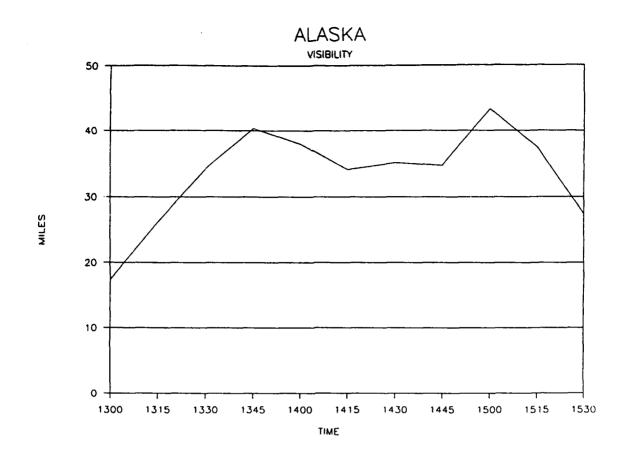
TRANSMISSION

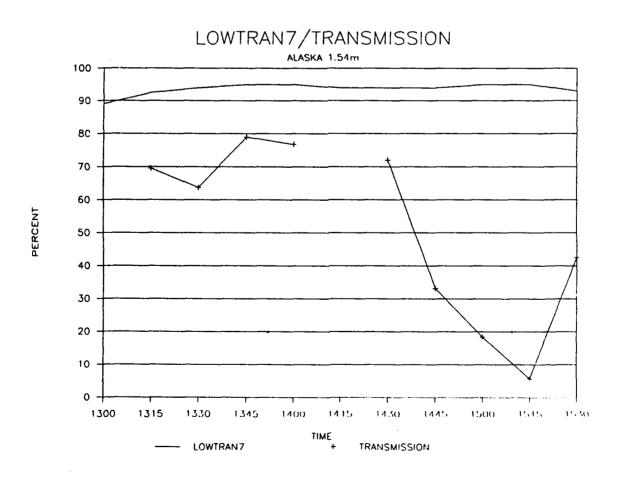




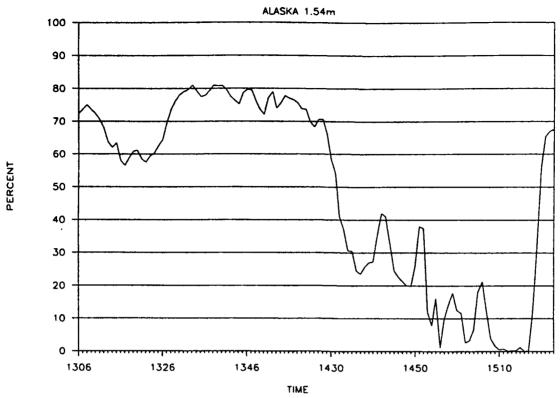


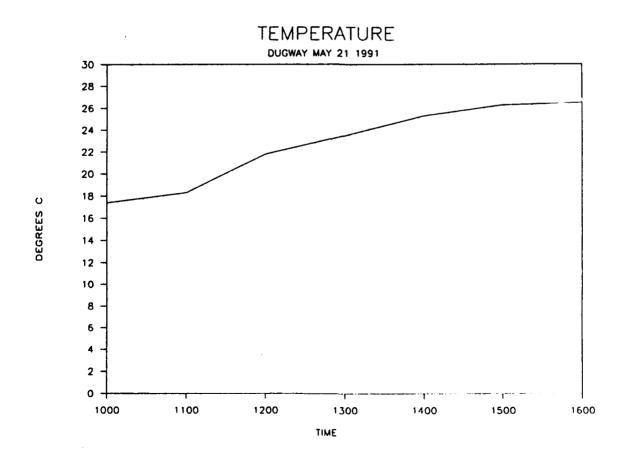


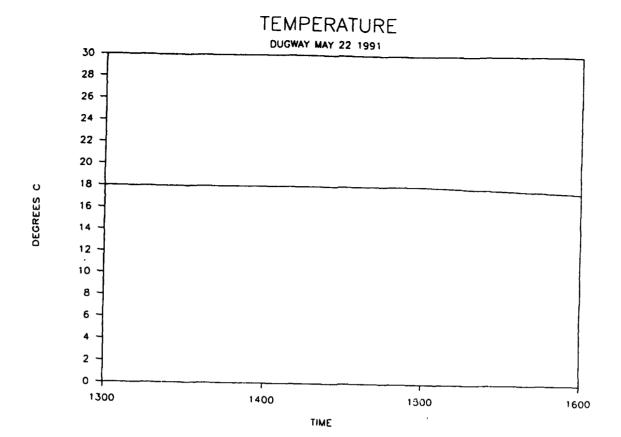


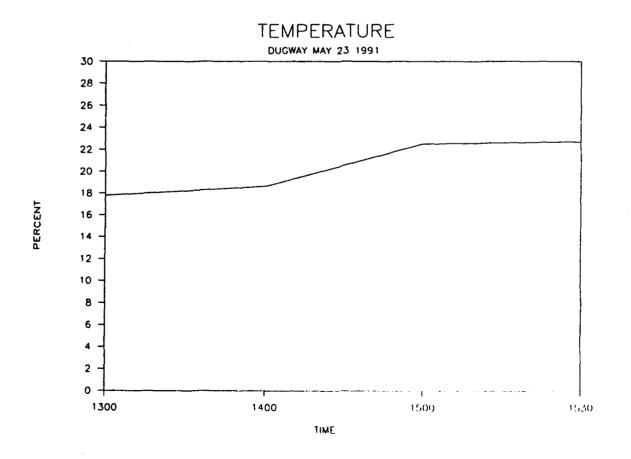




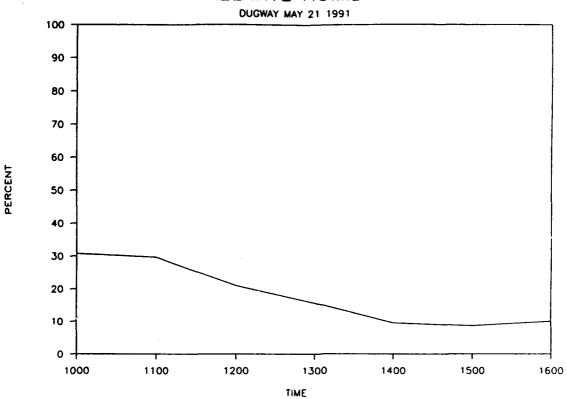


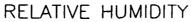


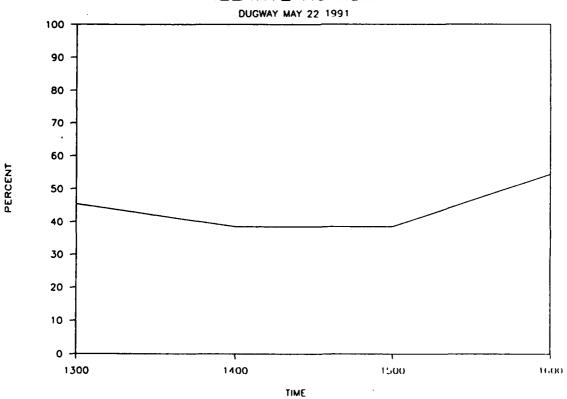


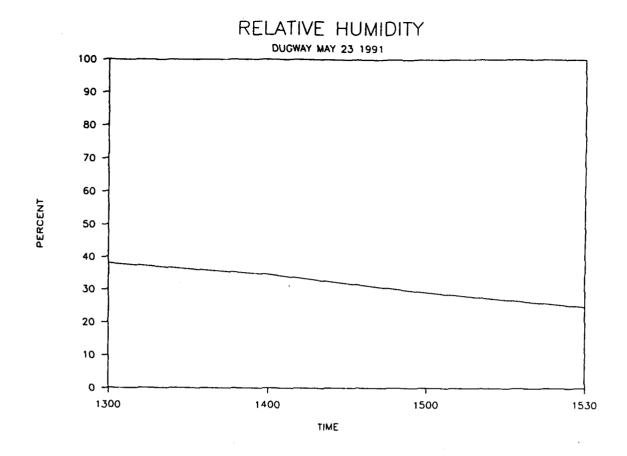


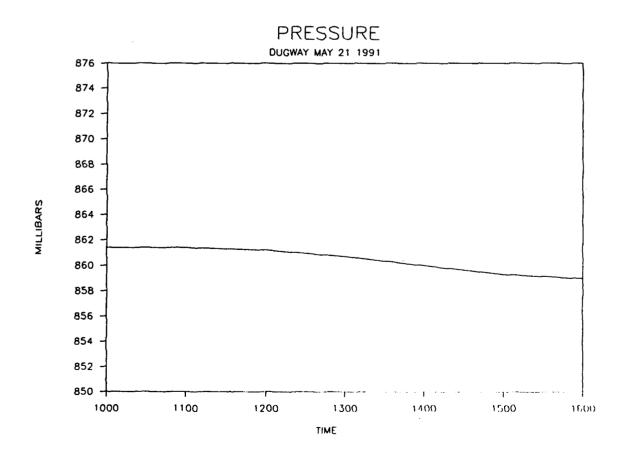
RELATIVE HUMIDITY



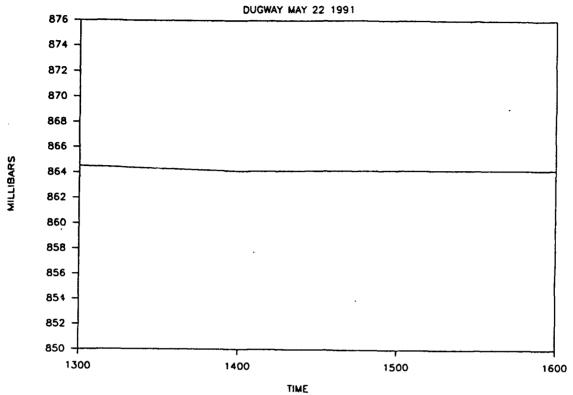


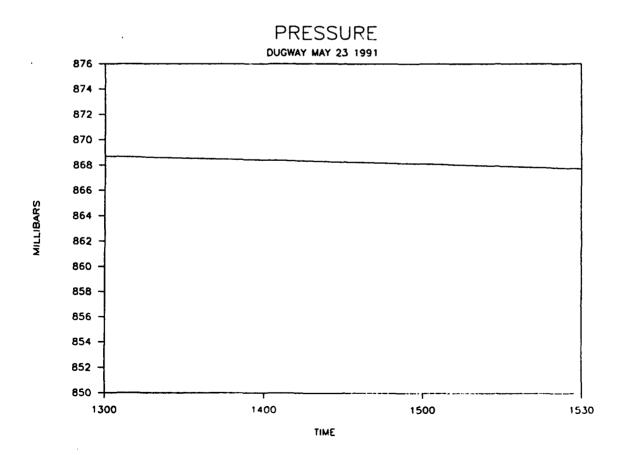


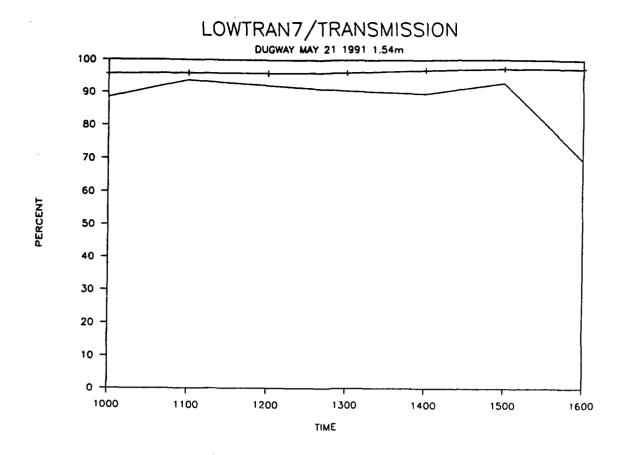


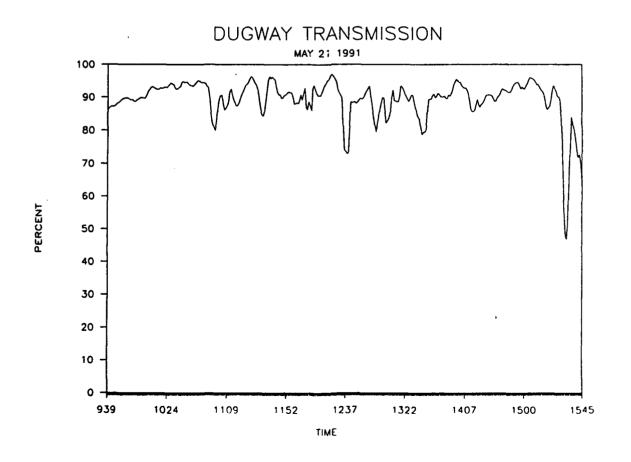




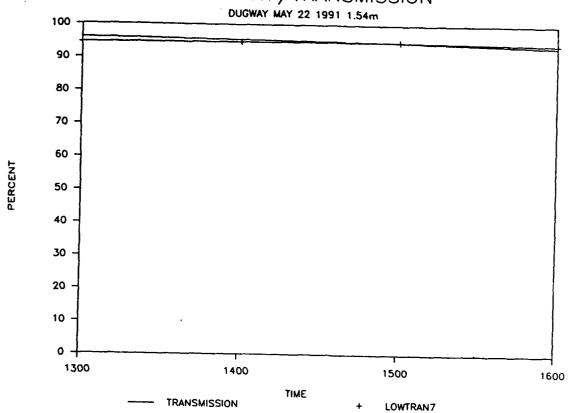




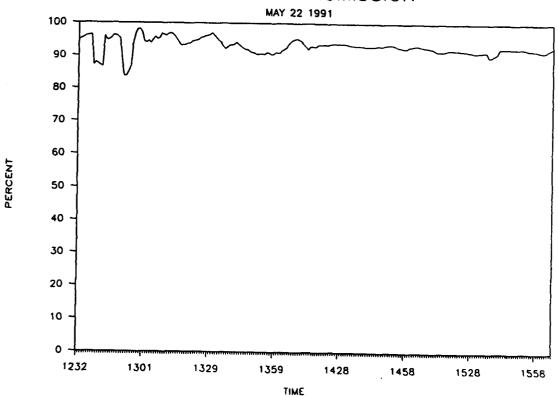




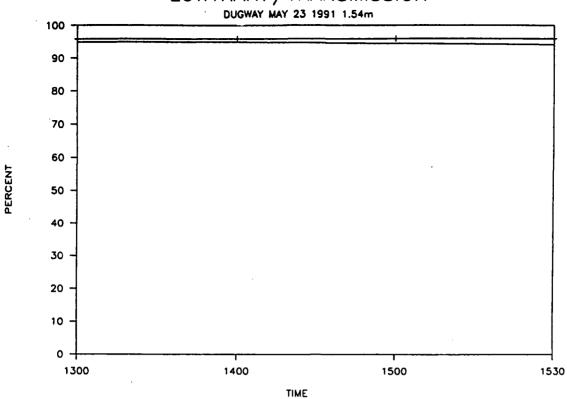






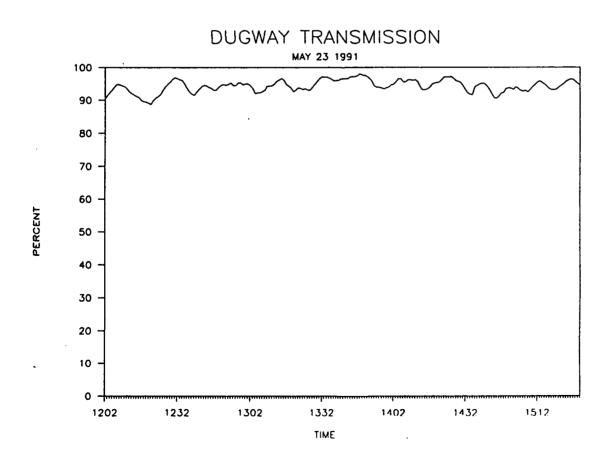


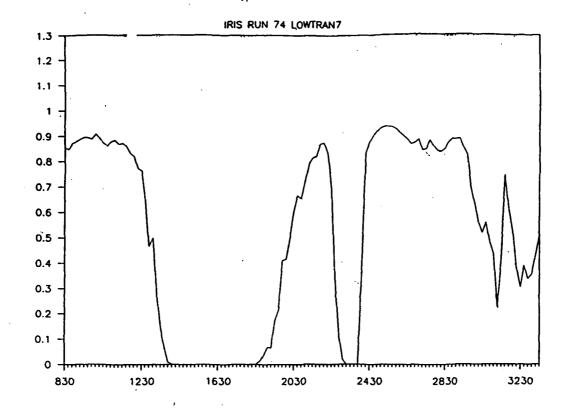
LOWTRAN7/TRANSMISSION

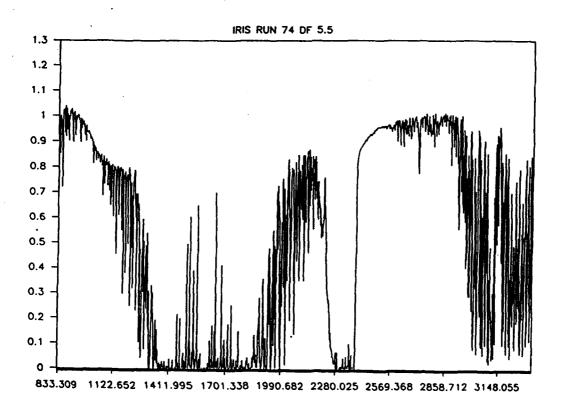


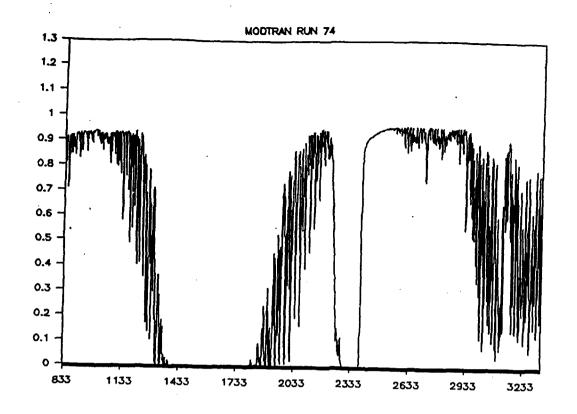
LOWTRAN7

TRANSMISSION









SPECTRAL SMOOTHING IN THE FOURIER DOMAIN: A SOFTWARE PACKAGE FOR LINE-BY-LINE CALCULATIONS

W. Gallery Atmospheric and Environmental Research, Inc., 840 Memorial Drive, Cambridge, MA 02139

M. Esplin Stewart Radiance Laboratory, 139 Great Road, Bedford, MA 01730

We have developed a software package which will convolve a spectrum with a spectral scanning function using Fourier transforms. This technique mimics the operation of Fourier transform spectroscopy and preserves the full extent of the scanning function, which is particularly important for functions like sinc. This package has the following features:

- 1. It gives the user a choice of 5 scanning functions commonly used in Fourier transform spectroscopy, including sinc, sinc², Hamming, Hanning, and Beer, plus triangle and Gauss, and may be easily modified to include other functions.
- 2. There is no limitation on the size of the spectrum (a disk-based Fourier transform method is used for spectra exceeding the available memory).
- 3. If possible, it optimizes the calculation by prescanning the spectrum with a rectangle narrow compared to the scanning function, resulting in significant time and size savings.
 - 4. It has been adapted to read and write FASCODE binary files.

Sample calculations will be shown comparing measured spectra with calculated spectra smoothed using this technique.

Spectral Smoothing in the Fourier Domain: A Software Package for Line-by-Line Calculations

William O. Gallery

OptiMetrics, Inc.

Mark Esplin
Stewart Radiance Lab, Bedford, MA

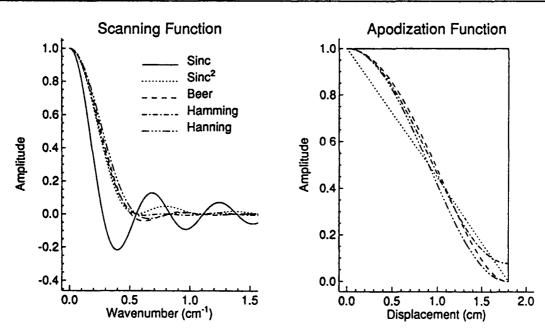
*Now with Atmospheric and Environmental Research, Inc., Cambridge, MA

Introduction

- Line-by-Line Calculation are Often Compared to FTS Measurements
 - e.g., SCRIBE, CIRRUS, HIS, ATMOS, Lab Measurements
- Scanning Function is Determined by the Apodization Function Applied to the Interferogram
- The Calculation Should Accurately Match the Scanning Function
 - Extent (Especially Important for Sinc, Sinc²)
 - Shape

- A Software Package for Convolving a Spectrum with a Spectral Scanning Function
 Using Fourier Transforms
- Mimics the Operation of a Fourier Transform Spectrometer
 - · Transforms the Calculated Spectrum Into an "Interferogram"
 - · Apodized the Interferogram
 - Transforms Back to the Spectral Domain
- Choice of 5 Common FTS Scanning Functions
 - Sinc, Sinc², Hamming, Hanning, Beer
 - Also Triangle, Gauss, and Box

Scanning Functions and Associated Apodization Functions



The Five Scanning Functions and Their Associated Apodization Functions. The functions shown here model the HIS interferometer, with a maximum optical path difference of 1.8 cm.

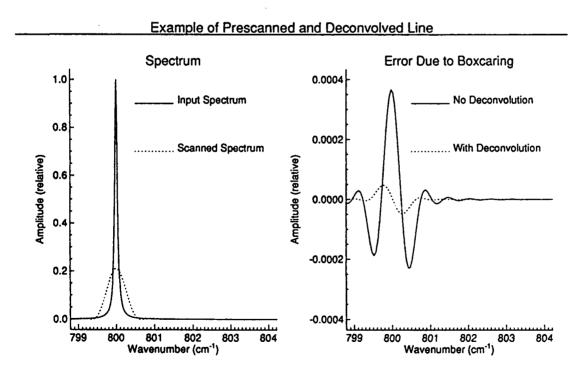
Program Details

- Program Reads and Writes Fascode Files
- Can Handle Arbitrarily Large Spectra By Using A Disk-Based FFT
- Input Spectrum Can be Prc-Scanned with a Boxcar and Deconvoled
- Apodization Function Can Be Calculated Either Analytically or As the Fourier Transform of the Scanning Function

Disk Based FFT

- Disk Based FFT Courtesy of Mark Esplin, Steward Radiance Lab
- If the Number of Points Exceeds the Available Memory, A Disk-Based FFT is Used
 - Input Data Points Are Sorted Into Blocks and Written To Disk as Direct Access Files
 - Only 2 Blocks Reside in Memory
 - A Standard FFT is Applied to Each Block
 - Data From the Various Blocks is Combined to Obtain the FFT of the Entire Dataset
 - Sorting of Data and Combining of the Blocks is Analogous to the Method of a Standard FFT
- Time Penalty For a Disk-Based FFT Compared to an In-Memory FFT is 35 % on a Sun 360 Workstation for the Same Total Number of Points
- Caution With Virtual Memory
- VAX: Direct Access Blocks Blocks Limited to 2048 Points

- Prescan Input Spectrum With a Boxcar (Rectangle) If Input δv < α/Μ
 - $\delta v = input$ frequency spacing, $\alpha = scanfunction$ halfwidth at halfmaximum, M = 5
- M Points From Input Spectrum Are Averaged To Obtain One Output Point
- Prescanning Results in Significant Time and Memory Savings
- Smoothing Effect of the Boxcar Can Be (Partially) Reversed By Deconvolving Resampled Spectrum



Lorenz Line, HWHM = 0.04 cm^{-1} , $dv = 0.01 \text{ cm}^{-1}$, Scanned with a Beer Scanning Function, HWHM = 0.2645 cm^{-1} (HIS Resolution), Prescanned With M = 5, Output $dv = 0.05 \text{ cm}^{-1}$

• Resolution:

- Half Width at Half Maximum of the Scanning Function, or
- Maximum Optical Path Difference of an Equivalent Interferometer

• Frequency Range

- Adjusted to Fit Input Spectrum
- User Must Allow For Edge Effects, Which Can be Quite Extensive For the Sinc Function

• Transmittance or Radiance

- Program Recognizes Different Fascode File Types
- Scanning Function
- Selectable Options:
 - Prescanning
 - Deconvolution
 - Apodization Function Calculated as the FFT of the Scanning Function

A COMPARISON OF COMPUTATIONAL APPROACHES FOR THE VOIGT FUNCTION

F. Schreier

DLR - Deutsche Forschungsanstalt für Luft- und Raumfahrt, Institute of Optoelectronics D-8031 Oberpfaffenhofen (Fed. Rep. Germany)

Several computational procedures for the Voigt function are discussed and compared for accuracy and speed. Vectorization of the codes was applied where possible. This resulted in a variation of computational speed over two orders of magnitude. However, even without vectorization restructuring of the programs can yield a significant acceleration. For applications with least-squares-fitting the evaluation of the complex error function provides an efficient way to calculate both the Voigt function and its partial derivatives.

on Atmospheric Transmission Models (1991)

A Comparison of Computational Approaches for the Voigt Function

F. SCHREIER

DLR — Deutsche Forschungsanstalt für Lust- und Raumfahrt Institute of Optoelectronics D-8031 Oberpfassenhosen (Fed. Rep. Germany)

ABSTRACT

Several computational procedures for the Voigt function are discussed and compared for accuracy and speed. Vectorization of the codes was applied where possible. This resulted in a variation of computational speed over two orders of magnitude. However, even without vectorization restructuring of the programs can yield a significant acceleration. For applications with least-squares-fitting the evaluation of the complex error function provides an efficient way to calculate both the Voigt function and its partial derivatives.

Voigt and complex error function: computational approaches

The Voigt Function — Definitions

$$g_V = g_L \otimes g_D = \frac{\sqrt{\ln 2/\pi}}{\gamma_D} K(x, y)$$

$$K(x, y) = \frac{y}{\pi} \int_{-\infty}^{+\infty} \frac{c^{-t^2}}{(x - t)^2 + y^2} dt$$

where

$$x = \sqrt{\ln 2} \frac{\tilde{\nu} - \dot{\nu}_0}{\gamma_D}$$
$$y = \sqrt{\ln 2} \frac{\gamma_L}{\gamma_D}$$

and

 $\tilde{\nu}_0$ line center

7L, 7D Lorentzian and Gaussian half width

representation in complex plane (z = x + iy):

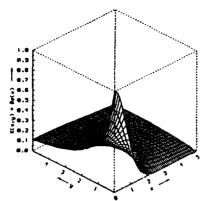
$$W(z) = K(x,y) + iL(x,y) = \frac{i}{\pi} \int_{-\infty}^{+\infty} \frac{e^{-t^2}}{z-t} dt$$

Complex error function:

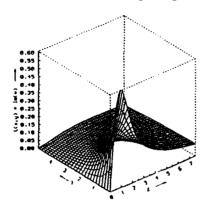
$$w(z) = e^{-z^2} \left(1 + \frac{2i}{\sqrt{\pi}} \int_0^z e^{t^2} dt \right)$$
$$= e^{-z^2} \operatorname{erfc}(-iz)$$

W(z) and w(z) are identical for positive y:

$$w(z) = \begin{cases} W'(z) & y > 0 \\ W'(z) + 2c^{-z^2} & \text{for} \\ y < 0 \end{cases}$$



Voigt function: Armstrong's algorithm

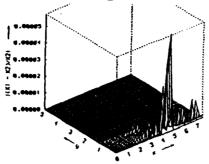


imaginary part of complex error function: Hui's algorithm

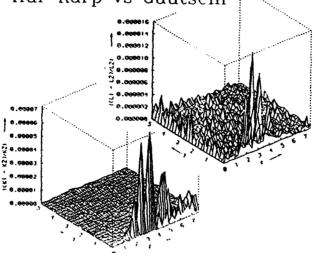
Voigt function: Overview of different algorithms

euthor(s)	regions	method	stated accuracy 1-2 digits in 6th significant figure	
Armstrong (1967)	$y < 1.0, x < 4 \text{ or } y < \frac{1.6}{x+1}, x > 4$ $1 < y < 2.6, x \le 4$ $y > 2.5, x < 4 \text{ or } y > \frac{1.6}{x+1}, x > 4$	Hummer-Faddeyeva/Terent'ev power series 20-term Gauß-Hintegration of mod. integrand 20-term Gauß-Hermite-integration		
Drayson (1976)	y < 1.0, x < 5 - 0.8y y > 1, x < 1.85(3.6 - y) else	Taylor expansion, Chebyshev expansion continued fraction 4-term or 2-term Gau8-Hermite-integration	one part in 10 ⁴	
Gautschi (1969)	all x,y	truncated Taylor expansion	10 decimal places after decimal point	
Hui et al. (1978)	all z, y	rational approximation	rel. error < 10 ⁻⁴	
Humlicek (1979)	y > 0.85 or x < 18.1y + 1.65 else	rational approximation rational approximation, modified for Re(w)	2·10 ⁻⁶ for real, 5·10 ⁻⁶ for imag. part	
Humlicek (1982)	$ x + y \ge 15$ 5.5 $\le x + y < 15$ $ x + y < 5.5 \text{ and } y \ge 0.195 x - 0.176$ else	rational approximations	10 ⁻⁴ relative error	
Karp (1978)	all x, y	Fourier transform		
Kielkopf (1973)	all z,y	weighted sum of Lorentz and Gauß function	10 ⁻⁴ relative to peak value	
Pierluissi et al. (1977)	0≤x>3,0≤y<1.8 3≤x<8,1.8≤y<8 x≥8,y≥8	series expansion 6-point Gauß-Hermite integration 4-point Gauß-Hermite integration	peak deviation $\leq 1.4 \cdot 10^{-3}$, RMS deviation $\leq 1.6 \cdot 10^{-5}$	
Whiting (1968)	all x,y	weighted sum of Lorentz and Gau's function	5% at worst	

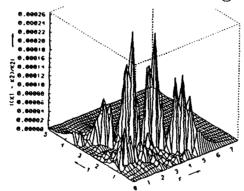
Armstrong vs Gautschi



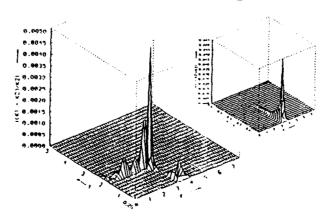
Hui-Karp vs Gautschi

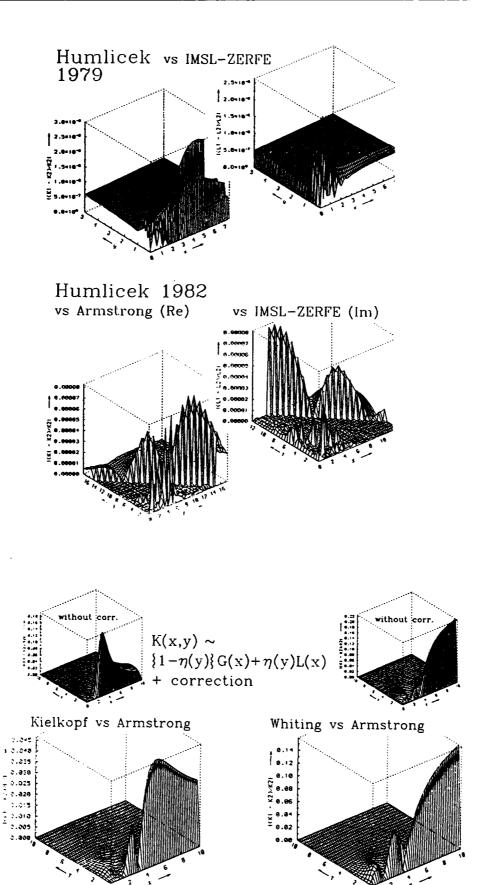


Drayson vs Armstrong



Pierluissi vs Armstrong





Comparison: Computational times

for 1000 $x \oplus 50$ y points $(0 < x < 10 \cdot x_{\perp})$

algorithm	Little (acc)					
	IBM 3090		CRAY Y-MP2			
	0 < y < 1	I < y < 10	0 <y<1< th=""><th>1 < y < 10</th></y<1<>	1 < y < 10		
		PUNCTION		·		
Armstrong	1.26	1.04	1.68	1.49		
Drayson	0.38	0.21	1.54	1.39		
llui et al.	0.48	0.48	1.42	1.42		
Humlicek 79	0.87	0.76	1.60	1.58		
Hamlicek 82	0.45	0.29	1.48	1.37		
imsl cerfe 🗶	5.07	3.18	3.75	2.60		
Pierluissi et al	0.51	0.24	1.54	1.39		
	St	BROUTINE	 	<u> </u>		
liui (vector)	0.093	0.093	0.020	0.020		
Kielkopf (vector)	0.051	120.0	0.015	0.015		
Kielkopf (novector)	0.17	0.17	0.13	0.13		
Whiting (vector)	0.15	0.15	0.036	0.037		
Whiting (novector)	0.36	0.36	0.38	0.39		

The CPU time used by each function or subroutine has been determined by the IMSL routine CTIME. John were run on a IBM 3090-30S VF(2) under MVS/XA operating system and mith VS FORTRAN Version 2 Release 4.8 Compiler. The CRAY Y-MP2/232 runs under UNICOS operating system with a CFT77 compiler. Highest optimization level has been used on both systems.

* implementation of funtschi algorithm

Voigt and complex error function: computational approaches

Vectorization of Hui's algorithm

rational approximation (Hui et al., 1978):

$$w(z) \approx \frac{\sum_{m=0}^{6} a_m (y - ix)^m}{\sum_{n=0}^{7} b_n (y - ix)^n} \quad \text{with} \quad b_7 = 1$$

 \implies computational effort (for each line and grid point $\tilde{\nu}$): 12 complex multiplications and one complex division, equivalent to 54 real multiplications and one real division

optimization:

complex polynomial in $\tilde{z} = y - ix$ with real coefficients c_m \longleftrightarrow polynomial in x with complex coefficients $d_m(y)$

$$P(\tilde{z}) = \sum_{m=0}^{M} c_m (y - ix)^m$$

$$= \sum_{m=0}^{M} d_m(y) x^m$$

$$= \sum_{m \text{ even}} d_m' x^m + i \sum_{m \text{ odd}} d_m'' x^m$$

where

$$d_{k} = (-i)^{k} \sum_{l=0}^{M-k} \binom{l+k}{k} c_{l+k} y^{l}$$

⇒ 21 real multiplications and one real division

Computing times: Hui's algorithm

	time (sec)			
	1BM 3090		CRAY Y-MP2	
	0 < y < 1	l < y < 10	0 < y < 1	1 < y < 10
Cunction	0.48	0.49	1.42	1.43
subroutine (voctor)	0.093	0.093	9.020	0.020
optimised subroutine (vector)	0.037	0.037	0.010	0.010
opi. subroutine, novector	0.14	0.14	0.048	0.048
ept. subr., Karp's mod., vector	6.840	0.037	0.010	0.010
opt. subr., Karp, novector	0.145	0.144	0.056	0.048

(Kerp's modification is used only for $y \le 0.1$)

Computing times: Humlicek's algorithm (1979)

· · · · · · · · · · · · · · · · · · ·	time (sec)			
	IBM 3090		CRAY Y-MP2	
	0< y< 1	1 < y < 10	0 < y < 1	1 < y < 10
function, region I and II, real*4 function, region I and II	0.87 1.29	0.76 0.95	1.60	1.58
subroutine, only region I	0.18	0.18	0.036	0.036
subroutine, region I and II	0.43	0.18	0.052	0.036
subroutine, I and II, novector	0.95	0.83	0.37	0.25

(Except for the first row double precision arithmetic has been used in the CIFI2 routine)

Fourier Transform Methods

advantage: simple Fourier representation of Voigt function

$$K(x,y) = \frac{1}{\sqrt{\pi}} \int_0^\infty e^{-q^2/4 - yq} \cos qx \ dq$$

- direct methods: n_ln_{\nu} evaluations Karp:

- FT methods:

only sines, cosines and exponentials for each line and two FFT's for entire frequency range

but:

FT method also requires $n_l n_{\nu}$ evaluations in the Fourier

domain plus two FFT's

comparable computational effort ??? for direct and FT methods

restriction for the number of grid points to powers of 2 problems: error sources like aliasing

Karp's Fourier Transform Algorithm

total absorption coefficient for n_l lines

$$k(\tilde{\nu}) = \sum_{l=1}^{n_l} S_l \frac{\sqrt{\ln 2/\pi}}{\gamma_l^D} K(x_l, y_l)$$

insert Fourier representation for K(x,y) use $\delta_l \equiv \gamma_l^D/\sqrt{\ln 2}$ and $\lambda_l \equiv \gamma_l^L$, change of variables $qx_l = p(\hat{\nu} - \hat{\nu}_l)$

 $k(\tilde{\nu}) = \frac{1}{\pi} \int_0^\infty dp \, \cos p\tilde{\nu} \left[\sum_l S_l \, e^{-(p\delta_l)^2/4 - p\lambda_l} \cos p\tilde{\nu}_l \right]$ $+ \frac{1}{\pi} \int_0^\infty dp \, \sin p\tilde{\nu} \left[\sum_l S_l \, e^{-(p\delta_l)^2/4 - p\lambda_l} \sin p\tilde{\nu}_l \right]$

estimate of computing time

$$t_{[...]} \approx n_l n_p \left(t_{exp} + 2t_{sin} + 6t_{mult} + 3t_{add}\right)$$

equidistant grid points $p_j = j\Delta p$: recursive relations for exponential and trigonometric functions

$$t_{Karp} = n_l n_p (12t_{mult} + 4t_{add}) + n_l (2t_{exp} + 2t_{sin} + 6t_{mult}) + 2n_\nu \log_2 n_\nu \tau_{FFT}$$

Voigt and complex error function: computational approaches

Absorption coefficient: Hui's rational approximation

total absorption coefficient for n_l lines

$$k(\tilde{\nu}) = \sum_{l=1}^{n_l} \frac{S_l}{\sqrt{\pi} \, \delta_l} \, \mathcal{R}e^{\frac{\int_{m=0}^{6} a_m (y_l - ix_l)^m}{\sum_{n=0}^{7} b_n (y_l - ix_l)^n}}$$

requires $n_l n_{\nu}$ evaluations of $x_l(\bar{\nu_i})$ and of fraction of polynomials define new coefficients for all lines

$$\alpha_{ml} \equiv \frac{S_l a_m}{\sqrt{\pi} \, \delta_l^{m+1}}$$

$$\beta_{nl} \equiv \frac{S_l b_n}{\sqrt{\pi} \, \delta_l^{m+1}}$$

⇒ absorption coefficient

$$k(\hat{\nu}) = \sum_{l=1}^{n_l} \mathcal{R}e^{\frac{\int_{0}^{c} \alpha_{ml} (\lambda_l - i(\hat{\nu} - \hat{\nu}_l))^m}{\frac{7}{n_l = 0} \beta_{nl} (\lambda_l - i(\hat{\nu} - \hat{\nu}_l))^n}$$

with rearrangement of the complex polynomials

$$t_{Hui} = n_l n_v \left(16t_{mult} + t_{div} + 13t_{add} \right)$$
$$+ n_l \left(10t_{mult} + t_{div} + t_{add} \right)$$

Derivatives of the Voigt function

Differential equation (z = x + iy)

$$w'(z) = \frac{2i}{\sqrt{\pi}} - 2z w(z)$$

use Cauchy-Riemann conditions

at

direct differentation of K(x, y) and partial integration

$$\frac{\partial K(x,y)}{\partial x} = -2 \operatorname{Re} \left(z w(z) \right)$$

$$\frac{\partial K(x,y)}{\partial y} = +2 \operatorname{Im} \left(z w(z) \right) - \frac{2}{\sqrt{\pi}}$$

Voigt function and derivatives calculated simultaneously !!!

numerics:

subtracting two numbers of approximately equal magnitude

Voigt and complex error function: computational approaches

Conclusions and Remarks

Accuracy:

sufficient accuracy of most algorithms, but for applications further aspects are important, too:

- other error sources:
 - limited accuracy of molecular line parameters
 - uncertainties from exact temperature dependance of γ_L
 - deviations from pure Lorentzian line shape
- least-squares-fits in molecular spectroscopy:
 higher accuracy for computation of derivatives

Computational Speed:

- "black boxes": quick implementation for single applications but possibly time consuming otherwise
- vectorization: significant acceleration (factor 140 for Hui)
- restructuring: subroutine instead of functions invariant code
- usefulness of imaginary part of w(z)

Session 4

Summary of the Topical Session on Spectral Line Shapes

The inclusion of the Topical Session on Spectral Line Shape, as part of the Annual Review Conference on Atmospheric Transmission Models, was an effort to introduce the workshop attendees to some of the basic physics of spectral line shape, to some of the recent research results in this field of study, to the ways those results are manifest in radiative transfer computer codes and to the effects the new results have on the problems of radiative transfer and remote sensing. A particular feature of the topical session was that special consideration was given to providing a tutorial overview of the subject with some emphasis on historical developments.

Within the constraint of time, there were two particular objectives. First, that there should be some presentation in outline tutorial form of the basic physics of spectral line shape. The intention was to stress the physics and not the mathematical theory. The second objective was that there should be detailed consideration of recent research results concerning (1) the shape of far wings of water vapor spectral lines and their aggregate affect on the water vapor continuum, especially in the "window" spectral regions, and (2) the shape of overlapped spectral lines, in particular in the microwave spectrum of oxygen and in the spectrum of carbon dioxide O branches in the fifteen micron spectral region. The question of the shape of the far wings of water vapor spectral lines is a long standing and much studied theoretical and experimental problem. The questions concerned with the shape of overlapping spectral lines were first addressed almost thirty-five years ago, both theoretically and experimentally in the study of the microwave spectrum of oxygen. However, the discovery, within the last ten years, of line coupling effects in laboratory and atmospheric spectra of many other molecules has brought this effect considerable new attention. Both problems are important to studies related to radiative transfer and remote sensing.

Five invited and five contributed papers composed the topical session. Both invited and contributed papers included original research results. In addition, however, the authors of the invited papers were asked to include tutorial and historical material, related to the general topic of their respective papers. The inclusion of historical material was considered appropriate and was specifically encouraged to address the lack of background knowledge of some of the conference attendees concerning the physics of spectral line shape. In compensation for the added requirement the invited presentations were allotted slightly more time than the contributed papers.

Copies of the transparencies of all of the presentations, both invited and contributed are collected together on the following pages. The authors of the invited papers were asked to prepare and submit summaries of their papers, including references, in particular because these papers contained interesting tutorial and historical materials. Some authors were not able to honor the request, and in part for that reason a very brief description of each paper, along with a few references, is given below.

The first paper, 4a1, "Basis of the Water Vapor Continuum Coefficients in the GL Models" was presented by S.A. Clough (Atmospheric and Environmental Research, Inc. and formerly of the Air Force Geophysics Laboratory). The results of the studies of S.A. Clough, F.X. Kneizys and their co-workers (1), are incorporated in the Geophysics

Directorate's computer code FASCODE. This paper covered some of the general dynamical and statistical considerations for spectral line shape. In particular as they apply to the shape of the far wings of water vapor spectral lines, the frequency dependence of the self and nitrogen broadened Chi-factors and continua. Some of their research is based on the studies of Huber and Van Vleck (2).

The second paper, 4a2, "Water Vapor Continuum Absorption Measurements with Line Shape Interpretations", was presented by M. Thomas (Johns Hopkins University Applied Physics Laboratory). This paper was concerned with the application of a line shape model developed by George Birnbaum (3). Birnbaum's stated objective was to develop a line shape which is applicable from resonance to the far wings. To achieve this he focused his attention on the dipole autocorrelation function, seeking to bridge the gap between the known long and short time behavior of the correlation function with a well chosen empirical interpolation function.

The third paper, 4a3, "Line Coupling for Microwave Oxygen Lines", was presented by P.W. Rosenkranz (Massachusetts Institute of Technology). This paper was concerned with the effect of line mixing in the microwave spectrum of oxygen. The line coupling effect was first observed in the microwave spectrum of oxygen and Rosenkranz was among the first to model the effect (5), employing a perturbation approximation to the line shape matrix. Rosenkranz's presentation included an historical overview of the study of the line coupling effect and recent results for the microwave oxygen band obtained in collaboration with H.J. Liebe (see contributed paper 4b2). Rosenkranz's data analysis technique is unique and differs from that of most other researchers in that the first order perturbation theory line coupling coefficients are inferred directly from the spectral data. Rosenkranz's presentation did not cover the technique but focused on the results of the analysis. However, a discussion of the technique has been presented by Rosenkranz in the literature (6).

The fourth paper, 4a4, "Laboratory Measurements of Line Coupling in CO₂ and N₂O" was presented by L.L. Strow (Univ. of Maryland). This paper considered laboratory measurements and analyses of spectra of carbon dioxide and nitrous oxide which Strow and his co-workers have made. The presentation also included a discussion of the technique most often used to model the line coupling effect in spectral data. Most often rate matrix parameters, and from them line coupling coefficients, are inferred from the spectral line widths, using "gap" laws, for example exponential gap or exponential-power gap laws, to model off diagonal elements of the rate matrix (7,8,9, see also contributed paper 4b3). First or second order perturbation theory is applied to the line shape operator (10) to yield the description in terms of the line coupling parameters (y_i).

The fifth paper, 4a5, "Line Mixing: A Near Wing and Far Wing Problem", was presented by J.M. Hartmann (Ecole Centrale, Paris). This paper, the last of the invited papers, was designed to iterate and tie together some of the basic physical ideas which were presented in the preceding four papers. Hartmann's presentation also illustrates those ideas with some of his and his co-worker's results (11,12) from studies of spectra of water vapor and carbon dioxide.

The sixth paper, 4b1, "Far Wing Line Shape Contribution to the Water Continuum in the Millimeter and Infrared Regions", was presented by R.H. Tipping (Univ. of Alabama). In this paper Tipping presented a theoretical collision broadened line shape, developed in collaboration with Q. Ma (Goddard Instituted for Space Studies) (13). The

theory assumes only the known values of (a) the permanent dipole moment, (b) the rotational constants and (c) the Lennard-Jones potential parameters. Their theory predicts, in particular, the experimentally observed negative temperature dependence of the molecular absorption by water vapor. Their theory partially follows the theoretical studies of Rosenkranz (14).

The seventh paper, 4b2, "Laboratory Measurements of the 60 GHz O₂ Spectrum in Air", was presented by Hans J. Liebe (Institute for Telecommunication Sciences). In this paper Liebe discussed his experimental apparatus which he used to make new measurements of the spectrum of O₂. Liebe also presented some of the experimentally recorded data and some data analyses. Liebe's data were the basis of analyses presented by Rosenkranz (see paper 4a3).

The eighth paper, 4b3, "Line Mixing in Polar and Nonpolar Molecules", was presented by A.S. Pine (National Institute of Standards and Technology; NITS). In this paper Pine presented data of HCN and HCCH which he collected and analyzed in collaboration with J.P. Looney (NITS). Pine reported new measurements and analysis of HCN; their studies of HCCH have been reported previously (15). Pines' presentation compared and contrasted results of data analyses employing various semi-empirical gap laws; an exercise which no one else has to date performed.

The ninth paper, 4b4, "Study of CO₂ Blue Wing in the 4.1 Micron Region", was presented by C.T. Delaye (Applied Physics Laboratory, the Johns Hopkins Univ.) and covered research performed in collaboration with M.E. Thomas (also of the Applied Physics Laboratory); see paper 4a2. Delaye presented interferometric data collected at the Applied Physics Laboratory of carbon dioxide in the 4.3 micron region. Delaye also presented an analysis of this data performed using the same Birnbaum line shape (3) which had been discussed by M. Thomas in paper 4a2. An important result of this study was the applicability of the line shape from the band head region into the far wing of the band and from this the implication that the Birnbaum line shape offered a convenient and accurate expression which would be useful in radiative transfer calculations.

The tenth paper, 4b5, "Theoretical Approach to the Line Wing Problem", was presented by L. Sinitsa (Institute of Atmospheric Optics, Tomsk, USSR). The presentation covered theoretical studies of spectral line shape and approximations with applications to a variety of experimental data from the infrared to the microwave region.

References:

- 1. S.A. Clough, F.X. Kneizys and R.W. Davies, "Line Shape and the Water Vapor Continuum", Atmospheric Research, 23, 229 (1989).
- 2. J.H. Van Vleck and D.L. Huber, "Absorption, Emission and Linebreadths: A semihistorical Perspective", Reviews of Modern Physics, 49, 939 (1977).
- 3. George Birnbaum, "The Shape of Collision Broadened Lines from Resonance to the Far Wings", J.Q.W.S.R.T., 21, 597 (1979).
- 4. Michel Baranger, "Problem of Overlapping Lines in the Theory of Pressure Broadening", Physical Review, 111, 494 (1958).

- 5. Philip W. Rosenkranz, "Shape of the 5 mm Oxygen Band in the atmosphere", IEEE Transactions on Antennas and Propagation, Vol. AP-23, 499 (1975).
- 6. P.W. Rosenkranz, "Interference Coefficients for Overlapping Oxygen Lines in Air", J.Q.S.R.T., 39, 287 (1988).
- 7. W. Lempert, G.J. Rosasco and W.H. Hurst, "Rotational Collisional Narrowing in the NO Fundamental Q Branch, Studied with CW Stimulated Raman Spectroscopy", J. Chem. Phys., 81, 4241 (1984).
- 8. L. Larrabee Strow, "Rotational Collisional Narrowing in an Infrared CO₂ Q Branch Studied with a Tunable Diode Laser", J. Chem. Phys., 84, 1149 (1986).
- 9. A.S. Pine and J.P. Looney, "Decoupling in the Line Mixing of Acetylene Infrared Q Branches", J. Chem. Phys., 93, 6942 (1990).
- 10. Earl W. Smith, "Absorption and Dispersing in the O₂ Microwave Spectrum at Atmospheric Pressures", J. Chem. Phys., 74, 6658 (1981).
- 11. J.M. Hartmann, L. Rosenmann and J. Taine, "Temperature and Pressure Dependence of Absorption in the Narrow R₆₆-R₆₈ Window of the ¹²C¹⁶O₂v₃ Band", J.Q.S.R.T., 40, 93 (1988).
- 12. M.Y. Perrin and J.M. Hartmann, "Temperature Dependent Measurements and Modeling of Absorption by CO₂-N₂ Mixtures in the Far Line Wings of the 4.3 um CO₂ Band", J.Q.S.R.T., 42, 311 (1989).
- 13. Q. Ma and R.H. Tipping, "A Far Wing Line Shape Theory and its Application to the Water Continuum Absorption in the Infrared Region. I", J. Chem. Phys., 95, 6390 (1991).
- 14. P.W. Rosenkranz, "Pressure Broadening of Rotational Bands. I. A Statistical Theory", J. Chem. Phys., 83, 6139 (1985).
- 15. A.S. Pine and J.P. Looney, "Decoupling in the Line Mixing of Acetylene Infrared Q Branches", J. Chem. Phys., 93, 6942 (1990).

BASIS OF THE WATER VAPOR CONTINUUM COEFFICIENTS IN THE GL MODELS

S.A. Clough Atmospheric and Environmental Research, Inc., 840 Memorial Drive, Cambridge, MA 02139

> F.X. Kneizys Geophysics Directorate, Hanscom AFB, MA 01731

> > R.W. Davies GTE Laboratories, Waltham, MA 02154

A formulation is developed in which the contribution of the far wings of collisionally broadened spectral lines to the water vapor continuum absorption is established. The effects of deviations from the impact (Lorentz) line shape due to duration of collision effects are treated semi-empirically to provide agreement with experimental results for the continuum absorption and its temperature-dependence. The continua due to both water-water molecular broadening (self-broadening) and water-air molecular broadening (foreign broadening) are discussed. Several atmospheric validations of the present approach are presented.

Line Shape and the Water Vapor Continuum

S.A. CLOUGH, F.X. KNEIZYS and R.W. DAVIES

Atmospheric and Environmental Research, Inc., Cambridge, MA 02139 (U.S.A.) Air Force Geophysics Laboratory, Hanscom AFB, MA 01731 (U.S.A.) GTE Laboratories, Waltham, MA 02154 (U.S.A.)

(Received May 1, 1988; accepted June 1, 1989)

ABSTRACT

Clough, S.A., Kneizys, F.X. and Davies, R.W., 1989. Line shape and the water vapor continuum. Atmos. Res., 23: 229-241. A formulation is developed in which the contribution of the far wings of collisionally broadened spectral lines to the water vapor continuum absorption is established. The effects of deviations from the impact (Lorent2) line shape due to duration of collision effects are treated semi-empirening) and water-air molecular broadening (foreign broadening) are discussed. Several atmospheric validations of the present approach are presented. ically to provide agreement with experimental results for the continuum absorption and its temperature-dependence. The continua due to both water-water molecular broadening (self-broad

RESUME

raise clargica par collision au continuum d'absorption de la vapeur d'eau. Les effeta des déviations de la forme de raie d'impact (Lorentz) sont traités de façon semi-empirique pour fournir un accord avec les résultats expérimentaux concernant le continuum d'absorption et sa dépendence en tem-On développe une formulation dans laquelle on établit la contribution des ailes éloignées des pérature. Les continus dùs à l'effet d'élargissement moléculaire eau-eau (self broadening) et air-eau (foreign broadening) sont discutés. Plusieurs validations atmosphériques de cette approche

INTRODUCTION

The continuum absorption due to water vapor has posed a complex problem versally accepted definition of continuum absorption has not been established for researchers concerned with atmospheric radiative problems. In fact, a unimaking more difficult the discussion of the effect. The regions of the atmos-

© 1989 Elsevier Science Publishers B.V. 0169-8095/89/\$03.50

ency, the windows, are strongly dependent on the water vapor continuum. These spectral regions are at 0 cm⁻¹, 800-1200 cm⁻¹ and 2000-3000 cm⁻¹. Labora. tory measurements of the water vapor continuum are made difficult by the pheric spectrum in the microwave and the infrared with the greatest transpar long path lengths required with conventional spectroscopic techniques or by ficulty in adequately characterizing the path, aerosol attenuation, turbulence, scintillation and instrument calibration. From a theoretical point of view, the pletely satisfactory explanation. The issue of whether the absorption represe its an excess or deficiency is fundamentally dependent on the line shape formulation chosen as reference as well as on the frequency regime of interest. A theoretical understanding of this problem entails a satisfactory description line wing requiring a proper treatment of the physical processes occurring in the complexities encountered with methods of high sensitivity such as spectrophone detection. Atmospheric measurements are adversely affected by the dif continuum has posed a comparably complex problem and still lacks a comof the line shape and its temperature-dependence from line center to the far the time associated with the duration of collision. Further, an adequate model must also address the issue of collision-induced spectra as well as the possibil ity of dimer absorption.

LINE SHAPE FORMULATION

tion for the absorption coefficient $k(\nu)$ (cm²/molec.), that is applicable from In our consideration of the continuum, we start with a line shape formulathe microwave to the infrared (Clough et al., 1983):

$$k(\nu) = R(\nu) \langle \phi(\nu) + \phi(-\nu) \rangle$$
with:
$$R(\nu) = \nu \frac{1 - e^{-\beta \nu}}{1 + e^{-\beta \nu}} \tag{2}$$

$$= \nu \tanh (\beta \nu/2) \tag{3}$$

8

where ν is the wavenumber value, $R(\nu)$ (cm⁻¹) is a radiation field term at temperature T with $\beta = hc/kT$ (cm), and $\langle \phi(\nu) + \phi(-\nu) \rangle$ is the symmetrized includes the effect of stimulated emission. This formulation has a number of attractive properties: its appropriateness to all spectral domains and the fact that the symmetrized power spectral density function satisfies an important intensity sum rule, the Nyquist theorem. For the application of this formalism power spectral density function (Van Vleck and Huber, 1977). The term $R(\nu)$ to the computation of spectra in terms of line transition data, we obtain:

232

$$k(\nu) = \nu \tanh(\beta \nu/2) \times \sum_{n} \hat{S}_{n}(T) \frac{1}{n} \left[\frac{\alpha_{n}}{(\nu - \nu_{n})^{2} + (\alpha_{n}^{2})^{2}} \chi(\nu_{n} - \nu) + \frac{\alpha_{n}}{(\nu + \nu_{n})^{2} + \alpha_{n}^{2}} \chi(\nu + \nu_{n}) \right]$$
(4)

where \hat{S}_i (cm²/molec.) is the intensity of the transition at wavenumber value ν_i (cm²¹) and halfwidth α_i (cm²¹). The Lorentz function, $f(\nu-\nu_i)$ (cm):

$$f(\nu - \nu_i) = \frac{1}{\pi} \frac{\alpha_i}{(\nu - \nu_i)^2 + \alpha_i^2}$$
 (5)

is the line shape function appropriate to the impact approximation for which the collision time is assumed to be instantaneous. The χ function is a semi-empirical function applied to the impact result to correct for duration of collision effects and to attain agreement between calculated and measured spectra. With $\chi=1$, this line shape reduces to the Lorentz shape in the infrared, since $R(\nu) \rightarrow \nu_i \ |\alpha-\nu_i| \ll \nu_i$ and to the Van Vleck-Weisskopf shape in the microwave, since $R(\nu) \rightarrow \beta \nu^2/2$. We adopt a notation in which a tilde over a quantity indicates that the radiation term, $R(\nu)$, has been excluded from that quantity.

At this stage we define a continuum absorption by excluding from the power spectral density function fast spectral components associated with the line center. The continuum, $\hat{\mathcal{C}}(\nu)$, is given by:

$$\tilde{C}(v) = \langle \phi(v) + \phi(-v) \rangle_c \tag{6}$$

$$=\sum \tilde{S}[f_c(\nu-\nu_i)\chi(\nu-\nu_i)+f_c(\nu+\nu_i)\chi(\nu+\nu_i)] \tag{7}$$

where f_c is a line shape with the strong central component excluded (Clough et al., 1980). We systematically define f_c ($\nu \mp \nu_i$) in the following way:

$$f_c(\nu \mp \nu_i) = \frac{1}{\pi} \frac{\alpha_i}{25^2 + \alpha_i^2} \qquad |\nu \mp \nu_i| \le 25 \text{ cm}^{-1}$$

$$\frac{1}{\pi} \frac{\alpha_i}{(\nu \mp \nu_i)^2 + \alpha_i^2} \qquad |\nu \mp \nu_i| \ge 25 \text{ cm}^{-1}$$
(8)

The function I_c is indicated schematically in Fig. 1 by the solid curve. Another function that has been used by Burch in some of his work is indicated by the dashed line in Fig. 1. The lack of agreement among researchers on the line shape formulation and on the definition of the function I_c has inhibited the intercomparison and validation of continua. It must be emphasized that the continuum and the details of the line-by-line calculation are inextricably related. The present formulation for the continuum is consistent with the FASCODE line-by-line model (Clough et al., 1986). Similarly, it is important to recognize that band models developed to describe molecular absorption, must also be derived in the context of a consistent treatment of the continuum. To

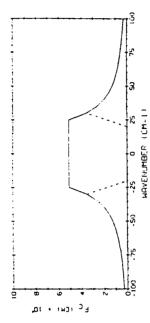


Fig. 1. The line shape function, $f_{\rm c}(\nu)$, used to develop the continuum (solid curve). The dashed curve represents the function used by Burch.

be more explicit, if a band model is to be used in conjunction with a continuum, then the absorption effects included in the continuum must be excluded from the band model. We should note that the continuum functions have been developed in such a way as to obey Beer's law.

It is an important consideration that the continuum coefficier., $\mathring{C}(\nu)$, is proportional to collider density, ρ . Since the collision frequency which is proportional to density determines the broadening, density is more appropriate as the dependent variable than pressure. At constant temperature the distinction is not relevant. The values for the self broadened halfwidths, $\alpha_i^{c_i}$, referred to atmospheric density, ρ_0 , are of the order of 0.1 cm⁻¹ (0.5 cm⁻¹ for self-broadened water vapor). With the halfwidth density-dependence given by:

$$\alpha_i = \alpha_i^0(\rho/\rho_0) \tag{9}$$

the α_i^i terms in eq. 8 may be dropped and the continuum shape function becomes:

$$f_{c}(\nu \mp \nu_{i}) = \frac{1}{\pi} \frac{\alpha_{i}^{0}(\rho/\rho_{0})}{25^{2}} \quad |\nu \mp \nu_{i}| \le 25 \text{ cm}^{-1}$$

$$f_{c}(\nu \mp \nu_{i}) = \frac{1}{\pi} \frac{\alpha_{i}^{0}(\rho/\rho_{0})}{(\nu \mp \nu_{i})^{2}} \quad |\nu \mp \nu_{i}| \ge 25 \text{ cm}^{-1}$$
(10)

The density scaling of the continuum is established as:

$$\tilde{C}(\nu) = \tilde{C}^{\circ}(\nu) (\rho/\rho_0) \tag{11}$$

since f_c is proportional to (ρ/ρ_0) for all values of ν .

The temperature-dependence of the absorption is dependent on the radiation term, $R(\nu)$ in eq. 2, the strength S_n , the halfwidth α_n^0 , and on the line shape factor χ . The dependence is known theoretically for $R(\nu)$ and for S_n^0 and is

234

satisfactorily described through an empirical exponent, m, determined from measurements for α , where:

 $\alpha_{\bullet}(\rho,T) = \alpha_{\bullet}^{\bullet}(T/T_{\circ})^{\bullet \bullet}(\rho/\rho_{\circ})$

For the line shape factor χ the situation is more complicated. Near line center, $|\nu\pm\nu|<5$ cm⁻¹, χ is essentially unity for all temperatures. However far from line center the temperature-dependence for χ must be inferred from the temperature of the absorption resulting from many overlapping lines.

WATER VAPOR

We are now in a position to apply the formulation we have developed to water vapor absorption. Performing a line-by-line calculation using the entire set of water vapor lines from 0 cm⁻¹ to 10,000 cm⁻¹, we obtain the power spectral density function for self-broadened water vapor shown in Fig. 2. The dotted curve is attained by utilizing the continuum line shape function, f_c , thus excluding from the power spectral density function the contribution of the line centers, and providing a spectral of low spectral content designated as the continuum. The well known water vapor bands associated with pure rotation $(0\,\text{cm}^{-1})$, ν_1 (1600 cm⁻¹), ν_1 of HDO (2720 cm⁻¹), $2\nu_2$ (3100 cm⁻¹), ν_1 (3660 cm⁻¹) and ν_3 (3760 cm⁻¹) are evident in Fig. 2. In Fig. 3 we indicate two

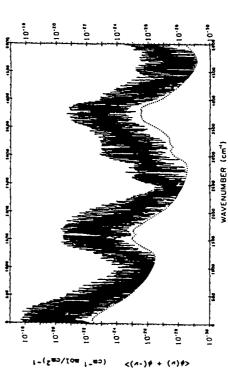


Fig. 2. The symmetrized power spectral density function for self-broadened water vapor at 26.7 mb. and 296 K (solid curve). The continuum is indicated by the dotted curve.

(cm²) = (cm²

Fig. 3. The continuum for self-broadened water vapor. The dashed line is the impact result and the dotted curve is with the χ function adjusted to fit the experimental data of Burch, 1981. The broadening pressure is 1992 mb.

continua, one obtained using the impact line shape $(\chi=1)$, and the other with a function obtained by adjusting the parameters in an empirical χ -function to attain agreement with the indicated spectral results (Burch, 1981; Burch and Alt, 1984; Burch, 1985)

Note that in Fig. 3 the continuum coefficient for self-broadened water vapor, Note that in Fig. 3 the continuum (χ =1) in the center of the bands at 0–500 cm⁻¹ and 1400–1800 cm⁻¹ and a deficiency between central band absorption regions, 800–1200 cm⁻¹ and 1800–3300 cm⁻¹. This result is consistent with theoretical requirements and is a direct consequence of the formulation. The χ function associated with the line shape for self-broadened water vapor, designated χ _s, is shown by the solid curve in Fig. 4. The functional form of χ is given by:

$$\chi = \frac{1 - (1 - \chi') \frac{(\nu \mp \nu_i)^2}{25^2} \quad |\nu \mp \nu_i| \le 25 \text{ cm}^{-1}}{|\nu \mp \nu_i| \ge 25 \text{ cm}^{-1}} \tag{12}$$

where for self-broadening χ_s is obtained by setting $\chi = \chi_s$ with:

$$\chi'_s = 8.63 \exp(-z_1^2) + (0.83z_2^2 + 0.033z_2^4) \exp(-|z_2|)$$
 (13)



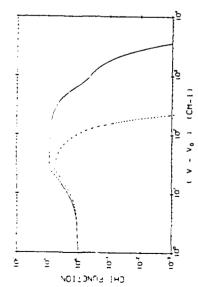


Fig. 4. The χ function for water at 296 K. The solid curve is for self-broadening, the dashed curve is for foreign-broadening.

where $z_1 = (\nu \mp \nu_i)/400$ and $z_2 = (\nu \pm \nu_i)/250$ at 296 K. From eq. 12 and Fig. 4 tinuous. This is a direct consequence of the choice of f_{ϵ} (eq. 8) but causes no we note that χ is continuous at 25 cm - ', but that the first derivative is disconparticular problems in the formulation.

tinuum in the window regions, is not explained. Rosenkranz (1985, 1987), in ture-dependence, particularly in the 1000 cm⁻¹ window. It is an important shortcoming of the current state of line shape theory for molecular collisions, that the temperature-dependence of the far wings, or alternatively of the contwo particularly interesting papers, has proposed an alternative formulation to eqs. I and 3, which leads to a strong temperature-dependence consistent with observations in the far-wing regions. This proposed formulation warrants additional scrutiny. The dimer has often been postulated as a source of the continuum absorption primarily as a consequence of its simple and attractive temperature-dependence. However, the absence of spectral structure, difficul-The self-continuum for water vapor demonstrates a rather strong temperaties in explaining spectral pressure-dependence and the fact that the absorption in the windows as developed in this paper represents an excess with re-On the other hand, dimers should be formed under atmospheric conditions so spect to the impact line shape are in direct contradiction with the dimer theory. that the central issue becomes the question of dimer lifetime (Suck et al., 1979).

K and 338 K. These parameters for 296 K and 338 K are then extrapolated to For pragmatic purposes the temperature-dependence of the continuum has by least-squares fitting the calculated continuum to the data of Burch at 296 been treated as follows: the parameters in an analytical x function are obtained

260 K and a continuum for that temperature is calculated. This is potentially a source of error; however, validations for atmospheric measurements have provided remarkably good results. Continua for 338 K, 296 K and 260 K are shown in Fig. 5.

ferred to as foreign broadening. Fig. 6 shows the empirical continuum, Cf, fit to the data of Burch as well as the continuum for the impact approximation. For the foreign-broadened case, the line wings decay much more rapidly as a ened case. This is reflected in the foreign chi-function, x, shown by the dashed curve in Fig. 4. For the foreign continuum χ_i is obtained by setting $\chi' = \chi'_i$ in function of wavenumber difference from line center than for the self-broad-An analogous treatment is performed for air-broadening of water vapor,

$$(14)^2 = 6.65 \exp(-z_1^2)$$

where $z_1 = (\nu \pm \nu_i)/75$. For the window regions of the foreign continuum, 1000 cm-' and 2500 cm-' in Fig. 6, an absorption coefficient has been added to the with atmospheric measurements (Roberts et al., 1975). The contribution of continuum resulting from the present formalism in order to attain agreement the foreign continuum is very small in these spectral regions making the measurements particularly difficult. The observed effect may be due to collision

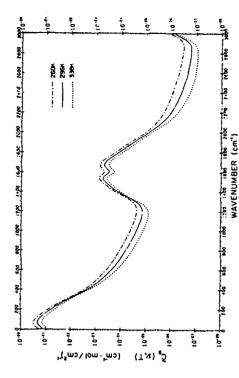


Fig. 5. The self-broadened water vapor continuum at 338 K, 296 K and 260 K. The continua at 338 K and 296 K have been fit to data and the 260 K continua have been extrapolated.



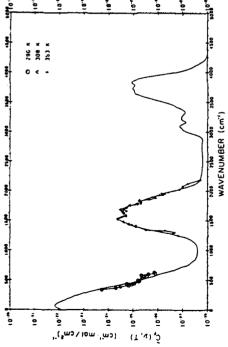


Fig. 6. The continuum for foreign-broadened water vapor. The solid curve is the calculated continuum with the χ function adjusted to fit the experimental data of Burch, 1981. The broadening pressure is 1013 mb.

induced spectra or humidity-dependent aerosols. No significant temperaturedependence has been observed for the foreign continuum.

The total absorption coefficient due to self- and foreign-water-vapor continuum, $k_{\epsilon}(\nu)$, is given by the relation:

$$k_{\bullet}(\nu) = \nu \tanh(\beta \nu/2) \left[\tilde{C}_{\bullet}^{0}(\rho_{\bullet}/\rho_{0}) + \tilde{C}_{\uparrow}^{0}(\rho_{i}/\rho_{0}) \right]$$
 (15)

It is an important point that for atmospheric conditions, the foreign continuum is dominant for in-band absorption and the self continuum is dominant for the out-of-band absorption, the window regions of water vapor spectrum.

ATMOSPHERIC VALIDATION

The most important element in the development of an atmospheric transmittance/radiance model is validation with atmospheric data. Since the atmospheric window at $1000 \, \mathrm{cm}^{-1}$ ($10 \, \mu\mathrm{m}$) is of such importance, we consider that spectral region in more detail. The continuum currently being used in FASCOD2 has been adjusted to fit the more recent measurements at $1000 \, \mathrm{cm}^{-1}$ of Burch and Alt, 1984 (Fig. 7). In Fig. 8 we show a plot of the optical depth for a 1-km path at 990 cm⁻¹ as a function of water vapor density from LOWTRAN7 (Kneizys et al., 1988) which incorporates this continuum de-

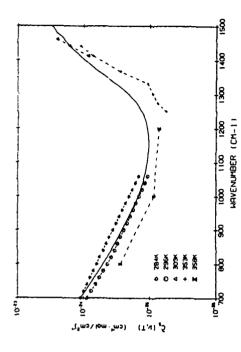


Fig. 7. Details of the self-broadened continuum at 1000 cm⁻¹. The solid line is the calculated continuum at 296 K. The data for 284 K and 296 K are from Burch and Alt (1984); the other data are from Burch (1981).

Air Force Wright Aeronautical Laboratories (AFWAL) taken over an 8-km molecules (intercept) and from the local water vapor lines. Spectral validation velopment. We consider two sets of atmospheric measurements: one from the path and for a range of visibilities (Kneizys et al., 1984) and the other from the Technion Institute in Israel over an 8.6-km path (Oppenheim and Lipson, 1986). Both of these sets of measurements were taken with circular variable ments. The calculations do take into effect the contribution from other of the continuum model with the Technion measurements for the 8–12 micron tained at 4.75 μm and 3.2 μm . These two regions demonstrate the predictive filter (CVF) spectrometers. Since the atmospheric measurements include excapability of the current formulation since there has been no adjustment with it should be emphasized that the calculations are essentially qualitative and tinction due to aerosol effects, the calculated optical depths, which do not include aerosol contributions, are less than those for the atmospheric measurewindow is shown in Fig. 9 and for the 3–5 micron window in Fig. 10. Of particular note is the excellent agreement between calculation and observation obdata in these spectral regions. With respect to the continua beyond $5000\,\mathrm{cm}^{-1}$ unvalidated. This is particularly the case for the seif-broadened continuum, mportant between the bands.

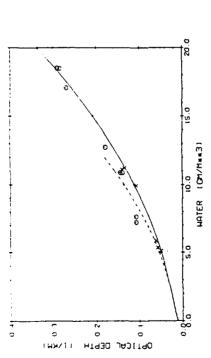


Fig. 8. The optical depth for a 1-km path at 990 cm⁻¹ as a function of water vapor density. The calculations are from LOWTRAN with the self-continuum of Fig. 7. The solid curve is for 296 K and the dashed curve is for 284 K. The data are from Kneizya et al., 1984. The X-symbols are for cases with visibilities > 15 km.

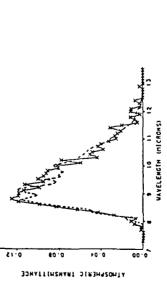
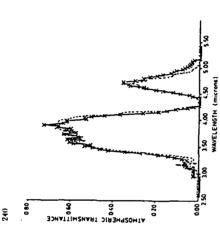


Fig. 9. Spectral comparison between a CVF measurement in the 8-12 micron window over a 8.637km path by Technion (Oppenheim and Lipson, 1985) and a LOWTRAN calculation with the FASCOD2 continuum (dotted curve). The measurement conditions: T=297.5 K, P=1008 mb, RH=85%, and visibility = 15 km.



239

Fig. 10. Spectral comparison between a CVF measurement in the 3-5 micron window over a 10.37-km path by Technion (Oppenheim and Lipson, 1985) and a LOWTRAN6 calculation (dotted curve). The measurement conditions: $T=283~\mathrm{K}$, $P=899~\mathrm{mb}$, RH=68% and visibility = 40 km.

SUMMARY

The present discussion is not intended as a comprehensive review of the water vapor continuum problem. It is rather a description of a specific approach that is consistent with the physics of the problem and that has ben constrained to provide results consistent with experimental measurements. The choice of measurements used for this discussion has been highly selective. This is related to a need for internal consistency of the observations, our estimation of the accuracy of the measurements and a treatment of the data that is in the context of the current development. The present status should be regarded as useful if not definitive. In order to meet current objectives in atmospheric remote sensing and related phenomena, more observations of high accuracy both in the laboratory and in the atmosphere are required, and significant advances in the theoretical treatment of the effects of collision on molecular line shape need to be achieved. A floppy disk containing a program to calculate continuum absorption coefficients as described here and consistent with FASCOD2 and LOWTRAN7 is available from the authors.

ACKNOWLEDGEMENTS

One of us, S.A.C., would like to acknowledge the invaluable support received while at AFGL during which time most of the work was performed. In particular we wish to recognize the contribution of James Chetwynd for the extensive

calculations leading to the current results. We would also like to thank our many colleagues, experimentalists and theoreticians, for the discussions that have clarified our understanding of a very difficult problem. The discussion and experimental results due to Darrel Burch have been invaluable in reaching the present state of understanding. To our other colleagues not mentioned here, we hope to do greater justice in a more extensive paper in preparation.

REFERENCES

Burch, D.E., 1981. Continuum Absorption by H₂O. AFGL-TR-81-0300. Burch, D.E., 1985. Absorption by H₂O in Narrow Windows Between 3000-4200 cm⁻¹. AFGL-

Burch, D.E. and Alt, R.L., 1984. Continuum Absorption in the 700-1200 cm -1 and 2400-2800 TR-85-0036

cm -1 Windows. AFGL-TR-84-0128.

Clough, S. A., Kneizys, F. X., Davies, R.W., Gamache, R. and Tipping, R.H., 1980. Theoretical line shape for H.O vapor: application to the continuum. In: A. Deepak, T.D. Wilkerson and L.H. Ruhnke (Editors), Atmospheric Water Vapor. Academic Press, London, pp. 25-46. Clough, S.A., Davies, R.W. and Tipping, R.H., 1983. The line shape for collisionally broadened molecular transitions: a quantum theory satisfying the fluctuation dissipation theorem. Proc. 6th Conf. Spectral Line Shapes. Waller de Gruyter, New York, N.Y., pp. 563-568. Clough, S.A., Kneizys, F.X., Shettle, E.P. and Anderson, G.P., 1986. Atmospheric radiance and transmittance: PASCOD2. Proc. 6th Conf. Atmospheric Radiance. AMS, Williamsburg, VA,

pp. 141-144.

Kneirys, F.X., Gruenzel, R.R., Martin, W.C., Schuwerk, M.J., Gallery, W.O., Clough, S.A., Chetwynd, J.H. and Shettle, E.P., 1994. Comparison of 8 to 12 Micrometer and 3 to 5 Micrometer CVF Transmissometer Data with LOWTRAN Calculations. AFGL-TR-84-0171.

Kneirys, F.X., Shettle, E.P., Abrev, L.W., Chetwynd, J.H., Anderson, G.P., Gallery, W.O., Selby, J.E.A. and Clough, S.A., 1988. User's Guide to LOWTRANT, AFGL. TR-88-0177.

mospheric water vapor in the regions 4.3-5.5 micron and 8-13 micron. Proc. Topical Meeting on Remote Sensing of the Atmosphere, OSA.

Roberts, R.E., Selby, J.E.A. and Biberman, L.M., 1976. Infrared continuum absorption by atmospheric water woop in the 8-12 µm window. Appl. Opt., 15: 2085. Oppenheim, U.P. and Lipson, S.G., 1986. Private Communication. See also A. Ben-Shalom, A.D. Devir, S.G. Lipson, U.P. Oppenheim and E. Ribak, 1985. Absorption of IR radiation by at-

Rosenkranz, P.W., 1985. Pressure broadening in rotational bands, I. A statistical theory. J. Chem. Phys., 83: 6139.

Rosenkranz, P.W., 1987. Pressure broadening in rotational bands, II. Water vapor from 300 to 1100 cm-1, J. Chem. Phys., 87: 163.

Suck, S. H., Kassner, J.L., Jr. and Yamagushi, Y., 1979. Water cluster interpretation of IR absorption aspectra in the B-14 µm wavelength region. Appl. Opt., 18: 2609.

Van Vleck, J.H. and Huber, D.L., 1977. Absorption, emission and linebreadths: a semihistorical

perspective. Rev. Mod. Phys., 49: 939.

WATER VAPOR CONTINUUM ABSORPTION MEASUREMENTS WITH A LINE SHAPE INTERPRETATION

M.E. Thomas, C.T. Delaye Applied Physics Laboratory, The Johns Hopkins University, Laurel, Maryland 20723

A review of water vapor continuum experimental data is presented as a function of frequency, partial pressures, and temperature for atmospheric windows from the millimeter wave to 1 μ m. The millimeter wave and 10 μ m regions are the most extensively characterized. The behavior of the continuum can be represented in the form of simple well behaved functions, yet a physical interpretation has been elusive. For the millimeter wave window, the continuum frequency dependence is frequency squared. For infrared windows, the continuum frequency dependence is exponential always decreasing away from strongly absorbing bands for both self and foreign broadening. These observations have lead to line shape interpretations of the water vapor continuum.

A particular line shape of interest has been developed by G. Birnbaum in the late 1970's. It has a closed form solution, has a continuous representation from line center to the far wing and thus is normalizable, has an exponential far wing and is consistent with many line shapes at line center. In short, it is a versatile and practical line shape. Line-by-line calculations based on this line shape are compared to the experimental data base with interesting results. The agreement with experimental data is best when the continuum is at a minimum, but deviates below observation towards the bordering absorption band. However, this formalism does not include line mixing (or coupling) and this is certainly important. Far wings must play some role in continuum absorption, but a definitive model will require a complete theory.

Water vapor continuum absorption heasurements with line shape interpretations

Michael E. Thomas and Corinne T. Delaye

The Johns Hopkins University Applied Physics Laboratory Laurel, Maryland 20723 Absorption by molecules defines the atmospheric windows and is an important mechanism of tropospheric attenuation at millimeter and infrared wavelengths, especially in the marine environment. Therefore, the understanding and accurate modeling of absorption by atmospheric molecules are important to atmospheric remote sensing, infrared imaging systems, long-path laser propagation, electro-optical systems, radar, and atmospheric meteorology. Figure la shows inov-resolution infrared transmittance of the atmosphere and demonstrates the importance of water vapor over other atmospheric constituents⁽¹⁾. The H₂O absorption bands, along with those of CO₂, define the atmospheric window regions in the infrared. At millimeter and microwave wavelengths, O₂ and H₂O determine the window regions.

The main rotational and vibrational bands have been extensively characterized by many investigators^(2,3,4). This work has resulted in a compendium of absorption-line parameters, maintained by the Air Force Geophysics Laboratory ^(3,6) (AFGL), which represents a significant contribution to absorption calculations. The database also contains parameters for weak absorptions lines in the window regions. However, this information is, in general, not a accurate as that of the main bands.

The comparatively weak absorption that does occur in the window regions can be described as arising from two distinct sources, local line and continuum absorption, as illustrated in the high-resolution computed spectrum of Fig. 1b for the 10 µm window region. Weak absorption bands of CO₂ and HDO, along with other H₂O absorption lines in the window regions, compose the local line contribution. The continuum contributes an additional, gradually varying, frequency-dependent background to the total absorption. A general empirical form for the continuum absorption coefficient used to represent the data⁽⁵⁾ is

$$\beta_{cont}(\nu, T, P_{\Omega_1} \dots P_{\Omega_1}, P_a) = \frac{P_a}{RT} \sum_i \left[G_{F1}(\nu, T) P_{E1} + G_b(\nu, T) P_a \right]$$
 (1)

where C_a , is the self-broadening coefficient of the absorbing gas, C_{Fl} is the foreign broadening coefficient due to the \mathbb{I}^{th} type foreign gas, and R is the ideal gas constant. The equation can be conveniently rewritten for I-2 to obtain

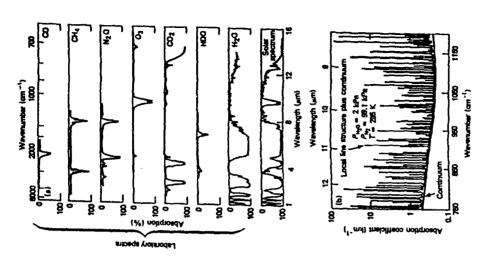


Figure 1. (a) Low-resolution solar spectrum compared with laboratory spectra of atmospheric gases. (b) Local line structure plus continuum in the 10-µm region.

$$\beta_{\text{cont}}(\nu, T) = \frac{G_{11}(\nu, T)}{KT} P_{41} [P_{\xi 1} + F(\nu, T) P_{\xi 2} + B(\nu, T) P_{4}]$$
 (2)

where $F = C_{TJ}/C_{TI}$ and $B = C_{u}/C_{TI}$ are the dimensionless broadening coefficients. Near line center, B has the value of 5 for water vapor relative to nitrogen. In the real atmosphere, the effects of oxygen broadening must also be included. The dimensionless broadening coefficient E accounts for oxygen. However, many laboratory experiments ignore the effects of oxygen and use only nitrogen as the broadening gas along with the absorbing gas.

Water vapor absorption

As previously mentioned, molecular absorption in the window regions manifests itself as local line and continuum type absorption. Narrow band systems can avoid local line effects but not continuum absorption. Broad band systems must account for both.

scal lines

Local line structure of the 10- and 4 μm vater vapor window regions has been experimentally characterized by Thomas(39), and Long and Damon(6b). The 1 to 1.1 μm local line structure based on experimental data has been reported by Gallery et. al. (66). The data demonstrate the importance of local line structure in the case of water vapor. The HITRAN database also represents local line structure structure based on experimental data and/or theoretical calculations.

ontinum

In 1942, Elemeser(*) recognized a continuum in the 13- to 8- µm window region, which he attributed to the far wings of the curong, nearby rotational and by obstational rotational bands of Hyū. Further verification of this nonlocal line absorption feature was provided by Yates and Taylor(*), who studies inflavored natemustron along horizontal paths at sea level, Solar spectra studies also indicated continuum absorption in the 13- to 8- µm window(**). The nature of the continuum, judged by those measurements, was uncertain. It could be due so fire wings (far from the band center) of strong absorption bands or to scattering and absorption by particulates.

It is deffort to determine the cause of continuum absorption in the 13- to a unished. Bignell's in 1963 examined solar spectra while monitoring the armosphere for aerosol concentrations and studying CO₂ far-wing contributions. He concluded that the amount of continuum absorption observed could not be required by aerosol attendation of the wing absorption observed could not be required to model the continuum by far wings of the bordering H₂O bands. The reportant contribution from this initial work was the realization of major water important contributions to the continuum. A second paper by Bignell'19 in 1970 with the contribution of major absorption in the window regions for a multiple-traversal absorption cell and grating spectrometer. Two if your of a multiple-traversal absorption cell and grating spectrometer. Two if your water vapor self-to-foreign-gas broadening ability (see Eq. 2) and (b) a strong negative temperature dependence. Neither of these findings was anticipated

on the basis of the far-wing approaches of Bignell's 1963 paper⁽¹²⁾. Also reported by Bignell⁽¹³⁾ was a stailar, but much weaker, continuum absorption in the 4 µm region. (The 4 µm region also features a collision-induced absorption band of nitrogen^(1,13). The band is of comparable strength to the water vapor continuum in the earth's atmosphere. It is a smooth absorption band showing no structure; thus, it is often referred to as the nitrogen continuum. Also, a far-wing continuum of CO₂ beyond the v₃ band head is observed between 4.1 and 4.0 µm⁽¹⁰⁾.)

Since those initial experimental efforts to characterize water vapor continuum absorption, many measurements have been made. They fall into three categories: (a) measurements within the earth's atmosphere or field measurements, (b) laboratory measurements using a long-path cell and a spectrometer, and (c) laboratory measurements using a long-path cell and a spectrometer, and (c) wariations measurements, its precise characterization variation a photoacoustic cell and measurements, its precise characterization requires control and knowledge of the propagation path. The effects of turbulence, particulates scattering, temperature pressure and temperature dependence of each atmospheric constituent. Spectrometer measurements and continuum absorption. Laser measurements are limited to discrete frequencies, but because of the laser's higher power and stability, greater accuracy can be obtained; this is particularly true for photoacoustic techniques. Laboratory transmission measurements require very long path lengths (%) km or longer) and thus are difficult to obtain. The photoacoustic cell, on the other hand, is compact (about 30 cm) but still maintains considerable sensitivity. Of atmospheric propagation computer codes.

As a result of these experiments, a good characterization of the commonly used window regions exists today. An excellent review of the field is given by the recent work of Hinderling et al. (17). They emphasize the 8- to 14- µm window region, which, along with the millimeter-wave window, is the most extensively measured. A review of the current experimental data for all the window regions is given in the next section, followed by a brief review of the theoretical and empirical models used to explain the experimental data.

Millimeter-wave window

Figure 1.3.10 (18-22) shows continuum absorption from 10 to 1000 GHz (total absorption minus local lines). The solid line represents an empirical formula given by Gaut and Raffenstein: (19)

$$\beta_{\text{continum}} = (1.08 \times 10^{-8}) \rho_{\bullet} \left[\frac{300}{7}\right]^{4} \left[\frac{P_{1}}{101}\right] f^{2} \qquad (km^{-1}),$$
 (3)

where ρ_{θ} is the water unpor density (g/m^3) , P_I is the total pressure (kPa), and f is the frequency (GHz). The plotted points indicate experimental data. The formula correctly demonstrates the frequency dependence of the continum but not

the temperature and pressure dependence. More recent work by Liebe⁽¹³⁾ uses a continum formula, fitted to experimental data at 138 GHz, of the form

$$\beta_{\text{continus}} \sim (4.73 \times 10^{-8}) \, \ell^2 \left[\frac{300}{T} \right]^3 P_a \left[p_{\text{c}} + 31.6 \left[\frac{300}{T} \right]^{3.5} P_a \right] \, (400^{-1}),$$
 (4)

where f is gigahertz, T is in kelvins, and P_a and P_f ($P_f = P_f - P_a$) are in kilopascals. A strong dependence on the water vapor partial pressure is shown (B >> 5). The continuum calculated using Eq. 4 is smaller than that calculated using Eq. 3 because of improved local line modeling. On the basis of the work by Liebe and Layton⁽²⁴⁾, the parameter B grows as the frequency decreases from B 33 co 110 GHz (see Table 1). This dependence is expected based on the far-wing model of Birrhaum⁽⁴²⁾ and leads to the following empirical model (for f < 1000 GHz and in units of km^{-1})⁽²⁴⁸⁾

where θ = (300/T) and the other variables have the same units as above.

Table 1. Experimental frequency dependence of B (u, 300)

В (v. 300)	32	31.6	20	7.4
, (cm ⁻¹)	3.7	4.6	7.1	27.8
f (CHZ)	110	138	213	833

As Eq. 4 indicates, B is not only a function of frequency but a strong function of temperature as well. Although Liebe⁽²³⁾ chooses to represent his data in a power law form, a comprehensive study at 213 GHz by Llewellyn-Jones⁽²³⁾ shows the data fits an Arrhenius plot with the functional form

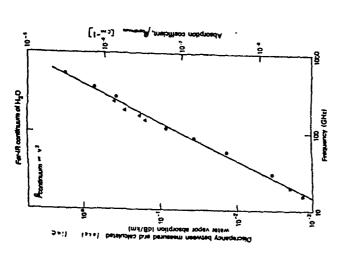


Figure 2. Water vapor continuum absorption coefficient as a function of frequency. The solid line is an empirical fit to the experimental data points as given by Eq. 1.3.92. The plotted points are (a) [20], (·) [21], and (m) [22] for $T \sim 300~K$, $P_{\rm f} = 101~k{\rm Pa}$ and $\rho_{\rm b} = 10^{-3}~k{\rm g/m}^3$.

$$C_a(\nu,T) \propto e^{b/T},$$
 (6)

 $b-5 \times 10^4$ K. Again, a strong negative temperature dependence is observed at this frequency as well. Figure 3 illustrates the experimental results of Llewellyn-Jones⁽²³⁾.

In summary, the millimeter-wave water wapor continuum falls off as frequency squared, has an enhanced self-broadening contribution that grows with decreasing frequency, and has a strong negative temperature dependence.

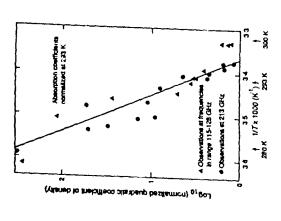


Figure 3. Temperature dependence of millimeter wave water vapor continuum. Solid curve represents empirical fit to data as given by Eq. 6.

The 8- to 12-um window

Figure 1.4(2?) shows the self-broadening water vapor continuum coefficient, Gereases exponentially as the frequency increase. The same functional degendence is exhibited by $G_{\rm w}$, the nitrogen-broadening coefficient, as shown in Fig. 5(2?), but the rate of decrease is more rapid. Thus, $B(-G_{\rm s}/G_{\rm w})$ increases as the frequency increases away from the rotational band. Long-path White cell and photoacoustic laser measurements indicate that B can be quite large. Values ranging from 100 to 600 have been measured in the $10-\mu m$ region with $G_{\rm s}$ issers. (15.2a.29) Figure 6 illustrates a laser measurement at 940.548 cm⁻¹ as a function of the water vapor partial pressure. The total pressure is maintained at 101 kpa (1 etc.) with nitrogen.

The observed temperature dependence at 10.6 μm features a rapid decrease virb increasing temperature (Fig. 7), just as in the millimeter window region, (30-33). The temperature dependence has the following functional form over a wide temperature range:

$$C_{\rm e}(\nu,T) = C_{\rm s}(\nu,T_{\rm o}) \, {\rm e}^{\rm b(1/T-1/T_{\rm o})},$$
 (7)

where $G_{\bf k}(94.0~{\rm cm}^{-1},296~{\rm K})$ = 1.83 x 10⁻²² cm⁻²/molecule-atm and b = 1680 k. This result at 10 μm is also consistent with other measurements in the $10-\mu m$ region and at 14.3 μm ^(19.27).

Based on the data presented and Birnbaum's line shape formula, a simple formula for the nitrogen broadened water vapor continuum absorption coefficient from 700 to 1100 cm⁻¹ and for typical atmospheric temperatures is given by (338)

$$\beta_{continuou} = 6.41 \text{x} 10^3 \text{exp}(-0.00839 \nu)$$

$$x((T_0/T)^3p_{M2} + 16.96exp(0.00374\nu + 1680(1/T - 1/T_0)p_{M20})p_{M20}/T$$
 [km⁻¹]

8

where p is atmospheres, ν is vave numbers and To = 296 K.

An excellent review of experimental measurements in the $10-\mu m$ region by $Grant^{(34)}$ makes the following additional points: 1. Oxygen does not broaden as effectively as nitrogen and must be included in

.. Oxygen does not broaden as effectively as nitrogen and must be included in a realistic model of the earth's atmosphere. A broadening coefficient of F 0.75 ± 0.1 for oxygen relative to nitrogen was measured by Nordstrom et al. (33) Using Eq. 3, this means air has an effective broadening of 0.95.

al. (35) Using Eq. 3, this means air has an effective broadening of 0.95.
2. Understanding the local line structure is critical in determining the true continum. Line positions are known reasonably well; however, line strength and half-width are not known with enough accuracy.

Long-path field measurements by Devir et al. $^{(16)}$ are in excellent agreement with the laboratory measurements of Burch and $\mathrm{Alt}^{(27)}$ and Peterson et al. $^{(28)}$ in this window region concerning the water vapor continuum. The measured spectral range of Devir extends the range covered by Burch and $\mathrm{Alt}^{(27)}$ and shows the water vapor continuum increasing with increasing frequency. The minimum occurs at 9.0 μ m (lll1 cm⁻¹). The nature of 8-12 μ m continuum absorption appears to be measurements.

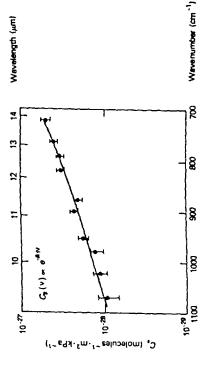


Figure 4. Self-broadening coefficient as a function of wave number from 700 to 1100 cm $^{-1}$ at 296 K.

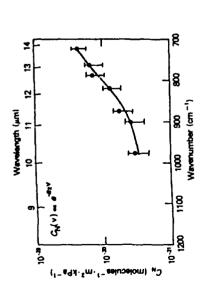


Figure 5. Nitrogen broadening coefficient as a function of wave number from 700 to $1000~{\rm cm}^{-1}$ at 296 K.

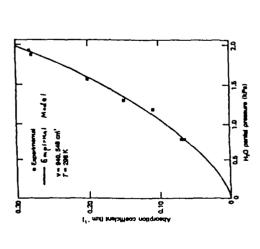


Figure 6. Water vapor partial pressure dependence in the 10 μm region.

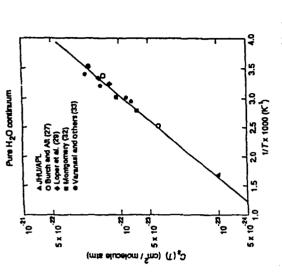


Figure 7. Temperature dependence of self-broadening coefficient in the 10 µm region.

The 3- to 5-µm window

The 3- to 5-µm continuum region has a different frequency dependence compared with the millimeter and 8- to 12-µm regions. Figure 1.3.16b displays a nearly parabolic dependence with a minimum at a wavenumber of 2600 cm⁻¹.

(27.37.39) As shown by the spectrometer measurements of Burch and Alt⁽²⁷⁾ (Fig. 8a), the self-broadening coefficient has an exponential falloff at wavenumbers up to 2550 cm⁻¹, then the falloff rate decreases as the frequency increases. Figure 8b shows long-path White cell DF laser measurements⁽²⁷⁾ taken under atmospheric conditions, which indicate continuum absorption lavels roughly 504 higher than those indicated by Burch and Alt⁽²⁷⁾. The lavel of absorption in the higher than those indicates the magnitude less than that in the 10-µm region. Long-path CO, DF, and HF laser measurements near room temperature again indicate large values for 8 in the continuum region, ranging from 10 to 20 at 5 µm⁽³⁹⁾ to approximately 50 to 60 at 4 µm⁽³⁷⁾ and back down to 10 at 3 µm⁽⁴⁰⁾.

A strong negative temperature dependence is again observed for the self-broadening coefficient. Figure 9 shows the results of laboratory long—path spectrometer measurements by Burch and $\mathrm{Alt}(^{27})$. The temperature dependence at 2400 cm⁻¹ exhibits exponential failoff similar to that in the $10^{-\mu\mathrm{m}}$ and millimeter regions. However, the curves at 2500 and 2600 cm⁻¹ show double exponential trends. The nature of the water vapor continuum in this window region is more complicated than the other windows previously discussed.

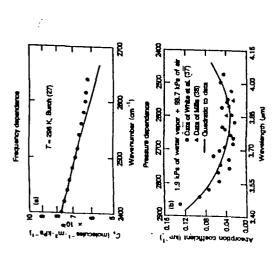


Figure 8. 4 μm water vapor continuum region at T= 296K. (a) C_s vs wavenumber [27] and (b) absorption coefficient vs wavelength [37,18].

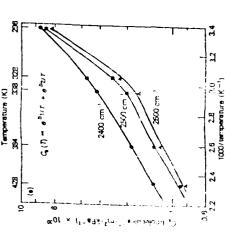


Figure 1. Plats of the water vapor self-broadening coefficients at 2400, 255, are 2500 each vs reciprocal temperature [27], the symbols \cdot , \blacksquare and \bullet represent the experimental data points.

::

More experimental data is needed to generate a meaningful empirical model of the continuum absorption coefficient. An attempt at representing the existing data is given by the following formula for the nitrogen broadened water vapor continuum absorption coefficient valid from 2400 to 2800 cm^{-1} [33a],

$$\begin{split} & \beta_{\text{continum}} = 7.34 \times 10^{26} (\text{PH}_{20}/\text{T}) \{ \text{C}_{\text{s}}(\nu, \text{T}) \text{Ph}_{\text{RO}} + \text{C}_{\text{s}}(\nu, \text{T}) \text{Ph}_{\text{R}2} \} \quad \text{[kn}^{-1}] \\ & \text{where} \\ & \text{C}_{\text{s}}(\nu, \text{T}) = 1.77 \times 10^{-29} \exp(-3.32 \times 10^{-3} \nu) \exp(1234(1/\text{T} - 1/\text{T}_{\text{0}})) \\ & + 3.91 \times 10^{-29} \exp(3.46 \times 10^{-3} \nu) \exp(2626(1/\text{T} - 1/\text{T}_{\text{0}})) \\ & \text{and} \\ & \text{C}_{\text{k}}(\nu, \text{T}) = (296/\text{T})^{3} \{ 7.16 \times 10^{-19} \exp(-6.45 \times 10^{-3} \nu) \} \\ & + 2.73 \times 10^{-39} \exp(6.45 \times 10^{-3} \nu) \}. \end{split}$$

Again, long-path field measurements by Devir et al. $^{(38)}$ are in good agreement with Butch and Alt $^{(27)}$ in this window region concerning the water vapor continuum. The results of Devir et al. $^{(36)}$ also point out the importance of the water vapor continuum between 4.5 and 5.0 μ m. In this region, local line contributions can be significant as well, thus masking to some extent water vapor continuum absorption. CO laser transmission measurements as a function of water vapor partial pressure show an increase in the dimensionless self-broadening coefficient, 8, over the near line center value $^{(39)}$. As observed in the previous window regions, this observation is indicative of continuum absorption.

Field measurements between 4.1 and 3.8 μm reveal that other continuum sources exist. The far blue wing beyond the band head of the fundamental ν_3 band of ${\rm CO}_2^{(41)}$ and the contistential expectation band of nitrogen⁽³⁵⁾ also contribute to continuum-type absorption in this window region and will be discussed later.

The 2.0- to 2.5-µm window

This window region has not received the same attention as the longer-wavelength windows; as a result, no experimental continuum absorption has been previously remotted. Recent measurements (*18), however, indirectly suggest that continuum absorption does exist. Transmission measurements on hot (T=685 K) high-pressure (up to 4.8 HPa) water vapor show the continuum absorption in the 2.1- and 4-µm regions (Fig. 10). Absorption levels at 4 µm are consistent with the extrapolated values from the curves in Fig. 9. The point to be made is that a similar continuum absorption process occurs in the 2.1-µm region, as shown in Fig. 10. If we assume that an extrapolation to lower temperature follows the same trend as at 4 µm, then a continuum exists in the 2.0- to 2.5-µm window that is very similar to the 3- to 5-µm window under normal atmospheric conditions.

1.7 to 1.5 µm window and beyond

Figure 10 shows the beginning of the continuum centered at 1.6 μ m. Again, this suggests a water vapor continuum in this window region at a weaker level than at 4 and 2 μ m. Based on this observation, it is expected that every window in the infrared has a water vapor continuum at some absorption level. This level should become weaker as the frequency increases.

13

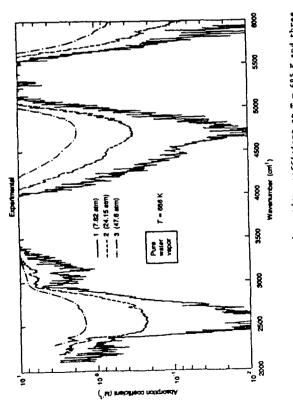


Figure 10. Pure water wapor absorption coefficient at T=685 K and three different pressures.

The 1 μ m window water vapor continuum has been measured by a novel interfarometric calorimeter technique^(1)b). A pulsed Nd-glass laser is used to hast a nitrogan buffared water vapor sample placed in the arm of He-Ne Machause measurable fringe shifts proportional to the absorption due to the heating cause measurable fringe shifts proportional to the absorption coefficient. The resulting continuum absorption coefficient measured at 9466 cm⁻¹ is 6×10^{-1} cm⁻¹ for water vapor partial pressure of 16.5 Torr buffered by nitrogen to a total pressure of 1 atmosphere at 30°C. Thus, the water vapor continuum is roughly two orders of magnitude weaker near 1 μ m than at 4 or 2 μ m. Further measurements to determine the water vapor partial pressure dependence and temperature dependence are needed.

The tragedy of experimental water vapor continuum characterization is that unlike $\mathrm{CO}_2^{(41)}$ and nitrogen⁽⁴²⁻⁴⁶⁾ continuum experiments, it presently cannot be done at high pressure. High-pressure water vapor measurements also require high-temperature and thus a theoretical understanding of the continuum absorption temperature dependence to extrapolate back to atmospheric temperatures.

Concepts and models

No universal interpretation of continuum absorption by water vapor presently exists. Clearly, far wings must play a role in continuum absorption because of the observed frequency dependence observed in every window and this belief has lead to various semi-empirical attempts(4),40,30-35). Work is continuing to tind a line-shape theory valid in the far wing(4)-300). The major shortcoming

of past line-shape theories is in their failure to predict the observed strong negative temperature dependence characteristic of all the window regions, except for the recent line shape model of Ma and Tipping at the millimeter wave window(199). But this weakness is the very strength of an alternative hypothesis window(199). But this weakness is the very strength of an alternative hypothesis to explain the water vapor continuum: the water dimer. The formation of water the temperature dependence of the continuum absorption in the 10-µm region(19,11). However, this near match does not occur in the microwave window this approach also requires dimer absorption bands to continuum. However, the hypothesis would require a dimer absorption band in continuum. However, the hypothesis would require a dimer absorption band in continuum. However, the hypothesis would require a dimer absorption band in continuum the water vapor window, a condition that has not been experimentally found or theoretically shown(16,32). Furthermore, measurements on supersaturated water vapor indicate that dimer absorption is an order of magnitude too small to shortcomings, the dimer hypothesis demonstrates the importance of understanding water-vapor water-vapor interaction to explain the continuum absorption temperature dependence⁽¹⁹⁾.

A semi-empirical line shape model developed by Birnbaum⁽⁴⁷⁾ with validity from line center to the far wing (when line mixing can be ignored) predicts an exponential wing as observed experimentally and can be properly normalized. This model has been successfully applied to the CO₂ blue wing of the 4.3 µm band⁽⁴³⁾. Application of this line shape to line-by-line calculations indicate that this model is not complete enough to represent the water vapor continuum in near band regions (probably because it lacks line mixing effects). However, the simple models given in the text for the water vapor continuum broadened by nitrogen are based on this formalism.

The continuum models for the popular Air Force Geophysics Laboratory codes FASCODE and LOWTRAN are based on the efforts of Clough et al. (*9), who used far-wing concepts to represent the water vapor continuum throughout the entire infrared region. The experimental data previously described are reasonably represented by these codes. The strength of this approach is accounting for spontaneous emission and the fluctuation dissapation theorem in enforcing detailed balance across the entire line shape. This results in a physically meaningful far wing and a more versatile line shape overall.

Although no definitive interpretation of the water vapor continuum exists, the experimental and theoretical evidence indicates that far-wing absorption contributions by the bordering strong water vapor bands play a dominant role. The evidence is based largely on the frequency dependence of the continuum in the first four spectral windows reviewed (i.e., the shape of the continuum in the function of frequency and growth of the dimensionless broadening coefficient, B, away from a band as a function of frequency). The shortcoming of the far-wing approach is predicting the temperature dependence, but the character of a far wing must be driven by close binary interactions much like the creation of a dimer, which does exhibit the observed temperature dependence in the $10-\mu m$ window region. This point has been verified by the recent work of Ma and Ilpping⁽¹⁹¹⁾.

REFERENCES

J. B. Shaw, Quig J., Stl., 53, 258 (1953).
 H. B. Benedict and R. F. Caifee, Line Parameters for the 1.9 and 8.3 Hicrom Mater Vapor Banda, 7858.
 Professional Paper 2, U.S. Government Printing Office, Washington, D.C. (Jun 1997).

- H. Gates, R. P. Calfes, D. M. Memam, and M. S. Benedict, "Line Parameters and Computed Spacing for ter Topics Endie at 1.7 pm." Estimate between of Standards Humsgraph 71, U.S. Government Printing Tites, Machington, D.C. (1981). Comp.Payrot and J. M. Flond, "Line positions and intensities in the band of EDG," Spi. DEGS, 23, 323
- - R. K. Long and E. K. Damma. "An Atlan of Para Water Paper Species from 500 to 2000 cm⁻¹ Vol. I and III," Chie East Shiver-II J. F. Long and E. K. Damma. "An Atlan Species of East Shiver-II J. P. Collisty, B. L. Faming, D. B. Longlin and L. S. London, "Trivined Water Vegor Line Parameters in the 1.0 to 1.1 and stronder Radies, "Properties Third in a Satisty, Species in the 1.0 to 1.1 and stronder Radies," Properties Third in a Satisty Species, Species in the 1.0 to 1.1 and stronder Radies, "Properties Third in a Satisty Species, Species

- 23. (as (1821). O. J. B. Hetchick, Sci. 88, 380 (1970).

 10. F. Careford, W. M. Malba, and J. L. Ledes, "Infrared absorption of erygen and mitrogen induced by the seminal context forces," Bry Rey. 3, 1607 (1840).

 2. Shankind and J. E. Searl, "Atmosphorite absorption near 2400 cml." J. Chunt. Specifics. Eddied. International of the 381 (1877).

 3. Historian, H. W. Sigiria, and P. E. Leadman, "Last photocontext specimens, of underrupor continuous and line-absorption in the 4th and atmospheric window," Inflanting, H. Y. Sigiria, and P. E. Leadman, "Last photocontext specimens, of underrupor continuous and line-absorption in the 4th atmospheric window," Inflanting Professional Continuous and Line-absorption in the 4th atmospheric window, "Inflanting Professional Continuous and Line-absorption in the 4th atmospheric window," Inflanting Professional Continuous and Line-absorption in the 4th atmospheric window, Inflanting Region, W. L. Berington, M. C. Reiffenstein III, Particommental Research and Technical Report, No. 13, Latington,
- Feat. (1971).

 G. E. Becker and S. Matlat, "Nater vapor absorption of electromagnetic radiation in the continuence overlampia range." [ED. Matlat, "Nat. 200 (1944).

 L. Frankel and D. Hoods, "The microwere absorption by EDO vapor and its attatase with other general networks to mad 300 ches, "The microwere absorption by EDO vapor and its attatase atta other (1900 p. 111. Absorption by EDO between 0.3 and 30 cm., "1204-2 cm.)." 2. [Ogt. Bot. 30, 30, 303 (1946).

 B. J. Liche, "A contribution to madeling stamphorie millimeter-wave properties," [EEGORGE 41, 31 **n** n
- 1875. Liche and P. B. Leyton, "Experiental and unsigital aspects of aimospheric EMF refrestivity," 18 Erst. 1883 Commission 2 1882 Errorium, Lovers, Baigism (Jem 1983). 18. E. Tommas, "Aimospheric cheespiton model from 0.01 to 10 wave numbers," <u>EEE Progressings</u>, 1312, 2 2 2
- Out I. Lieselly. Jones, 'Inducatory measurements of absorption by enter vepour in the frequency range 100 to 1006 CER, in ALMORPHINIS WINEY 1950. A. Despai, T. D. Hilterson, and L. E. Enhabe, Eds., Academic Press, Few York, pp. 225 (1981). March 1950. A. Despai, T. D. Hilterson, and L. E. Rahabe, Eds., E. J. Liebe, "As explained model for millimater wave propagation is moist air," <u>Englo St.,</u> 29, 1069

2 2

- D. E. Burch and R. L. Alt, Continues Absorption by E20 is the 700-1200 cm⁻¹ and 2400-2800 cm⁻¹ Windows, APG-TER+-0128, Ford Astropace and Communications Corporation, Astronactoric Division (May
-
- Just).

 Justing M. Thomas, H. J. Bordstrow, E. E. Damen, and E. E. Long, "Mater vapor militogen absorption at GGD Lasset frequencies," 4602-1054, 130 (1789).

 G. Lupser, H. A. O'shill, and J. A. Calbarcha, "Mater vapor continue GGD Lasse absorption spectra between 17 cf. 411, °C. and 18cf. 411, °C
- H. 7. Grant, A Critical Series of Newstreemics of Mater Vapor Absorption in the 848 to 1130 cm⁻¹ Special Registral Registral Co. 77, Publication 87-34, 46 Trepsisted Laboratory (Dec 1887).
 2. Recidence, H. E. Therman, J. G. Peterson, E. E. Domos, and R. E. Long, "Effects of crypes addition as pressure breadment water vapor checopies in the 10-ms region," ADDL, Opp. 17, 2724 (1878). 2 2 2

2

- 10. Deptit, A. Ben-Malen, E. Striberniky, E. Res, H. Dagel, S. G. Lipens, and U. P. Oppstadel.

 "Experimental validation of stronghorist transmittence cades." DES. EXT. EXEC. Stilled. Integrational validation of stronghorist transmittence cades." DES. EXPERIM. 2016.

 10. United Structured and Structured Education Col. N. Philos and R. P. Expelta. Education and Structured Structured Structured Structures and Structured Col. Structured Structured Structured Structured Col. Structured Structur
- - : # # # #
- į **4**2.
 - Ž,
 - - * * * * * *

- S.
 - Š
- 22
- Amorphies (1981).

 1. Though and C. T. Davis, "Collision induced infrared absorption of the binary absorption of confined and the binary absorption of summitted distorts and all the profession of the binary and the confined and the profess and the confined and the confined and the profess and the confined and the confined and the profess and the confined and the confined and the confined and the confined and the profess and the confined and the confined and the profess and the confined and the profess and the confined and the profess and the confined and the confined and the profess and the confined and the confirmant and the confined and the confirmation at the fined and the confirmation at the fined and the confirmation z z
 - H. E. Thomas and R. J. Bordatrom, "Lime shape undel for describing infrared abserption by woter vaper," Appl. Opt. 2, 3:26 (1003). ž.
- Annual Review Conference on Atmospheric Transmission Wodels Prepared for:
 - Geophysics Directorate, Phillips Laboratory Topical Session on Spectral Line Shapes Hanscom Air Force Base June 12, 1991

16



WATER VAPOR CONTINUUM ABSORPTION MEASUREMENTS WITH LINE SHAPE INTERPRETATIONS

M. E. Thomas and C. T. Delaye Applied Physics Laboratory The Johns Hopkins University Laurel, Maryland 20723

BIRNBAUM'S LINE SHAPE

IGNORING LINE MIXING, THE ABSORPTION COEFFICIENT IS:

$$\beta(\nu) - \sum_{j} S_{j} \frac{\nu}{\nu_{j}} \frac{\tanh \frac{hc\nu}{2k_{B}T}}{\tanh \frac{hc\nu_{j}}{2k_{B}T}} j(\nu,\nu_{j})$$

WHERE $S_{\mathbf{j}}$ is the line strength of the \mathbf{j}^{TH} line,

. IS THE FREQUENCY IN WAVE NUMBERS.

 $J(\nu, \nu_j)$ is the Fourier transform of the Dependent autocorrelation function $C(\tau)$:

$$j(\nu,\nu_{j}) = \frac{1}{N} \cdot \frac{1}{\pi} \int_{0}^{\pi} d\tau \, \cos 2\pi c \nu \tau \, \left(e^{j2\pi c \nu_{j} \tau} \, C(\tau) + e^{-j2\pi c \nu_{j} \tau} \, C^{*}(\tau) \right)$$

N is the normalization factor of the line profile. At infrared frequencies N ≈ 1 .

BIRNBAUM USES THE FOLLOWING SEMI-EMPIRICAL EXPRESSION FOR C(7):

$$C_{a}(\tau) = \exp[\tau_{a2} - (\tau_{a2}^2 + \tau^2 - 2i\tau_0\tau)^{1/2}]/\tau_{a1}$$

and
$$C(r) = C_a(r) \cdot C_b(r) \dots C_a(r)$$

WHERE THE SUBSCRIPTS DESIGNATE THE DIFFERENT MOLECULES IN THE SYSTEM.

TAL AND TAL REPRESENT THE LONG TIME AND SHORT TIME BEHAVIOR OF THE AUTOCORRELATION FUNCTION RESPECTIVELY.

TO IS A THERMAL TIME DEFINED BY:

$$r_o = \frac{h}{4\pi k_B T}$$

In the case of pure gases, $J(u,u_3)$ is written (with $u=2\pi c_r$):

$$\begin{split} j(\omega,\omega_{j}) &= \frac{1}{N} \frac{r_{1}}{\pi} e^{r_{2}/r_{1}} \left\{ e^{(\omega-\omega p r_{0})} \cdot \frac{Z_{-}K_{1}(Z_{-})}{1 + ((\omega-\omega_{j}) r_{1})^{2}} \right. \\ &+ e^{(\omega-\omega p r_{0})} \cdot \frac{Z_{-}K_{1}(Z_{+})}{1 + ((\omega+\omega_{j}) r_{1})^{2}} \right\} \end{split}$$

WHERE
$$Z_{\pm} = (\tau_1^2 + \omega_{\pm}^2)^{\frac{1}{4}} (\tau_2^2 + \tau_0^2)^{\frac{1}{4}}$$
 AND $\omega_{\pm} = \omega_{\pm} \omega_{J}$

 $K_1\left(Z\right)$ is the modified Bessel function of the second kind. τ_1 is written as

$$r_1 = \frac{1}{2\pi c \gamma_1}$$

WHERE τ_1 IS THE SELF BROADENED COEFFICIENT FOR EACH ABSORBER MOLECULE I. WE ASSUME THAT τ_2 IS CONSTANT FOR EACH MOLECULE AND FOR EACH STUDIED FREQUENCY RANGE.

Far Wing line shape.

$$\epsilon_{N}(*;*_{j}) = \frac{1}{*_{j}} \frac{\tanh(\hbar c_{v}/2k_{\parallel}T)}{\tanh(\hbar c_{v}j/2k_{\parallel}T)} j_{N}(*)$$

--4

$$j_{H}(v) = (\frac{\tau_{12}}{2\pi})^{1/2} \frac{1}{\tau_{11}\sqrt{2\pi c}} \frac{\exp(-2\pi c | v - v_{1}| | \tau_{12})}{\tau_{11}\sqrt{2\pi c}} \exp(2\pi c (v - v_{1}) | \tau_{0})$$

The exponential wing is consistent with experimental observation [13,18]. The general farwing result for a binary mixture can be obtained by solving a convolution integral of the individual line shape functions $(j_i \text{ and } j_i)$ in the far wing limit. Thus, given

$$j_{\lambda}(v) = \frac{1}{2\pi} \int_{-\pi}^{\pi} d\tau e^{-i2tc_{\nu}} G_{\lambda}(\tau),$$

$$j_b(v) = \frac{1}{2\pi} \int_{-a}^a d\tau \ e^{-i2\pi\epsilon_b} \ C_b(\tau),$$

#nd

$$j(x) = \int_{-1}^{1} j_{2}(x) j_{3}(x - y_{3} - x) dx$$

then using contour integration and in the far wing limit

$$j_{H}(v) = (\frac{\tau_{12}}{2\pi})^{1/2} \frac{1}{\tau_{11}} \frac{\exp(-2\pi c |v-v_{j}|\tau_{12})}{\sqrt{2ed} |v-v_{j}|^{1.5}} \exp(2\pi c (v-v_{j})\tau_{0})$$

$$+ \left(\frac{\tau_{bl}}{2\pi}\right)^{1/2} \frac{1}{\tau_{bl}} \frac{\exp\left(-2\pi c \left[v - v_{j}\right] \tau_{bl}\right)}{\sqrt{2\pi c} \left[v - v_{j}\right]^{1.5}} \exp\left(2\pi c \left(v - v_{j}\right) \tau_{o}\right).$$

Note:

A general empirical form for the continuum absorption coefficient used to represent the data (5) is

$$\beta_{cont}(v,T,P_{li}\dots P_{li},P_a) = \frac{P_a}{RT} \sum_i \left[C_{fi}(v,T) P_{li} \cdot C_s(v,T) P_a \right]$$

where C_i , is the self-broadening coefficient of the absorbing gas, C_{ii}) is the foreign broadening coefficient due to the i^{th} type foreign gas, and R is the ideal-gas constant. The equation can be conveniently rewritten for i=2 to obtain

$$\beta_{cost}(\mathbf{v},\mathbf{T}) = \frac{C_{fl}(\mathbf{v},\mathbf{T})}{RT}P_{g}[P_{fl}+F(\mathbf{v},\mathbf{T})P_{fl}+B(\mathbf{v},\mathbf{T})P_{g}]$$

where $F = C_{II}/C_{II}$ and $B = C_{I}/C_{II}$ are the dimensionless broadening coefficients. Near line center, B has the value of 5 for water vapor relative to nitrogen. In the real atmosphere, the effects of oxygen broadening must also be included. The dimensionless broadening coefficient P accounts for oxygen. However, many laboratory experiments ignore the effects of oxygen and use only nitrogen as the broadening gas along with the absorbing gas.

EXPERIMENTAL WATER VAPOR CONTINUUM DATA

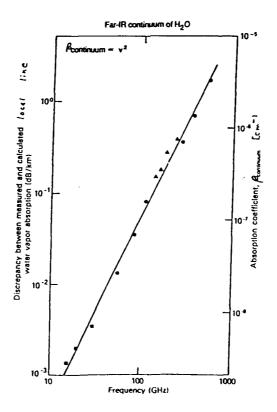


Figure 1.3.10. Water vapor continuum absorption coefficient as a function of frequency. The solid line is an empirical fit to the experimental data points as given by Eq. 1.3.92. The plotted points are (a) [20], (*) [21], and (m) [22] for T = 300 K, P_T = 101 kPa and ρ_0 = 10⁻⁹ kg/m³.

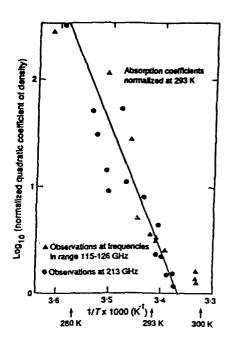


Figure 1.3.11 Temperature dependence of millimeter wave water vapor continuum. Solid curve represents empirical fit to data as given by Eq.

Table 1 Experimental frequency dependence of B (ν , 300)

f (GHz)	ν (cm ⁻¹)	Β (ν, 300)
110	3.7	32
138	4.6	31.6
213	7.1	20
833	27.8	7.4

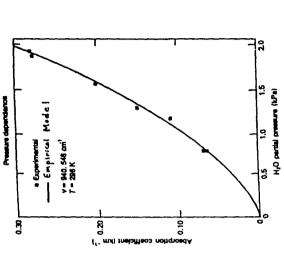


Figure 1.3.14 Water vapor partial pressure dependence in the 10 µm region.

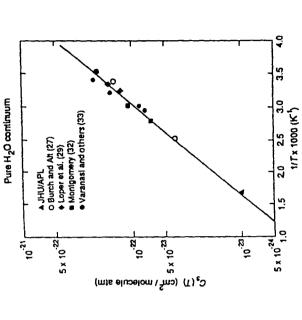
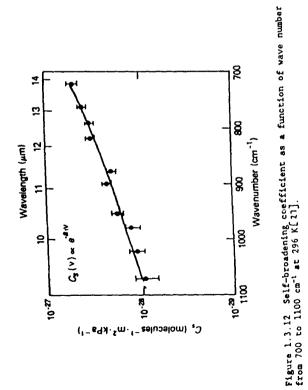


Figure 1.3.15 Temperature dependence of self-broadening coefficient in the 10 μm region.



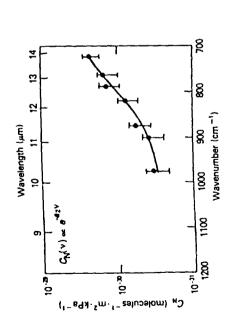


Figure 1.3.13 Nitrogen broadening coefficient as a function of wavenumber from 700 to 1000 cm $^{-1}$ at 296 KL21],

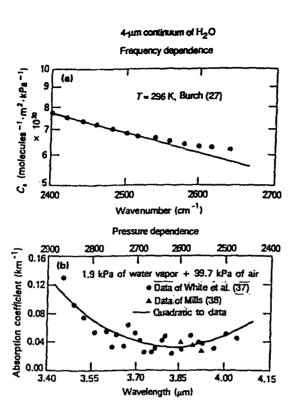


Figure 1.3.16 4 µm water vapor continuum region at T- 296K. (a) C_s vs wave number [27] and (b) absorption coefficient vs wavelength [37,38].

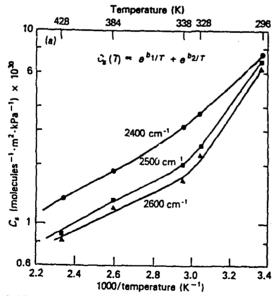
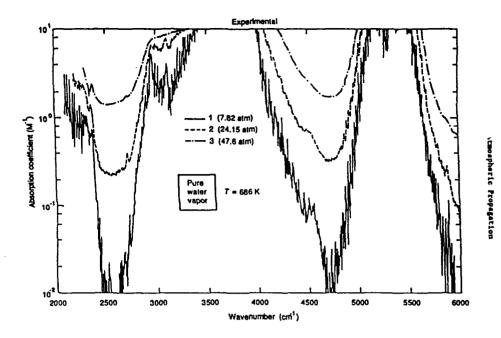


Figure 1.3.17 Plots of the water vapor self-broadening coefficients at 2400, 2500 and 2600 $\rm cm^{-1}$ vs reciprocal temperature [27], the symbols and a represent the experimental data points.



Pure water vapor absorption coefficient at T=685K and three different pressures.

* The 1 µm window water vapor continuum has been measured by a novel interferometric calorimeter technique.

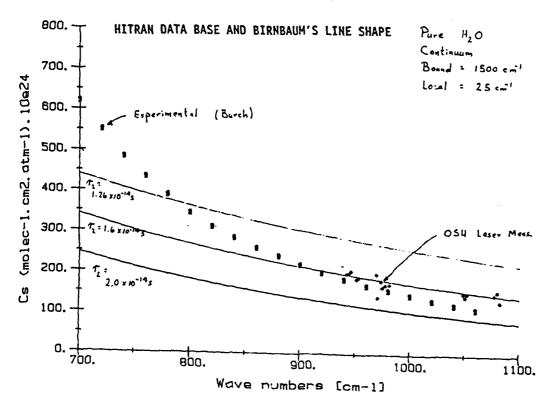
A pulsed Nd-glass laser is used to heat a nitrogen buffered water vapor sample placed in the arm of He-Ne Mach-Zehnder interferometer. Variations in the index of refraction due to the heating cause measurable fringe shifts proportional to the absorption coefficient.

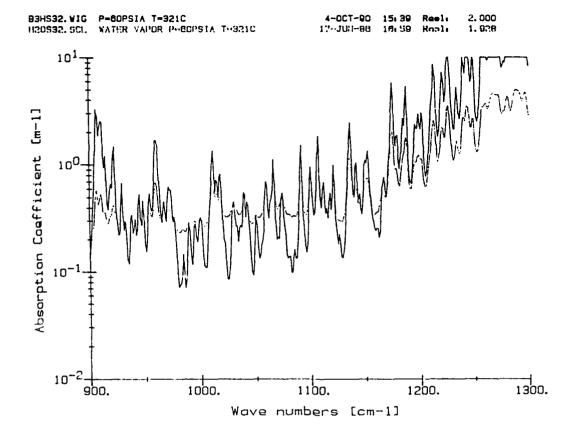
The resulting continuum absorption coefficient measured at 9466 cm⁻¹ is 6x10 ¹⁰ cm⁻¹ for a water vapor partial pressure of 16.5 Torr buffered by nitrogen to a total pressure of 1 atmosphere at 30°C.

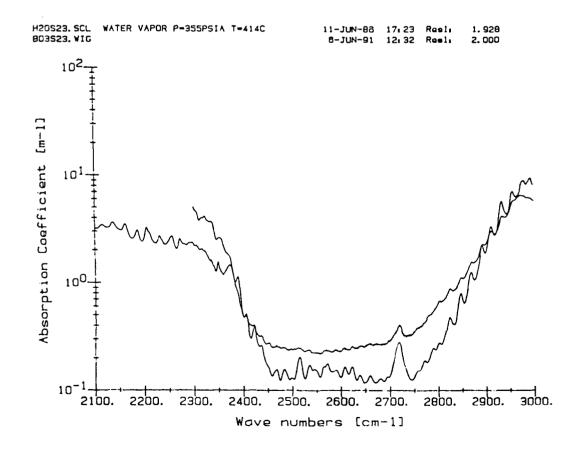
Thus, the water vapor continuum is roughly two orders of magnitude weaker near 1 µm than at 4 or 2 µm.

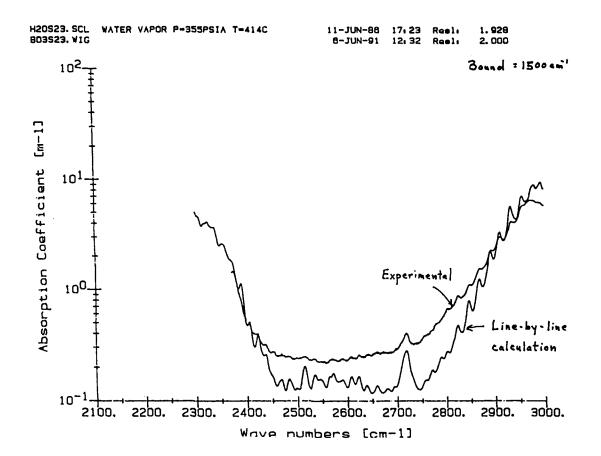
 Purther measurements to determine the water apor partial pressure dependence and temperature dependence are needed. The tragedy of experimental water vapor continuum characterization is that unlike nitrogen and CO₂ experiments, it presently cannot be done at high pressure. High-pressure water vapor measurements also require high-temperature and thus a theoretical understanding of the continuum absorption temperature dependence to extrapolate back to atmospheric temperatures.

LINE-BY-LINE CALCULATIONS









OVERVIEW OF LINE COUPLING IN THE 5 mm BAND OF OXYGEN

P.W. Rosenkranz Massachusetts Institute of Technology, 77 Massachusetts Avenue, Cambridge, MA 02139

Nearly forty years ago, measurements of microwave absorption in oxygen indicated that pressure broadening became less effective, by approximately a factor of two, at pressures approaching one atmosphere than at lower pressures where the individual lines in the band were resolved. The explanation of this behavior of oxygen by means of overlapping line theory eventually led to methods of calculating absorption by oxygen that could be based on parameters determinable from careful laboratory measurements. Only recently, however, have such measurements explored an extensive range of frequency, pressure and temperature. These measurements (made by H.J. Liebe) are interpreted to determine the variation with temperature of the parameters that characterize line coupling. Possible revisions in transmittances for weather satellite frequencies are discussed.

Overview of Line Coupling in the 5 mm Band of Oxygen

P. W. Rosenkranz Massachuseus Institute of Technology Cambridge, MA 02139

Abstract-Nearly forty years ago, measurements of microwave absorption in oxygen indicated that pressure broadening became less effective, by approximately a factor of two, at pressures approaching one atmosphere than at lower pressures where the individual lines in the band were resolved. The explanation of this behavior of oxygen by means of overlapping line theory eventually led to methods of calculating absorption by oxygen that could be based on parameters determinable from careful laboratory measurements. Only pressure and temperature. These measurements (made by H. J. Liebe) are interpreted to determine the variation with temperature of the parameters that characterize line coupling. Possible revisions in transmittances for weather satellite frequencies are discussed.

When microwave absorption in oxygen began to be measured, it was recognized very early (e.g. Crawford and Hogg., 1956 - Fig. 1) that at pressures near 1 atmosphere where the lines overlapped into a band, pressure broadening seemed to be less effective, by approximately a factor of two, than at much lower pressures where the individual lines were resolved. Meeks and Lilley (1963) proposed the use of the oxygen band for remote measurement of atmospheric temperature from satellites. They also devised a scheme for calculating absorption by assuming that the ratio of linewidth to pressure varied with altitude (Fig. 2). Similar absorption models were devised by Carter, Mitchell and Reber (1968) and Reber (1972). By and large, these models represented atmospheric opacity on the far wings of the original reasonably well. However, when the Nimbus 5 Microwave Spectromer is launched into space in 1972, some systematic discrepancies from calculated brightness temperatures were observed, in particular near 58.8 GHz (Waters et al., 1975 - Fig. 3).

Gordon (1967) had already explained the relative narrowness of the oxygen band at high pressures by means of the theory of overlapping lines. This theoretical framework had been originated by Baranger (1958) and Kolb and Griem (1958) and had been further developed by Fano (1963) and Ben-Reuven (1966). In the impact approximation, the pressure-proportional width parameter that applies to an isolated line is replaced, for a band of lines. by a pressure-proportional matrix w whose diagonal elements are width parameters for each line, and whose off-diagonal elements represent the coupling of each pair of lines by collisions. Calculation of the band shape involved the inversion of a

complex matrix (Fig. 4); however, a first-order perturbation expansion (Rosenkranz, 1975 - Fig. 5) made it feasible to use the theory for atmospheric radiative-transfer calculations. In the first-order approximation, the influence of the off-diagonal matrix elements occurs through the addition of dispersion-shaped functions to the usual resonant line shapes that describe isolated lines. Because of the way in which the signs of the coefficients associated with the former terms depend on rotational quantum number, the effect is an increase in absorption near the band center, and a decrease on the wings (Fig.6).

Initially these coefficients (of the dispersion-shaped terms) were obtained from a method that estimated the largest of the off-diagonal elements of w. A later refinement (Rosenkranz, 1988) allowed their determination directly from laboratory measurements. Direct calculation of the w matrix has been carried out by Lam (1977) (whose results were revised by Smith, 1981 - Fig. 7), and by Mingelgrin et al. (1972, 1979 - Fig. 8). These calculations obtained agreement with measurements at normal laboratory temperature and at pressures up to at least seven atmospheres (although the exact matrix inversion is required above one atmosphere).

Despite the success of overlapping-line theory in accounting for laboratory measurements of absorption and dispersion as well as atmospheric opacity on the far wings of the band, it has not eliminated all discrepancies between calculations and measurements for satellite-based radiometers. Grody (1983) discusses some of these systematic offsets in data from the Microwave Sounding Unit on NOAA satellites (Fig.9). They reach I to 2 K in the channels at 55 and 58 GHz, which measure thermal emission from the upper troposphere and lower stratosphere. These brightness temperature differences could be explained by an increase in absorption of approximately 10%.

The association of these offsets with the colder parts of the atmosphere suggested that the temperature dependence of the line coupling might be different from that which had been assumed. A recently completed series of measurements by Liebe et al. (1991) on dry air at 279, 303 and 327 K provide the opportunity to test this hypothesis (Fig. 10). Coefficients for the line interference effect have been extracted from these measurements by the method described by Rosenkranz (1988). For the lower rotational quantum levels (1, 3, 5, 7) their temperature dependence is T^{-0.8} (Fig. 11), similar to the line widths. The higher levels have some further variation with temperature, to which a linear function of the reciprocal temperature variable θ = 300/T was fitted.

Atmospheric absorption can be calculated by extrapolating this fitted temperature dependence, and the new coefficients produce slightly less absorption than previously calculated at 53.7 and 55 GHz. The calculated brightness temperatures at these frequencies

have changed by less than 0.4 K. At 58 GHz there is essentially no change from the older calculation. Possibly, one could choose different functions to represent the variation with temperature that might fit the data equally well over the measured temperature range, yet estrapolate differently to colder temperatures. On the basis of the present laboratory measurements, however, the discrepancies observed by the MSU do not find an explanation.

An aircraft-based radiometer experiment is planned for the summer of 1991. It is hoped that these measurements, in the zenith-observing mode, will provide the lower-temperature test points that could validate (or not validate) the new oxygen-band line parameters.

References

Baranger, M., Phys. Rev. 111, 494-504 (1958).

Ben-Reuven, A., Phys. Rev. 145, 7-22 (1966).

Carter, C. J., R. L. Mitchell, and E. E. Reber, J. Geophys. Res. 73, 3113-3120 (1968).

(.rawford, A. B., and D. C. Hogg, Bell System Tech. J. 35, 907-916 (1956).

Fano, U., Phys. Rev. 131, 259-268 (1963).

Gordon, R. G., J. Chem. Phys. 46, 448-455 (1967).

Grody, N. C., J. Climate and Appl. Meteor. 22, 609-625 (1983).

Kolb, A. C., and H. Griem, Phys. Rev. 111, 514-521 (1958).

Lam, K. S., J. Quant. Spectros. Radiat. Trransfer 17, 351-383 (1977). Liebe, H. J., G. A. Hufford, and R. O. DeBolt, "The Atmospheric 60-GHz Oxygen

Spectrum: Modeling and Laboratory Measurements," NTIA Report 91-272, U. S. Dept. of Commerce (1991).

Meeks, M. L., and A. E. Lilley, J. Geophys. Res. 68, 1683-1703 (1963).

Mingelgrin, U., R. G. Gordon, L. Frenkel, and T. E. Sullivan, J. Chem. Phys. 57, 2923-2931 (1972).

Mingelgrin U., and R. G. Gordon, J. Chem. Phys. 70, 3828-3839 (1979).

Reber, E. E., J. Geophys. Res. 77, 3831-3845 (1972).

Rosenkranz, P. W., IEEE Trans. Antennas Propagat. AP-23, 498-506 (1975).

Rosenkranz, P. W., J. Quant. Spectros. Radiat. Transfer 39, 287-297 (1988).

Smith, E. W., J. Chem. Phys. 74, 6658-6673 (1981).

Waters, J. W., K. F. Kunzi, R. L. Pettyjohn, R. K. L. Poon, and D. H. Staelin, J.

Amos. Sci. 32, 1953-1969 (1975).

Viewgraphs:

- 1. Absorption in air at sea level, from Crawford and Hogg (1956).
- Oxygen line-width parameter, from Meeks and Lilley (1963).
- 3. Calculated minus measured NEMS brightness temperatures at 58.8 GHz, from Waters et al. (1975).
- 4. Complex index of refraction.
- 5. Absorption at 58.8 GHz, from Rosenkranz (1975).
- 6. The effect of off-diagonal elements of w.
- 7. Dispersion at 59.59 GHz, from Smith (1981).
- 8. O2 spectrum, from Mingelgrin et al. (1972).
- 9. Measured versus computed MSU brightness temperatures, from Grody (1983).
- 10. New laboratory measurements on dry air by Liebe et al. (1991). Interference coefficients were fitted to the 101 kPa data.
- 11. Derived interference coefficients at three temperatures. The plotted coefficients are adjusted to 100 kPa pressure and normalized by the factor $\,\theta^{0.8}$.

Note: Figs. 10 and 11 were revised after the conference.

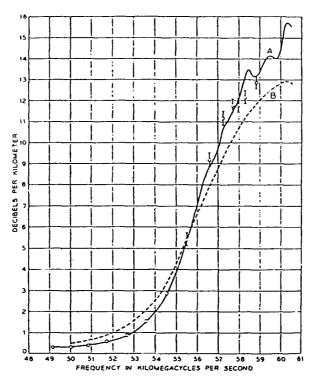
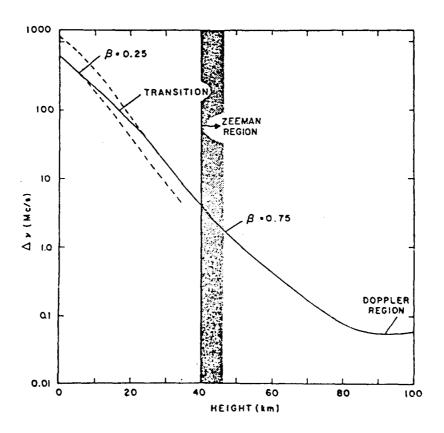
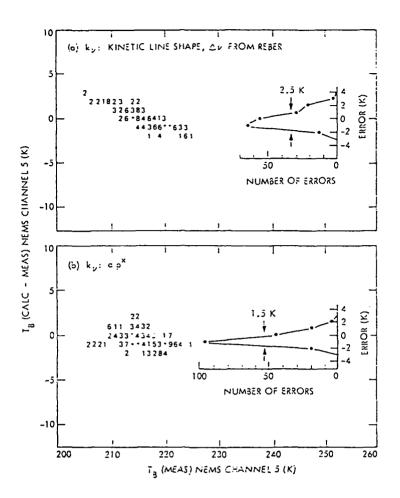
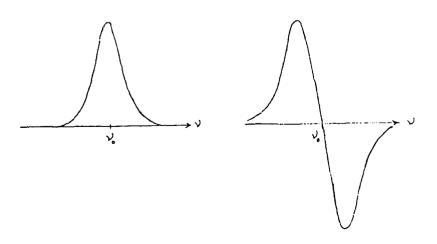


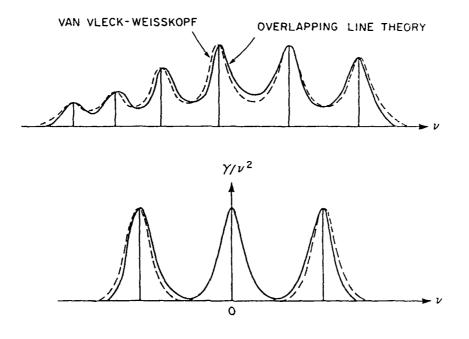
Fig. 8 — Calculated and measured absorption by air at sea level. The dots represent the experimental data; the vertical lines indicate the spread in the measured values. Curves A and B are calculated curves of oxygen absorption using line-breadth constants of 600 and 1200 mc, respectively, and a temperature of 293° K. (Courtesy of T. F. Rogers, Air Force Cambridge Research Center.)





Complex index of refraction:





IEEE TRANSACTIONS ON ANTENNAS AND PROPAGATION, JULY 1975

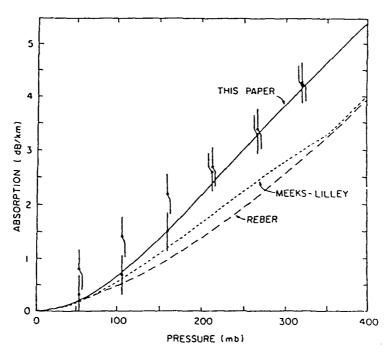


Fig. 3. Absorption in dry air at 58.82 GHz and 295 K, computed for three models. Measurements are by Poon [30].

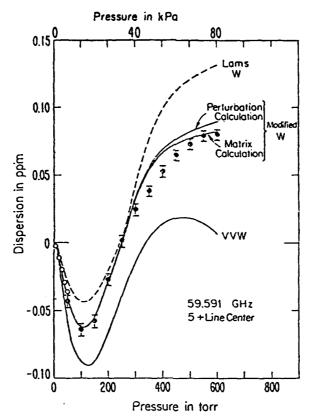


FIG. 8. Dispersion²¹ at 59.591 GHz as a function of pressure at a temperature of 300 K. Experimental points, solid and open circles, obtained from two independent unpublished measurements.⁶

MINGELGRIN, GORDON, FRENKEL, AND SULLIVAN

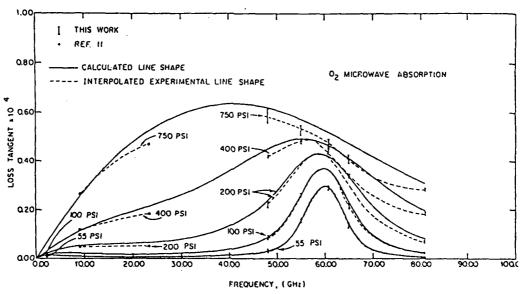
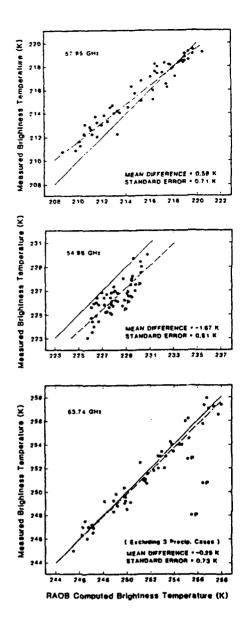
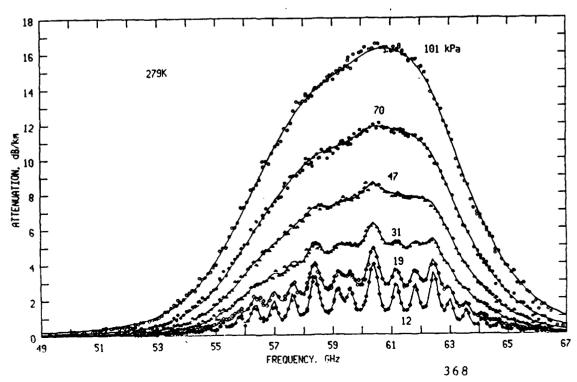
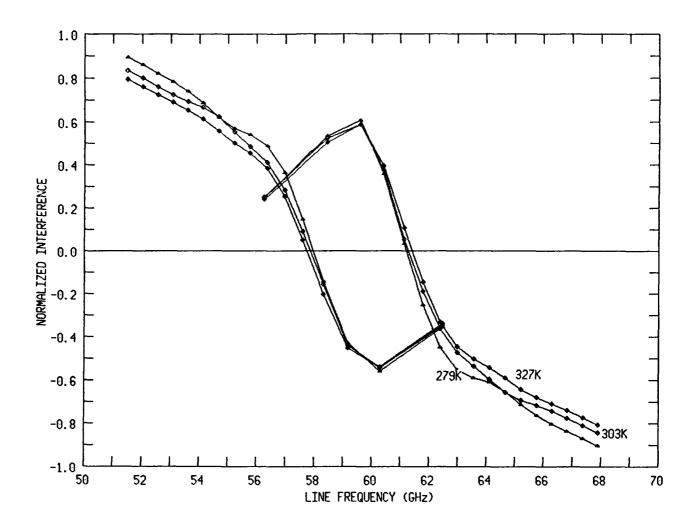


Fig. 7. Calculated vs experimental line shape of pure Oi.







LABORATORY MEASUREMENTS OF LINE COUPLING IN CO₂ AND N₂O

L.L. Strow

Physics Department, University of Maryland Baltimore County, Baltimore, MD 21228

Laboratory studies of line coupling in a number of CO_2 and N_2O Q-branches will be presented. Coupling calculations based on very simple scaling laws for rotational relaxation give good agreement with observation for self-broadened spectra over a wide temperature range (200 to 350K). N_2 -broadened CO_2 Q-branches, however, exhibit more line coupling than calculated unless one forces the $f \rightarrow f$ collision rate in the Π state to be larger than the $f \rightarrow e$ collision rate. These two collision rates are approximately equal for self-broadened line coupling. Similar, but more extreme differences in these collision rates have been observed in CO_2 Q-branches broadened by He. Laboratory measurements of line coupling in the Q-branch at the $\Pi - \Delta$ band of CO_2 will also be presented. All previous measurements of Q-branch line coupling in CO_2 have involved $\Pi - \Sigma$ bands. Examples of line coupling in N_2O Q-branches will also be presented.

Laboratory Measurements of Line Coupling in CO2 and N2O

L. Strow University of Maryland Baltimore County

• Line Mixing - also known as

Line Coupling

Rotational Collisional Narrowing

Q-branch Collapse

• Previous Work

Raman - CO2, NO, N2, O2, CO

1932, 2070 cm⁻¹ CO₂ Q branches, self- and N₂-broadened; 597 cm⁻¹ Q -branches, N₂-broad.

720 cm⁻¹ CO₂ Q branch, self-broadened

 N_2O Q branches, self-broadened (1880, 2800 cm⁻¹), N_2 -broadened (2800 cm⁻¹)

C₂H₂, HCN, etc. Q branches, self-broadened

ν₃ R-branch bandhead of CO₂

Atmospheric Implications

Temperature Sounding: UARS (CLAES, ISAMS), EOS (AIRS, TES), ATMOS, HIS

Line Coupling Theory

- $\Pi \Sigma$ band, l=1 in Π state
- · Line mixing absorption coefficient given by

$$k(\nu) = \frac{N}{\pi} \text{IM} \left\{ \sum_{j,k} d_j \langle \langle j | [(\nu - \nu_o) - iPW]^{-1} | k \rangle \rangle d_k \rho_k \right\},$$

• Determine W matrix $(\Pi - \Sigma \text{ bands})$ from

$$W_{jj} = -\frac{1}{2} \left(\sum_{j' \neq j} K_{j'j}^{\Sigma(e \leftarrow e)} \right) - \frac{1}{2} \left(\sum_{j' \neq j}^{f \, levels} \beta K_{j'j}^{\Pi(f \leftarrow f)} + \sum_{j' \neq j}^{e \, levels} (1 - \beta) K_{j'j}^{\Pi(e \leftarrow f)} \right),$$

where W_{jj} is the linewidth, and $K_{j'j}$ is modeled with the hybrid power-exponential-gap (PEG)

$$K_{j'j} = a_1 (T_o/T)^{0.5} \left(\frac{|\Delta E_{j'j}|}{B_o} \right)^{-a_2} \exp\left(\frac{-a_3 |\Delta E_{j'j}|}{kT} \right),$$

for j' > j. Detailed balance gives $K_{j'j}$ for j' < j. $\Delta E_{j'j} = E_{j'} - E_j$ is the rotational energy gap. For CO₂-CO₂, N₂O-N₂O collisions $\beta \approx 0.50$. For CO₂-N₂ collision $\beta \approx 0.625$, for CO₂-He collisions $\beta \approx 0.75$. W is obtained by letting

$$W_{j'j} = -\beta K_{j'j}^{\Pi(f \leftarrow f)}.$$

• Only β must be determined from spectra exhibiting mixing

Calculational Details

$$k(\nu) = \frac{N}{\pi} \text{IM} \left\{ \sum_{j,k} d_j \langle \langle j | [(\nu - \nu_o) - iPW]^{-1} | k \rangle \rangle d_k \rho_k \right\},$$

can be rewritten as

$$k(\nu) = \frac{N}{\pi} \text{IM} \{ \mathbf{d} \cdot \mathbf{G}(\nu)^{-1} \cdot \rho \cdot \mathbf{d} \},$$

where

$$G = \nu - H$$
, $H = \nu_o + iPW$.

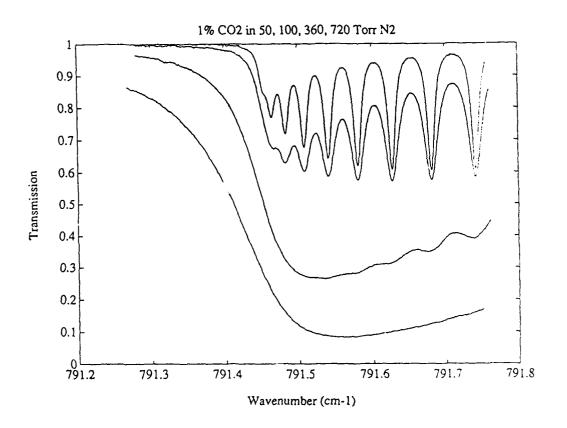
Diagonalizing H with L

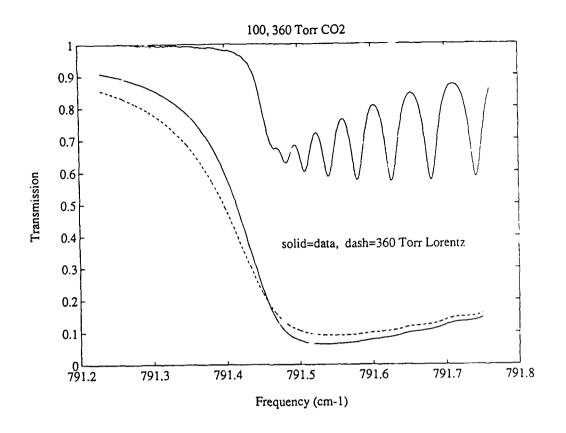
$$A^{-1} \cdot H \cdot A = L$$

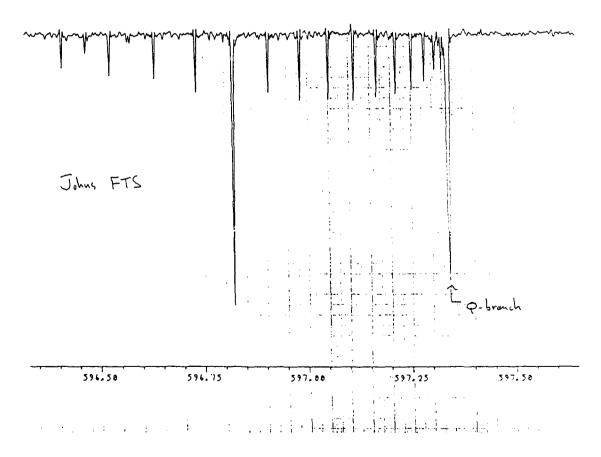
allows $k(\nu)$ to be rewritten

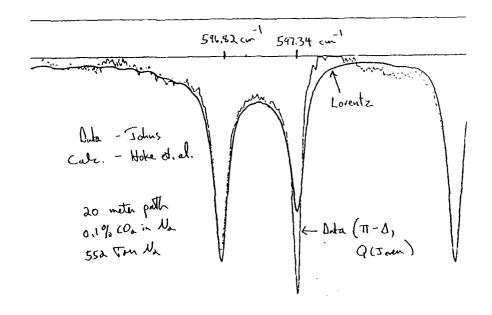
$$k(\nu) = \frac{N}{\pi} \operatorname{IM} \left\{ \sum_{i} \frac{(\mathbf{d} \cdot \mathbf{A})_{i} (\mathbf{A}^{-1} \cdot \boldsymbol{\rho} \cdot \mathbf{d})_{i}}{\nu - l_{i}} \right\}$$

which is an algebraic sum.









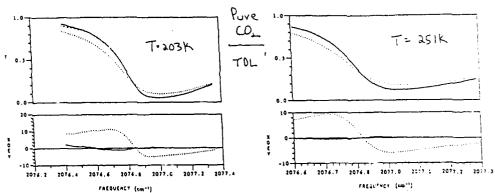
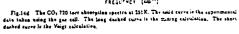


Fig.14a The CO, 120 fore absorption spectra at 202K. Tae colld curve is the experimental data taken using the gas cell. The long dashed curve is the mixing calculation. The abort dashed curve is the Voigt calculation.



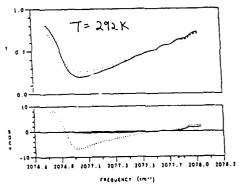


Fig. 14g. The CO, 720 terr absorption spectrs at 202K. The solid curve is the apperimental data taken using the gas cell. The long dashed curve is the midlag calculation. The short deshed curve is the Vorgt execulation.

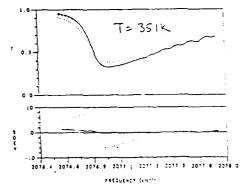
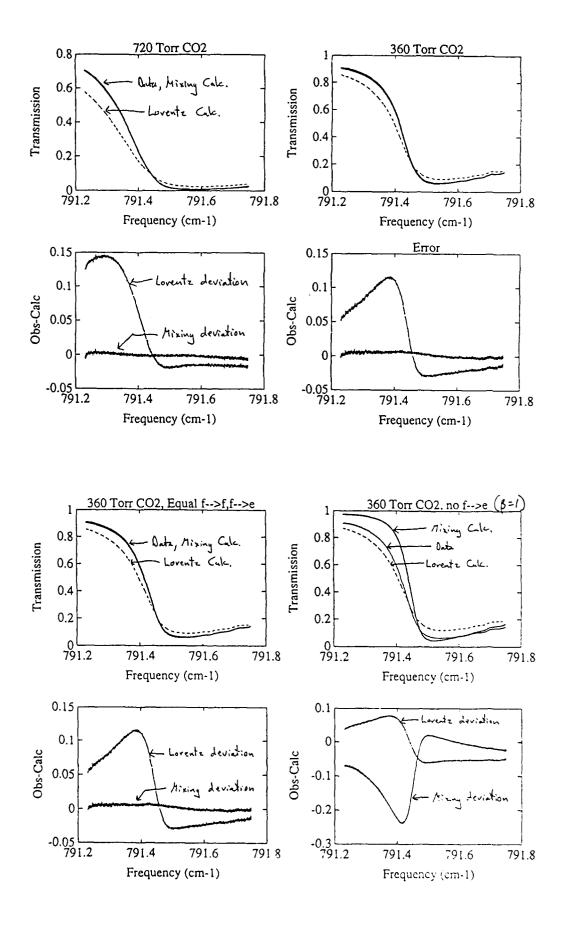
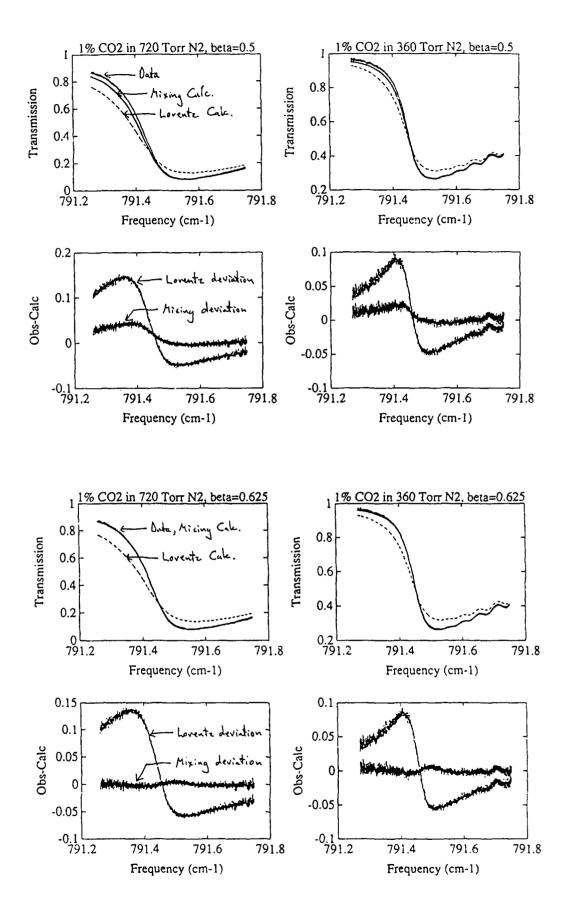
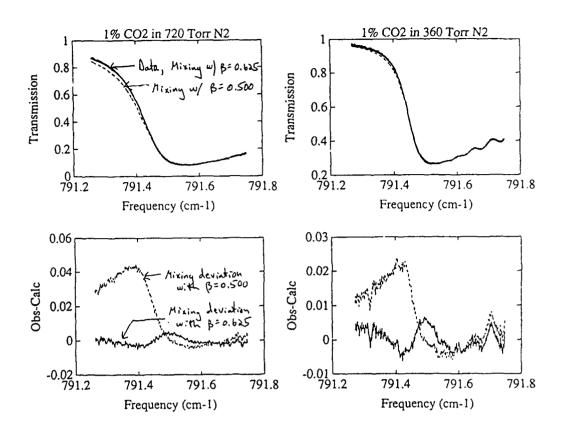
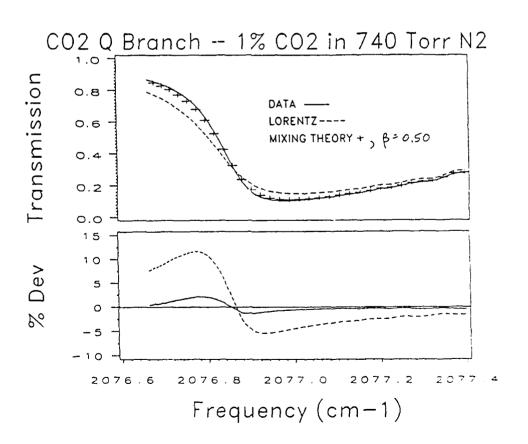


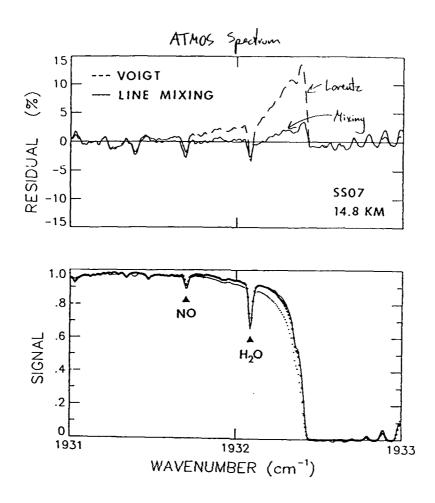
Fig.14). The CO₂ 720 terr absorption spectra at 2314. The solid curre is the experimental data taken using the gas cell. The long dashed curre is the musing taltuistion. The about dashed curre is the Vogs calculation.

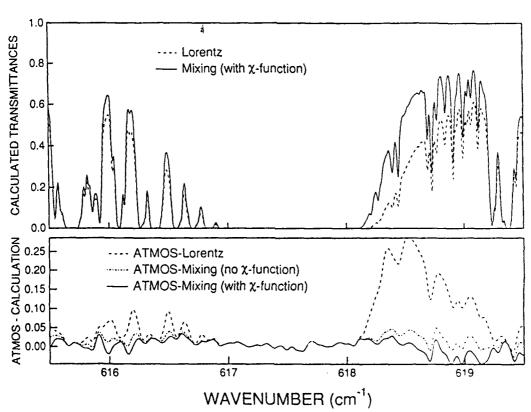


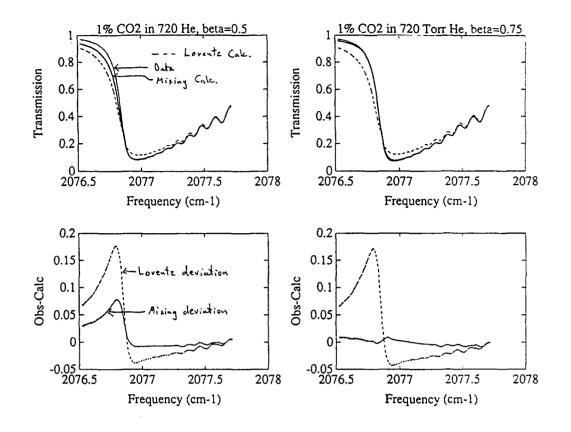


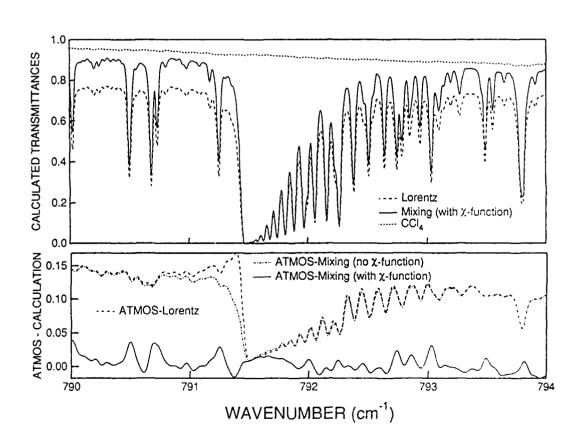


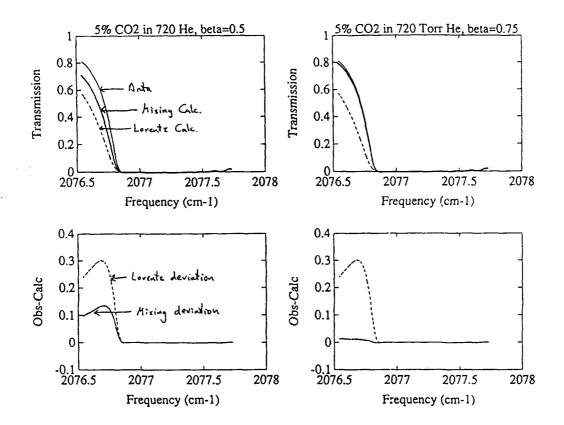


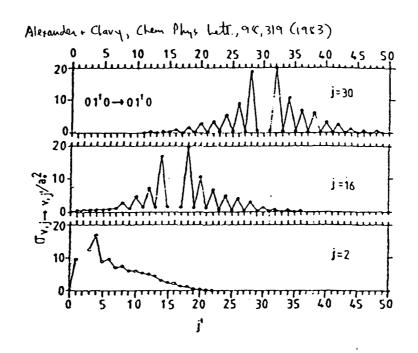


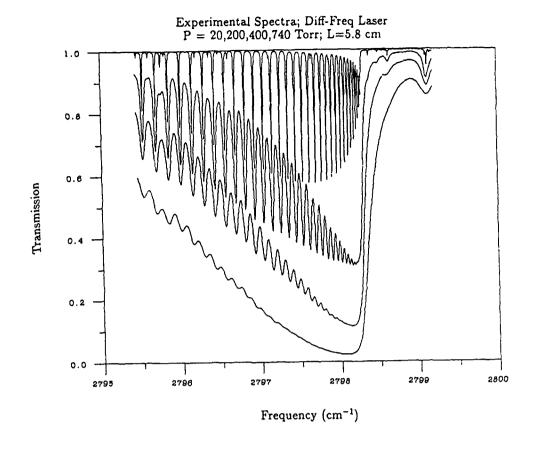


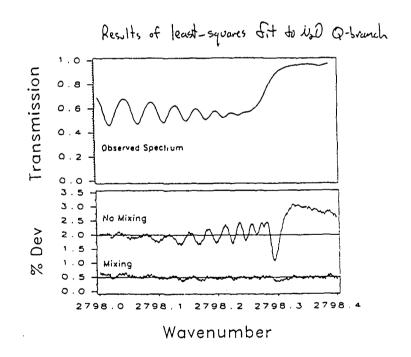


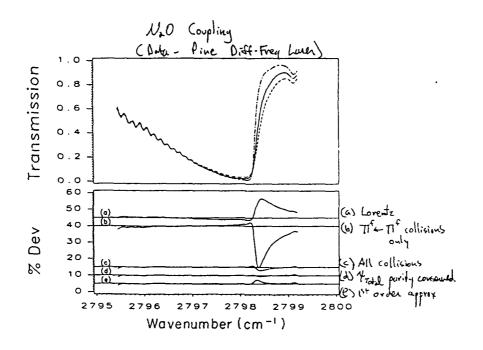


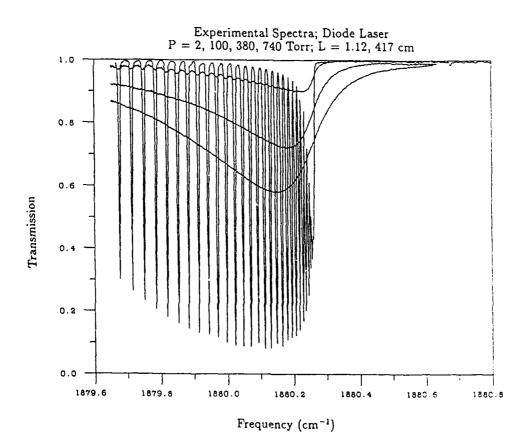


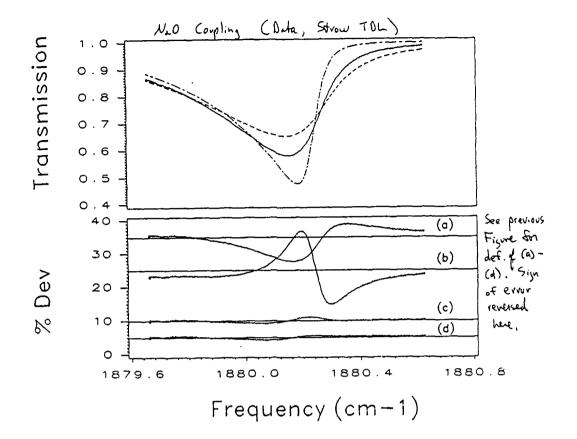


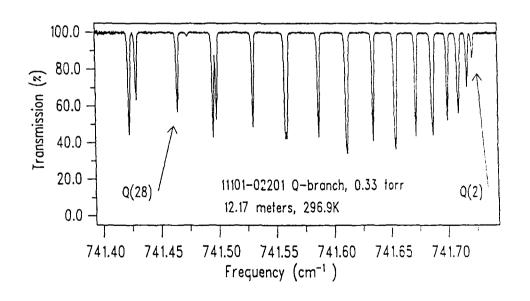


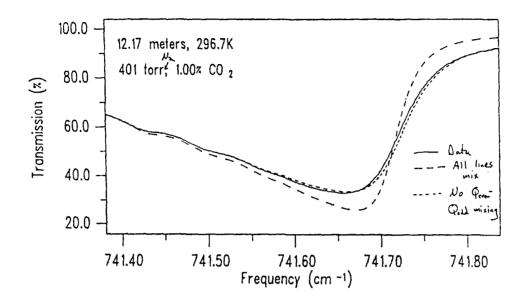


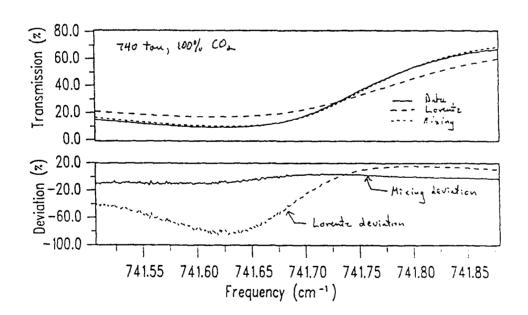












Line Coupling in the ν_3 Bandhead of CO_2 at 4.3 μ m

- Line coupling accounts for much of the sub-Lorentz absorption in the bandhead region which is used for temperature sounding
- Duration-of-collision effects may also be important inside the bandhead
- Trade-offs between high-J behavior of rotational relaxation (is the scaling law any good at high J?) and the duration-of-collision parameter give good results for room-temperature spectra of pure CO₂

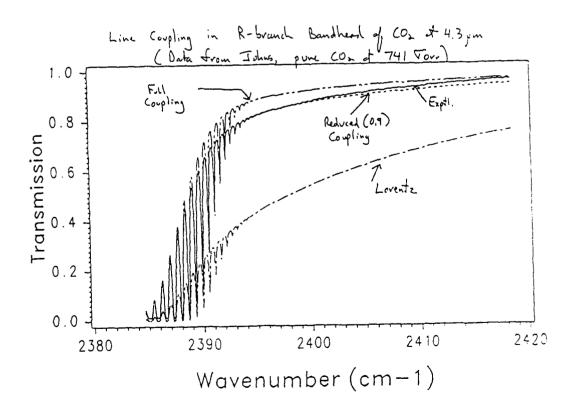
We use a semi-empirical lineshape in this region

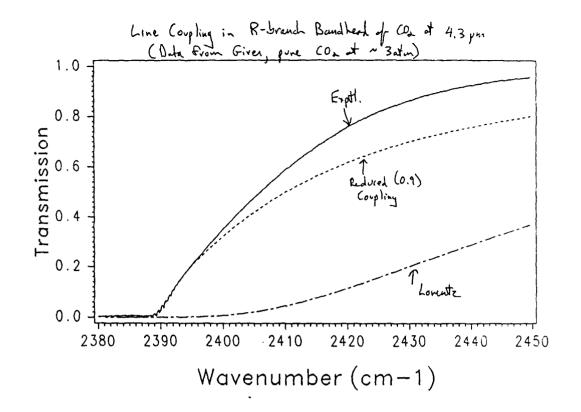
$$k(\nu)_{empirical} = k_{mixing}(\nu) * \chi(\Delta\nu), \quad \Delta\nu_i = \nu - \nu_i.$$

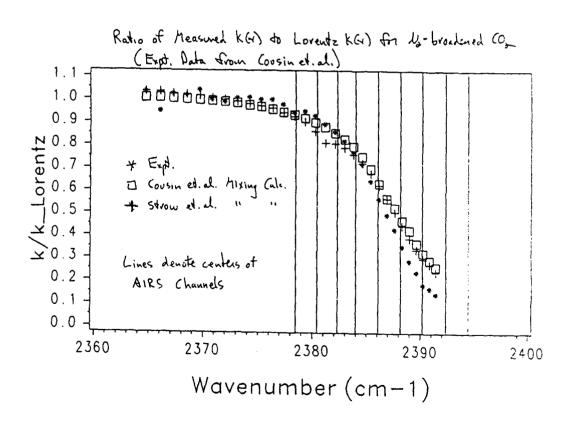
$$\chi_i = z_i K_1(z_i) exp(\tau_2 \alpha_{L_i} + \tau_o \Delta\nu_i),$$

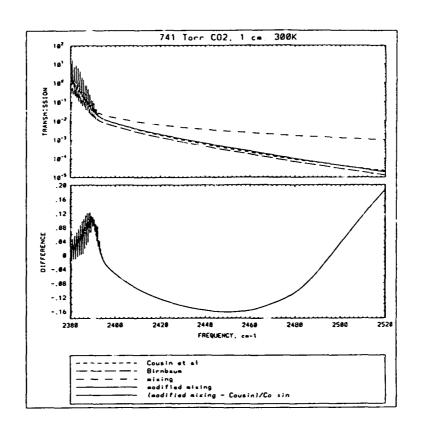
where

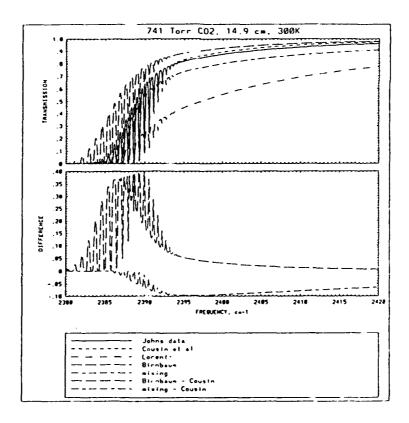
$$z_i = \sqrt{(\alpha_{L_i}^2 + \Delta \nu_i^2)(\tau_o^2 + \tau_2^2)}, \ \tau_o = \frac{0.72}{T}, \ \tau_2 \sim 0.0275.$$

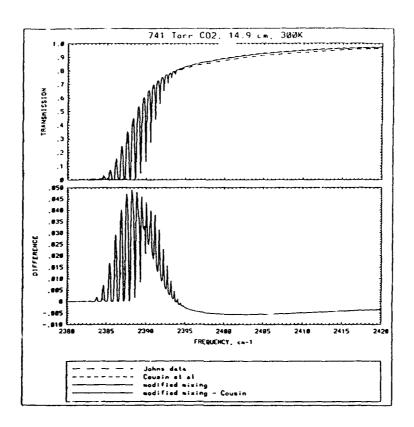












Conclusions

- CO₂-N₂ calculations predict less coupling than observed indicating some propensity to conserve vibrational angular momentum, this propensity is more pronounced for CO₂-He collisions
- CO₂ self-broadening models also very accurate over a wide temperature range
- Line coupling models sufficiently accurate for Q-branches important for CLAES, AIRS, HIS retrievals
- Atmospheric measurements (ATMOS, HIS) indicate that temperature dependence of line coupling is in relatively good shape for air-broadening
- More parameters needed to model Π - Δ Q-branches at 740 and 597 cm⁻¹?
- One N_2 -broadened N_2 O study shows good agreement using self-broadened collision model ($\beta=0.50$), some further work warranted on other bands, and with O_2 -broadening
- Good progress made with R-branch coupling at 4.3 μ m. Further work with N₂-broadening, low temperature, high-resolution spectra required for AIRS temperature sounder which operates inside the R-branch

LINE-MIXING: A NEAR AND FAR LINE WING PROBLEM

J.-M. Hartmann
Laboratoire E.M2.C., de CNRS (UPR288) et de l'Ecole Centrale Paris,
Grand voie des vignes, 92295 Chatenay-Malabry Cede, France

Line mixing is a problem of crucial importance for modeling of gas absorption spectra. For this reason, much experimental and theoretical studies have been made in the infrared and Raman domains. In particular, absorption in Q-branches and troughs between lines of P and R-branches, which are affected by line-interferences at moderate densities have been widely investigated. Various models have been proposed for the modeling of such phenomenon, which are generally based on the impact approximation. Studies of absorption at elevated density and in the very far wings of lines have demonstrated that these models can be very inaccurate. Other approaches, which account for the finite collision duration, have been proposed quite recently which lead to satisfactory results.

The author will try to present a comprehensive revue of experimental and theoretical results connected with the influence of line-mixing on absorption spectra. The advantages and limits of approaches based on the impact approximation will be discussed. The state of the art and perspectives for measurements and calculations of high density spectra and continuum absorption will be discussed.

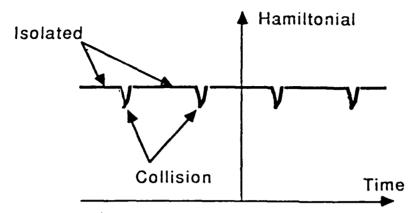
LINE - MIXING : NEAR AND FAR LINE - WING PROBLEMS

Jean. Hichel HARTHANN Laboratoire E.HZ.C, École Centrale France.

- . WHAT HAPPENS?
- " IMPACT APPROXIMATION
 - HODELLING
 - REHAINING PROBLEHS
- FAR WING

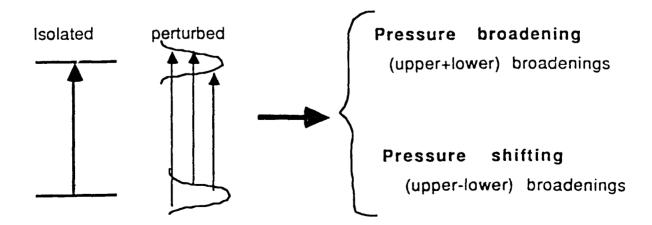
COLLISIONAL BROADENING: WHAT IS HAPPENING

Hamiltonial



The hamiltonian of the isolated molecule is perturbated during each collision. The energy levels of the molecule are then modified and functions of time

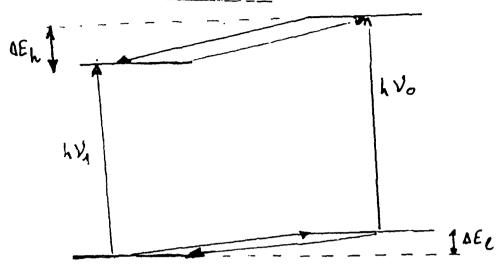
Transitions



All the more important that the interaction potential is large and spread (long range), and that the collision duration is long (low T)

LINE- HIXING: What happens.

T NEAR LINE CENTER



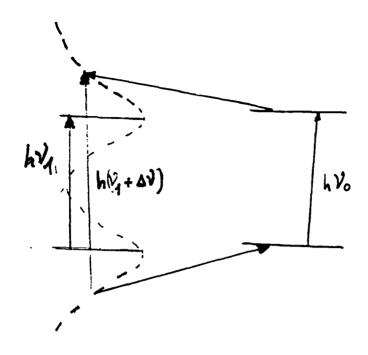
- Energy of collisional process: $|\Delta E| = |\Delta E| |\Delta E| = h(\nu_1 \nu_0)$ efficient if $|\nu_0 \nu_1| \ll \chi$
- Dominant process: po To-1 = P1 T1-0
 - -s if (po>p, i.e. So>Si) J→0 More

efficient

- -> molecules which are on a object the My
- -> uitensites taken from veak lines given to strong lines

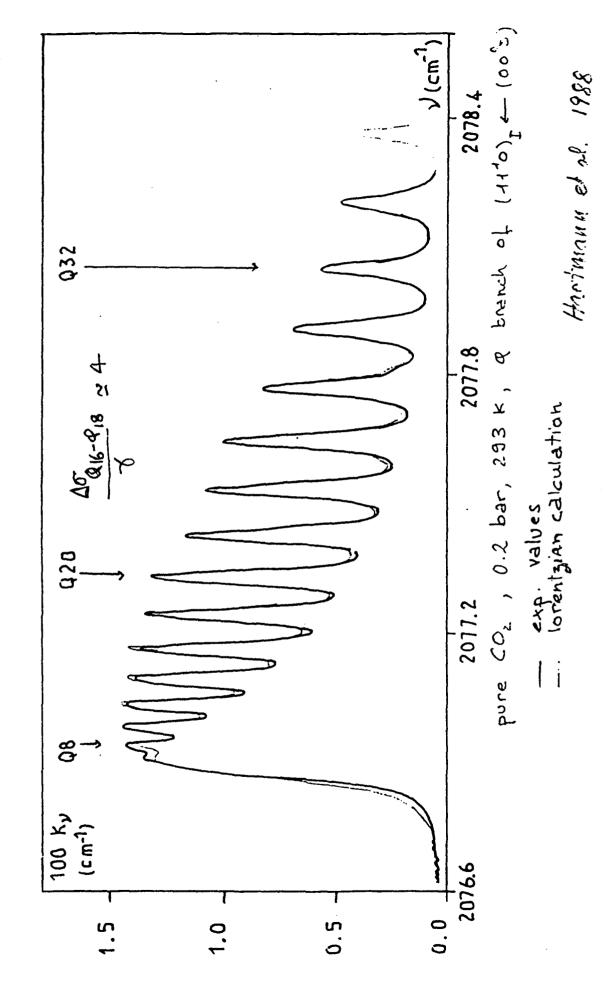
Conclusion: from lene conter to leve center

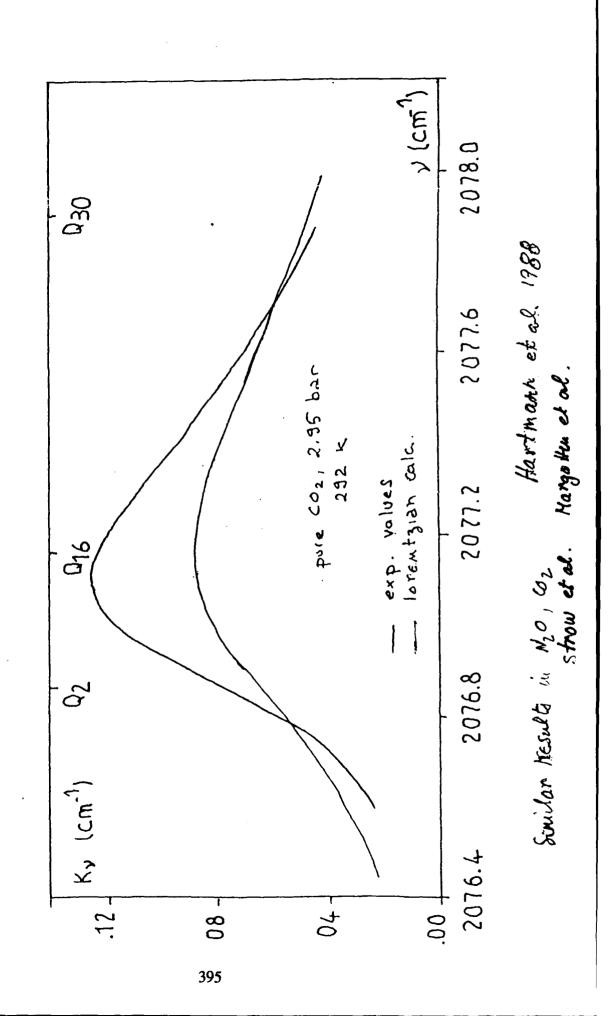
- only if 8>> | Vo-Vi (-> large potential)
- only if & populations on the levels (low T)
- from Weak to strong lines

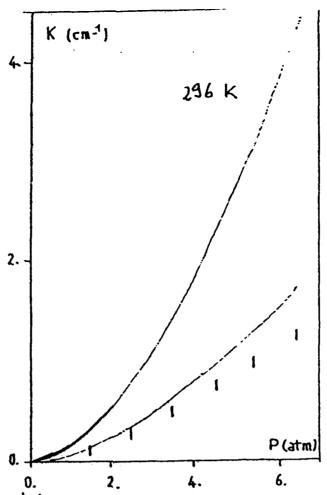


- Energy | AE| = | h(Vo-7, + AV) |
- efficiency: when 100-0,1<< 00

 the jump is or as efficient as the broadening up to av
- -> Take intensity in the wings to give to line centers
 - alxaption will go to zero in for wing





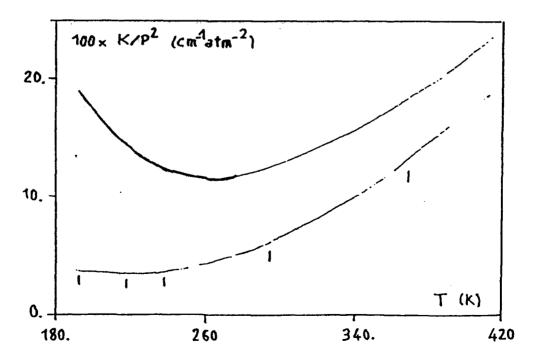


0. 2. 4. 6.

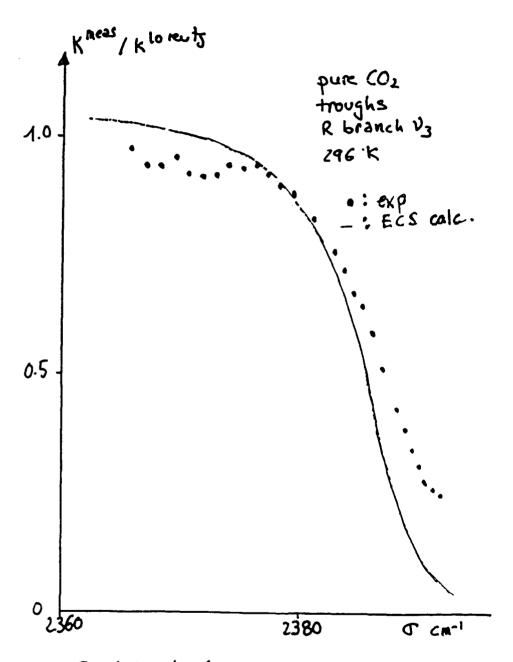
1: experimental

-: torent sian calculation

-: EGL fitting naw line-mixing coloulation.



Trough Between R66-R68 C/2 lines Co2-N2



C. Boulet et al. Similar hesult for Co, N20:... Bubrin et st.

W: relaxation operator - All the unfluence of collisions.

- , 2TC | 0-0ig| 2° (<1 -> W udependant on 0 (Impact afformation)
- . W diagonal -> Lorent shape : <<ili W ||if>> = Tip - i Di6
- . In Roman (isotopièce)

. In informed (within 108A)

W(= 3)

Statistically based FITTING LAWS

Exponential Gap Law = ρ_i , exp[-. $|E_i-E_{ii}|$]
Polynomial Energy Gap Law = ρ_i , $\left(\sum_{k} - |E_i-E_{ii}|^{-k}\right)$

Isotropic Raman Sum Rule

Widely used in Raman (Greenhalgh, Hall, Rasasco, Robert, Bonamy,...)

in IR (Strow, Gentry, Lacome, Boalet, Hargottin-Hacloux, ...)

Dynamically based Scaling LAWS (De Pristo, Rabitz, 1979)
(105, ECS)

CifIW(0) 1i161> & Effici, 6, 6', L) To-L

Augular momenta

Energy Corrections

Detailed Balance

Direct colculation (10s, cs, cc) (Green, Boulet 1989: Inversion from broadening (De Pristo, Rubitz Bonamy, Robert 1989

Hore accurate than fitting bus. Correct J dependence (interbranch mixing)

MODELS within the IMPACT APPROX

Absorption coefficients

$$\begin{split} \text{K}_{\text{V}}^{\text{LC}}(\text{T},\text{P}) &= \text{Im } \{\text{P} \ (8\pi^2\text{v}) \, / \, (3\text{hc}) \ \{\text{1-exp}(-\text{hv/kT})\} \ \sum_{\text{If}} \rho_{\text{I}}(\text{T}) \ d_{\text{IF}} \\ & \times \ \{\sum_{\text{I'f'}} d_{\text{I'F'}} \, < \text{IF} \, | \, (\text{V} - \text{V}_{\text{IF}} - \text{iPW}(\text{T}))^{-1} \, | \, \text{I'F'} > \,] \, \} \end{split}$$

W(T): relaxation operator. Contains all the influence of collisions. Relation with line-broadening:

$$<$$
IF|W(T)|IF> = γ_{IF} (T) - $i\Delta_{IF}$ (T)}

No line-mixings--> W diagonal --> lorentzian shape.

$$K_V^{LR}(T,P) = \sum_{i \in I} [PS_{iF}(T)] [P\gamma_{iF}(T)] / \{\pi[[v-v_{iF} - P\Delta_{iF}(T)]^2 + [P\gamma_{iF}(T)]^2]\}$$

Problem: Model the off-diagonal elements of W

Fitting laws

$$\langle IF|W(T)|1'F' \rangle = f(a_1, a_2, ..., a_n, I, I')$$
 (I $\neq I'$)

Exponential Gap Law) : ρ_{I} , a exp(-b|E_I-E_I,|)

parameters deduced from isotropic Raman sum rule : $\Sigma < \text{IF}|W(T)|I'F'> = - < \text{IF}|W(T)|IF>$

Scaling relations (Energy Corrected Sudden Approximation).

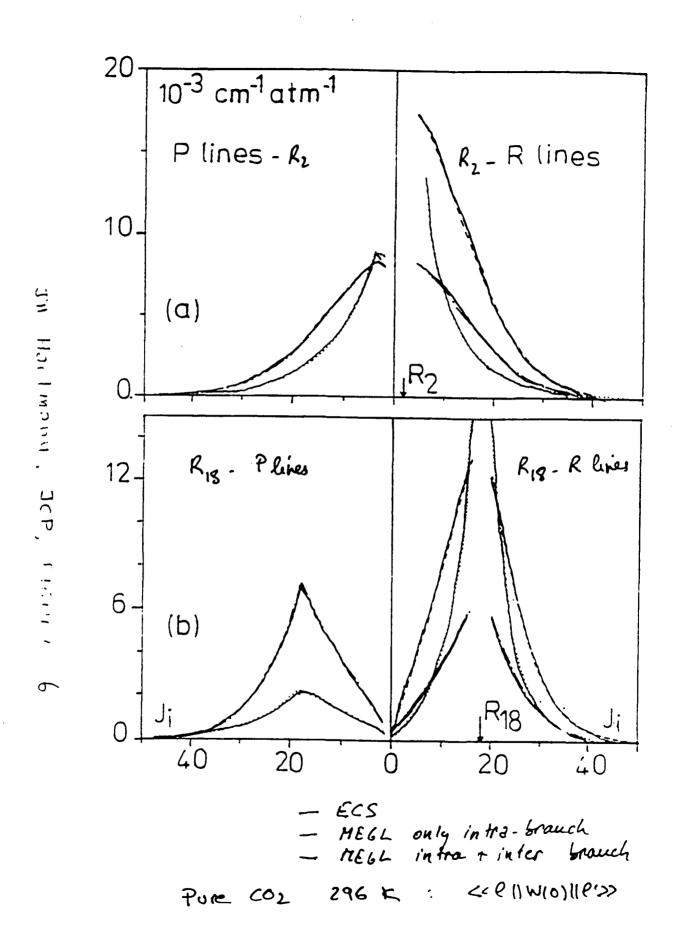
$$A(j,j') = (1 + (\Omega(j,j') \ell_{c}/v)^{2/24})^{-1} , (\ell_{c} \text{ scaling length})$$

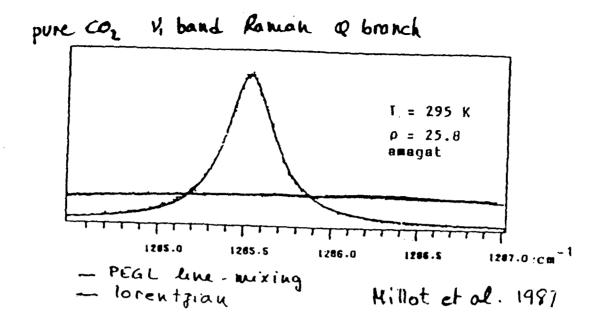
calculation or analytical law for σ_{OL} (exemple : A (L(L+1))- α)

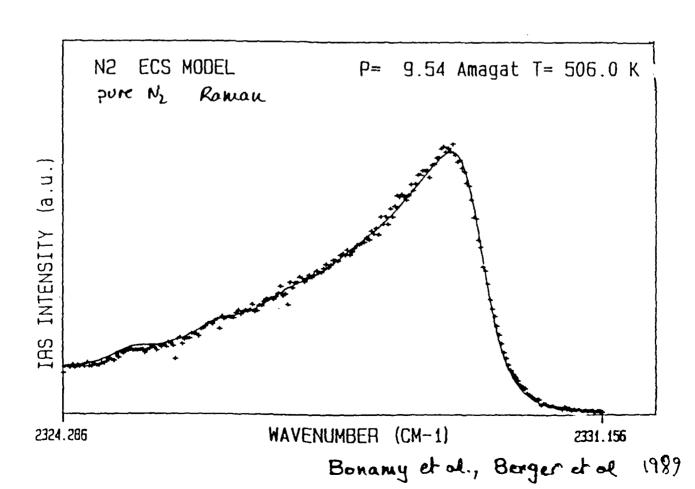
parameters (including ℓ_{c}) deduced from line-broadening :

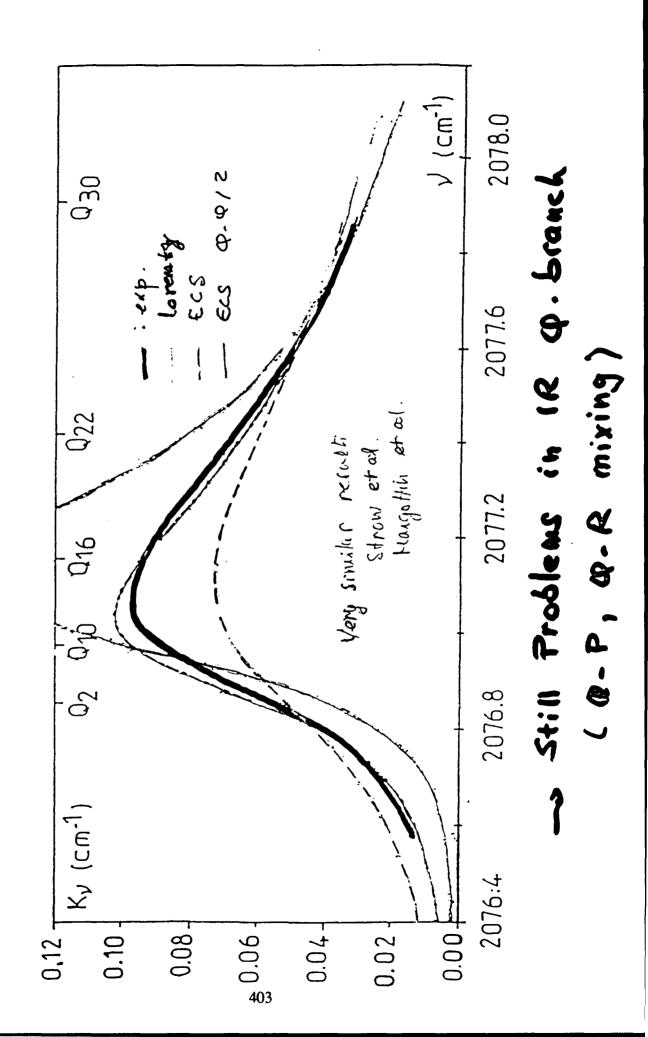
$$(j_ij_f|W^{ECS}|j_ij_f) = \gamma_{iij_f} = (Nv/2\pi c) A(ji,ji)A(jf,jf)$$

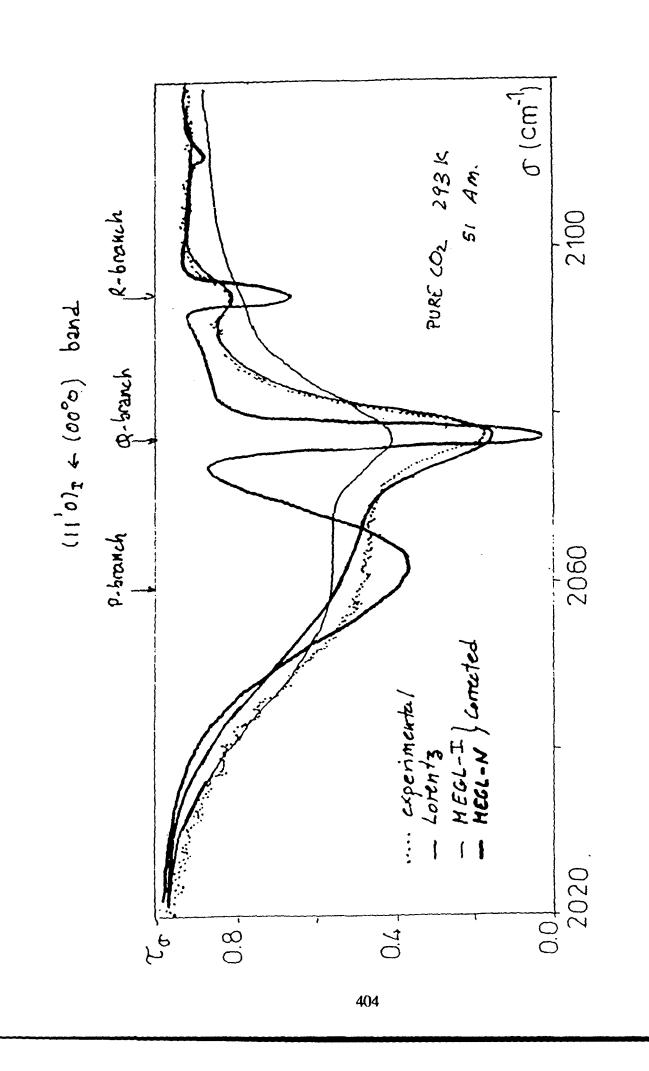
$$\{\sum 1 - \{F_n(j_ij_f|j_ij_f|L00\} A(L,0)^{-2} (2L+1) \sigma_{OL}$$





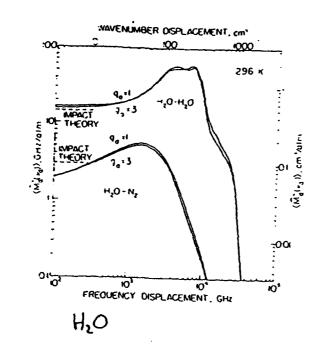


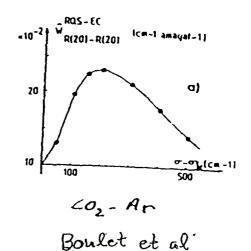




JH Hartmann Jr D Ficore 124

A CALLACT TO BE A CALLED TO SECURITY OF THE SE





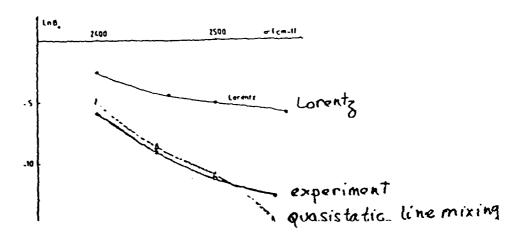
Tipping

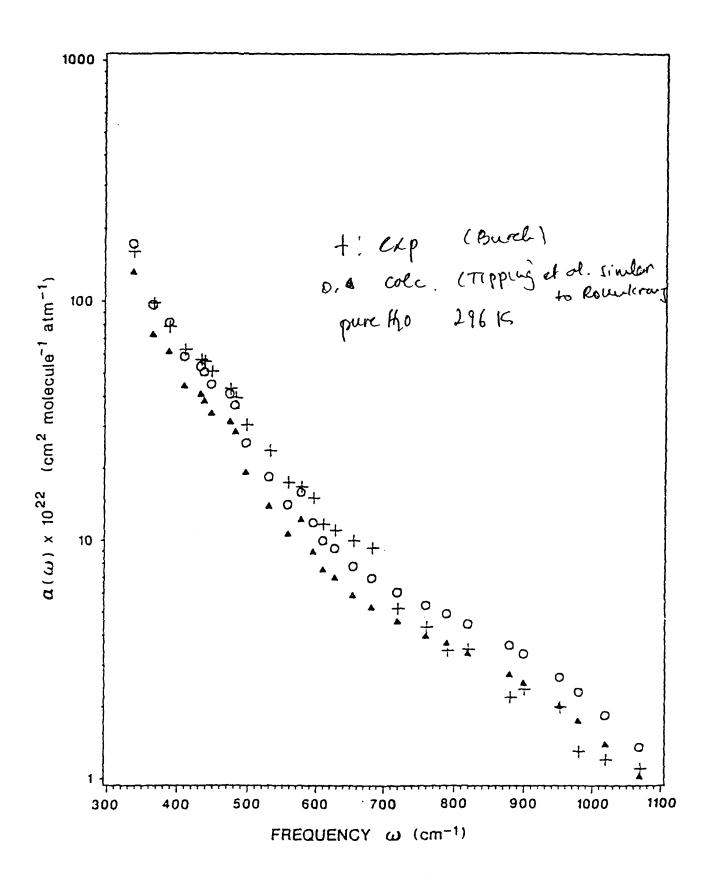
Statistical questistatic approach

Danies et al.)

From first principles

CO2-Ar 296 K IR Boulet et Al





CONCLUSION

Impact Models

- QUITE ACCURATE BY USING EMPIRICAL FACTORS FOR INTER/INTRA BRANCH OR e/f LEVELS
- STILL PROBLEMS: WHY INTRA BRANCH
 MIXING HAS TO BE COWERED IN THE IR (OKIN PAI
 EVEN WITH HODELS (105, ECS) WHICH
 SHOULD ACCOUNT CORRECTLY FOR
 COUPLING BETWEEN LEVELS OF \$ SYMMETRY
- EFFORTS ON Q-brouched (602-He? Close coupling?
 FAR WING
 - VERY DIFFICULT PROBLEM
 - RESULTS ARE VERY SENSITIVE TO THE INTERACTION POTENTIAL particularly in far wing short rauge interactions)
 - THEORY ONLY FOR VERY FAR WING (QUASISTATIC)
 - STILL QUITE UNTRACTABLE FOR HOLECULE. HOLECULE
 WITH HANY LEVELS AND MULTI-COMPONENT
 INTERACTION

FAR-WING LINESHAPE CONTRIBUTION TO THE WATER CONTINUUM IN THE MILLIMETER AND INFRARED REGIONS

R.H. Tipping
Department of Physics and Astronomy, University of Alabama, Tuscaloosa, AL 35487

O. Ma

Center for the Study of Global Habitability, Columbia University and Institute of Space Studies, Goddard Space Flight Center, New York, NY 10025

Theoretical calculations of the contributions from the far wings of allowed transitions to the continuous absorption by water vapor have been carried out for both the millimeter and infrared spectral regions. The theory is based on the quasistatic approximation and assumes as input only the known rotational constants and dipole moment matrix elements, and two Lennard-Jones potential parameters describing the isotropic interaction between two molecules. Results will be compared to recent laboratory data, and the implications for atmospheric applications discussed.

FAR WING LINESHAPE CONTRIBUTION

TO THE WATER CONTINUUM IN THE

MILLIMETER AND INFRARED REGIONS

R. H. Tipping
University of Alabama

Q. Ma

Goddard Institute for Space Studies

INTRODUCTION

- 1.1) IMPORTANCE OF MILLIMETER AND INFRARED RADIATION IN ATMOSPHERES
- (1) Controls the energy balance and affects the climate of the Earth.
- (2) Widely used in remote sensing, atmospheric communications, etc.
- (3) To determine characteristics of planetary atmospheres from experiment data.

1.2) ATMOSPHERIC WINDOWS AND CONTINUUM ABSORPTION

OPAQUE REGIONS AND WINDOWS: The opaque regions are mainly determined by $\rm H_2O$ lines, along with $\rm O_2$ and $\rm CO_2$ lines. Between them there are "WINDOWS".

THE WEAK ABSORPTION IN WINDOWS:

- (1) Some weak local lines of H_2O , O_2 and CO_2 .
- (2) A gradually varying background,i.e. continuum absorption.

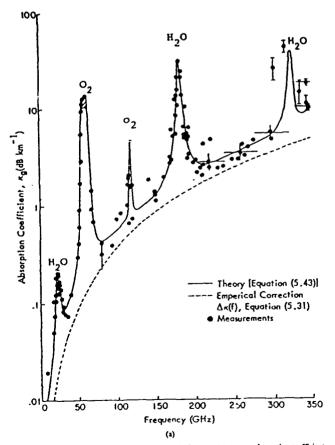


Fig. 5.7 Microwave absorption due to atmospheric gases; (a) gaseous absorption coefficient $n_i(f)$ at sea level and (b) remith opacity, both for the surface conditions $P_0 = 1013$ mbar, $T_0 = 293$ K, and $p_0 = 7.5$ gcm⁻³. Solid curves are calculated according to theory, and dots are measured within $N_0 = 0.000$ to $N_0 = 0.000$.

SEMANTIC/NOTATIONAL

- 1. "CONTINUUM" ABSORPTION NOT ASSOCIATED
 WITH NEARBY LINES. THIS DOES NOT IMPLY
 THAT IT IS ASSOCIATED WITH UNBOUND STATES.
- 2. EXCESS ABSORPTION OR DEFICIENT ABSORPTION?

1.3) BASIC CHARACTERISTICS OF CONTINUA

There are two kinds of water continua:

- (1) H₂O H₂O (self) continuum
- (2) $H_2O N_2$, O_2 (foreign) continuum Usually, the self-continuum is dominant.

CHACTERISTICS OF THE SELF-CONTINUUM:

- (1) Varies smoothly with frequency.
- (2) Proportional to n².
- (3) Very strong negative temperature dependence.

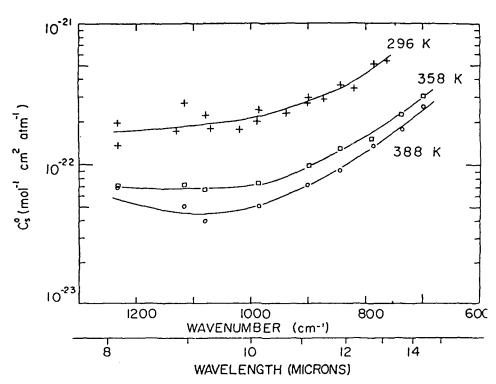


FIG. 3-4. Comparison of the continuum absorption coefficient at three temperatures.

1.4) MAIN THEORIES OF WATER CONTINUUM THREE MECHANISMS FOR SELF-CONTINUUM:

- (1) Collision broadened far-wings of allowed water vapor lines.
- (2) Collision-induced absorption.
- (3) Water dimers.

All three mechanisms vary as n², but there are large differences in the temperature dependencies and in the magnitudes of the absorption.

BRIEF HISTORY OF COLLISION-BROADENING MECHANISM FOR THE WATER CONTINUUM:

- (1) In 1938, Elsasser first proposed that the water continuum was due to far-wings of allowed lines.
- (2) Anderson-type theories with the impact approximation.
- (3) Clough et al. considered the finite duration of collisions.
- (4) Boulet and Robert, Birnbaum, etc.
 obtained exponential-like far wings.
- (5) Rosenkranz's quasistatic method based on two approximations:
 - (a) the far wing limit: $\omega \gg \omega_{fi}$
 - (b) the narrow band approximation: $\omega \ \ \, \text{$\omega$} \ \ \, \text{$\omega$} \ \, \text{$\omega$}$

RESULTS:

In the IR, the temperature dependence and the magnitude of $\alpha(\omega)$ were in reasonable agreement with experiment

BUT

there are significant differences in some regions, and this method is NOT APPLICABLE IN THE MILLIMETER REGION.

THEORY MILLIMETER REGION

$$\alpha(\omega) = \frac{4\pi^2}{3\hbar c} \omega \tanh(\beta\hbar\omega/2) [F(\omega) + F(-\omega)]$$

$$= \frac{4\pi^2}{3\hbar c} \omega (e^{\beta\hbar\omega} - 1) F(\omega)$$

$$F(\omega) = (2\pi)^{-1} \int_{-\infty}^{+\infty} e^{i\omega t} \langle \vec{\mu}(0) \cdot \vec{\mu}(t) \rangle dt$$

$$\langle \vec{\mu}(0) \cdot \vec{\mu}(t) \rangle \equiv \sum_{i} \rho_{i} \langle i | \vec{\mu}(0) \cdot \vec{\mu}(t) | i \rangle$$

$$F(\omega) = -(\pi)^{-1} \text{ Im Tr } \{\vec{\mu}(0) | \frac{1}{\omega - \mathfrak{F}} \rho \vec{\mu}(0)\}$$

APPROXIMATIONS

- 1. BINARY COLLISIONS
- 2. PAIR POTENTIAL

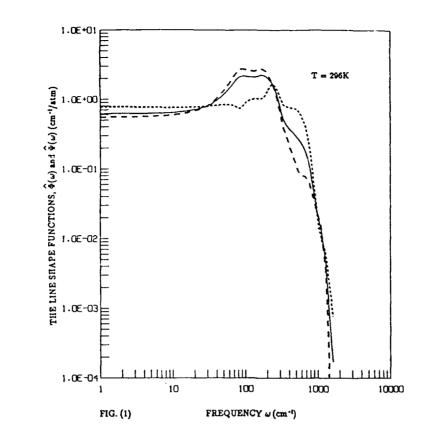
$$V = V_{ISO} + V_{d-d}$$

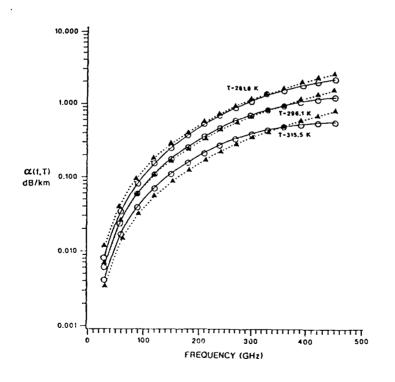
3. QUASISTATIC

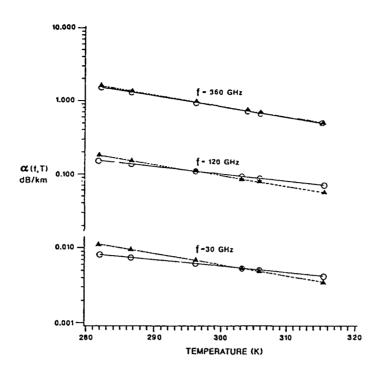
INPUT DATA

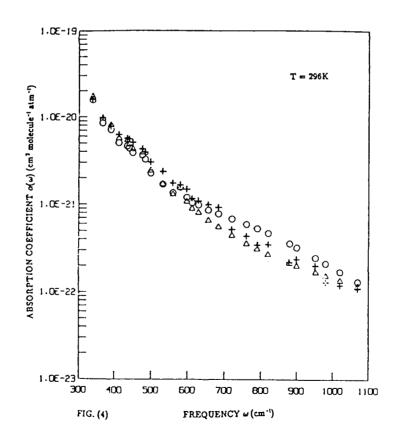
A, B, C,
$$\mu$$

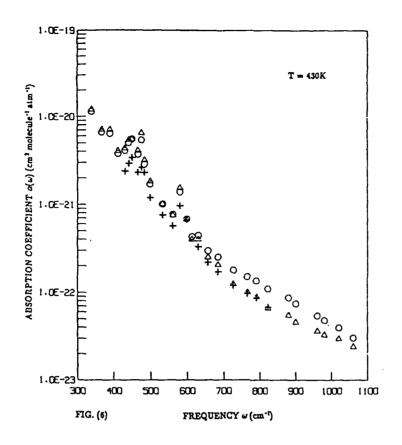
$$S_{if} \in \sigma$$

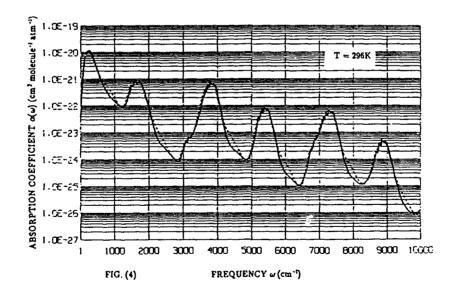












LABORATORY MEASUREMENTS OF THE 60-GHz O2 SPECTRUM IN AIR

H.J. Liebe

Institute for Telecommunication Sciences, National Telecommunications and Information Administration, U.S. Department of Commerce, NTIA/ITS.S1, 325 Broadway, Boulder, CO 80303

The O_2 -spectrum of dry air was studied with a resonance spectrometer under controlled laboratory conditions. Key parts of the instrumentation were an automatic network analyzer and a one-port Fabry-Pérot resonator affording an effective path length of 240 m. Measurements were made at frequencies between 49.3 and 67.2 GHz in 0.1 GHz increments for eleven pressure steps (1-100 kPa) and three different temperatures (7-30-53°C). More than 5×10^6 data points (S_{11} parameters) have been recorded and reduced to about 5,000 absorption values α (dB/km). Measurement uncertainties were estimated to be typically the worse of ±0.05 dB/km or 2 percent. The collective spectral behavior of 38 pressure-broadened O_2 lines is described by the model MPM (NTIA Report 91-272, March 1991). A comparison of the absorption results with MPM predictions reveals systematic differences which correlate with O_2 line width and overlap parameters. An interpretation of the extensive data set with Rosenkranz's overlap theory [JQSRT 39(4), 287-297, 1988] is underway.

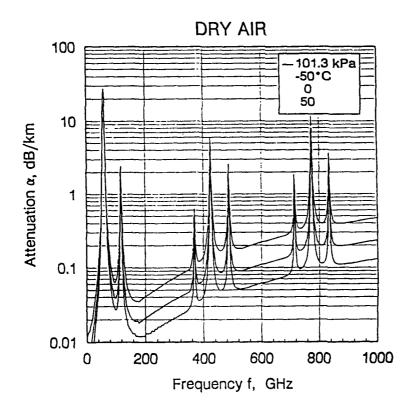
LABORATORY MEASUREMENTS OF THE 60-GHz O, SPECTRUM IN AIR

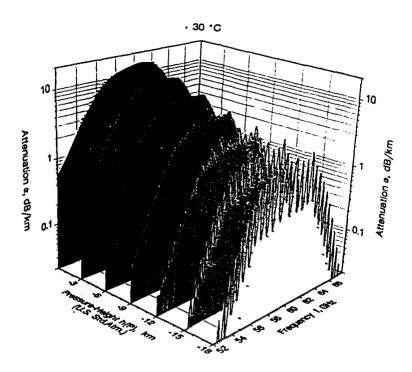
Hans J. Liebe

Institute for Telecommunication Sciences

National Telecommunications and Information Administration U.S. Department of Commerce

NTIA/TTS.S1, 325 Broadway, Boulder, CO 80303, USA





Microwave Line Spectrum of Dry Air

Line-by-line summation of 40 O_2 transitions ($R^2=1$ to 39) to yield the complex refractivity (6 \times 40 = "240-parameter" problem),

where the line strength is

$$s_k = a_1 P \theta^3 \exp(a_2(1-\theta))$$
 kHz

and P_k is a complex shape function in GHz^{-1} . The Van Vleck-Weisskopf shape function of a pressure-broadened line was modified by Rosenkranz (1988) to account for overlap interferences,

$$F(\mathcal{E}) = \frac{\mathcal{E}}{\nu_k} \left[\frac{1 + j \mathcal{I}_k}{\nu_k - \mathcal{E} + j \gamma_k} - \frac{-1 - j \mathcal{I}_k}{\nu_k + \mathcal{E} - j \gamma_k} \right]$$

which rationalizes to absorption (\mathbf{f}'') and dispersion (\mathbf{f}') profiles

$$F''(f) = A(X + Y) - I_k[(1 - B)X + (1 + B)Y]$$

$$F'(f) = (1 - 8)X - (1 + 8)Y + I_1A(X - Y),$$



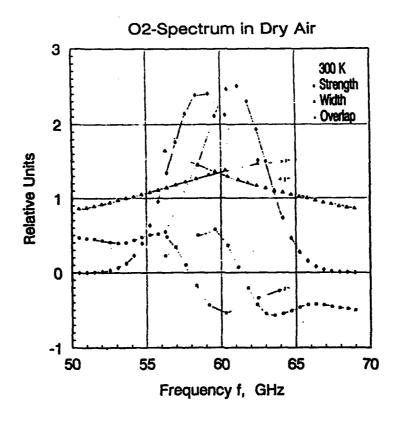
with the abbreviations

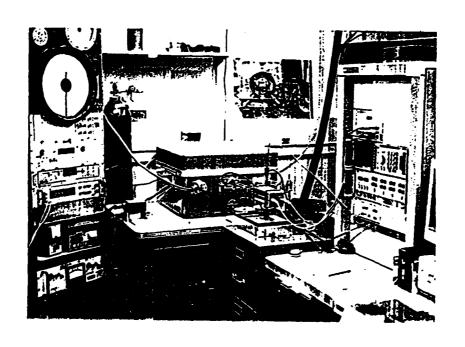
$$\begin{array}{ll} A = \gamma_{k}/r_{k}, & B = \ell/r_{k}, \\ X = \ell/((r_{k} - \ell)^{2} + \gamma_{k}^{2}), & x = \ell/((r_{k} + \ell)^{2} + \gamma_{k}^{2}). \end{array}$$

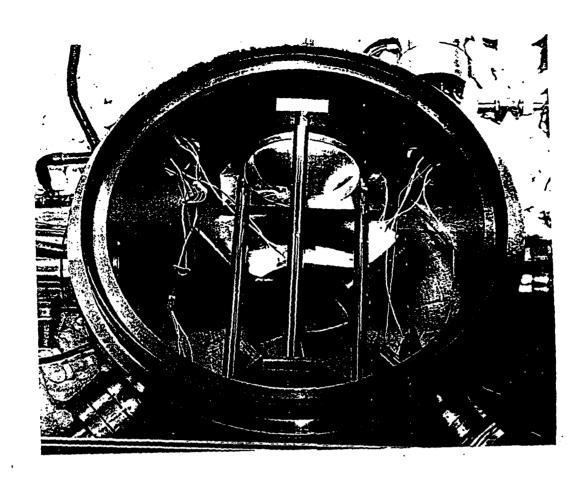
Width and interference parameters are for O_2 lines in air,

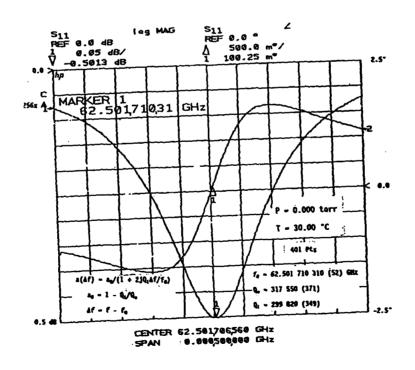
$$\gamma_{c} = a_{3}P^{(0,0)} - \frac{g(c)}{2} i$$
 GHz $e^{-c_{1}} g(c_{2})$

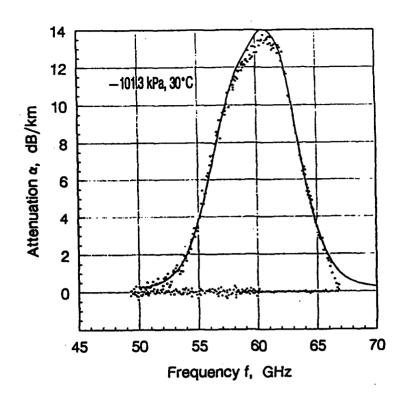
an(

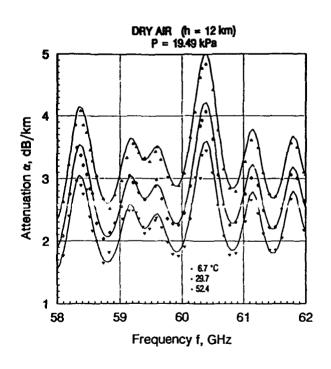


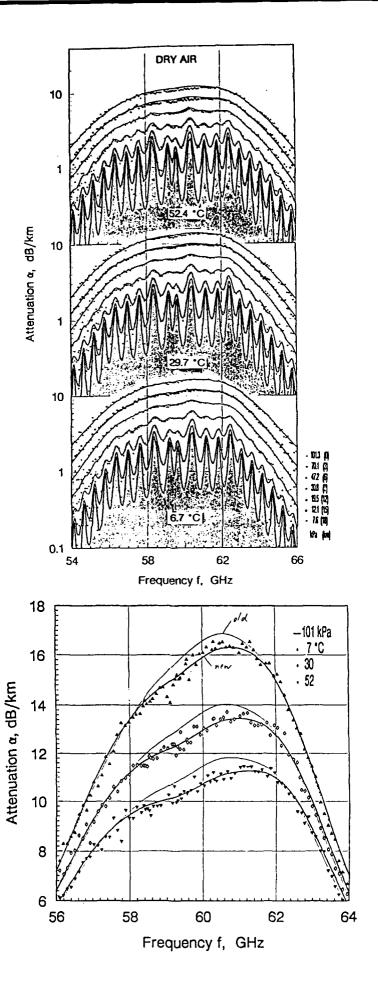


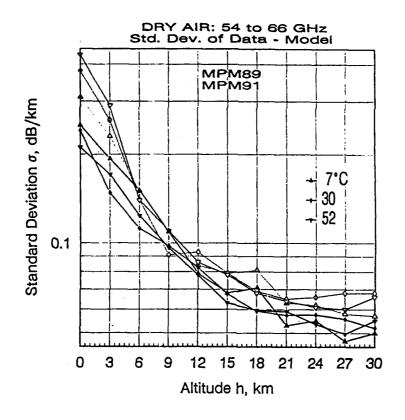


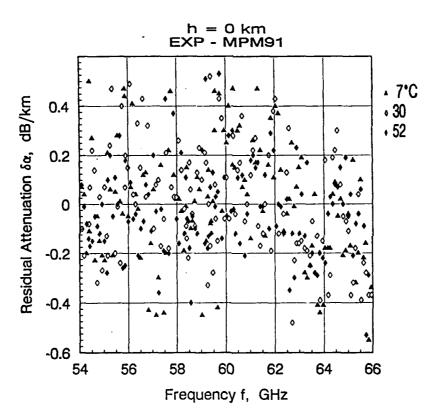


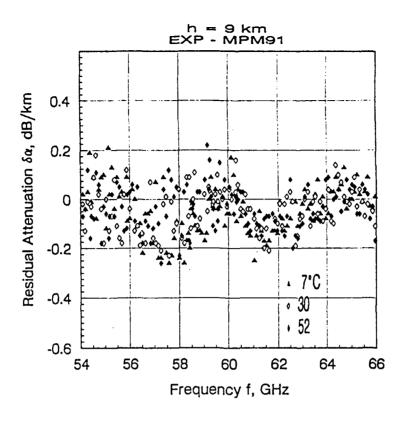


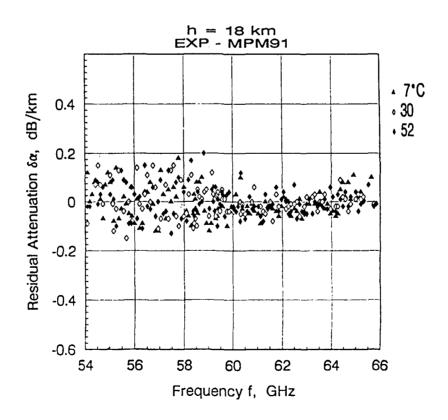


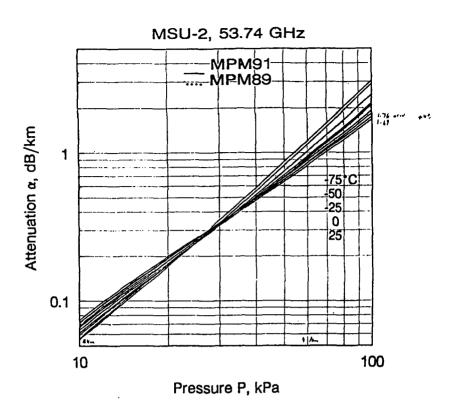












LINE MIXING IN POLAR AND NONPOLAR MOLECULES

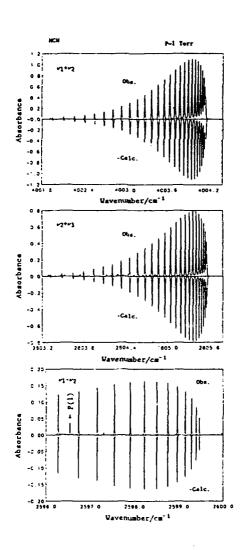
A.S. Pine, J.P. Looney
Molecular Physics and Thermophysics Divisions, National Institute of
Standards and Technology, Gaithersburg, MD 20899

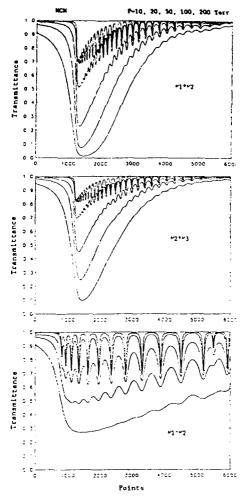
Line mixing has been observed for three infrared Q branches of HCN and HCCH, self-broadened at subatmospheric pressures, using a difference-frequency laser spectrometer. Broadening coefficients and line-coupling effects are independent of vibration in these species. The broadening coefficients monotonically decrease with J for HCCH whereas they peak near the Boltzmann population maximum for HCN. Empirical energy-gap rate laws adequately describe the broadening and line mixing in HCCH provided that a decoupling factor, representing collisional cross relaxation between the earn of levels of the II bending vibrations, be included. These rate laws do not fit the line mixing in HCN whereas an energy-corrected-sudden (ECS) scaling law does. Here the cross relaxation decoupling is smaller than for HCCH, indicating a slight propensity for preserving vibrational angular momentum in polar molecule collisions.

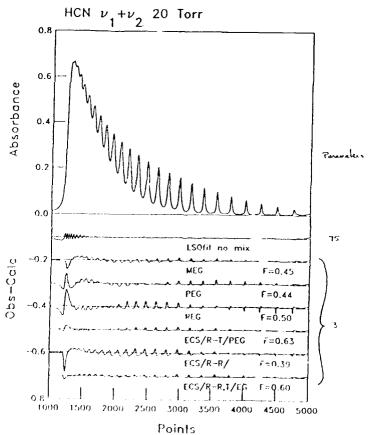
LINE MIXING IN POLAR AND NONPOLAR MOLECULES (HCN) (HCCH)

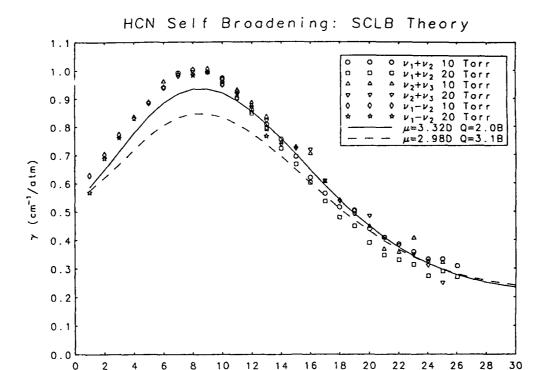
A. S. Pine and J. P. Looney

Molecular Physics and Thermophysics Divisions
National Institute of Standards and Technology
Gaithersburg, MD 20899









EMPIRICAL COLLISION RATE FITTING LAWS

R-T Hybrid Power-Exponential-Gap (PEG) Law

$$R_{J\rightarrow K} = a_1 (E_{KJ}/B)^{-a_2} \exp(-a_3E_{KJ}/kT)$$

where $E_{KJ} = E_{K}-E_{J}$ and $k = k_B/hc$

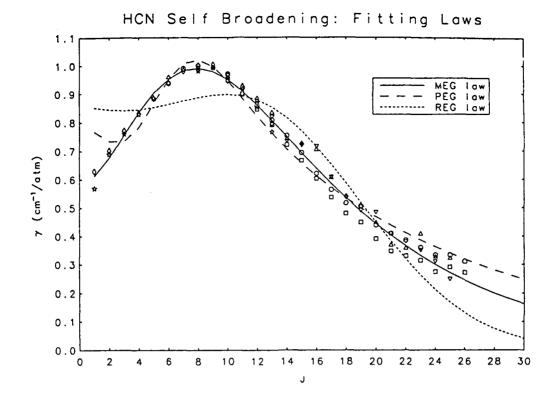
R-T Modified-Exponential-Gap (MEG) Law

$$R_{J\to K} = a_1 \frac{[1+1.5(E_J/a_2kT)]}{[1+1.5(E_J/kT)]} \exp(-a_3E_{KJ}/kT)$$

R-R Resonant-Exponential-Gap (REG) Law

$$R_{J\rightarrow K}$$
 = a₁ $\rho_K \Sigma_{LM} \rho_L \rho_M \exp(-a_3|E_{KJ}+E_{ML}|/kT)$
where ρ_J = $g_J(2J+1)\exp(-E_J/kT)/Z_R$

for upward collisional transitions, K > J. Downward transitions related by detailed balance, $R_{K\to J} = R_{J\to K} \rho_J/\rho_K$.



ENERGY-CORRECTED-SUDDEN (ECS) SCALING LAWS

R-T Inelastic Collision Rates

$$R_{J\to K} = (2K+1)\exp(-E_{KJ}/kT) \Sigma_L(2L+1) \begin{pmatrix} J & K & L \\ 0 & 0 & 0 \end{pmatrix}^2 R_{L\to 0}$$

$$\times [1+(a_4E_{L-})^2/BkT]^2/[1+(a_4E_{K-})^2/BkT]^2$$

where
$$E_{KJ} - E_K - E_J$$
 and $k - k_B/hc$,
 $E_{K-} - E_K - E_{K-I}$ for $I - 1$ (dipole)
or $I - 2$ (quadrupole),
 $R_{L\to 0} - a1$ (E_L/B)^{-a2} exp(-a3 E_L/kT) (PEG)

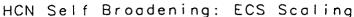
R-R Inelastic Collision Rates

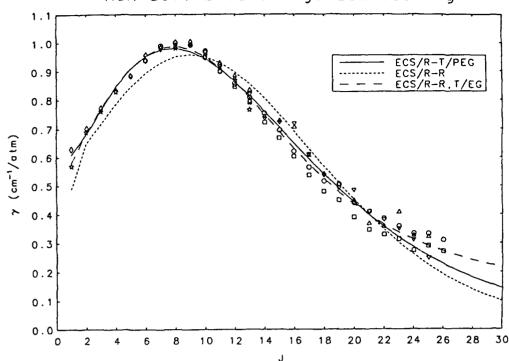
$$R_{J\to K} - a_1(2K+1) \Sigma_L \rho_L \exp(-\Delta E/kT) \begin{pmatrix} J & K & I \\ 0 & 0 & 0 \end{pmatrix}^2 \begin{pmatrix} L & M & I \\ 0 & 0 & 0 \end{pmatrix}^2 \times (2M+1)(2I+1)/[1+(a_4(E_{KJ}+E_{ML}))^2/BkT]^2$$

where
$$\rho_L = g_L(2L+1) \exp(-E_L/kT)/Z_R$$
, $K = J+I$, $M = L-I$, for $I = 1$ or 2, $\Delta E = E_{KJ} + E_{ML}$ if > 0 or $= 0$ if ≤ 0

for upward collisional transitions, K > J.

Downward transitions related by detailed balance, $R_{K\to J} - R_{J\to K} \rho_J/\rho_K$.





LINE COUPLING or LINE MIXING

Absorption Coefficient (impact approximation)

$$\kappa(\nu) = (N/\pi) \text{ Im} \{ \Sigma_J(d \cdot A)_J(A^{-1} \cdot \rho \cdot d)_J/(\nu - \omega_J) \}$$

where

 $\mathrm{d}_{\mathrm{J}} = \mu_{\mathrm{V}} \left[1 + \alpha_{\mathrm{HW}} \mathrm{J} \left(\mathrm{J} + 1 \right) \right]^{\mathrm{I}_{\mathrm{S}}}$

 $\rho_{JJ'} = \delta_{JJ'} g_J (2J+1) \exp(-hcE''(J)/k_BT)$

 ω_J are complex eigenvalues of complex matrix

 $H = \nu_0 + iPW$

whose eigenvectors are columns of matrix A

 $A^{-1} \cdot H \cdot A = \Omega$ where $\Omega_{JJ'} = \delta_{JJ'} \omega_{J}$

 u_0 is a diagonal matrix of transition

frequencies, vj

W is relaxation matrix whose diagonal elements are broadening coefficients and off-diagonal elements are line-coupling coefficients.

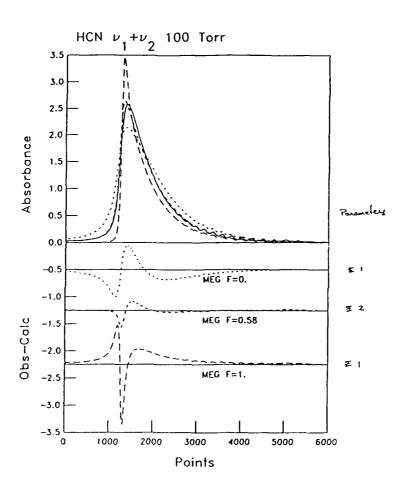
RELAXATION MATRIX

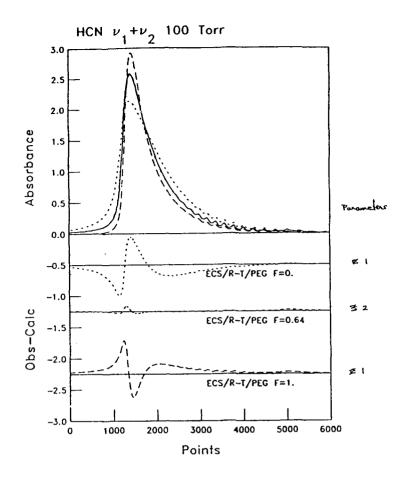
Diagonal Elements (Broadening)

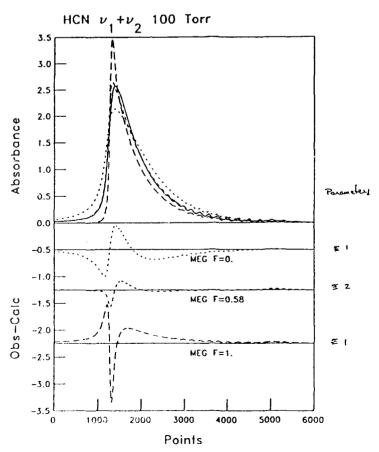
Off-Diagonal Elements (Coupling)

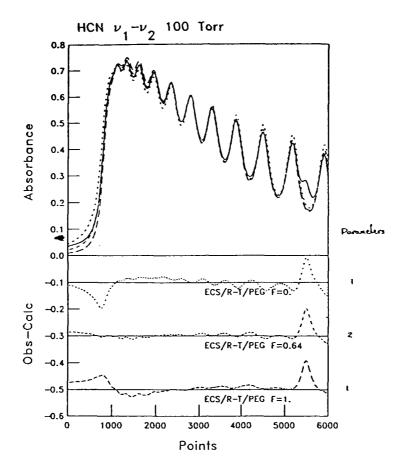
 $\mu_{JK} = -F R_{J\rightarrow K}(\Pi, f\rightarrow f)$

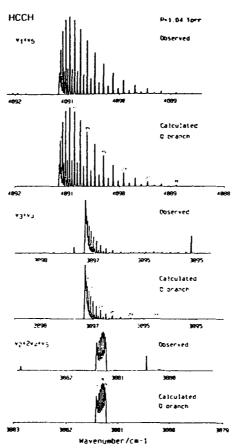
F is an empirical coupling factor.

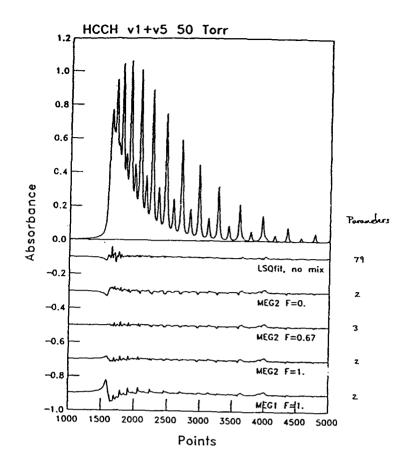


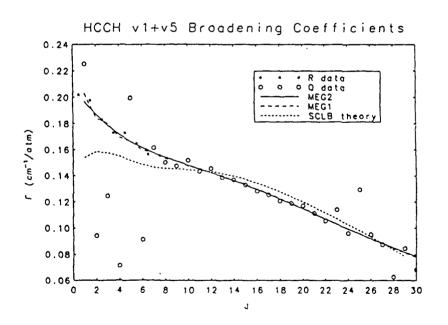


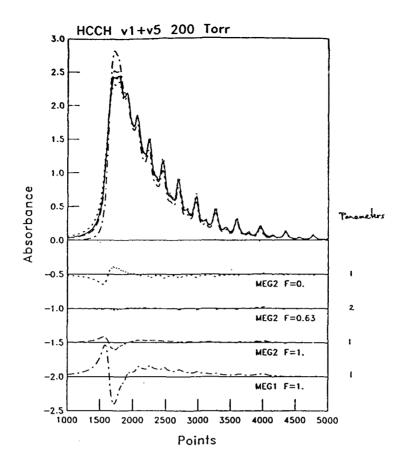


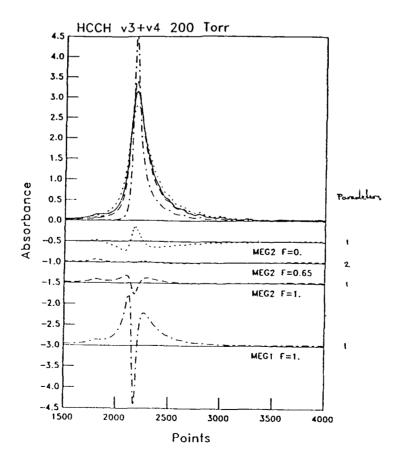


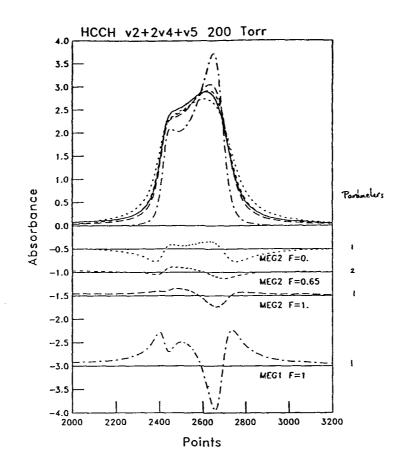












STUDY OF THE CO₂ BLUE WING IN THE 4.1 μM REGION

C.T. Delaye, M.E. Thomas Applied Physics Laboratory, The Johns Hopkins University, Laurel, MD 20723

In the 4.1 μ m region, continuum type absorption by CO₂ is the blue wing of the υ_3 fundamental band. Correct modeling of absorption in the wings of CO₂ vibrational bands

is required to calculate the shape of atmospheric windows.

Birnbaum's line shape is used to calculate absorption coefficients beyond 2380 cm⁻¹. This line shape allows a continuous representation from local calculations near resonance to continuum calculations in the far wings. It is incorporated in a line by line calculation, where it can be used with up to date spectroscopic databases. The calculation duplicates the shape of the wing, but not the magnitude. Line mixing effects are not taken into account in this model and an empirical scaling factor is required to match the model with the experimental data. This scaling factor remains constant below 1 atmosphere and increases, as expected, with increasing density. However, it is not possible to deduce a relation between this coefficient and the pressure. At high pressure, collision induced absorption (CIA) bands appear, which are forbidden, in the infrared. These bands are centered at 2669 cm⁻¹ and at 3015 cm⁻¹, and they modify the shape of the far wing. Beyond 2380 cm⁻¹, no strong temperature dependence has been observed. Experimental data have been obtained with a 10 meter long White cell and with a 30 cm long high pressure high temperature cell. Comparisons with calculations are presented.



STUDY OF CO₂ BLUE WING IN THE 4.1 µm REGION

C. T. Delaye and M. E. Thomas Applied Physics Laboratory The Johns Hopkins University Laurel, Maryland 20723

STUDY OF CONTINUUM ABSORPTION

- RADAR
- ELECTRO-OPTICAL SYSTEMS
- ATMOSPHERIC REMOTE SENSING
- INFRARED IMAGING SYSTEMS
- ATMOSPHERIC METEOROLOGY ...

CO, $\label{eq:constraint} 4.1~\mu m~REGION~[2380~-~2600]~cm^{-1}$ CO, - N,

BIRNBAUM'S MODEL

EFFECTS OF LINE MIXING -- EMPIRICAL SCALE FACTOR

In the far wing

$$g_{pw}(\omega) = \frac{\lambda}{\pi} \left\{ \sum_{i} \frac{\rho_{i} d_{j}^{2}}{\Delta_{i}^{2}} B_{ij}(\Delta_{j}) + \sum_{i} \sum_{k \neq i} \frac{\rho_{i} d_{k} d_{j}}{\Delta_{i} \Delta_{k}} B_{ij}(\Delta_{j}) \right\}$$

$$\Delta_{\rm j} = \omega_{\rm j} - \omega$$

ρ_i POPULATION OF THE ACTIVE MOLECULE

d, REDUCED DIPOLE MATRIX ELEMENT

 $B_{ii}(\Delta_i)$ FREQUENCY DEPENDENT LINE WIDTH

 $B_{iq}(\Delta_j)$ FREQUENCY DEPENDENT CROSS-RELAXATION FUNCTION WHICH PRODUCES LINE INTERFERENCE

BIRNBAUM'S MODEL:

$$B_{ii}(\Delta_j) = \gamma_{ii} h_{ji}(\Delta_j)$$

$$B_{ki}(\Delta_i) = \gamma_{ki} h_{ki}(\Delta_i)$$

$$h_{kj} (\Delta_j) = \frac{H_{kj}(\Delta_j)}{H_{kj}(0)}$$

$$H_{ij}(\Delta_j) = \frac{1}{2} \frac{\pi^{in}}{r^i (3/2)} e^{\frac{4\hbar \Delta_j}{4\pi}} \cdot \frac{\tau_{ij} x K_i(x)}{1 + (\tau_i/\tau_{ij})^2}$$

$$x = |\Delta_i| [\tau_{ki}^2 + \tau_0^2]^{4}$$

approximations
$$\rightarrow$$
 $h_{i,j}$ $(\Delta_j) = h_{jj}$ (Δ_j)
 \rightarrow $\tau_{i,j} = \tau_1$
 \rightarrow $\Delta_k = \Delta_j + \delta\omega$

sum rule
$$-\sum_{j\neq k} \rho_j d_k d_j \gamma_{kj} = \rho_j d_j^2 \gamma_{ij}$$

$$g_{FW}(\omega) = \frac{1}{\pi} \left\{ \sum_{i} \frac{\rho_{i} d_{i}^{2} \gamma_{ii}}{\Delta_{i}^{2}} h_{ii}(\Delta_{j}) \left[1 - (1 - \frac{\delta \omega}{\Delta_{i}}) \right] \right\}$$
scale factor
$$\alpha = \frac{\delta \omega}{\Delta_{i}}$$

MIXTURE CO₂ - N₂

$$\tau_{1}(CO_{1}-CO_{1}) = \tau_{1}(CO_{1}-N_{1})$$

$$Y_{IJ} = Y_{IJCO_1-CO_1} + Y_{IJCO_1-N_2}$$

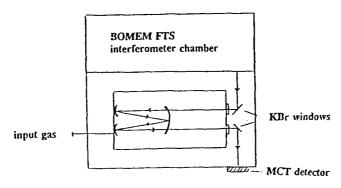
$$\rightarrow g_{FW}(\omega) = \frac{1}{\pi} \left\{ \sum_{i} \frac{\rho_{i} d_{i}^{2} \gamma_{ji}}{\Delta_{i}^{2}} h_{jj}(\Delta_{j}) \right\} \cdot \alpha$$

• ABSORPTION CELL

10 M WHITE CELL (40 TRAVERSALS)

 $P < 1 \Lambda TM$

ROOM TEMPERATURE

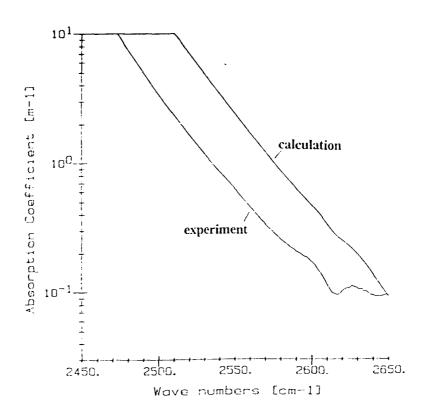


• HIGH PRESSURE - HIGH TEMPERATURE CELL

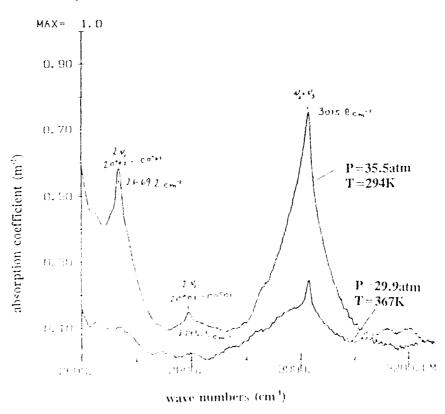
L = 30 CM

P = 1 ATM - 35 ATM

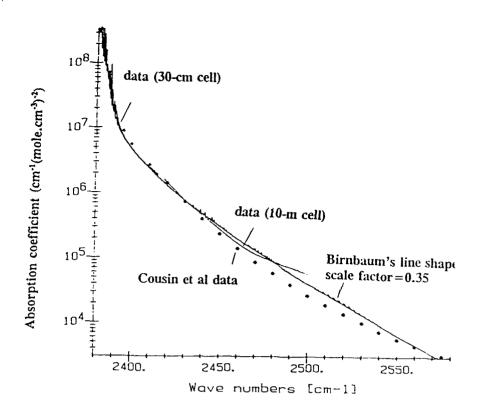
T = 296K - 370K



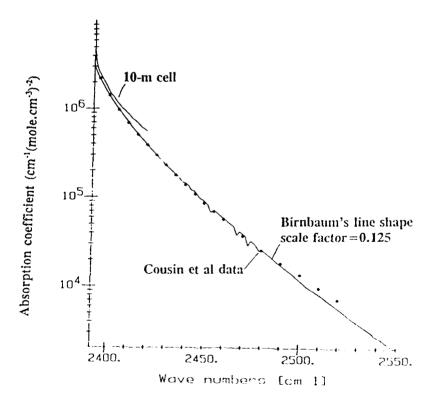
 CO_2 absorption coefficient in $m^{\text{-}1}$ at $T=329\mathrm{K}$ and $p=28.9\mathrm{atm}$.



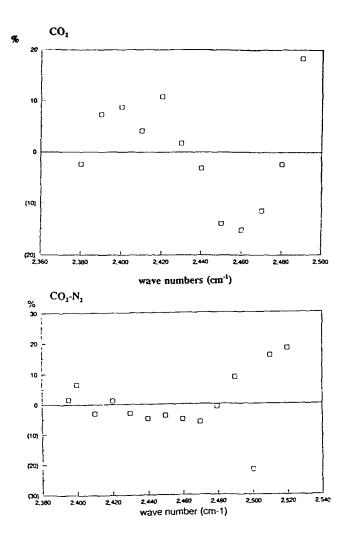
 CO_2 absorption coefficient in m^3 at 295K and p=35.5 atm and at T=367K and p=29.9 atm.



CO₂ absorption coefficient in (cm⁻¹(mole.cm⁻³)⁻²) at 295K.



CO₂-N₂ absorption coefficient in (cm⁻¹(mole.cm⁻³)⁻²) at 295K.



Relative difference in percent between experimental and calculated data.

$$CO_{2}$$

$$T = 296K 329K 367K 534K 627K$$
 $\alpha 0.35 0.25 0.19 0.22 0.14$

Scale factor α for CO_1 and $CO_2 \cdot N_2$ at different temperatures.

CONCLUSIONS

BIRNBAUM'S LINESHAPE

VERSATILE LINE SHAPE (II,O,CH,,...)

EASILY UTILIZED IN A LINE-BY-LINE CALCULATION

AGREEMENT WITH EXPERIMENTAL DATA AT ROOM TEMPERATURE FOR ${\rm CO_2}$ AND ${\rm CO_2}$ - ${\rm N_2}$

UNDERSTANDING OF TEMPERATURE DEPENDENCE OF THE CONTINUUM ABSORPTION (TEMPERATURE DEPENDENCE OF THE SCALE FACTOR)

THEORETICAL APPROACH TO THE LINE WING PROBLEM

L. Sinitsa Institute of Atmospheric Optics Tomsk, USSR

THEORETICAL APPROACH TO THE LINE WING PROBLEM

Presented by

L. Sinitsa

Institute of Atmospheric Optics

Tomsk, USSR

Theoretical approach
to the line wing problem

$$H = H_S + H_{OR} = (H_1 + H_2 + H_3 + U) + H_{OR}$$
 (1)

 H_1 -absorbing molecules | dynamic slbsystem P_1
 H_2 -surrounding molecules | dissipative P_2
 H_3 -kinetic energy of subsystem P_3
mass centers | interaction fetwern subsystems | P_3

First order perturbation theory in P_3
 P_4 -kinetic energy of subsystem P_5
 P_5 -kinetic energy of

Theoretical approach to the line wing problem

H=H_s+H_{OR}=
$$(H_1+H_2+H_3+U)+H_{OR}$$
 (1)

H₁-absorbing molecule | dynamic | stissystem | P_1

H₂-surrounding molecules | dissipative | P_2 | dissipative | P_2 | subsystem | P_3 | dissipative | P_2 | subsystem | P_3 | dissipative | P_2 | subsystem | P_3 | dissipative | P_2 | subsystems | P_3 | dissipative | P_2 | subsystems | P_3 | dissipative | P_2 | subsystems | P_3 | dissipative | P_2 | dissipative | P_3 | P_4 | P_4

$$i(\omega - \omega_{mn}) \mathcal{Q}_{cm} + (M\rho_{I})_{mn} = (\omega - \omega_{mn})^{2} I_{mn} + J_{mn}$$

$$\varphi(V) \mathcal{U} \qquad \qquad (4)$$

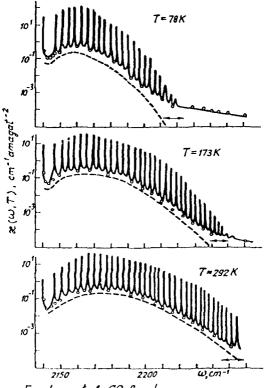
Asymptotic cases

Small
$$\Delta \omega$$
 large $\Delta \omega$ Line wing theory

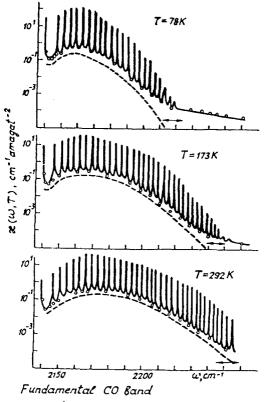
$$\begin{aligned}
& \approx \sum \frac{\gamma}{\gamma^2 + \Delta \omega^2} & \approx = D_a \sum S \Delta \omega^{-1-3/\alpha} F(R(\Delta \omega), T) \quad (5) \\
& \qquad \qquad \mathcal{P}(V), \mathcal{U} \\
& \qquad \qquad F(R(\Delta \omega), T) = \frac{1}{R_i} \int_0^{R_i} dR e^{-V(R)/kT} R(R_i^2 - R^2)^{1/2} \quad (6) \\
& \qquad \qquad V, \mathcal{U} \\
& \qquad \qquad R_i = C \alpha \Delta \omega^{-1/\alpha} \quad (7) \\
& \qquad \qquad \mathcal{U} \\
& \qquad \qquad R_i - the \ root \ of \ the \ Equation \\
& \qquad \Delta E_{mn} = \hbar \omega \quad (8) \\
& \qquad \Delta E_{mn} \sim \frac{C \alpha}{R^\alpha} \quad (9)
\end{aligned}$$

$$i(\omega - \omega_{mn}) \mathcal{Q}_{mn} + (M\rho_{t})_{mn} = (\omega - \omega_{mn})^{2} I_{mn} + J_{mn}$$

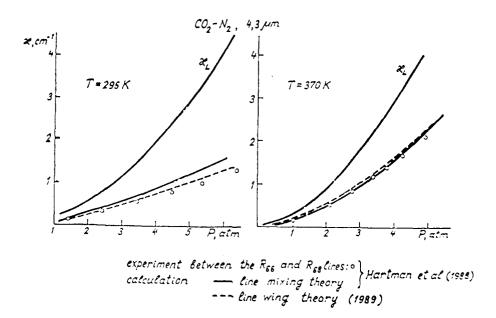
$$\phi(V), U \qquad (4)$$

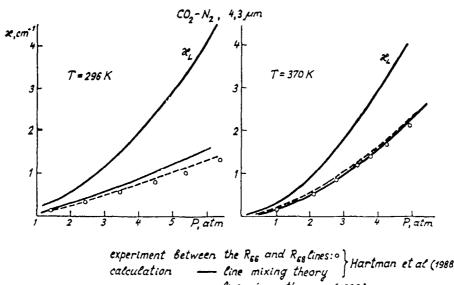


Fundamental CO Band experiment: • - Bulanin et al (1984)
calculation: — line wing theory (1988)
--- calculations using four
nearest lines with Lorentz profile

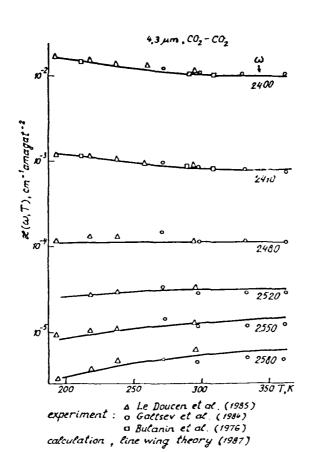


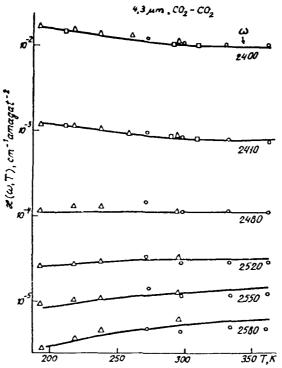
experiment: o - Bulanin et al (1984)
calculation: —— line wing theory (1988)
--- calculations using four
nearest lines with Lorentz profile

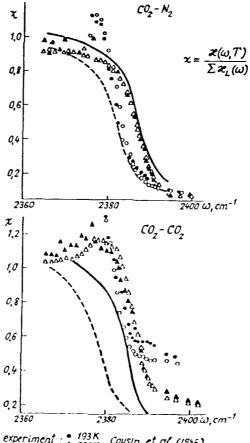


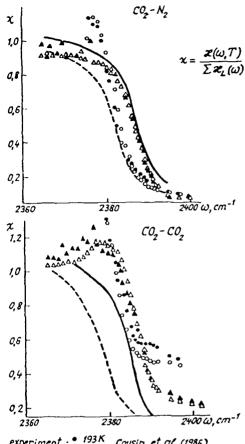


experiment between the R_{66} and R_{68} lines:0 Hartman et al (1988) calculation — line mixing theory (1989)









DEPARTMENT OF THE AIR FORCE

GEOPHYSICS LABORATORY (AFSC) HANSCOM AIR FORCE BASE, MASSACHUSETTS 01731-5000

REPLY TO OPS/F.X. Kneizys, 617-377-3654/L.W. Abreu, 617-377-2337

28 January 1991

SUBJECT

Annual Review Conference on Atmospheric Transmission Models

DISTRIBUTION

- 1. The extended DoD Plan for Atmospheric Transmission Research and Development tasks the Air Force to conduct an annual review conference to provide for tri-service discussion of model deficiencies and recommend corrective action.
- 2. The 14th Annual Review Conference will be held at the Geophysics Laboratory (now designated the Geophysics Directorate, Phillips Laboratory), Hanscom Air Force Base, Bedford, Massachusetts during the second week in June (11-12 June 1991). The objectives of the meeting are to review the current status of transmittance/radiance models and in hearing your recommendation regarding how we can overcome any identified deficiencies.
- 3. Areas of interest include molecular and aerosol effects on atmospheric radiative transfer, lidar, turbulence, remote sensing, the impact of trace atmospheric constituents on climate, and the general topic of spectral line shapes including both continua and line coupling effects.
- 4. This letter is intended to solicit contributions to this conference. If you would like to present a paper, please provide an unclassified abstract which should be double-spaced and no more than 12 lines. Please send abstracts to L.W. Abreu, GL/OPS (AFSC), HANSCOM AFB, MA 01731-5000 by 19 April 1991 (Telephone 617-377-2337).
- 5. Note all sessions will be open, and it is anticipated that foreign nationals will be permitted to attend. Allow sufficient time to obtain the necessary clearances for your papers. Immediately following this meeting, on 13-14 June the workshop on the HITRAN database will be held. For those interested in also attending this workshop, contact L.S. Rothman, GL/OPS, Hanscom AFB, MA 01731 (Telephone 617-377-2336).
- 6. If you plan to participate in the conference, but not make a presentation, <u>please notify us in writing</u>, by 19 April 1991 (non-US citizens should allow at least 6 weeks for visit approval). Send your letter to L.W. Abreu, GL/OPS (AFSC), Hanscom AFB, MA 01731-5000, (Telephone 617-377-2337). If you have any questions contact us at the numbers listed. AUTOVON prefix for Hanscom AFB is 478.

FRANCIS X. KNEIZYS

Simulation Branch

Optical Environment Division

LECNARD W. ABREU Simulation Branch

Optical Environment Division



DEPARTMENT OF THE AIR FORCE

GEOPHYSICS LABORATORY (AFSC)

HANSCOM AIR FORCE BASE, MASSACHUSETTS 01731-5000

REPLY TO OPS/F. Kneizys/617-377-3654/L.W. Abreu/617-377-2337

1 May 1991

SUBJECT:

Annual Review Conference on Atmospheric Models (11-12 June 91) (OPS Ltr, 28 Jan 91, same subject)

10

DISTRIBUTION

- 1. On the basis of responses to our January 28th letter announcing the Annual Peview Conference on Atmospheric Transmission Models, we have constructed the enclosed tentative agenda for a two-day meeting on 11-12 June 1991. In general, we have reduced some initial time requests slightly to allow for adequate discussion. Speakers should plan on a maximum total presentation time of 15 minutes. Viewgraphs are preferable as visual aids in the talks. The meeting will be unclassified.
- 2. We ask that all conference speakers provide us with hard copies of viewgraphs used in your presentation at the meeting. You can either mail them to L.W. Abreu GL/CPS, Hanscom AFB, MA 01731-5000, or bring a copy to the meeting.
- 3. We will meet on 11-12 June (starting at 0845 on the 11th and 0830 on the 12th in the GL Science Center, Bldg 1106, Hanscom AFB. (See attached map). Please plan to arrive by 0830 on the eleventh to allow time for registration on the first day.
- 4. We do not intend to make motel reservations for any participants, but we have enclosed a list of motels which are reasonably close to Hanscom AFB (although you will need a car for transportation). On-base government quarters are limited, so if you require VOQ accommodations, please make your reservations early by calling 617-377-2112. The AUTOVON prefix for Hanscom AFB is 478.

FRANCIS X. KNEIZYS

Simulation Branch

Optical Environment Division

LEONARD W. ABREU

Simulation Branch

Optical Environment Division

3 Atchs

1. Agenda

2. Map

3. List of Motels

ANNUAL REVIEW CONFERENCE ON ATMOSPHERIC TRANSMISSION MODELS

11-12 June 1991

Geophysics Directorate, Phillips Laboratory
Hanscom Air Force Base
Science Center, Building 1106

PROGRAM

Tuesday, 11 June 1991 (0845 - 1200)

WELCOME - R.E. Good, OP/Geophysics Directorate

KEYNOTE - Col. G. Aufderhaar, USAF (OUSDA)

SESSION 1 - AEROSOLS AND CLOUDS (Co-Chairpersons: E.P. Shettle (NRL) and J.R. Hummel (SPARTA)

"Boundary Layer Illumination Radiation Balance Model: BLIRB" A. Zardecki (Science and Technology Corporation)

"Relations Between Giant Aerosols Near the Surface and Solar Aureole Brightness" F.E. Volz (Geophysics Directorate)

COFFEE BREAK (1000 - 1015)

"The Computation of Radiative Transfer Through the Atmosphere Incorporating Various Aerosol Scenarios"

L.C. Rosen (University of California, Lawrence Livermore National Laboratory)

"BACKSCAT Lidar Backscatter Simulation: Version 2.0" J.R. Hummel, D.R. Longtin, N.L. Paul, J.R. Jones (SPARTA, Inc.)

"Cirrus Cloud Transmission Modelling"
W.M. Cornette, J.G. Shanks (Photon Research Associates, Inc.)

"ICE-CLOUD - A Model for IR Transmittance Through Cirrus Cloud" W.T. Kreiss, R. Vik (Horizons Technology, Inc.)

"The Status of the Navy Oceanic Vertical Aerosol Model" S. Gathman (Naval Ocean Systems Center)

LUNCH (1130 - 1330)

Tuesday, 11 June 1991 (1330 - 1700)

SESSION 2 - ATMOSPHERIC PROPAGATION MODELS

Co-Chairpersons: L.W. Abreu (PL), R. Shirkey (ASL) and J.E.A. Selby (Grumman)

"MODTRAN/LOWTRAN: Current Status, Future Plans"

L.W. Abreu, F.X. Kneizys, G.P. Anderson, J.H. Chetwynd (Geophysics Directorate)

"FASCODE3: An Update"

G.P. Anderson, F.X. Kneizys, J.H. Chetwynd, L.W. Abreu, M. Hoke (Geophysics Directorate), S.A. Clough, R.D. Worsham (Atmospheric and Environmental Research, Inc.), E.P. Shettle (Naval Research Laboratory)

"EOSAEL92"

A.E. Wetmore (U.S. Army Atmospheric Sciences Laboratory)

"HITRAN'91: The Contemporary Spectroscopic Molecular Database"

L.S. Rothman (Geophysics Directorate)

"SHARC, An Atmospheric Radiation and Transmittance Code for Altitudes from 50 to 300 km"

D. Robertson, L. Bernstein, J. Duff, J. Gruninger, R. Sundberg (Spectral Sciences, Inc.),

R. Sharma (Geophysics Directorate), R. Healey (Yap Analytics, Inc.)

"Recent Developments of the GENLN2 Line-by-Line Model: Studies in Support of the UARS Project"

D.P. Edwards (National Center for Atmospheric Research)

COFFEE BREAK (1500 - 1515)

"Present Status of Transmittances and Radiances Modelling at L.M.D."

N.A. Scott, A. Chédin, F. Chéruy, B. Tournier (ARA/LMD - Ecole Polytechnique)

"AURIC (Atmospheric Ultraviolet Radiance Integrated Code): an Update"

R. Huguenin, R. Hickey, K. Minschwaner (Aerodyne Research, Inc.), G.P. Anderson, L.A. Hall, R.E Huffman (Phillips Laboratory)

"Ontar's PC Compatible LOWTRAN Package"

J. Schroeder, P. Noah (Ontar Corporation)

"Coupling Atmosphere and Background Effects"

W.M. Cornette (Photon Research Associates, Inc.)

Tuesday, 11 June 1991 (1330 - 1700)

SESSION 2 - ATMOSPHERIC PROPAGATION MODELS (continued) Co-Chairpersons: L.W. Abreu (PL), R. Shirkey (ASL) and J.E.A. Selby (Grumman)

"SENTRAN7: A Sensitivity Analysis Package for LOWTRAN7 and MODTRAN" D.R. Longtin, F.M. Pagliughi, N.L. Paul (SPARTA, Inc.)

"Atmospheric Models in the Strategic Scene Generation Model" W.M. Cornette, D.C. Anding (Photon Research Associates, Inc.)

"Review of the Chemical Kinetic Rate Constants Used in the SHARC Model" V.I. Lang, A.T. Pritt, Jr., (The Aerospace Corporation)

SOCIAL HOUR/DINNER

Wednesday, 12 June 1991 (0830 - 1200)

SESSION 3 - MEASUREMENTS AND MODELS Co-Chairpersons: G.P. Anderson (PL), R. Smith (TECOM) and H. Revercomb (Univ. of Wisconsin)

"Atmospheric Ultraviolet Radiance and its Variations"
R. Link, D.J. Strickland and D.E. Anderson Jr. (Computational Physics, Inc.)

"Photoabsorption Cross Sections in the Transmission Window Regions of the Schumann-Runge Bands of Oxygen"

K. Yoshino, J.R. Esmond, D.E. Freeman, W.H. Parkinson (Harvard-Smithsonian Center for Astrophysics), A.S-C. Cheung (Chemistry Department - University of Hong Kong)

"Incorporation of LOWTRAN7 into the ACQUIRE Model" S.G. O'Brien (Las Cruces Scientific Consulting)

"High-resolution Spectral Measurements of Upwelling and Downwelling Atmospheric Infrared Emission with Michelson Interferometers" H.E. Revercomb (University of Wisconsin - SSEC)

"Validation of HIS Spectral Measurements with the FASCODE Line-by-Line Model" S.A. Clough, R.D. Worsham (Atmospheric and Environmental Research, Inc.), W.L. Smith, H.E. Revercomb, R.O. Knuteson, H.M. Woolf (U. of Wisconsin), G.P. Anderson, M.L. Hoke, F.X. Kneizys (Geophysics Directorate), M.V. Wagner, R.M. Goody (Harvard University)

"Improved HNO3 Band Model Parameters"

N. Jones, A. Goldman, D. Murcray, F. Murcray, W. Williams (University of Denver, Department of Physics)

COFFEE BREAK (1000 - 1015)

"Line-by-line Calculations of Atmospheric Fluxes and Heating Rates"
S.A. Clough, M.J. Iacono, J.-L. Moncet (Atmospheric and Environmental Research, Inc.)

"Comparison of FASCOD2 and LOWTRAN7 Models with FIT Spectral Transmittance Measurements in the 3-12 μ m Region"

J.M. Thériault (DREV-Defense Research Establishment Valcartier)

"Spectral Solar Radiation Modeling, Measurement, and Data Base Activities at the Solar Energy Research Institute"

C.J. Riordan, R.L. Hulstrom (Solar Energy Research Institute)

Wednesday, 12 June 1991 (0830 - 1200)

<u>SESSION 3</u> - MEASUREMENTS AND MODELS (continued) Co-Chairpersons: G.P. Anderson (PL), R. Smith (TECOM) and H. Revercomb (Univ. of Wisconsin)

"LOWTRAN 7 Comparisons with Field Measurements"
R. Smith, N. McNabb, K. Hammerdorfer, T. Corbin (TECOM Fort Belvoir Met Team)

"Spectral Smoothing in the Fourier Domain: A Software Package for Line-by-Line Calculations"

W. Gallery (Atmospheric and Environmental Research, Inc.), M. Esplin (Stewart Radiance Lab)

"A Comparison of Computational Approaches for the Voigt Function"
F. Schreier (Deutsche Forscungsanstalt für Luft- und Raumfahrt, Institute of Optoelectronics)

LUNCH (1200 - 1330)

Wednesday, 12 June 1991 (1330 - 1700)

SESSION 4 - TOPICAL SESSION ON SPECTRAL LINE SHAPES Chairperson: M.L. Hoke (PL)

SESSION 4a - INVITED PAPERS

"Basis of the Water Vapor Continuum Coefficients in the GL Models" S.A. Clough (Atmospheric and Environmental Research, Inc.)

"Water Vapor Continuum Absorption Measurements with Line Shape Interpretations"

M. Thomas (Johns Hopkins University)

"Line Coupling for Microwave Oxygen Lines"
P.W. Rosenkranz (Massachusetts Institute of Technology)

"Laboratory Measurements of Line Coupling in CO₂ and N₂O" L.L. Strow (University of Maryland)

COFFEE BREAK (1500 - 1515)

"Line Mixing: A Near Wing and Far Wing Problem" J.-M. Hartmann (Ecole Centrale Paris)

SESSION 4b - CONTRIBUTED PAPERS

"Far-wing Lineshape Contribution to the Water Continuum in the Millimeter and Infrared Regions"

R.H. Tipping (University of Alabama), Q. Ma (Goddard Space Flight Center)

"Laboratory Measurements of the 60-GHz O₂ Spectrum in Air" H.J. Liebe (U.S. Department of Commerce)

"Line Coupling in Polar and Nonpolar Molecules" A.S. Pine and J.P. Looney (NITS)

"Study of CO₂ Blue Wing in the 4.1 µm Region" C. Delaye, M. Thomas (Johns Hopkins University)

Name	Affiliation	Phone Number
Lt. Col. Mike Abel	ESD/WE Hanscom AFB, MA 01731-5000	617-377-3237
Mr. Leonard Abreu	PL/OPS Hanscom AFB, MA 01731-5000	617-377-2337
Mr. Donald E. Anderson, Jr.	Computer Physics, Inc. PO Box 360 Anandale, VA 22003	703-642-8728
Gail P. Anderson	PL/OPS Hanscom AFB, MA 01731-5000	617-377-2335
Stacy Angle	Loral IRIS 2 Forbes Road, Mail Stop 391 Lexington, MA 02173	617-863-3918
Roblin Antoine	ONERA(FR)	
Col. Grant Aufderhaer	OUSDA (R&AT/E&LS) The Pentagon/Room 3D129 Washington, DC 20301	703-695-9604
Stuart D. Augustin	Scitec, Inc. 100 Wall Street Princeton, NJ 08540	609-921-3892
Dr. Robert R. Beland	PL/OPA Hanscom AFB, MA 01731-5000	617-377-4604
Capt. Leslie O. Belsma	AFSD/AWS-OL-F Los Angeles AFS, CA 90009	213-416-7720
Dr. Larry Bernstein	Spectral Sciences, Inc. 111 S. Bedford Street Burlington, MA 01803	617-273-4770
Ron Bieniek	U. Missouri Rolla 102 Physics Rossa, MS 05401	314-341-4786
Dr. W. A. M. Blumberg	GL/OPS Hanscom AFB, MA 01731	617-377-3688

Name	Affiliation	Phone Number
Barry W. Bryant	Nichols Research Corporation 251 Edgewater Drive Wakefield, MD 01880	617-246-4200
Mr. James T. Bunting	PL/LYS Hanscom AFB, MA 01731-5000	617-377-3495
Georgette Burgen	MIT/Lincoln Lab P.O. Box 73 Lexington, MA 02173-0073	617-981-2870
Mark Caccui	York University 4700 Keele Street North York, Toronto Canada M3J 1P3	416-736-2100
Dr. Ken Champion	PL/LY Hanscom AFB, MA 01731	617-377-3033
Dr. Kelly Chance	Harvard Smithsonian Center for Astrophysics 60 Garden Street Cambridge, MA 02138	617-495-7389
Frederique Cheruy	Centre National de la Recherche Scientifique Ecole Polytechnique Palaiseau Cedex F-91128 France	331-693-34533
Mr. James H. Chetwynd	PL/OPS Hanscom AFB, MA 01731-5000	617-377-2613
Robert W. Cleary	USA-Materials Technology Lab Tecom Watertown, MA 02172	617-923-5440
Marianne Clinarella	Creative Optics, Inc. One DeAngelo Drive Bedford, MA 01730	617-275-8823
Dr. William M. Cornette	Photon Research Associates, Inc. 9393 Town Center Drive San Diego, CA 92121	619-455-9741

Name	Affiliation	Phone Number
Willam T. Creoss	Horizons Technology, Inc. 3990 Ruffin Road San Diego, CA 92123	619-292-8331
Lt. Kevin M. Crupi	Det. 10 2nd Weather Sqdn. Eglin AFB, FL 32542	904-882-5960
Frank DelGreco	PL/LIM Hanscom AFB, MA 01731	617-377-4758
John DeVore	Physical Research Inc. 350 South Hope Avenue Suite A201, PO Box 30129 Santa Barbara, CA 93130	805-682-1605
Dr. Edmond Dewan	PL/OPS Hanscom AFB, MA 01731-5000	617-377-4401
Paul Dorian	General Electric Building A, Room 37A30 PO Box 8048 Philadelphia, PA 19101	215-531-3863
Dr. Laila Dzelzkalns	GL/OPS Hanscom AFB, MA 01731	617-377-3671
Dr. John F. Ebersole	Creative Optics, Inc. One DeAngelo Drive Bedford, MA 01730	617-275-8823
Dr. David Edwards	NCAR/GOMOT Box 3000 Boulder, CO 80307	303-497-1467
Dr. Paul Eitner	General Electric Building A, Room 37A30 PO Box 8048 Philadelphia, PA 19101	215-531-1195
Vin Falcone	GP/LYS Hanscom AFB, MA 01731	617-377-4029
Hans Fast	AES (ARQX) 495 Dufferin Street Downsview, Ontario M3H 5T4 Canada	416-739-4627

Name	Affiliation	Phone Number
Patrick Freeman	Science & Technology Corp. 555 Telshor Blvd., Suite 200 Las Cruces, NM 88001	505-678-8013
Stuart Friedenreich	NOAA/GFDL PO Box 308 Princeton, NJ 08542	609-452-6645
William O. Gallery	Atmospheric and Environmental Research, Inc. 840 Memorial Drive Cambridge, MA 02139	617-547-6207
Margaret E. Gardner	Visidyne 10 Corporate Place South Bedford Street Burlington, MA 01803	617-273-2820
Dr. Dennis Garvey	ARMY Atmospheric Sciences Laboratory White Sands Missile Range, NM 88002	505-678-5677
Stuart Gathman	NOSC, Code 4320 Naval Research Laboratory Washington, DC 20375	619-553-1418
Mimi Gerstell	Center for Earth and Planetary Physics Harvard University 29 Oxford Street Cambridge, MA 02139	617-846-9117
Dr. James R. Gillis	Boeing Aerospace PO Box 3999 MS 87-08 Seattle, WA 98124-2499	206-773-9956
Dr. R. Earl Good	PL/OP Hanscom AFB, MA 01731-5000	617-377-2951
Melanie Gouviea	STX 109 Massachusetts Avenue Lexington, MA 021378	617-862-0405
Allen S. Grossman	Lawrence Livermore National Laboratory P.O. Box 808 Livermore, CA 94550	510-423-6371

Name	Affiliation	Phone Number
Dr. L. A. Hall	PL/LIU Hanscom AFB, MA 01731	617-377-3322
J. Hartney	MIT/Lincoln Laboratory P.O. Box 73 Lexington, MA 02173-0073	617-981-4727
Mr. Robert Hawkins	PL/OPS Hanscom AFB, MA 01731-5000	617-377-3614
Rebecca Healey	Yap Analytics 594 Marrett Road Lexington, MA 02173	617-863-1599
Mr. Glenn J. Higgins	TASC 33 Walkers Brook Drive Reading, MA 01867	617-942-2000
Don Hirst	AFTAC/Advanced Systems Patrick AFB, FL 32925-6001	407-494-2531
Helen Hoover	MIT/Lincoln Laboratory P.O. Box 73 Lexington, MA 02173-0073	617-981-2869
Mr. Robert E. Huffman	PL/LIU Hanscom AFB, MA 01731-5000	617-377-3311
Robert L. Huguenin	Aerodyne Research Inc. 45 Manning Road Billerica, MA 01821	508-663-9500
Dr. John R. Hummel	SPARTA, Inc. 24 Hartwell Avenue Lexington, MA 02173	617-863-1060
Dr. Nicole Husson	Laboratoire de Meteorologie Dynamique C.N.R.S. Ecole Polytechnique 91128 Palaiseau France	33 16933h02
Priscilla Ip	Mission Research Corporation 1 Tara Boulevard, Suite 302 Nashua, NH 03062-2801	603-891-0070

Name	Affiliation	Phone Number
Ronald G. Isaacs	Atmospheric and Environmental Research, Inc. 840 Memorial Drive Cambridge, MA 02139	617-547-6207
Douglas R. Jensen	Naval Ocean Systems Center San Diego, CA 92152	619-553-1415
Rana Jones	MIT	617-981-2970
Dr. Frank Kantrowitz	U.S. Army Atmospheric Sciences Lab Attn: SLCAS-AA-A White Sands Missile Range, NM 88002	505-678-1526
Dieter Klaes	PL/LYS Hanscom AFB, MA 01731	617-377-3317
Mr. Francis X. Kneizys	PL/OPS Hanscom AFB, MA 01731-5000	617-377-3654
Dr. Olga Lado-Bordowsky	Ecole Nationale Superieure de Sciences Appliques et de Technologie Universite de Rennes 6 Reude Kerampont 22305 Lannion FRANCE	33-96465030
Capt. Bob Lawconnell	USAFA, FJSRL/NP Colorado Springs, CO 80840-6528	719-472-3503
Dr. Edward Lee	GL/PL Hanscom AFB, MA 01731	617-377-2338
Dr. Hans Liebe	NTIA/TIS.S3 Boulder, CO 80303	303-497-3310
Mr. David R. Longtin	SPARTA, Inc. 24 Hartwell Avenue Lexington, MA 02173	617-863-1060
Charles LoPresti	Battelle Pacific Northwest Labs PO Box 999 MS K7-34 Richland, WA 99352	509-375-3923

Name	Affiliation	Phone Number
Qiancheng Ma	The Goddard Institute for Space Studies 2880 Broadway New York, NY 10025	212-678-5574
Arvind S. Marathay	PL/OPS Hanscom AFB, MA 01731	617-377-2810
William R. Mark	Det 1, HQAWS SAF/SS Pentagon Room 4C, 1052 Washington DC 20330-1000	703-614-1772
Mary Martin	Complex Systems Research Center SERB University of New Hampshire Durham, NH 08324	603-862-4098
Prof. Arthur Mason	Univ. of Tennessee Space Institute Tullahoma, TN 37388	615-455-0631
Ms. Susan M. McKenzie	Atmospheric & Space Sciences Division Mission Research Corporation 1 Tara Boulevard, Suite 302 Nashua, NH 03062-2801	603-891-1986
John L. Mergenthaler	Lockheed P. A. Research Lab Org: 97-90 Bldg. 201 3251 Hanover St. Palo Alto, CA 94304	415-424-2483
Ken Minschwaner	Harvard University Center for Astrophysics 60 Garden Street Cambridge, MA 02138	617-496-8318
H. Nebel	Alfred University Dept. of Geology Alfred, NY 14802	607-871-2208
ът. Flemming M. Nicolaisen	University of Copenhagen The H.C. Orsted Institute Universitetsparker 5 DK-2100 Kobenhavn DENMARK	

Name	Affiliation	Phone Number
Mr. Edward R. Niple	Aerodyne Research, Inc. 45 Manning Road The Research Center at Manning Park Billerica, MA 01821-3976	508-663-9500
Paul Noah	Ontar Corp. 129 University Rd. Brookline, MA 02146	617-739-6607
Dr. Sean G. O'Brien	L.C. Scientific Consultants 3373 Solar Ridge St. Las Cruces, NM 88001	505-382-0285
Valdar Oinas	NASA Goddard Institute for Space Studies 2880 Broadway New York, NY 10025	212-778-5528
Armand J. Paboojian	ARCON Corp. 260 Bear Hill Rd. Waltham, MA 02154	617-377-2262
Ms. Nanette L. Paul	SPARTA, Inc. 24 Hartwell Avenue Lexington, MA 02173	617-863-1060
Dr. Richard H. Picard	PL/OPS Hanscom AFB, MA 01731-5000	617-377-2222
Ms. Angela Phillips	E-O & Data Systems Group Hughes Aircraft Company P.O. Box 902 El Segundo, CA 90245	213-616-0124
Damon J. Phillips	MIT/Lincoln Laboratory P.O. Box 73 Lexington, M \ 02173-0073	617-981-4716
William J. Phillips	Sverdrup Technology AEDC Group MS 900 Arnold AFS, TN 37389	615-454-4664
Chuck Pritt	Aerospace Corp. P. O. Box 92957 Los Angeles, CA 90009	213-396-6701

Name	Affiliation	Phone Number
Dr. Anthony Ratkowski	PL/OPS Hanscom AFB, MA 01731-5000	617-377-3655
Kenneth W. Reese	DET 3 AWS Okizaka CA	
Mr. H.E. Revercomb	Cooperative Institute for Satellite University of Wisconsin 1225 W. Dayton Street Madison, WI 53706	608-263-6758
Ms. Carol J. Riordan	Solar Energy Research Institute 1617 Cole Boulevard Golden, CO 80401-3393	303-231-1344
Dr. Rolando Rizzi	European Centre for Med. Range Weather Forecasting Shinfield Park, Reading RG2 9AX UNITED KINGDOM	447-344-99080
Dr. David C. Robertson	Spectral Sciences, Inc. 111 S. Bedford Street Burlington, MA 01803	617-273-4770
Mr. Ron Rodney	Wright Laboratory - Staff Metoeorology WRDC/WEA WPAFB, OH 45433-6543	513-255-1978
Dr. L. C. Rosen	Lawrence Livermore National Laboratory P.O. Box 808 Livermore, CA 94550	415-422-1834
P.W. Rosenkranz	Massachusetts Institute of Technology 77 Massachusetts Avenue Cambridge, MA 02139	617-253-3073
Sam Rosenzweig	SAIC 6 Fortune Drive Billerica, MA 01821	617-275-2200
Dr. Laurence S. Rothman	GL/OPS Hanscom AFB, MA 01731-5000	617-377-2336
Robert Rubio	U.S. Army Atmospheric Science Lab White Sands Missile Range, NM 88002	505-678-2926

Name	Affiliation	Phone Number
Ms. Crystal Schaaf	GL/LYA Hanscom AFB, MA 01731-5000	617-377-2963
Franz Schreier	DFVLR, Institut fur Optoelectronik 8031 Oberpfaffenhofen Post Wessling Federal Republic of Germany	8153 28777
Dr. John Schroeder	ONTAR Corporation 129 University Road Brookline, MA 02146	617-739-6607
Dr. Bertram D. Schurin	MS E-55-MS/G-223 Hughes Aircraft Company P.O. Box 902 El Segundo, CA 90245	213-616-6978
Noelle A. Scott	Centre National de la Recherche Scientifique Ecole Polytechnique Palaiseau Cedex F-91128 France	33-1-69334532
Dr. John E. A. Selby	Research Department, MS A08-35 Grumman Aerospace Corporation South Oyster Bay Road Bethpage, NY 11714	516-575-6608
Lt. Scott Shannon	GL/OPS Hanscom AFB, MA 01731-5000	617-377-7396
Mr. Eric P. Shettle	NRL, Code 6522 Washington, DC 20375	202-404-8152
Mr. Richard C. Shirkey	Atmospheric Sciences Laboratory DELAS-EO-S White Sands Missile Range, NM 88002	505-678-5470
Dr. Lewis L. Smith	Mail Stop A01-26 Grumman Corporate Research Center Bethpage, NY 11714-3580	516-575-2196

Name	Affiliation	Phone Number
Shaoann Shon	MIT/Lincoln Laboratory P.O. Box 73 Lexington, MA 02173-0073	617-275-0111
M.O. Shyluf	NOAA/GFDL PO Box 308 Princeton, NJ 08542	609-452-6521
Robert W. Smith	Chief, TECOM Ft. Belvoir Met Team AMSTE-TC-AM (BE) CCNVEO Fort Belvoir, VA 22060	703-664-1188
Dr. J. William Snow	GL/LYS Hanscom AFB, MA 01731-5000	617-377-3496
Doug Strickland	Computer Physics, Inc. PO Box 360 Anandale, VA 22003	703-642-8728
L. Larrabee Strow	University of Maryland 5401 Wilkins Avenue Baltimore, MD 21228	301-455-2528
Mr. Frank Suprin	PL/OPA Hanscom AFB, MA 01731-5000	
Capt. Andrew Terzakis	WL/WE Kirtland AFB, NM 87117-608	505-846-4722
Jean-Marc Theriault	DREV P.O. Box 8800 Courcelette, Quebec GOA 1RO Canada	418-844-4335
Patrice Y. Thrash	MIT/Lincoln Lab P.O. Box 73 Lexington, MA 02173-0073	617-981-2870
Dr. Richard H. Tipping	University of Alabama Dept. of Physics & Astronomy 206 Gallalee Box 870324 Tuscaloosa, AL 35487	205-348-3799

Name	Affiliation	Phone Number
C.N. Touart	STX 109 Massachusetts Avenue Lexington, MA 021378	617-862-0405
D. Shawn Turner	Atmospheric Environment Service Atm: ARMA 4905 Dufferin Street Downsview, Ontario CANADA M3H 5T4	416-739-4885
Capt. Glen Van Knowe	RL/WE Griffiss AFB, NY 13441	DSN-587-9836
Marty Venner	PL/RFT Hanscom AFB, MA 01731	805-275-5584
R.C. Vik	Horizons Technology, Inc. 3990 Ruffin Road San Diego, CA 92123	619-453-7024
Dr. Fred Volz	PL/OPS Hanscom AFB, MA 01731-5000	377-3666
R. J. Waldeon	Aerospace Corporation P. O. Box 92957 Los Angeles, CA 90009	213-416-7324
James Wallace	Far Field, Inc. 6 Thoreau Way Sudbury, MA 01776	508-443-9214
Dr. Alan E. Wetmore	Atmospheric Sciences Laboratory White Sands Missile Range, NM 88002-5501	505-678-5563
Gerald Wetzel	Institute for Meteorologie und Klimaforschung Karlsruhe Postfach 3640 D-7500 Karlsruhe 1 Federal Republic of Germany	49 07247-5947
Mr. P. P. Wintersteiner	ARCON Corporation 260 Bear Hill Road Waltham, MA 02154	617-890-3330

Name	Affiliation	Phone Number
Mr. Robertt D. Worsham	Atmospheric and Environmental Research, Inc. 840 Memorial Drive Cambridge, MA 02139	617-547-6207
Dr. Al S. Zachor	Atmospheric Radiation Consultants 59 High Street Acton, MA 01720	508-263-1931
Dr. Andrew Zardecki	Science & Technology Corp. 555 Telshor Blvd., Suite 200 Las Cruces, NM 88001	505-678-8013
Gerald J. Zdyb	PL/OP Hanscom AFB, MA 01731	617-377-2089

Appendix

AUTHOR INDEX

Abreu, Leonard W64, 73	Looney, J.P.	429
Anderson, Donald E., Jr202	McNabb, Norman	
Anderson, Gail P 64, 73, 130, 231	Ma, Qiancheng	409
Anding, David C	Minschwaner, Ken	
Bernstein, Larry107	Moncet, Jean-Luc	
Chédin, Alain	Murcray, D.	
Chéruy, Frederique129	Murcray, Frank	242
Chetwynd, James H64, 73	Noah, Paul V.	
Cheung, A.S-C203	O'Brien, Sean G.	
Clough, Shepard A73, 231, 249, 333	Pagliughi, Frank M.	
Corbin, Ted	Parkinson, W.H.	
Corbin, Ted	Paul, Nanette L	
Davies, R.W	Pine, A.S.	
Delaye, Corinne T	Pritt, A.T., Jr.	
Duff, James	Revercomb, Henry E.	
Edwards, David P	Riordan, Carol J.	276
Esmond, J.R	Roberson, David C.	
Esplin, Mark	Rosen, L.C.	
Freeman, D.E	Rosenkranz, P. W	
Gallery, William O314	Rothman, Laurence S	
Gathman, Stuart54	Schreier, Franz	
Goldman, Aaron242	Schroeder, John	
Goody, Richard M231	Scott, Noelle A	
Gruninger, John107	Shanks, Joseph G	
Hall, L.A	Sharma, R.	
Hammerdorfer, Karl282	Shettle, Eric P.	
Hartmann, Jean-Michel389	Sinitsa, L.	
Healey, Rebecca107	Smith, Robert W	282
Hickey, R	Strickland, Douglas J.	202
Hoke, Michael L 73, 231	Strow, Larry L	370
Huffman, Robert E	Sundberg, Robert	
Hugeunin, Robert L	Thériault, Jean-Marc	263
Hulstrom, Roland L276	Thomas, Michael E 341,	441
Hummel, John R28	Tipping, Richard H	409
Iacono, Michael J249	Tournier, B	129
Jones, James R28	Vik, R.C	. 47
Jones, Nicholas242	Volz, Fred E	
Kneizys, Francis X 64, 73, 231, 333	Wagner, M.W.	231
Kreiss, William T47	Wetmore, Alan E	. 86
Lang, V.I188	Williams, Walter	242
Liebe, Hans J	Worsham, Robert D73,	231
Link, R202	Yoshino, A	
Longtin, David R	Zardecki, Andrew	2